

## Calhoun: The NPS Institutional Archive DSpace Repository

---

Theses and Dissertations

1. Thesis and Dissertation Collection, all items

---

1991-12

### An analysis of middle ultraviolet dayglow spectra.

Walden, Billie S.

Monterey, California. Naval Postgraduate School

---

<http://hdl.handle.net/10945/27971>

---

*Downloaded from NPS Archive: Calhoun*



<http://www.nps.edu/library>

Calhoun is the Naval Postgraduate School's public access digital repository for research materials and institutional publications created by the NPS community.

Calhoun is named for Professor of Mathematics Guy K. Calhoun, NPS's first appointed -- and published -- scholarly author.

Dudley Knox Library / Naval Postgraduate School  
411 Dyer Road / 1 University Circle  
Monterey, California USA 93943









# NAVAL POSTGRADUATE SCHOOL

## Monterey, California



# THESIS

AN ANALYSIS OF MIDDLE  
ULTRAVIOLET DAYGLOW  
SPECTRA

by

Billie S. Walden

December, 1991

Thesis Advisor:

David D. Cleary

Approved for public release; distribution is unlimited.

T259078



## Unclassified

SECURITY CLASSIFICATION OF THIS PAGE

Form Approved  
OMB No 0704-0188

## REPORT DOCUMENTATION PAGE

1a REPORT SECURITY CLASSIFICATION Unclassified		1b RESTRICTIVE MARKINGS	
2a SECURITY CLASSIFICATION AUTHORITY		3 DISTRIBUTION/AVAILABILITY OF REPORT Approved for public release; distribution is unlimited.	
2b DECLASSIFICATION/DOWNGRADING SCHEDULE			
4 PERFORMING ORGANIZATION REPORT NUMBER(S)		5 MONITORING ORGANIZATION REPORT NUMBER(S)	
6a NAME OF PERFORMING ORGANIZATION Naval Postgraduate School	6b OFFICE SYMBOL (if applicable) 33	7a NAME OF MONITORING ORGANIZATION Naval Postgraduate School	
6c ADDRESS (City, State, and ZIP Code) Monterey, CA 93943-5000		7b ADDRESS (City, State, and ZIP Code) Monterey, CA 93943-5000	
8a NAME OF FUNDING/SPONSORING ORGANIZATION	8b OFFICE SYMBOL (if applicable)	9 PROCUREMENT INSTRUMENT IDENTIFICATION NUMBER	
8c ADDRESS (City, State, and ZIP Code)		10 SOURCE OF FUNDING NUMBERS PROGRAM ELEMENT NO      PROJECT NO      TASK NO      WORK UNIT ACCESSION NO	
11 TITLE (Include Security Classification) AN ANALYSIS OF MIDDLE ULTRAVIOLET DAYGLOW SPECTRA			
12 BRIEF STATEMENT OF AUTHOR(S) B. S. Walden			
13a TYPE OF REPORT Master's Thesis	13b TIME COVERED FROM _____ TO _____	14 DATE OF REPORT (Year, Month, Day) December 1991	15 PAGE COUNT 231
16 SUPPLEMENTARY NOTATION The views expressed in this thesis are those of the author and do not reflect the official policy or position of the Department of Defence or the U.S. Government.			
17 COSATI CODES FIELD      GROUP      SUB-GROUP		18 SUBJECT TERMS (Continue on reverse if necessary and identify by block number) Dayglow, Ionosphere, Ultraviolet Spectroscopy	
19 ABSTRACT (Continue on reverse if necessary and identify by block number) Middle ultraviolet spectra from 1800 to 3400 Å are analyzed. These spectra were obtained from the March 1990 rocket flight of the NPS MUSTANG instrument over the altitudes 105km to 315km. The data were compared with computer generated synthetic spectra. A least squares fitting procedure was developed for this purpose. Each data point was weighted using the standard deviation of the means. Synthetic spectra were generated for the following emissions: N <sub>2</sub> Vegard-Kaplan; N <sub>2</sub> Lyman-Birge-Hopfield; NO $\gamma$ , $\delta$ , and $\epsilon$ ; OI 2972 Å, OII 2470 Å; and NII 2143 Å. Altitude profiles for the emissions were obtained. Tentative identification was made of the OIII 2853 Å emission. A comparison of VK and LBH profiles demonstrates the process of N <sub>2</sub> A-state quenching by atomic oxygen.			
20 DISTRIBUTION/AVAILABILITY OF ABSTRACT <input checked="" type="checkbox"/> UNCLASSIFIED/UNLIMITED <input type="checkbox"/> SAME AS RPT <input type="checkbox"/> DTIC USERS		21 ABSTRACT SECURITY CLASSIFICATION Unclassified	
22a NAME OF RESPONSIBLE INDIVIDUAL D. Cleary		22b TELEPHONE (Include Area Code) (408)646-2828	22c OFFICE SYMBOL Ph-cl

Approved for public release; distribution is unlimited.

An Analysis of Middle  
Ultraviolet Dayglow  
Spectra

by

Billie S. Walden  
Lieutenant, United States Navy  
B.S.E., Duke University, 1986

Submitted in partial fulfillment  
of the requirements for the degree of

MASTER OF SCIENCE IN PHYSICS

from the

NAVAL POSTGRADUATE SCHOOL  
December 1991

## ABSTRACT

Middle ultraviolet spectra from 1800 to 3400Å are analyzed. These spectra were obtained from the March 1990 rocket flight of the NPS MUSTANG instrument over the altitudes 105km to 315km. The data were compared with computer generated synthetic spectra. A least squares fitting procedure was developed for this purpose. Each data point was weighted using the standard deviation of the means. Synthetic spectra were generated for the following emissions: N<sub>2</sub> Vegard-Kaplan; N<sub>2</sub> Lyman-Birge-Hopfield; NO  $\gamma$ ,  $\delta$ , and  $\epsilon$ ; OI 2972Å, OII 2470Å; and NII 2143Å. Altitude profiles for the emissions were obtained. Tentative identification was made of the OIII 2853Å emission. A comparison of VK and LBH profiles demonstrates the process of N<sub>2</sub> A-state quenching by atomic oxygen.

10313  
6/22/16  
C.J.

TABLE OF CONTENTS

I.	INTRODUCTION	1
A.	THESIS OBJECTIVES	2
B.	THESIS OUTLINE	3
II.	BACKGROUND	5
A.	THE ATMOSPHERE	5
1.	General Description	5
2.	Atmospheric Airglow	8
B.	ATOMIC AND DIATOMIC SPECTRA	10
1.	Atomic Emissions	10
2.	Molecular Emissions	11
III.	DAYGLOW EMISSION FEATURES	16
A.	MOLECULAR NITROGEN	16
1.	Vegard-Kaplan	16
2.	Lyman-Birge-Hopfield	17
3.	Second Positive	17
B.	ATOMIC NITROGEN	18
C.	ATOMIC OXYGEN	19
D.	NITRIC OXIDE	20
1.	Delta	20
2.	Gamma	21

3. Epsilon . . . . .	22
IV. THE EXPERIMENT . . . . .	
A. Introduction . . . . .	23
B. Instrument Description . . . . .	23
C. Data Collection . . . . .	24
V. DATA ANALYSIS & RESULTS . . . . .	
A. TECHNIQUE . . . . .	26
1. Introduction . . . . .	26
a. Fitting Method . . . . .	26
b. Synthetic Spectra . . . . .	27
2. General Programming Technique . . . . .	30
a. Fitting Routine . . . . .	30
b. Weighting Program . . . . .	33
B. RESULTS . . . . .	34
1. Comparison of Data and Fit . . . . .	34
a. Nitric Oxide Bands . . . . .	34
b. Nitrogen Bands . . . . .	34
c. Oxygen Atomic Emissions . . . . .	38
2. Profiles . . . . .	38
a. Nitric Oxide . . . . .	38
b. Nitrogen Bands . . . . .	43
c. Atomic Emissions . . . . .	47
3. Discussion . . . . .	48
a. V-K Quenching . . . . .	48

b. Adjustments to Franck-Condon Factors . . . . .	48
c. Temperature Profile . . . . .	54
VI. CONCLUSIONS . . . . .	55
A. SUMMARY OF FINDINGS . . . . .	55
B. TOPICS FOR FURTHER INVESTIGATION . . . . .	56
APPENDIX A . . . . .	58
APPENDIX B . . . . .	73
APPENDIX C . . . . .	96
APPENDIX D . . . . .	105
APPENDIX E . . . . .	110
LIST OF REFERENCES . . . . .	216
BIBLIOGRAPHY . . . . .	218
INITIAL DISTRIBUTION LIST. . . . .	220

## LIST OF TABLES

TABLE	PAGE
2-1 SUMMARY OF SELECTION RULES FOR MOLECULAR TRANSITIONS. . . . .	14
2-2 MOLECULAR ELECTRONIC STATES. . . . .	15
5-1 NO COLUMN DENSTIES . . . . .	43
5-2 ATOMIC INTENSITY VALUES . . . . .	47
5-3 ADJUSTMENTS TO FRANCK-CONDON FACTORS . . . . .	51

## LIST OF FIGURES

FIGURE	PAGE
2-1 Temperature profile and corresponding atmospheric layers. . . . .	5
2-2 Atomic processes induced by incident radiation. . . . .	10
2-3 Molecular absorption transitions. . . . .	12
2-4 Graphical representation of molecular spectrum. . . . .	13
2-5 Instrument response to molecular transition. .	13
3-1 N <sub>2</sub> energy level diagram. . . . .	16
3-2 Energy level diagram for N <sup>+</sup> . . . . .	19
3-3 Energy level diagram for neutral atomic oxygen. . . . .	20
3-4 Energy level diagram for O <sup>+</sup> . . . . .	21
3-5 Transitions for nitric oxide. . . . .	22
4-1 MUSTANG "hot pixels". . . . .	25
5-1 "Other Atomics" synthetic spectrum . . . . .	29
5-2 Functions to simulate instrument slit response.. . . . .	32
5-3 Nitric oxide synthetic bands at 115km. . . . .	35
5-4 NO data vs. synthetic spectra at 305, 165, 105km.. . . . .	36

5-5	Comparison of data & LBH synthetic spectrum for 295, 155, 105km. . . . .	37
5-6	VK data & fit comparison for 105, 135, 165, 195km. . . . .	39
5-7	Data & fit of OI 2972Å emission at 115, 155, 295km. . . . .	40
5-8	Data & fit of OII 2470Å emissions at 135, 205, 305km. . . . .	41
5-9	Nitric oxide column density profile. . . . .	42
5-10	Nitrogen LBH intensity profile. . . . .	44
5-11	Intensity profile for N <sub>2</sub> VK(0,5) transition. .	45
5-12	Intensity profiles for OI, OII, OIII, NII. . .	46
5-13	Intensity plots for LBH & VK showing quenching of VK. . . . .	49
5-14	Data and best-fitting synthetic spectrum at 135km. . . . .	52
5-15	Data and best-fitting synthetic spectrum at 305km. . . . .	52
5-16	Unidentified feature at 2955Å. . . . .	53
5-17	Temperature profile of analysis. . . . .	54

#### **ACKNOWLEDGEMENT**

This work is incomplete without rendering proper credit to my husband, Cleon, whose computer knowledge was constantly challenged by my total ineptitude at word processing. His refusal to give up on me resulted in a far better composition than I could ever have produced alone.

## I. INTRODUCTION

The composition of the earth's atmosphere is important to many areas of science, such as weather prediction, satellite operations, and communications. Properties of the upper atmospheric region known as the ionosphere are of specific interest to the military, as they strongly influence such systems as high frequency (HF) radio communications, over-the-horizon radar (OTH), ballistic missile early warning (SDI), and the Ground Wave Emergency Network (GWEN). The electron density profile, a plot of electron density versus altitude for a given time and location, is needed for effective use of the ionosphere. Electron density is a factor that varies not only with altitude, but with time and geographical location as well. In 1986, the Joint Chiefs of Staff prioritized the determination of ionospheric electron density as fifth on a list of 43 critical geophysical parameters for inclusion in a defense satellite (The Joint Chiefs of Staff, 1986).

Currently, electron density profiles are determined using ground-based ionosonde stations. This is very effective locally, but is inherently inaccurate for global forecasting since there are only about 20 stations worldwide. A satellite-based method of forecasting the ionosphere would be

globally effective, but to place an ionosonde in orbit is unfeasible due to size and power limitations. One alternative to ionosondes is to infer electron density profiles from spectrographic measurements of the atmospheric airglow. An operational spectrograph is small and relatively low-powered; it can easily be included in a defense satellite package. The Naval Research Lab and the Naval Postgraduate School have a joint spectrographic project scheduled to be included in a satellite to be launched in 1995. The NRL project is a high resolution airglow and aurora spectrograph (HIRAAS) and the accompanying NPS effort is the middle ultraviolet spectrograph (MUSTANG). The inclusion of the duo represents a significant improvement in the global determination of electron density profiles over ground-based ionosondes.

The inference of electron densities from emission observations by the HIRAAS/MUSTANG is performed by relating measurements of natural ultraviolet emissions to the neutral species' densities. A rocket-launched HIRAAS/MUSTANG experiment was first tested in March 1990. The data from the launch is the topic of this thesis.

#### **A. THESIS OBJECTIVES**

This thesis focuses on the analysis of data obtained from the March 1990 flight. The analysis extends methods used previously on subsets of the data to the entire observed range,  $1800\text{\AA}$  to  $3400\text{\AA}$ . All known synthetic models with

emissions in this range are used in the fitting. The result of the fitting algorithm is a set of relative scale factors for the various spectra by altitude. The relative scale factors are converted into absolute terms and plotted against altitude. These absolute plots of intensity and column density can be used to infer an electron density profile (see e.g., Meier, 1991; McCoy, 1985). A secondary goal is to determine the feasibility of an approximation for the N<sub>2</sub> Second Positive spectrum given the unavailability of a synthetic spectrum. The determination of the Second Positive spectrum would allow an estimation of photoelectron flux, since it is produced by transitions from a state which can only be populated by collisions.

#### **B. THESIS OUTLINE**

The thesis is divided into six chapters. Chapter II gives general background information on the descriptions and designations of the atmosphere and existing emissions. A basic explanation of atomic and molecular spectra is also summarized in this chapter. Chapter III addresses the specific emission features in the wavelength range of interest. Chapter IV presents a summary of the experiment and the subsequent data reorganization. Chapter V gives a complete treatment of analysis of the data and results of the study. Chapter VI concludes the paper with a summary of findings and suggestions for future study. The Appendices

contain the computer programs which generated the synthetic spectra and the fitting programs, as well as plots of the final fits to the data.

## II. BACKGROUND

### A. THE ATMOSPHERE

#### 1. General Description

The Earth's atmosphere is designated by horizontal layers, and these divisions are determined by one of two primary methods. One method designates the layers based upon temperature characteristics; the other uses density to categorize the strata. The layers and a typical temperature profile are shown in Figure 2-1.

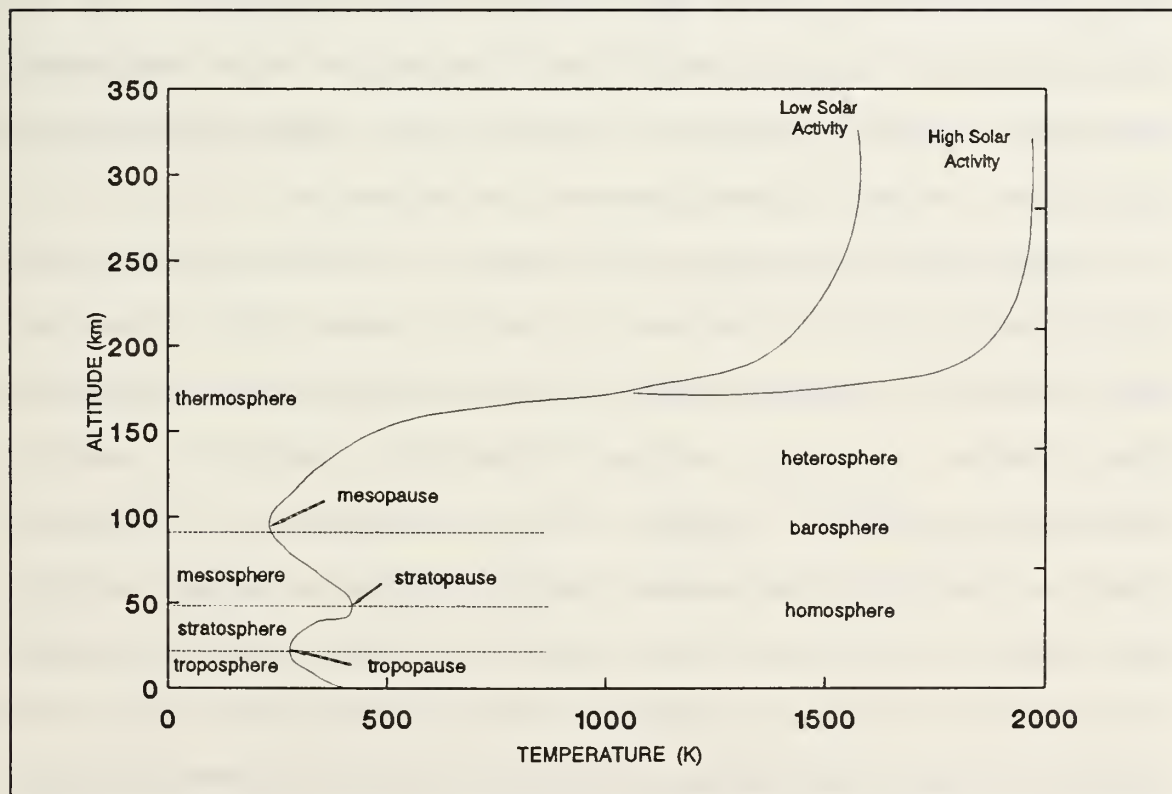


Figure 2-1 Temperature profile and corresponding atmospheric layers.

With respect to the temperature designations, the *troposphere* is the region closest to the Earth's surface where temperatures decrease with altitude, typically from about 300K at the surface to 220K at 10 km. The point at which temperature begins to rise again is called the *tropopause* and it indicates the start of the next region, the *stratosphere*. The stratosphere is a relatively warm layer due to absorption of solar radiation (primarily 2000-3000Å) by ozone. The top of the stratosphere is marked by the *stratopause*. At this point the *mesosphere* begins. The temperature again begins to decrease with altitude until a low of about 100K occurs at around 85 kilometers. This is the *mesopause*, which marks the beginning of the next layer, the *thermosphere*. In the thermosphere, temperature rises steadily with increasing altitude until reaching an equilibrium temperature between 1000K and 2000K, depending on solar activity.

Studying the atmosphere in terms of density gives rise to a different set of atmospheric layers. Under this convention, the lowest 80 kilometer layer of the atmosphere is called the *homosphere*. In this region, vertical mixing of the air currents provides a uniform relative density ratio between various species. The primary components are nitrogen, oxygen, and argon in a ratio of 78:21:0.9. The remaining 0.1 percent is primarily helium, hydrogen, and carbon dioxide. The 20 km from 80 to 100 is designated the *barosphere*, or tropopause, and it is a region of transition above which very little

vertical mixing occurs. Above the barosphere, from 100 km to around 1000 km, lies the *heterosphere*. Due to the absence of mixing in this region, the ratio of constituents varies with altitude. At extremely high altitudes of 1000 kilometers or so, the atmosphere becomes so tenuous that particle trajectories are essentially parabolic orbits. This "outer atmosphere" is called the *exosphere*.

The data analysis in this paper is concentrated in the lower heterosphere, the first 200 km of the thermosphere, where there is an obvious positive temperature gradient and the convective mixing is minimal. This region is also termed the ionosphere.

The ionosphere is so termed due to the ionization of the atmosphere by absorbed solar radiation. The actual height and thickness of the four layers(D,E,F1,F2) vary with solar activity and atmospheric composition. The D region is typically from 70 km to 90 km during the day; the E region is typically from 90 to 130 km; F1 generally exists from 130 to 160 km during the day; and F2 is above 160 km. Each of these regions is formed by ionization due to solar radiation at different wavelengths. For example, longer wavelength radiation can penetrate deeper into the atmosphere. Since solar activity changes daily, seasonally, and yearly, the intensity of sunlight at a particular wavelength and hence the depth of penetration is variable. Ionization depends on the composition of the neutral atmosphere as well. Combining

these two factors of composition and solar activity, one can see that the flux of radiation is greatest at high altitude but density is lowest and vice versa. The maximum ionization occurs somewhere between these two extremes, and the result is an overall layer known as a Chapman layer. The composition and formation of the ionosphere is quite complex and is not unique to Earth. An excellent discussion of planetary ionospheres is written by Chamberlain (1978).

## 2. Atmospheric Airglow

Airglow is the naturally occurring radiation in the Earth's atmosphere. The daytime emissions, called dayglow, are primarily driven by photoexcitation. Also contributing to dayglow are emissions which result from photoelectron impacts and, to a lesser degree, photochemical reactions. During daylight hours photochemical reactions are negligible compared to the abundance of emissions due to sunlight, but the same reactions are significant at night since there are obviously few direct solar photons to stimulate transitions. Because the data analyzed in this work were obtained during the day, photochemical reactions are not specifically addressed in this work.

The primary source of dayglow emissions is photoexcitation. Photoexcitation is the absorption of a photon as a result of inelastic collision between a photon and an atom or molecule to raise the particle to an excited state.

When the photon collides with the particle, the photon is absorbed and the particle jumps to a higher energy level. When the particle drops back to a lower energy state, it emits a photon with energy equal to the transition. This process will be further described in the next section on atomic and molecular emissions.

Although not as important to dayglow as photoexcitation, photoelectron collisions are significant because they can produce transitions which are otherwise forbidden. Observations of forbidden transitions can be used to find the photoelectron flux, since only photoelectron collisions could excite the particle to the upper state. Given the importance of whether a transition is allowed or forbidden to calculations of photoelectron flux, a knowledge of basic selection rules is desirable for the analysis of dayglow emissions.

It is also worthy to note that some of the forbidden transitions which are prominent in the low density unconfined gas of the thermosphere cannot be produced in earthbound lab experiments (Rees, 1989). Such emissions, seen in dayglow data collected by space-borne equipment, do not match any of the spectra which have been observed using lab or ground-collected data. These emissions are identified with transitions of known elements, by wavelength matching. One needs to be familiar with spectral nomenclature and selection rules in order to understand the explanations of these identifications.

## B. ATOMIC AND DIATOMIC SPECTRA

### 1. Atomic Emissions

The primary atom-photon interactions are shown in Figure 2-2. In elastic scattering, no energy transfer takes place between the photon and the atom during collision, although the photon may change directions. In inelastic scattering, the incident photon may not only change direction, but may impart energy to the atom. In this case, the atom is excited to a level  $\Delta E$  above its original state and the deflected photon will have an energy  $\Delta E$  less than its incident energy. A photon with energy  $\Delta E$  will be emitted when the atom relaxes to the initial state. Resonance scattering occurs when the incident photon is absorbed, raising the atom to an excited

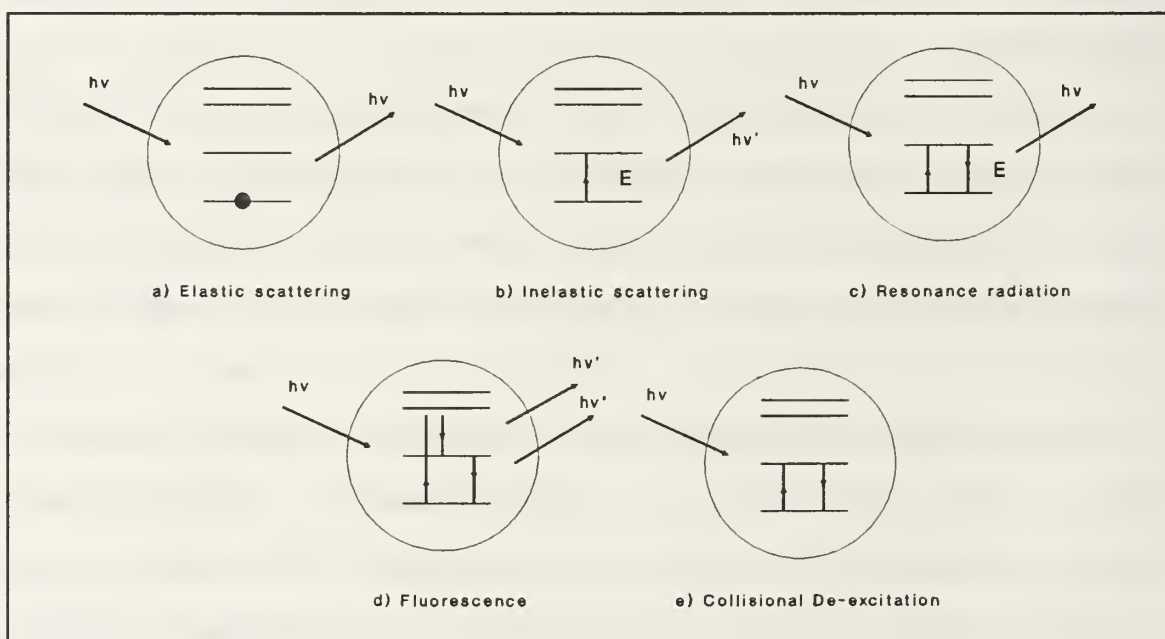


Figure 2-2 Atomic processes induced by incident radiation (Brehm & Mullin, 1989).

state. A photon with wavelength equal to the incident photon is emitted when the atom falls back to its initial state. Fluorescence is the phenomenon which occurs when the excited atom undergoes several downward transitions in returning to the initial state, giving a cascade of photons. An atom can also return to the ground state by colliding with another particle, thus returning to the ground state without emitting a photon. This is called collisional de-excitation or quenching.

Similar to photon-atom collisions, electron-atom collisions may be elastic or inelastic. In an electron-atom collision, the scattered electron loses kinetic energy, rather than actually being absorbed, when the atom is excited to a higher energy level. Photon emissions occur when the atom relaxes to the ground state.

## **2. Molecular Emissions**

Molecular spectra may occur as the result of electronic state changes, but they may also result from purely vibrational and rotational state changes. Each of these types of transitions has typical energy gaps, with electronic being on the order of 10 eV, vibrational of .1 eV, and rotational of .001 eV. These three types of transitions are illustrated in Figure 2-3. As seen in the figure, for a given electronic energy level there are many vibrational energy levels. Similarly, for a given change in vibrational energy there are

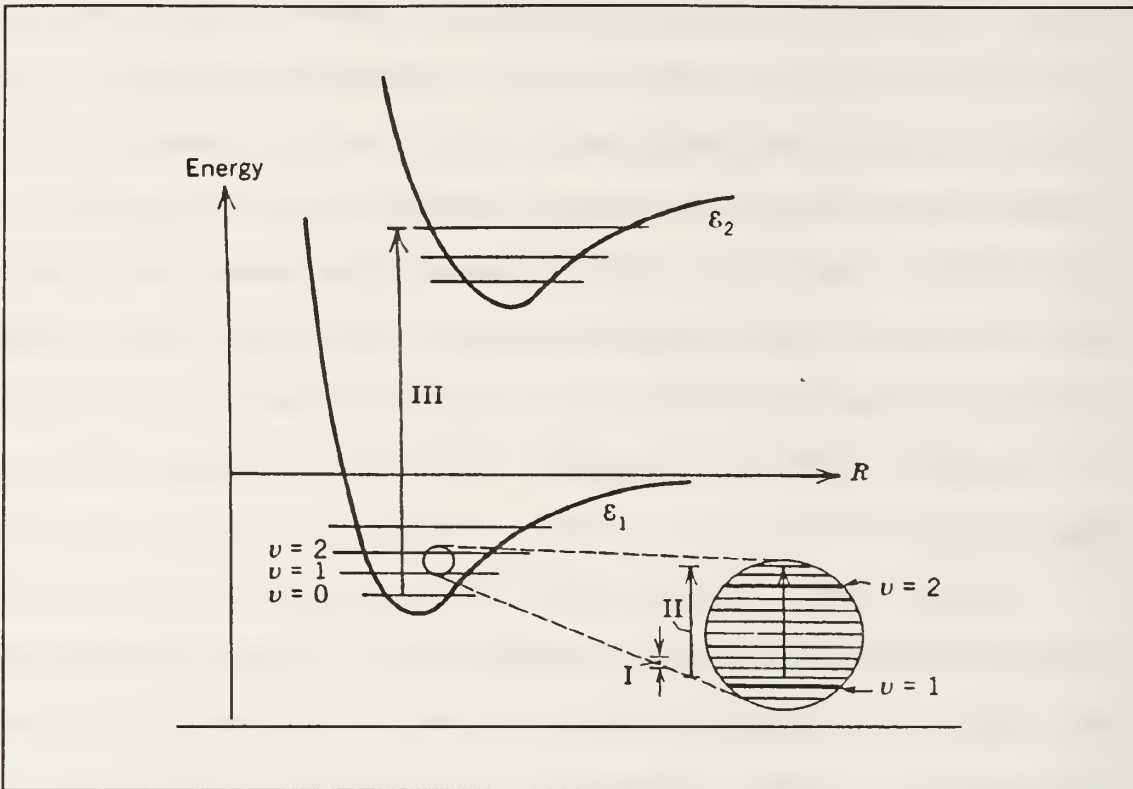


Figure 2-3 Molecular absorption transitions:  
 Transition I is pure rotational  
 Transition II, vibrational change  $\Delta\nu=1$   
 Transition III, electronic change of state  
 (Brehm & Mullin, 1989).

many possible initial and final rotational levels. As a result of the many vibrational and rotational levels which can be populated for any given electronic transition, the emission feature is composed of many closely spaced lines. Figure 2-4 shows a molecular spectrum, exhibiting a distribution of emissions. When the separation of component lines is smaller than instrument resolution, the transition may appear as a hump, as shown in Figure 2.5. This is the case for the data studied in this paper.

The study of quantum mechanics explores transitional possibilities, and develops a set of guidelines for those emissions one expects to observe. These so-called selection rules require that rotational transitions only occur for  $\Delta j = \pm 1$ , where  $j$  is the total quantum number ( $j=0, 1, 2, 3, \dots$ ). Vibrational transitions occur within the confines of selection rules  $\Delta j = \pm 1$  and  $\Delta v = \pm 1$ , where  $v$  is the vibrational quantum number ( $v=0, 1, \dots, j$ ). These rules are not strictly adhered to, as they are based on electronic dipole behavior, and some molecules exhibit quadrupole and magnetic dipole characteristics. There are also cases where, though only slightly probable, emissions occur when  $\Delta v > \pm 1$ . Electronic transition selection rules are complex, and a full treatment is given to the development and explanation of them by Green and Wyatt (1965). A summary of these is shown in Table 2-1.

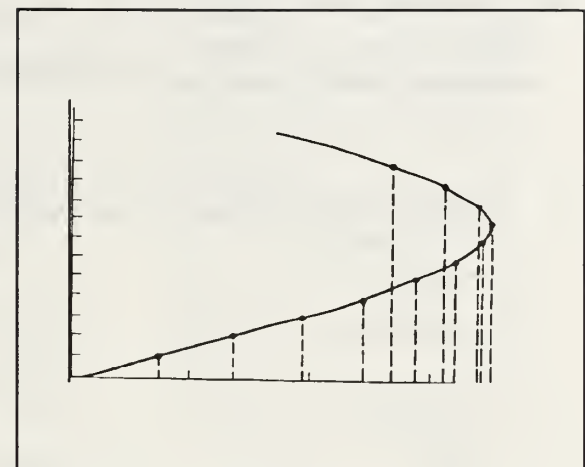


Figure 2-4 Graphical representation of molecular spectrum.

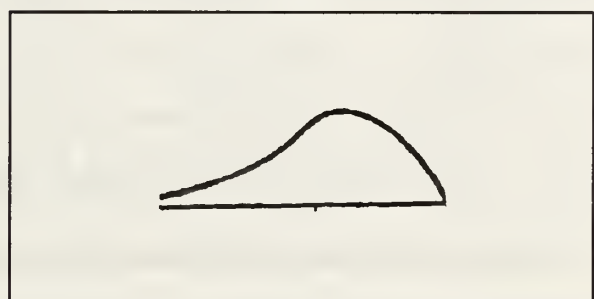


Figure 2-5 Instrument response to molecular transition.

TABLE 2-1 SUMMARY OF SELECTION RULES FOR MOLECULAR TRANSITIONS (Green & Wyatt, 1965).

	Electric Dipole (E1)	Magnetic Dipole (M1)	Electric Quadrupole (E2)
Total inversion	$+ \leftrightarrow -$	$+ \leftrightarrow + - \leftrightarrow -$	$+ \leftrightarrow + - \leftrightarrow -$
Electronic inversion	$g \leftrightarrow u$	$g \leftrightarrow g \quad u \leftrightarrow u$	$g \leftrightarrow g \quad u \leftrightarrow u$
$\Delta J$	$0, \pm 1$	$0^*, \pm 1 \quad (0 \leftrightarrow 0)$	$0, \pm 1, \pm 2 \dagger$
$\Delta S$ (a), (b)	0	0	0
$\Delta \Sigma$ (a)	0	See $\Delta \Lambda$	0
$\Delta \Lambda$ (a)	$0, \pm 1$	$\pm 1 \text{ if } \Delta \Sigma = 0;$ $0 \text{ if } \Delta \Sigma = \pm 1$	$0, \pm 1, \pm 2$
$\Delta \Omega$ (a)	$0^*, \pm 1$	$\pm 1$	$0, \pm 1, \pm 2$
$\Delta \Lambda$ (b)	$0^*, \pm 1$	$0, \pm 1$	$0, \pm 1, \pm 2$
$\Delta K$ (b)	$0 \ddagger, \pm 1$	$0, \pm 1 \ddagger$	$0, \pm 1 \ddagger, \pm 2$

\* Not  $0 - 0$ .

† Not  $0 - 0, 0 - 1, \frac{1}{2} - \frac{1}{2}$ .

‡ If  $0 - 0$  then  $\Delta J = 0$ .

Derivation of these rules is not essential to this data analysis, but an understanding of the corresponding molecular nomenclature is necessary in order to understand the discussion.

The component of total angular momentum which lies along the internuclear axis of a molecule is designated  $\Lambda$ , and is used to label molecular electronic state. Each state is given a capital Greek letter depending on its value of  $\Lambda$ . These designations are shown in Table 2-2. The spin of the molecule is designated  $\Sigma$  (which should not be confused with the  $\Sigma$  symbol for the  $\Lambda=0$  state). It can take on values from  $-S$  to  $S$ , where  $S$  is the resultant of individual electron spins in the

TABLE 2-2 MOLECULAR ELECTRONIC STATES.

molecule. *Multiplicity*, which is  $2S+1$ , is written as a left superscript on the state letter. The ground state of a diatomic molecule is labelled with a leading X. Successive excited states of the same multiplicity are labelled A,B,C, and so forth. Excited states of different multiplicity are alphabetically designated by small letters. If these labels are strictly followed, then in general the selection rules allow transitions between like-labelled states (e.g. capital ⇔ capital). As with any rule, there are exceptions. For instance,  $N_2$  diagrams have capital and small letters assigned conversely.

DESIGNATIONS OF MOLECULAR STATES	
Greek Letter	$\Lambda$ of Molecule
$\Sigma$	0
$\Pi$	$\pm 1$
$\Delta$	$\pm 2$
$\Phi$	$\pm 3$

### III. DAYGLOW EMISSION FEATURES

#### A. MOLECULAR NITROGEN

Figure 3-1 is an  $N_2$  energy level diagram including the three transition bands of interest in the 1800-3400Å range. The states are indicated by molecular notation, and the transitions are identified by name.

##### 1. Vegard-Kaplan

The Vegard-Kaplan system is so designated because Vegard discovered the system in 1932, and Kaplan determined the specific wavelengths involved a few years later. The emissions range from 1250Å to 5325Å and represent the  $A^3\Sigma_u^+ \rightarrow X^1\Sigma_g^+$  transition. In this transition, the total

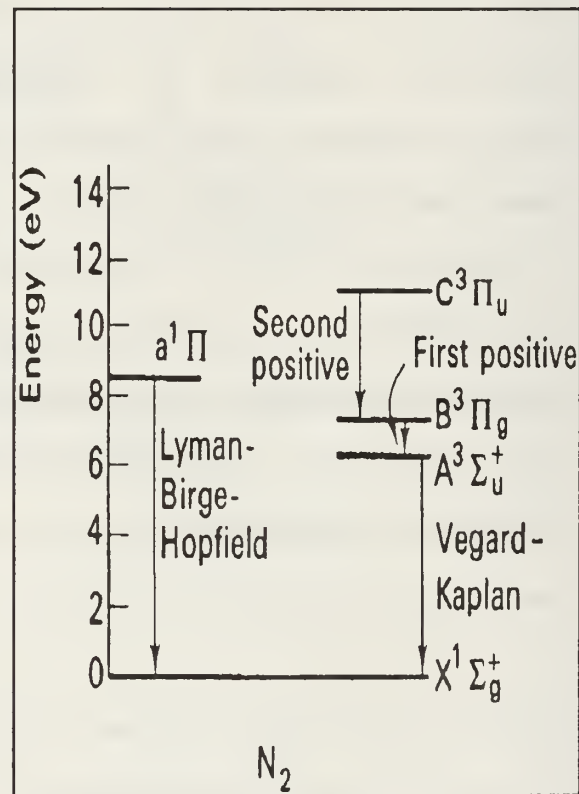


Figure 3-1  $N_2$  energy level diagram (McEwan, 1975).

transformation is  $\leftrightarrow$ , the electronic inversion is  $u \rightarrow g$ ,  $\Delta\Sigma=-1$ , and  $\Delta\Lambda=0$ . From the molecular selection rules summarized in Table 2-1, this is a forbidden transition, yet it has been

observed as an electric dipole transition. A thorough discussion of the band system is given in Meier (1990).

A-state nitrogen molecules are produced by cascading downward from the B and C states or as a result of photoelectron collisions. Because the relationship of emission bands to photoelectron flux is complicated by cascading N<sub>2</sub> molecules and quenching effects, the V-K band is not generally used to infer photoelectron flux.

## 2. Lyman-Birge-Hopfield

The Lyman-Birge-Hopfield system is the name given to the a<sup>1</sup>Π<sub>g</sub>→X<sup>1</sup>Σ<sub>g</sub><sup>+</sup> transition of N<sub>2</sub>. The emission bands arising from this transition extend from 1160Å to 3020Å and are due to both electric quadrupole and magnetic dipole transitions. Unlike the V-K system, the upper state of the LBH system can only be populated by photoelectron collision excitation. This system can therefore be used to directly infer the photoelectron flux. The LBH bands found in the data were particularly significant in the wavelength region from 1800Å to 2400Å. An intensive investigation of the LBH system as it pertains to the MUSTANG data was performed by Mack (1991).

## 3. Second Positive

The Nitrogen Second Positive system (C<sup>3</sup>Π<sub>u</sub>→B<sup>2</sup>Π<sub>g</sub>) extends from 2680Å to 5460Å. It is a particularly important transition because the upper level is not directly populated through photoexcitation, but only by collision. Thus a

measurement of the Second Positive intensity profile can be used to infer the photoelectron flux. This result can be compared with those obtained from the LBH bands. Unfortunately, there is no synthetic spectrum model developed for the Second Positive. It was originally intended to determine the  $N_2$  Second Positive spectrum by subtracting known contributions from the data and assuming the remaining data was Second Positive. This means of estimating a spectrum was found to be impractical due to inaccuracies in the data caused by data drops.

#### **B. ATOMIC NITROGEN**

Figure 3-2 shows the transitions which have been observed in the airglow due to  $N^+$ . Two transitions are in the wavelength range of this study. The 3070Å emission falls in the same range of wavelengths as the  $N_2$  Second Positive spectrum, so it could not be definitively seen in the data. The emission shown at 2143Å was considered in the synthetic fit to the MUSTANG data. It is actually a doublet at 2143.55Å and 2139.68Å with a ratio of 100:58, respectively. This intensity ratio was determined by Bucsela and Sharp (1989) from dayglow observation. Theoretical and laboratory estimates of relative line strength range from 100:60 to 100:23. Since the data source for the Bucsela and Sharp ratio was similar to the experimental data being analyzed, the 100:58 relation was used in the synthetic model.

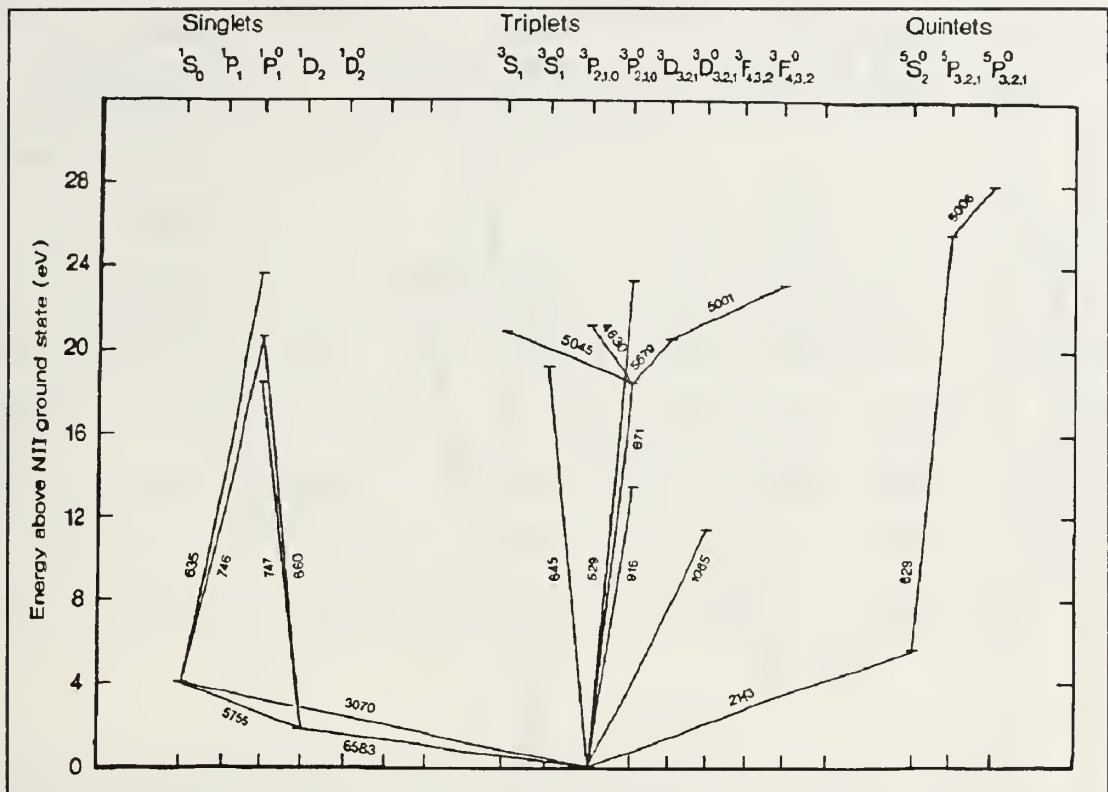


Figure 3-2 Energy level diagram for N<sup>+</sup> (Rees, 1989).

### c. ATOMIC OXYGEN

Figures 3-3 and 3-4 diagram the atomic oxygen emissions which have been viewed in the airglow. Two of these emissions fall in the wavelength range explored by this analysis.

The neutral oxygen atom emits a photon with wavelength 2972Å when it falls from the <sup>1</sup>S state to the <sup>2</sup>P ground state. This transition is depicted in Figure 3-3. Singly ionized oxygen, shown in Figure 3-4, produces a line at 2470Å when it falls from the <sup>2</sup>P state to the <sup>1</sup>S ground state.

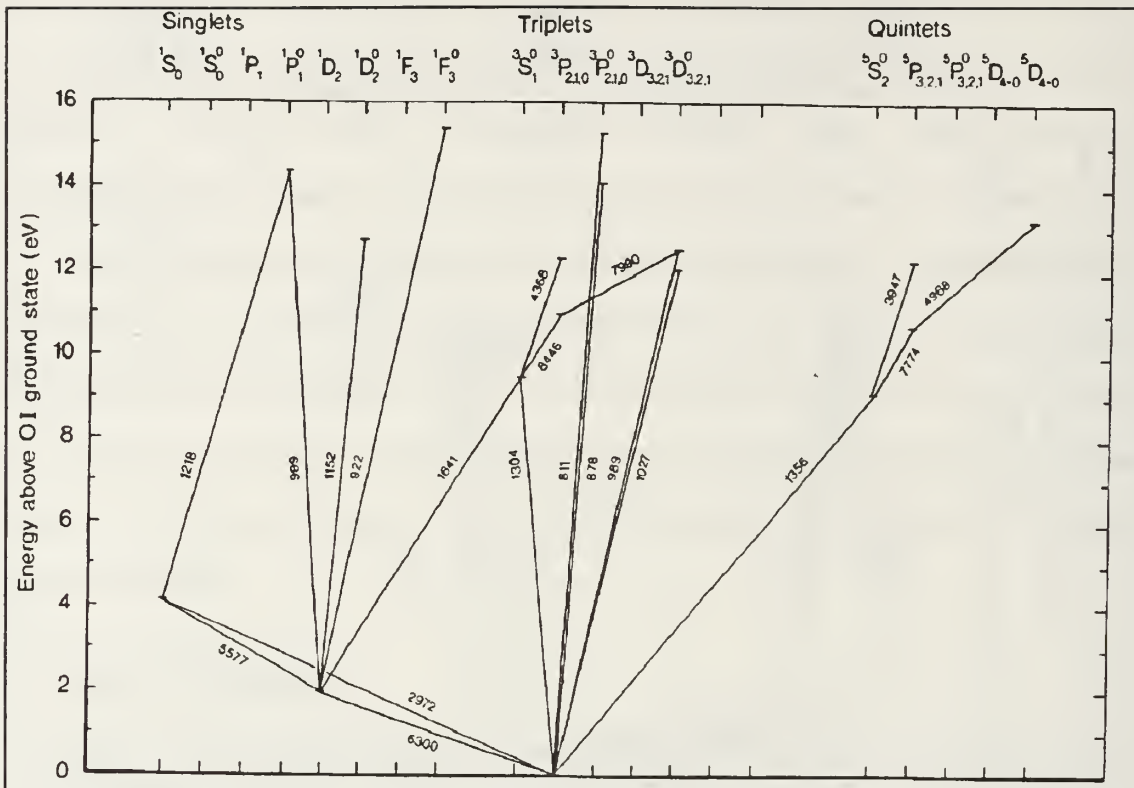


Figure 3-3 Energy level diagram for neutral atomic oxygen (Rees, 1989).

#### D. NITRIC OXIDE

Nitric oxide emissions, shown in Figure 3-5, dominate much of the dayglow data. There are four primary bands in the range 1800Å - 3400Å,  $\gamma$ ,  $\delta$ ,  $\beta$ , and  $\epsilon$ . The  $\beta$  bands are several orders of magnitude less intense than the other emissions, so they have been neglected.

##### 1. Delta

The  $C^2\Pi \rightarrow X^2\Pi$  transition band system, designated  $\delta$ , ranges from 1621Å to 4288Å (Barth, 1965). Using standard notation, the upper electronic state's vibrational level is designated  $v'$ , and the lower state vibrational level,  $v''$ . The  $\delta$  transition band includes vibrational levels corresponding to

$v'=0,1,2,3,4$  and  $v''=0,1,\dots,23$ . Nitric oxide will dissociate at  $v'>0$  for  $C^2\Pi$ , so  $v'$  is limited to  $v'=0$  and  $v''\leq 14$  in creating the synthetic  $\delta$  spectrum.

## 2. Gamma

The  $\gamma$  bands of nitric oxide extend from 1873Å to 6126Å. The emissions arise from the  $A^2\Sigma^+\rightarrow X^2\Pi$  transition, and the ground state has  $v''=0,\dots,23$  as previously stated. The dissociation energy for nitric oxide is lower than the energy of the  $v'=4$  level in the  $A$  state, so only transitions arising from  $v'=0,1,2,3$  contribute to the synthetic  $\gamma$  spectrum.

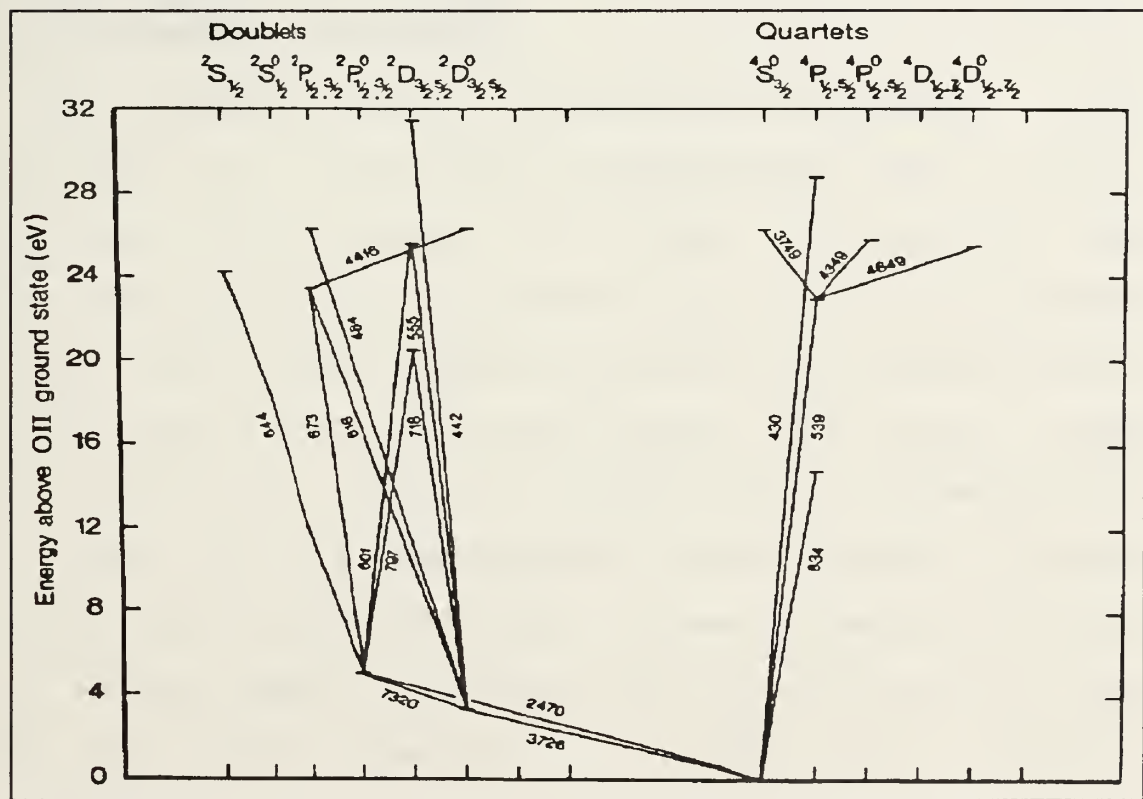


Figure 3-4 Energy level diagram for  $O^+$  (Rees, 1989).

### 3. Epsilon

The nitric oxide  $\epsilon$  system is the result of molecules transitioning from  $D^2\Sigma^+ \rightarrow X^2\Pi$ . The wavelengths of emissions range from  $1800\text{\AA}$  to  $2385\text{\AA}$ . D-state molecules populate vibrational levels  $v'=0, 1, 2$ .

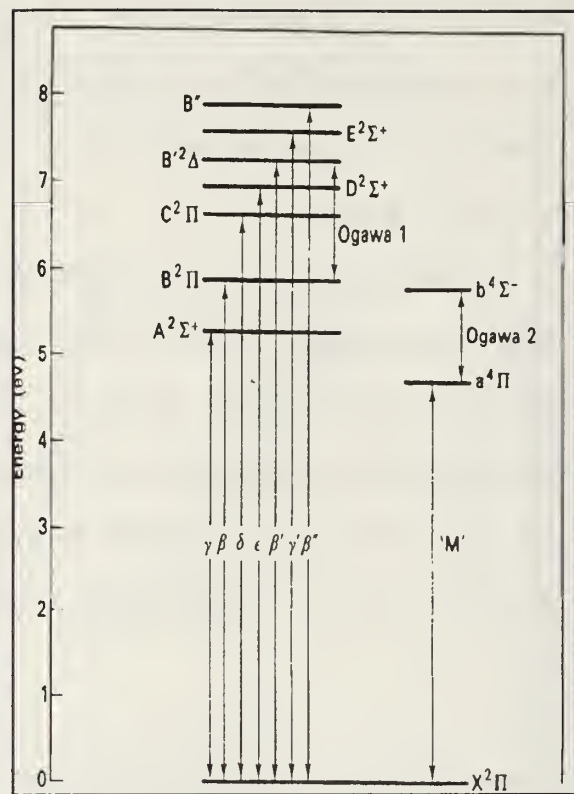


Figure 3-5 Transitions for nitric oxide (McEwan, 1975).

## IV. THE EXPERIMENT

### A. Introduction

The middle ultraviolet spectra analyzed in this thesis were obtained from the NPS MUSTANG spectrograph flown on a NASA sounding rocket launched March 30, 1990, from White Sands Missile Range, New Mexico. The spectrograph was launched on a Terrier boosted Black Brant, which carried the payload to an apogee altitude of 320 km. The spectrograph was looking in the anti-solar direction with an observation zenith angle of 90°. From 320 to 180 km on the downleg no useful data were obtained due to the payload attitude.

### B. Instrument Description

The MUSTANG (Middle Ultraviolet Spectrograph) is a modified 1/8 m Ebert-Fastie spectrograph with a 1/8 m telescope. The entrance slit is 5mm x 140  $\mu$ m and a 10 $\text{\AA}$  wavelength resolution is provided by a 1200 g/mm grating ruling. The detector assembly consists of an ultraviolet-to-visible image intensifier using a quartz input window, a CsTe photocathode, and a fiber optic output window. The detector is an array of 512 photodiodes giving voltage outputs proportional to intensity using a 50 msec integration period. This voltage output is fed serially to an A/D converter and then to rocket telemetry via a FIFO shift register.

Calibration/sensitivity curves were obtained using a deuterium lamp for the wavelength range 1800-2800 Å and a FEL tungsten lamp for 2400-3400 Å. A more precise calibration of the 1800-2000 Å range, which is affected by O<sub>2</sub> absorption, was performed in a vacuum chamber (Mack, 1991).

### C. Data Collection

Over 8000 spectra were collected by MUSTANG. These spectra were then averaged into 25 altitude bins, disregarding spectra which were contaminated by the instrument's electronics. Each of the 25 resultant spectra covers a 10 km layer and is identified by its central altitude.

Because of a timing difference between clocking and reading functions, only 480 of the 512 photodiodes' responses were recorded. It was first determined that every seventeenth word was dropped, and these blanks were inserted as averages of the two adjoining data values (Clayton, 1990). This still did not produce a suitable wavelength match with known emissions, so a mathematical spline was performed on the data in order to match a uniform wavelength grid (Mack, 1991). Although this provided an excellent fit to assumed models, it had no physical justification. Laboratory testing was performed by Quint (1991) to determine which values were lost in the timing error. His results accounted for the 32 expected data dropouts, but two additional dropouts remained unexplained. These two shifts were inserted at positions

which were consistent with the findings of Quint and also provided the best agreement with three previous studies. It should be pointed out that this was not confirmed with the electronics. The corrected spectra are delineated in Appendix A, noting each dropped pixel. At these spots an average of the adjacent values was inserted into the original 480 data points, to obtain an array of 512 values.

The adjusted spectra were then divided by instrument sensitivity. The first six values were set to zero, since the uncertainty in sensitivity of the instrument at the endpoint is extremely large. It was found that one further correction had to be made to the data. In both pre-launch and post-launch high voltage dark count spectra, two voltage spikes existed. These hot spots occurred at points corresponding to  $2850\text{\AA}$  and  $3373\text{\AA}$ , as shown in Figure 4-1. These dark count hot spots were converted to  $\text{R}/\text{\AA}$  and then subtracted from the averaged spectra before analysis.

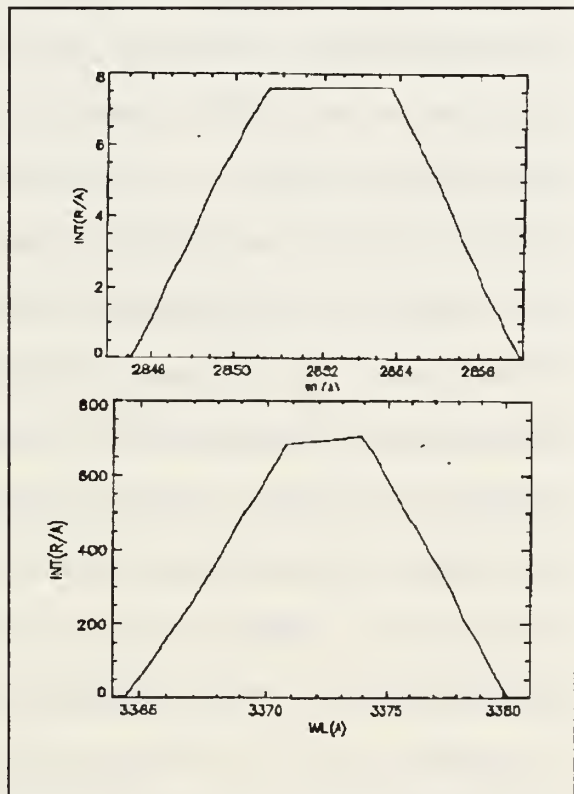


Figure 4-1 MUSTANG "hot pixels" plotted as intensity (in  $\text{R}/\text{\AA}$ ) versus wavelength.

## V. DATA ANALYSIS & RESULTS

### A. TECHNIQUE

#### 1. Introduction

##### a. Fitting Method

Synthetic spectra were fit to the data using a least squares fit process (hereafter referred to as GRIDLS). It was developed by Bevington (1969) and applied in limited portions of the wavelength range by Clayton (1990), Andersen (1990), and Mack (1991). This method is an extension of a basic least-squares regression, minimizing error between the fit and the data as measured by the variable  $\chi^2$  with weighting for confidence in the data. The program fits a linear combination of synthetic spectra to the data, with each synthetic spectrum having an independent coefficient, or scale factor. The program is adaptable for any number of desired parameters. The final analysis used nine parameters, which will be discussed in the Results section. The fitting program (GRIDLS) and its accompanying subprograms are in Appendix B.

The output of the program is the scale factors for the linear combination of models. What each models' scale factors represent depends on the normalization dimensions used in creating the corresponding synthesized spectrum. The model spectra do not all have the same dimensional units. In the

case of atomic spectra, the scale factors are absolute intensity measured in Rayleighs. For the VK and LBH bands the scale factors are a measure of relative intensity and must be converted to absolute values to obtain an intensity profile. The Nitric Oxide scale factors are column density, in molecules per square centimeter.

### *b. Synthetic Spectra*

Previous analysis of the March 1990 MUSTANG data includes: an analysis of NO at 2000-2500Å (Clayton, 1990); analysis of OI 2972Å and OII 2470Å emissions (Andersen, 1990); and a study of LBH and NO at 1800-2100Å (Mack, 1991). An analysis combining all the contributing spectra and spanning the full MUSTANG wavelength range had not been performed, but previous work provided many of the computer programs as well as "initial guesses" for the fitting routine. Other models and programs arose as a result of the fitting analysis. Computer models written by Cleary (1986) were used for the generation of Nitrogen Lyman-Birge-Hopfield and Nitric Oxide  $\gamma$ ,  $\delta$ , and  $\epsilon$  band emissions. The Nitrogen Vegard-Kaplan model was written by Siskind and Barth (1987).

The synthetic spectra for individual atomic emissions were created by convolving appropriate impulse functions with the slit function of the instrument. As already discussed, in the case of the N<sup>+</sup> 2143Å doublet a pair of impulse functions in the ratio 100:58 was used. The previously identified atomic

contributions to the MUSTANG spectrum include OI 2972Å, OII 2470Å, and NII 2143Å.

One other atomic spectrum, a prominent line emission at 2853Å at higher altitudes, has been included in the fitting routine as a result of observation. Elements with emissions at that wavelength include nickel, copper, manganese, iron, sodium, cobalt, and oxygen. Of these, oxygen is the most abundant in the atmosphere where the emission is seen, above 200km. Doubly ionized oxygen has an emission at 2853Å that although not previously identified in dayglow data, is classified "predicted" by Kelly (1979).

A collection of atomic emissions observed during the fitting process, but not verified by other literature, was classified as a separate spectrum. As discussed in Chapter II, an atomic emission is a single line vice the "hump" of a molecular transition. Even after convolution with the instrument slit function, the form of an atomic emission feature is distinctive from a molecular band. There were several areas in the data which matched the form at a sufficient number of altitudes as to suggest an atomic emission. These wavelengths were then checked against tables for possible origins and included in the synthetic spectrum if a likely emission existed, based on atmospheric composition and transition probability. The resultant synthetic spectrum (designated "Other Atomics") is shown in Figure 5-1. The program used to create this spectrum, along with possible

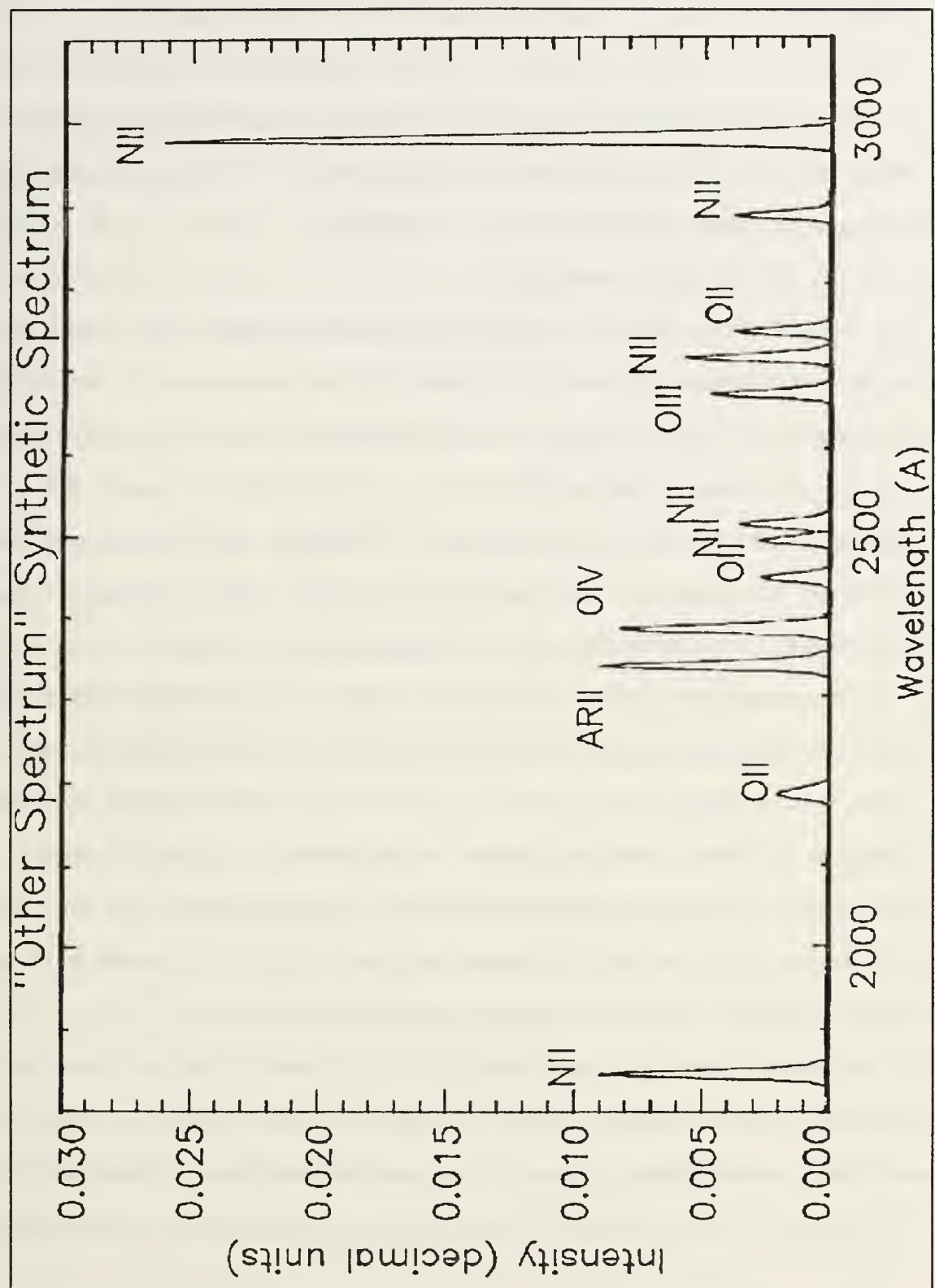


Figure 5-1 "Other Atomics" synthetic spectrum

identifications for each emission, is in Appendix B. None of these emissions occurred with sufficient intensity and regularity to merit being considered as a separate parameter. They are included only to facilitate the fitting procedure.

## 2. General Programming Technique

### a. Fitting Routine

The GRIDLS program which successfully handled 72 points of data with three parameters (Mack, 1991) was overloaded by the inclusion of all 512 points of wavelength and nine parameters (i.e., the scale factors for V-K, OI, OII, OIII, LBH, NO, NII, Other Atomics, and Background). Several modifications were made to improve the data handling capabilities of the program, and other characteristics were accepted as limitations.

Previously, the program would allow negative scale factors, effectively allowing subtraction of a spectrum. It also would enter an infinite loop if the scale factor equalled zero. These problems were eliminated in the program by requiring that zero be the minimum scale factor allowed, and by performing a simple global minimum check to prevent a zero scale factor from causing an infinite loop.

The program had great difficulty converging to a value if the "initial guess" for the scale factor was far from the minimum deviation value. This problem was not corrected, but a test-plotting program was written to allow one to visually

match the synthetic curve to the data so as to obtain reasonable first guess values.

The standard function of instrument response was an 11-element symmetric slit function (Clayton, 1990; Andersen, 1990; Mack, 1991). When convolved with a 512-element synthetic spectrum, this slit function would sufficiently represent the instrument's response to the modeled molecular spectrum. However, in the case of an atomic emission, which occurs as a line at a particular wavelength vice a band of lines, the slit function could shift the apparent peak as much as 1.7Å. The symmetric function centered the response on the applied pixel, a 3.133Å range, instead of at the particular desired wavelength. A new set of five slit functions, shown in Figure 5-2, was developed to correctly model atomic emissions, allowing for emissions which are not centered on a pixel.

A major limitation of the previous version of the GRIDLS fitting routine was that there existed no absolute measurement of "goodness of fit." Although the program minimized a  $\chi^2$  value, the values were not weighted and thus could not be compared between runs or altitudes to determine goodness of fit as parameters were tweaked. Creating a proper weighting for the data evaluation so that these comparisons could be made was a major task.

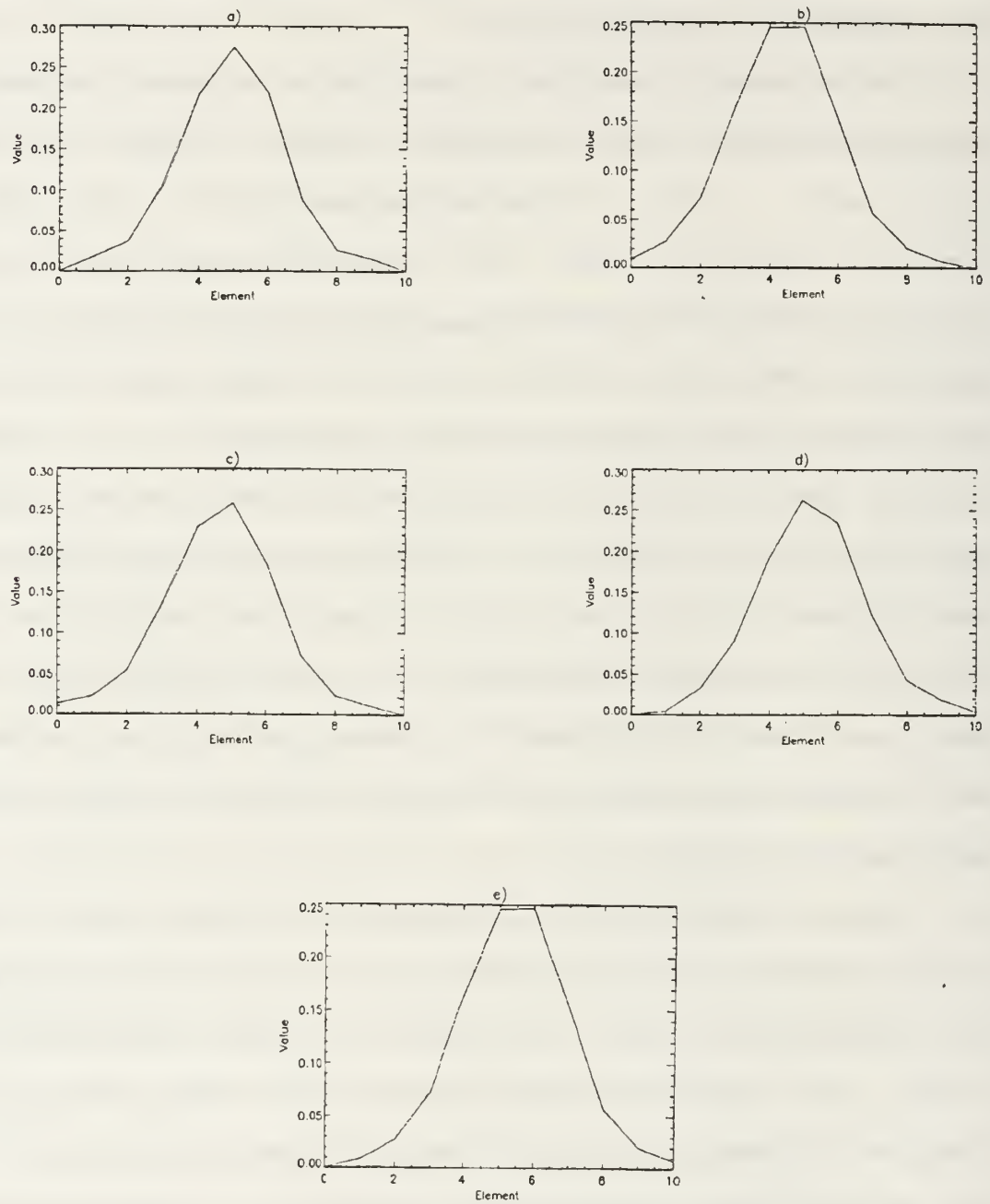


Figure 5-2 Functions to simulate instrument slit response. Delta function is placed: a)centered b) $\frac{1}{2}$  pixel right of center c) $\frac{1}{4}$  pixel right d) $\frac{1}{4}$  pixel left e) $\frac{1}{2}$  pixel left.

### *b. Weighting Program*

The GRIDLS program allows for statistical weighting of the data, instrumental weighting, or no weighting. Instrumental weighting was chosen for its advantage of stressing datapoints which have small uncertainties. The first step in producing instrumental data weights was to determine the standard deviations of the mean (sdom) for every data point in each altitude bin. A second source of instrumental uncertainty was instrument response. It was determined that the detector had a linear response for most output values, but reached saturation above 900 decimal units (divided by instrument sensitivity to get  $R/\text{\AA}$ ), so data points in the saturation range were given weights based on the sdom being equal to the data value itself. The exception to this was when the data value was so small as to give a large weight to the point (since weight  $\propto \text{sdom}^{-1}$ ), in which case the weight was assigned 1/10 the largest weight factor for that altitude (Cleary, private communication, 1991). Additionally, the data points which were merely averages of adjoining values due to lost data points were given weights based on the sdom being equal to the data value. Since the sdom and saturation points are different for each altitude, a set of values for weighting of the 512 data points was stored for each data spectrum.

The data pixels corresponding to nitrogen Second Positive emissions had no synthetic input being matched to them. The pixel corresponding to each wavelength of these emissions as

determined by Barth (1965), plus a buffer of  $\pm 1$  pixel to account for instrument response, were given essentially zero weight. The final weight program, designated WEIGHTS2, is Appendix C.

## B. RESULTS

### 1. Comparison of Data and Fit

#### a. Nitric Oxide Bands

In the plots of the fits, nitric oxide is viewed as one entity rather than plotting the  $\gamma$ ,  $\delta$ , and  $\epsilon$  bands separately. This is for ease in reading the plots. Figure 5-3 shows the components of the nitric oxide synthetic spectrum for 115km. The bands are not equal contributors, as the  $\delta$  band has a 25% fluorescent efficiency factor.

Figure 5-4 is a plot of the observed data and its corresponding fit. The data is indicated by the solid line, and the fit obtained from the computer procedure by a dotted line. The dashed line is that portion of the synthetic fit which is nitric oxide. From the plots in Figure 5-4, one can see the importance of nitric oxide with decreasing altitude. In the 105km plot, nitric oxide accounts for almost all of the dayglow from 1800-2600Å, but at 295km the NO is less prevalent.

#### b. Nitrogen Bands

Figure 5-5 shows an intensity plot (in R/Å) of the LBH contribution to the fit, along with the observed spectrum, for

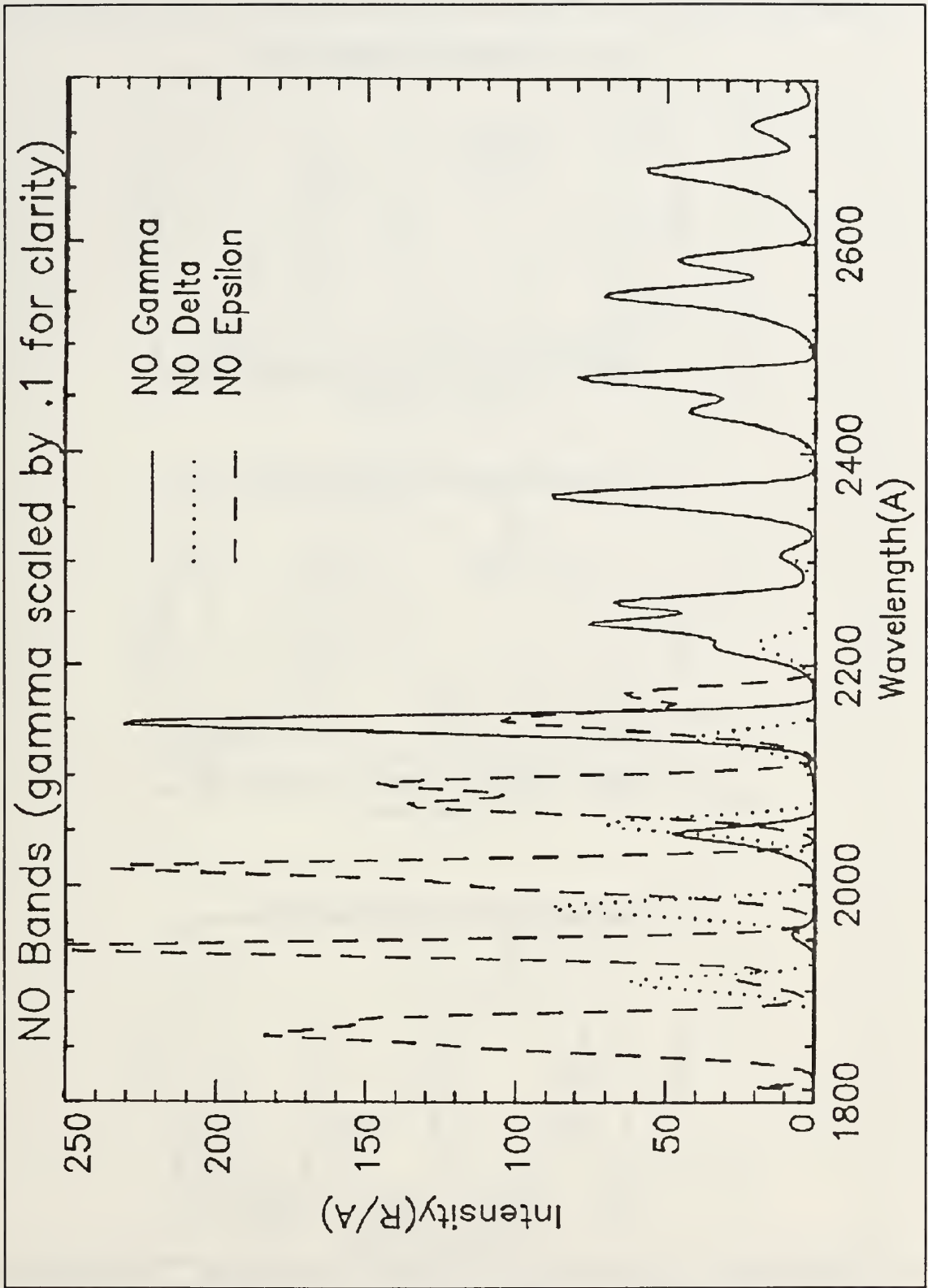


Figure 5-3 Nitric oxide synthetic bands at 115km.

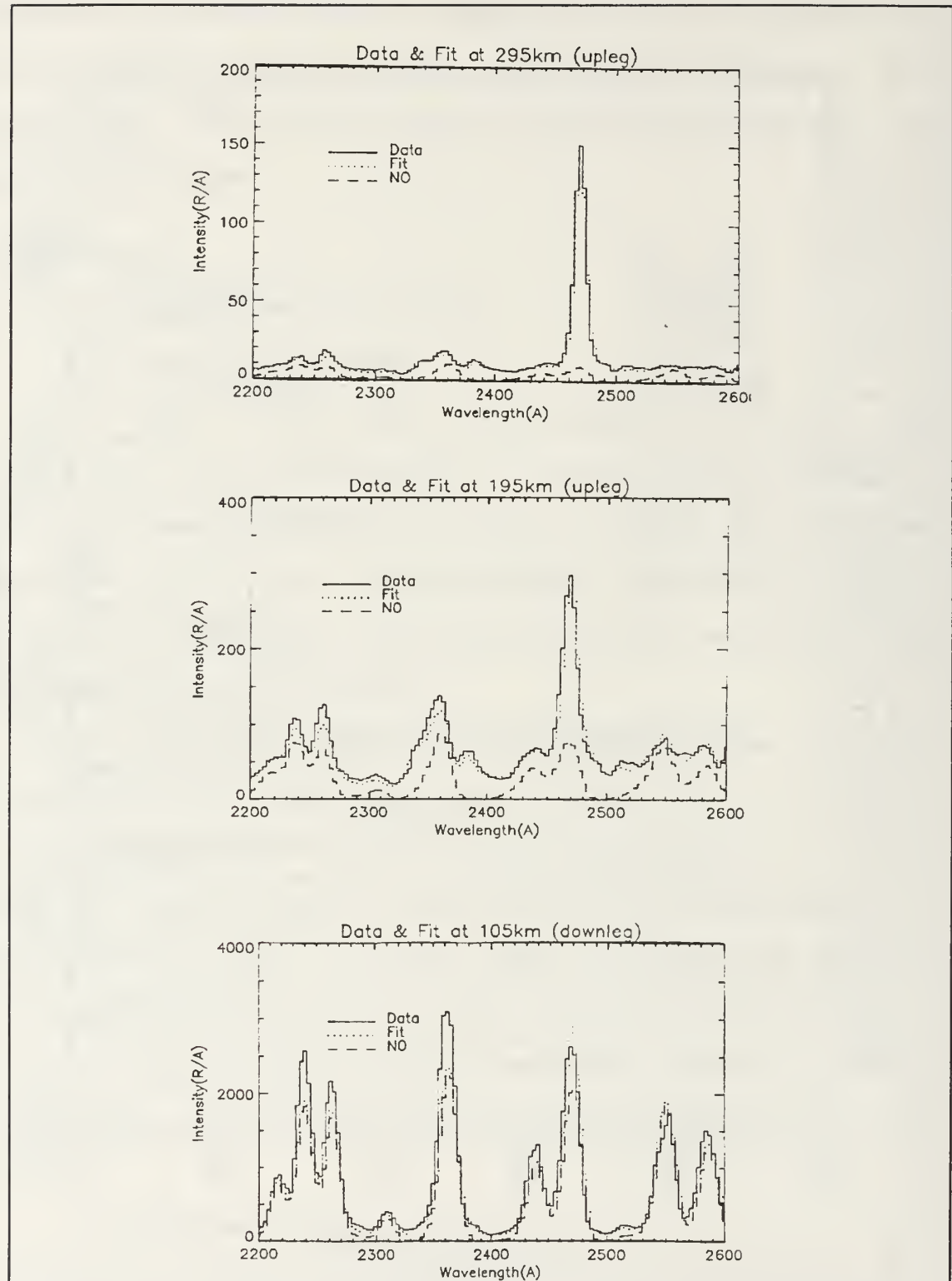


Figure 5-4 NO data vs synthetic spectra at 305, 165, 105 km. The bright emission at 2470 Å is an O<sup>+</sup> line.

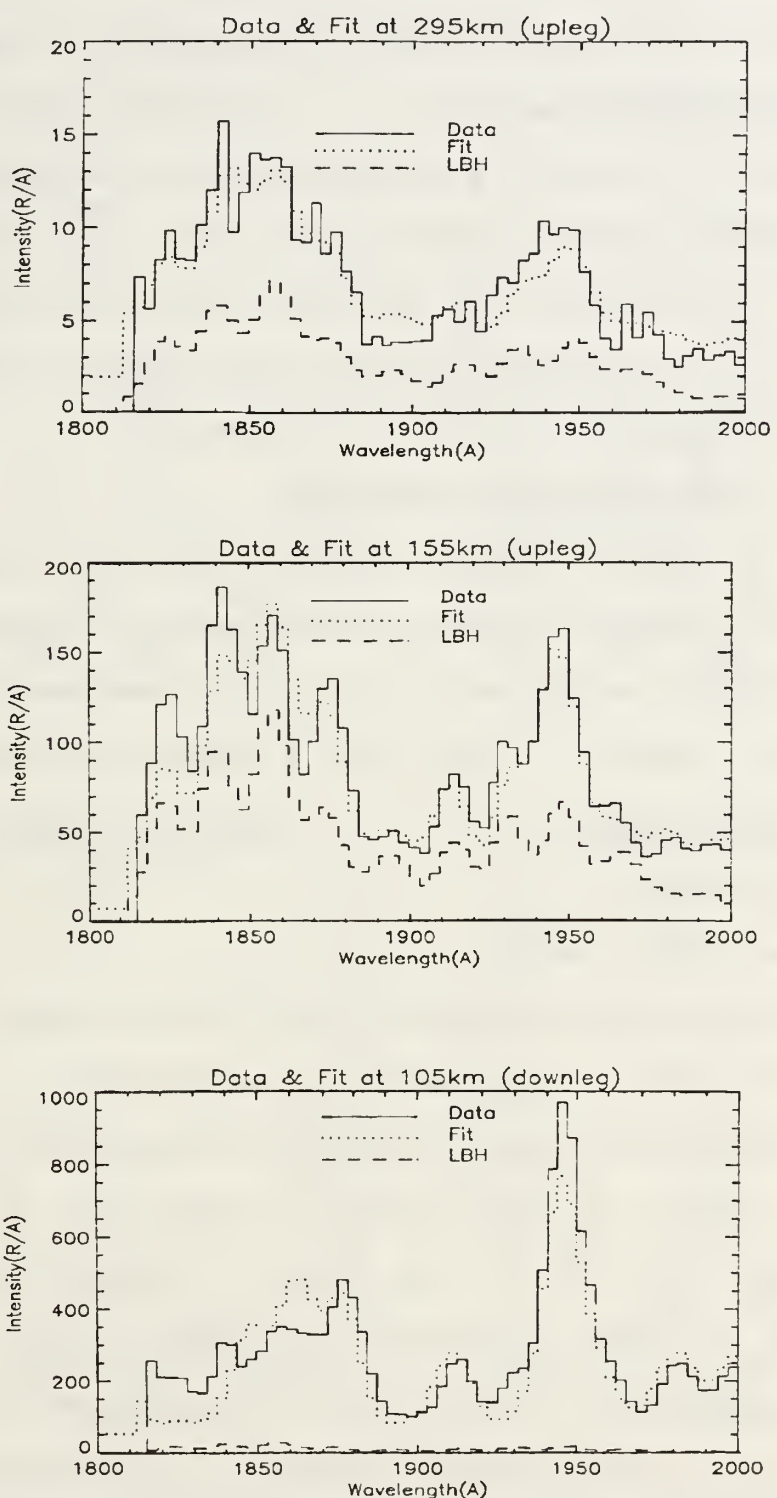


Figure 5-5 Comparison of data & LBH synthetic spectrum for 295, 155, 105km.

three different altitudes. From these plots, one can see that the Lyman-Birge-Hopfield band of  $N_2$  emissions dominates the wavelength range 1800-2000Å.

Figure 5-6 shows a similar altitude progression for the Vegard-Kaplan system, emphasizing the (0,5) transition at 2605Å. VK emissions are prominent from 2200-3300Å, and in general all the emission features show the same characteristic growth as exhibited by the (0,5) transition.

### *c. Oxygen Atomic Emissions*

The OI 2972Å emission as fit to the data at three different altitudes is shown in Figure 5-7. The poor fit of this feature is addressed in the Discussion section. The OII 2470Å line, shown in Figure 5-8, becomes more important with increasing altitude.

## **2. Profiles**

### *a. Nitric Oxide*

The column density profile for Nitric Oxide is shown in Figure 5-9, with the corresponding values given in Table 5-1. Values obtained from upleg data are indicated with squares and downleg values by triangles. There is a systematic uncertainty of 15%. The values obtained show general agreement in both magnitude and slope with the column densities obtained by Mack (1991), Clayton (1990) and Andersen (1990), all of whom analyzed subsets of the MUSTANG data. The maximum and minimum values best agreed with those obtained by

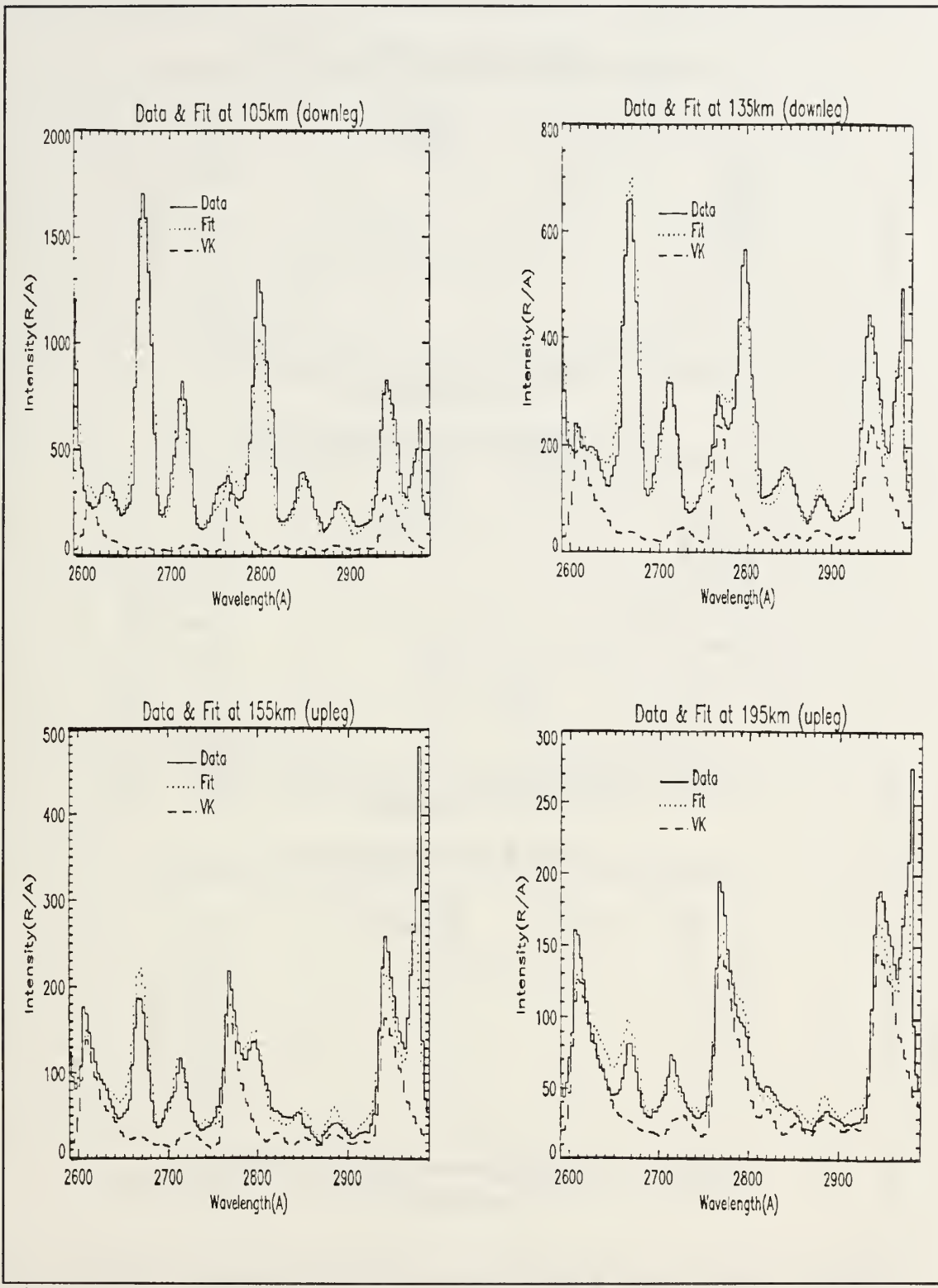


Figure 5-6 VK data & fit comparison for 105, 135, 165, 195km.

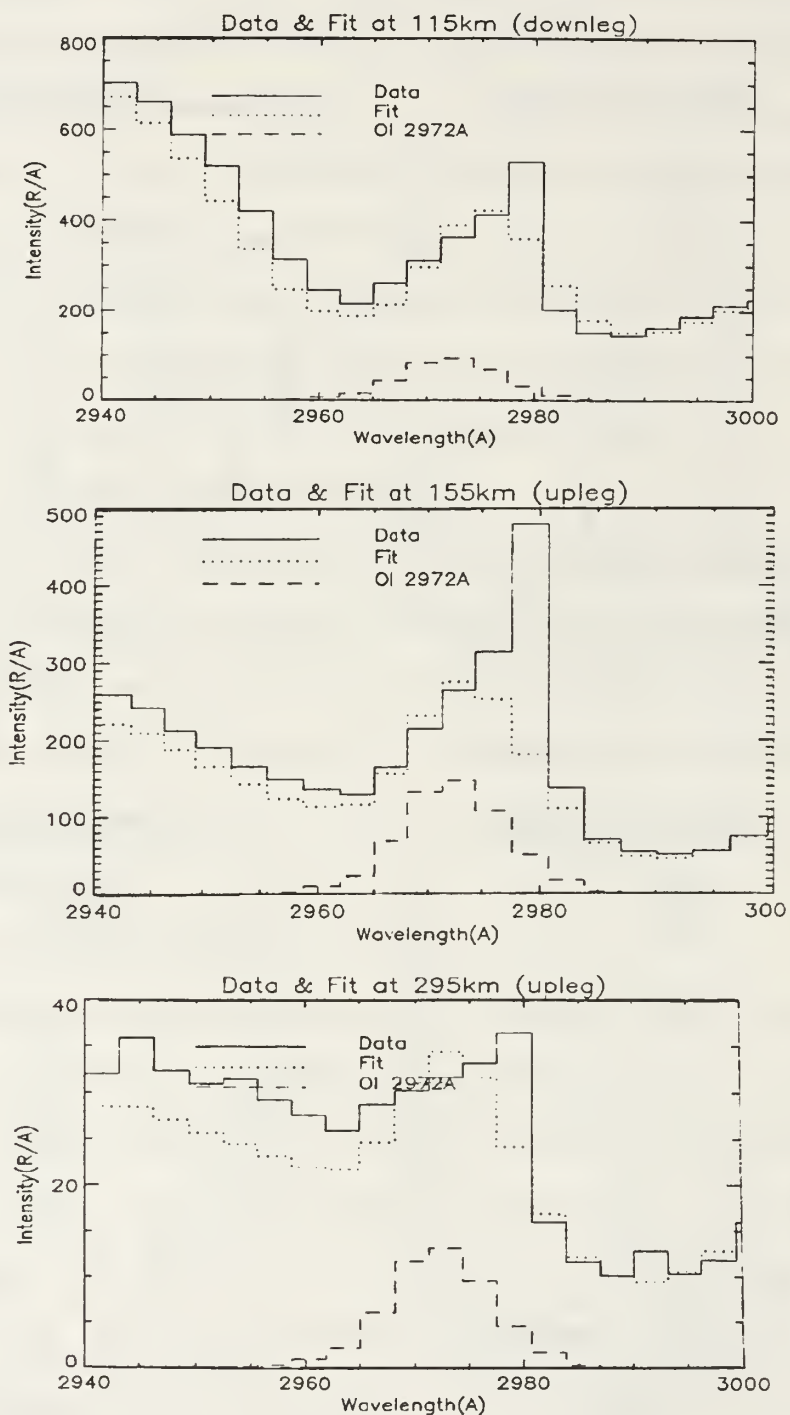


Figure 5-7 Data & fit of OI 2972 Å emission at 115, 155, 295 km.

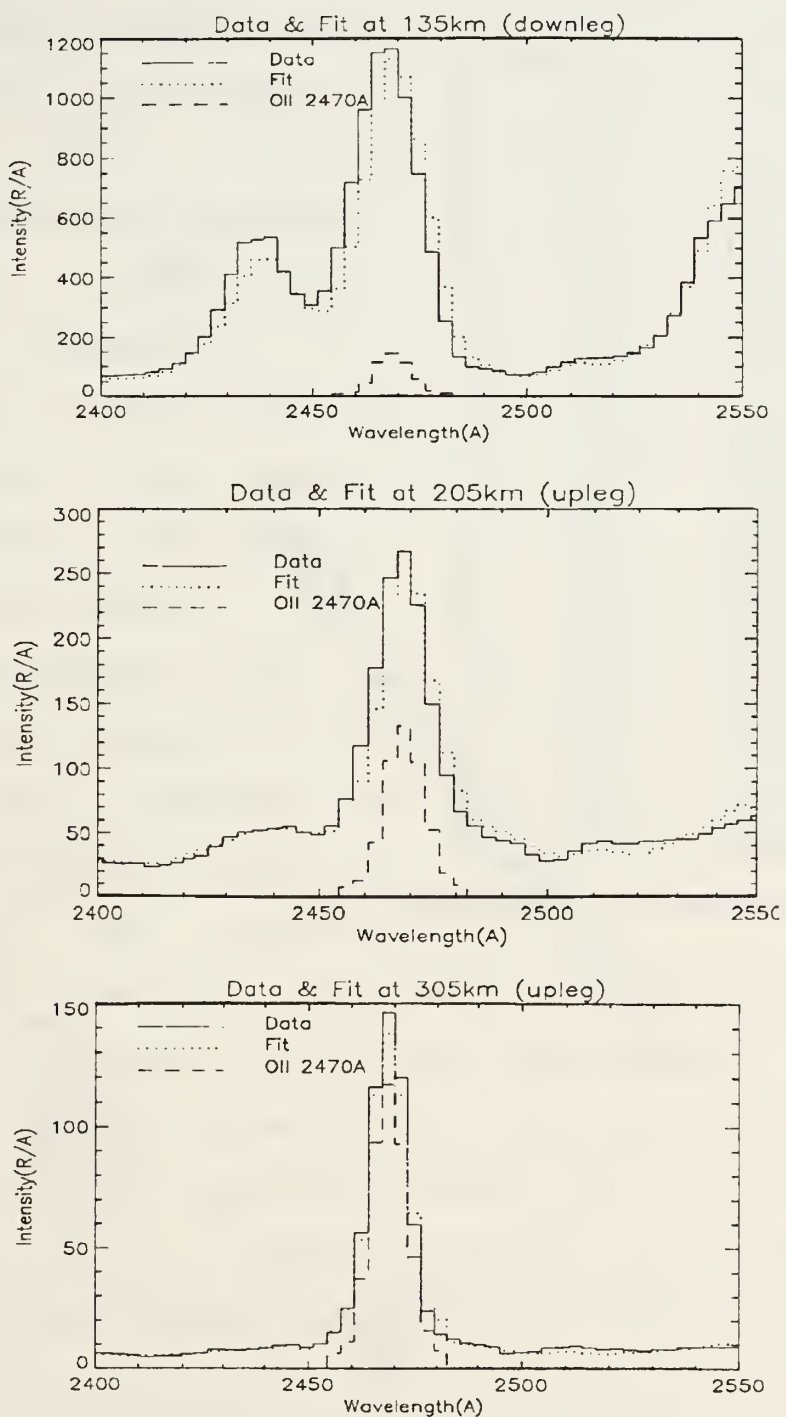


Figure 5-8 Data & fit of OII 2470 Å emission at 135, 205, 305km.

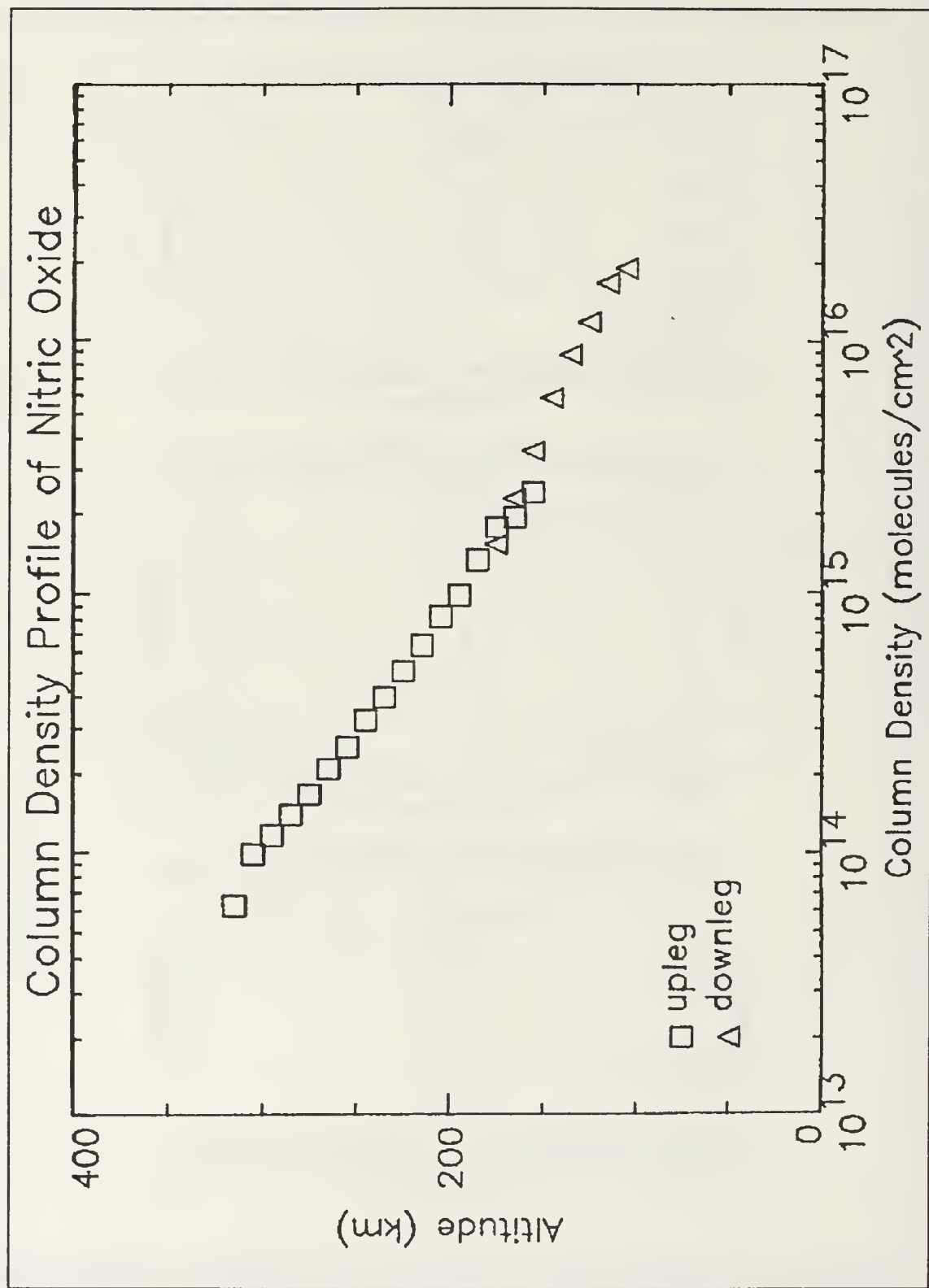


Figure 5-9 Nitric oxide column density profile.

TABLE 5-1 NO COLUMN DENSITIES

Mack (1991), with the intermediate values best matching the fit obtained by Clayton (1990). The significance of this agreement is that a full spectrum fitting procedure (i.e., including all species and all wavelengths) is not required to accurately determine the Nitric Oxide density.

*b. Nitrogen Bands*

The scale factors for LBH bands were converted to absolute intensity using the algorithm and computer programs in Appendix D. The resultant LBH intensity profile is shown in Figure 5-10, and is a measurement of total LBH intensity as it includes all  $a \rightarrow X$  transitions. The intensity profile for VK can only be calculated for a particular  $v' \rightarrow v''$  band, and Figure 5-11 shows this calculation for one of the more prominent systems, the (0,5).

ALTITUDE(km *)	COLUMN DENSITY (molecules/cm <sup>2</sup> )
125*	1.908e+16
115*	1.681e+16
125*	1.186e+16
115*	8.785e+15
145*	5.883e+15
155	2.427e+15
155*	3.596e+15
165	1.938e+15
145*	2.299e+15
185	1.779e+15
125*	1.520e+15
185	1.332e+15
165	9.850e+14
205	8.222e+14
215	6.321e+14
205	5.062e+14
235	4.003e+14
205	3.248e+14
255	2.554e+14
265	2.103e+14
275	1.665e+14
285	1.388e+14
295	1.158e+14
305	9.824e+13
315	6.240e+13

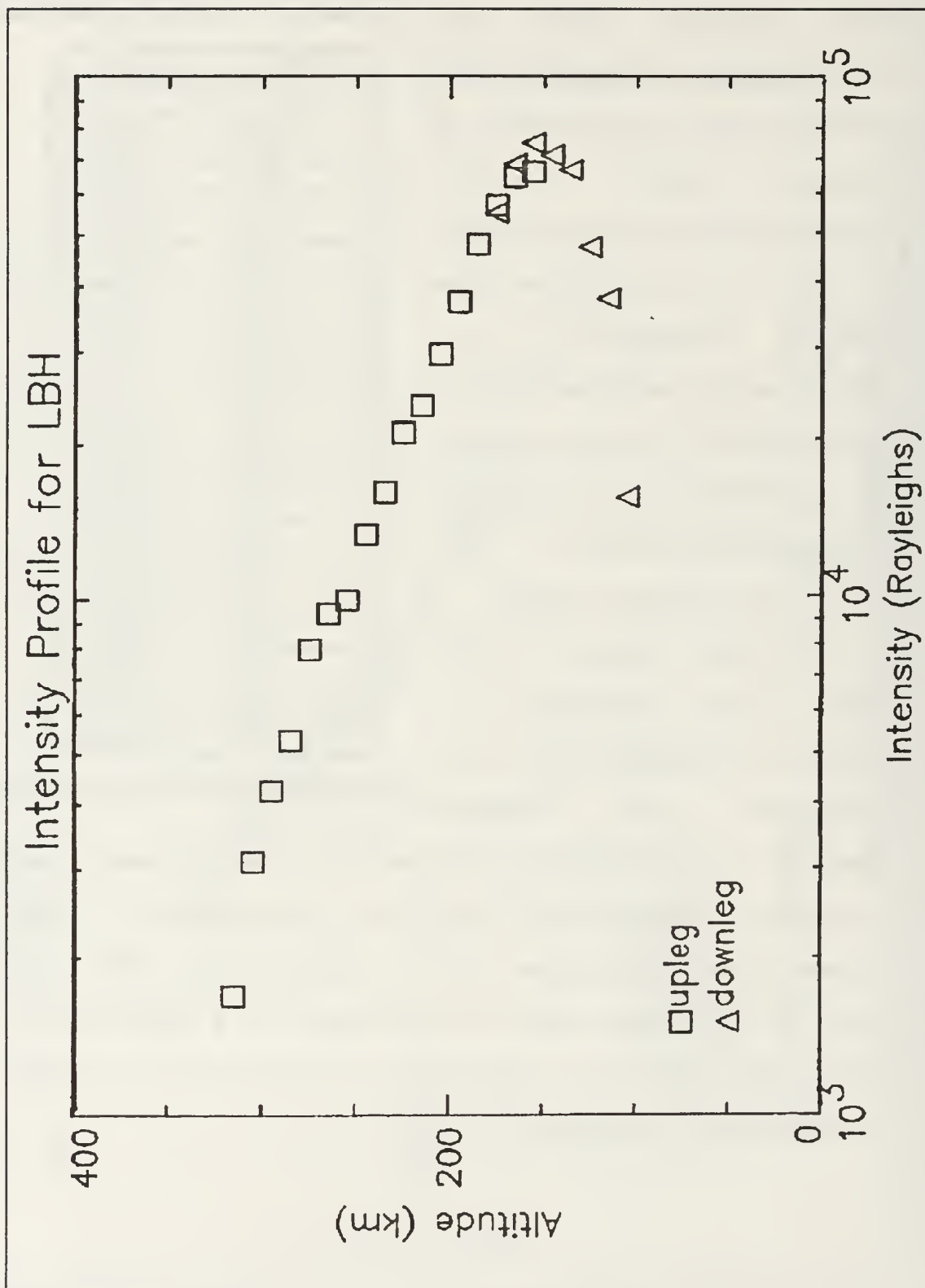


Figure 5-10 Nitrogen LBH intensity profile.

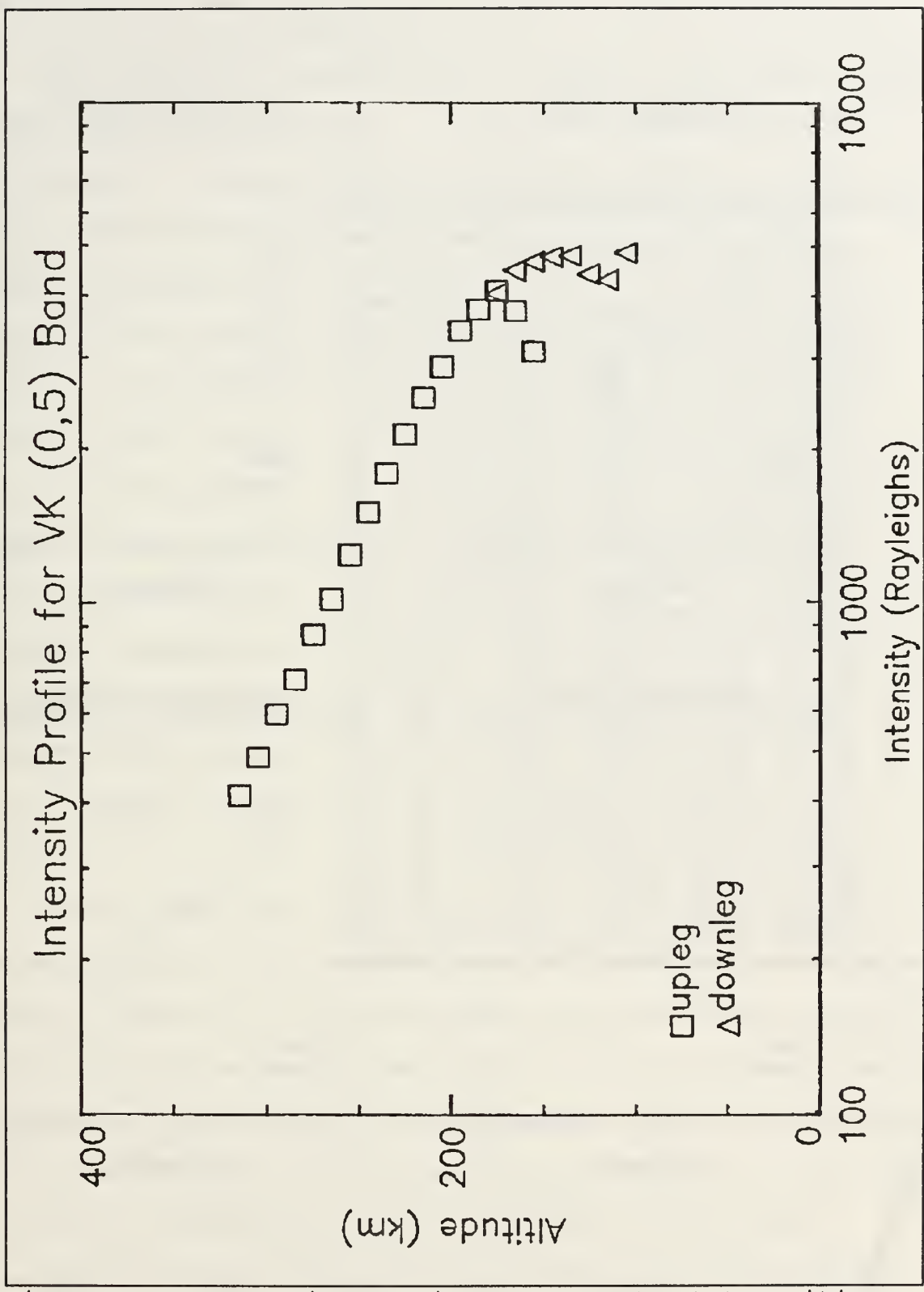


Figure 5-11 Intensity profile for  $N_2$  VK(0,5) transition.

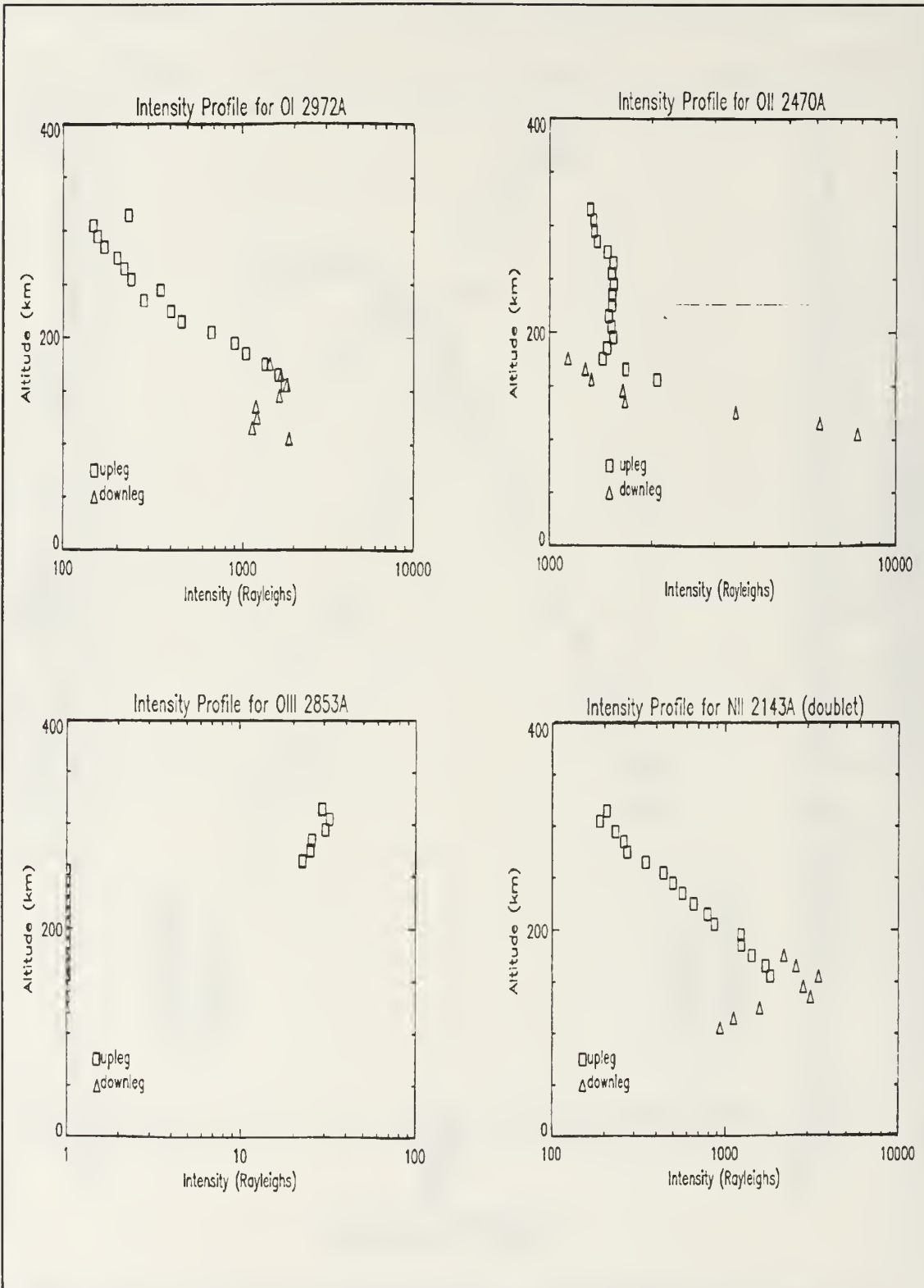


Figure 5-12 Intensity profiles for OI, OII, OIII, NII.

### c. Atomic Emissions

The intensity profiles for OI 2972Å, OII 2470Å, OIII 2853Å, and NII 2143Å

are shown in Figure 5-12, with the values given in Table 5-2.

The OI 2972Å profile shows a distinctive peak at about 150km; the O<sup>+</sup> 2470Å profile shows a broad peak at about 250km; the OIII profile suggests a peak at around 300km; and the NII reaches its maximum around 150km.

The OI 2972Å line emission profile was found to have very little agreement with previous analysis. The maximum found by this analysis was 50% of that found when fitting only the OI 2972Å line (Andersen, 1990). This is due to the uncertainty of the wavelength for the data, since two of the data dropouts were in this region. The overall

TABLE 5-2 ATOMIC INTENSITY VALUES

ALT(km) *down leg	OI 2972Å	OII 2470Å	OIII 2853Å	NII 2143Å doublet
105*	1878.70	7816.57	0.00	934.11
115*	1131.50	6120.95	0.00	1113.95
125*	1207.23	3477.89	0.00	1579.08
135*	1187.29	1660.38	0.00	3106.81
145*	1652.85	1633.97	0.00	2824.51
155	1777.33	2065.98	0.00	1824.37
155*	1828.75	1323.66	0.00	3469.86
165	1623.30	1671.16	0.00	1715.49
165*	1692.26	1264.87	0.00	2559.10
175	1351.22	1436.91	0.00	1431.54
175*	1448.04	1127.43	0.00	2175.71
185	1045.54	1478.36	0.00	1243.45
195	907.09	1535.49	0.00	1238.92
205	677.06	1517.33	0.00	865.34
215	461.95	1492.67	0.00	786.54
225	404.27	1523.80	0.00	654.12
235	283.24	1525.33	0.00	563.59
245	353.83	1540.24	0.00	496.13
255	240.10	1522.03	0.00	436.25
265	219.15	1537.10	22.56	348.22
275	200.13	1481.19	25.02	273.15
285	169.77	1383.26	25.48	260.23
295	156.30	1350.18	30.51	232.33
305	147.63	1342.65	32.31	186.90
315	232.63	1310.17	29.27	206.432

uncertainty in the OI profile should reflect the data drops, thus caution is urged for any subsequent analysis of this emission profile.

### 3. Discussion

#### a. V-K Quenching

Figure 5-13 shows an overlay of the nitrogen LBH and VK profiles, with the VK scaled up by a factor of 9.5 for comparison. The most interesting aspect of the nitrogen profiles is that they have roughly the same slope above 200 kilometers, but the VK intensity drops off rapidly below this height. This is due to the quenching effect of  $N_2$ , NO, O,  $O_2$ , and N at the lower altitudes. From auroral studies, atomic oxygen is thought to be the primary quenching agent with molecular oxygen playing a role below 135km (Sharp, 1971). As previously discussed, the upper state for the VK emissions is the  $N_2$  A-state. The A-state to ground-state energy for  $N_2$  corresponds to an excitation energy for atomic oxygen. Below 200 km, the O density is high enough that during their metastable lifetime in the excited state,  $N_2$  molecules collide with and excite oxygen, thus losing their energy without emitting a photon. This is believed to be the first simultaneous observation of these two profiles in the dayglow.

#### b. Adjustments to Franck-Condon Factors

The first set of spectra to be fitted to the data included Nitric Oxide  $\gamma$ ,  $\delta$ , and  $\epsilon$  bands, Nitrogen LBH and V-K bands, OI

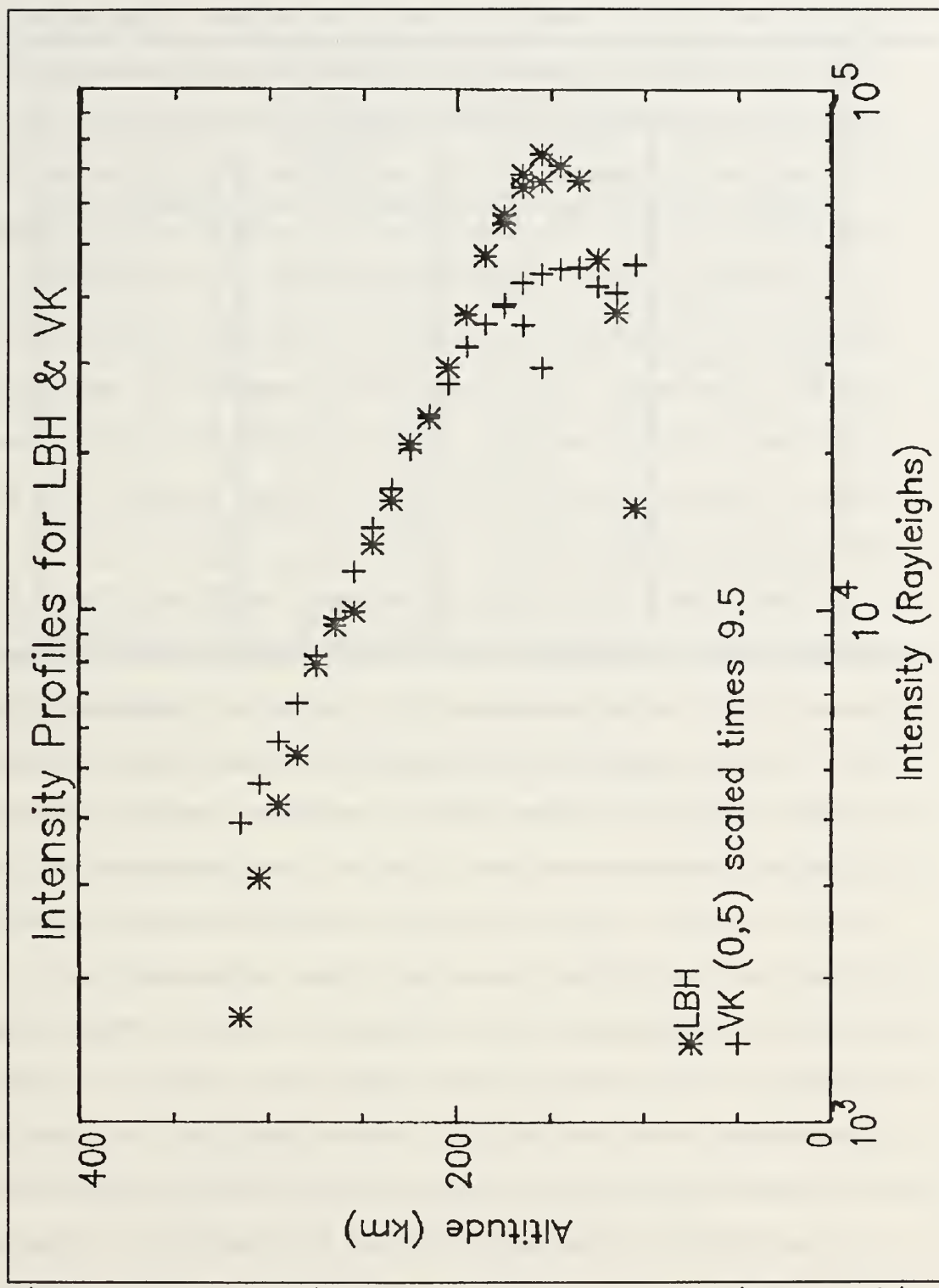


Figure 5-13 Intensity plots for LBH & VK showing quenching of VK.

2972Å, OII 2470Å, and OIII 2853Å emissions. The first fine-tuning of the fit was accomplished by plotting the fit and data simultaneously in 400Å segments and looking at each band for trends in undershooting or overshooting at a particular altitude, or for all altitudes at a particular wavelength. Any trend was then adjusted up or down in the original model spectrum, a procedure equivalent to varying the Franck-Condon factor (the factor which quantifies probability of transition for the synthetic models). This process was very tedious and time intensive, but a second fitting yielded an average decrease of 30% in  $\chi^2$ .

After the first set of changes had been made to the Franck-Condon factors, the same process of plotting and observing trends was repeated. Several unidentified peaks were seen in the data which are believed to be unidentified atomic emissions, since their profiles matched that of an impulse function convolved with the instrument slit function. Other than the well-documented NII 2143Å doublet, which was added as a synthetic spectrum, these emissions had not been previously reported in the literature, so the "Other Atomics" spectrum was created (see discussion above). The two parameters, NII and "Other", were included in the fitting routine. Once these parameters were included, the adjustments to the Franck-Condon factors found for the Nitric Oxide bands' synthetic spectra confirmed those used by Mack (1991) and Clayton (1990). The adjustments to the Franck-Condon factors

TABLE 5-3

Adjustments to Franck-Condon Factors							
Vegard-Kaplan		Lyman-Birge-Hopfield		Nitric Oxide $\gamma$		Nitric Oxide $\epsilon$	
$v', v''$	factor	$v', v''$	factor	$v', v''$	factor	$v', v''$	factor
0, k k=0...9	2.6	1,7	1.7	0, k k=0...8	1.2	0,0	.63
1, j j=0...9	1.5	3,9	1.203	1,0	1.125	0,1	.9
6,9	.83	5,11	1.4	1,1	1.3	0,2	1.03
4,8	.67	1,8	1.3	1,2	1.8	0,3	1.11
7,10	.6	3,10	.8	1,3	1.6		
11,13	.7	4,11	.9	1, j j=4...10	1.3		
12,14	.67	5,12	.757	2,0	.75		
2,8	.67	3,11	.8	2,2	1.26		
5,10	.5	4,12	.9	2,3	1.6		
8,12	.5	5,13	1.2				

are summarized in Table 5-3. These changes to the accepted probabilities of transition are believed to be actual corrections and not just a function of the instrumentation. It is expected that further independent measurements will verify these corrections.

The intensity profiles were derived from the final parameters of the fitting routine, but analysis of the data includes looking not only at the profiles but at the fits themselves. A complete set of plots of the data showing a comparison of data and fits, as well as accompanying plots showing the breakdown of the fits by constituent, are in Appendix E. Figures 5-14 and 5-15 show sample fits of the entire wavelength range at low altitude and high altitude. It

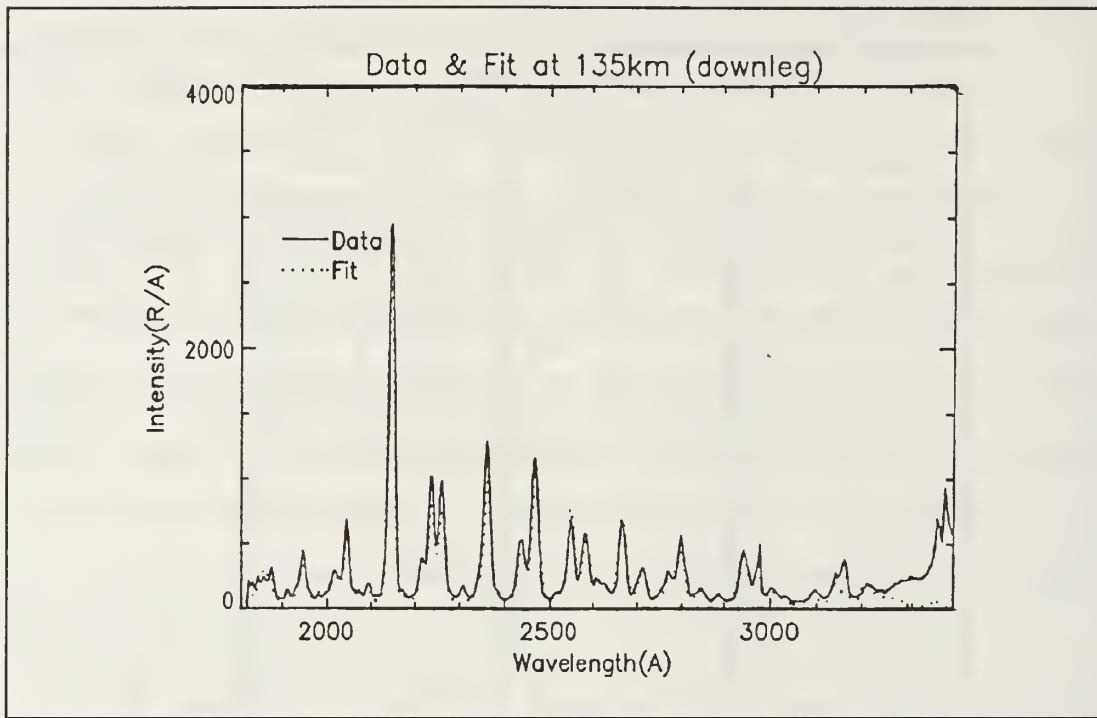


Figure 5-14 Data and best-fitting synthetic spectrum at 135km.

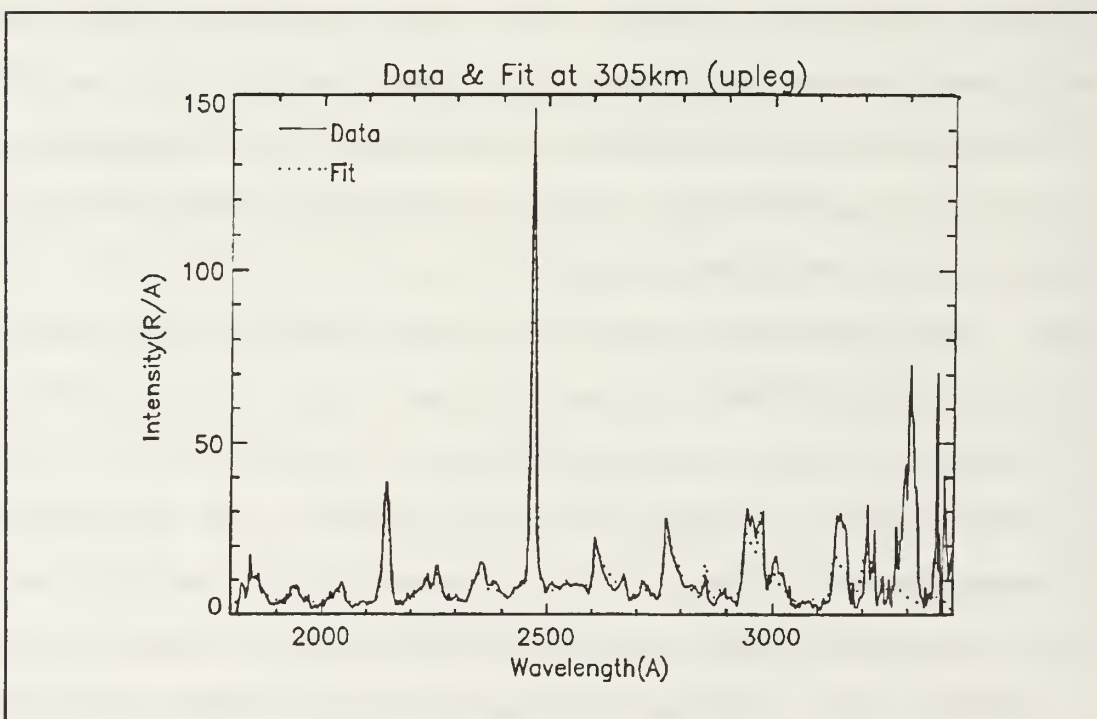


Figure 5-15 Data and best-fitting synthetic spectrum at 305km.

is apparent from these figures that the overall fit was excellent.

It should be pointed out that there is a disagreement between the data and fit at the wavelengths where the nitrogen Second Positive emissions are present. Additionally, the only other poorly fit feature was the 2930 $\text{\AA}$  to 2990 $\text{\AA}$  range at altitudes above 200 km. This is one of the areas one would like to be able to fit well, since it includes the OI 2972 $\text{\AA}$  emission. Unfortunately, two of the dropped data points are at 2969.7 $\text{\AA}$  and 2972.9 $\text{\AA}$ , exactly where the peak of OI is expected. Also, there seems to be another emission at about 2955 $\text{\AA}$  which is not explained by the VK bands or OI emission, creating three peaks in the data where theory predicts only two. This feature is shown in Figure 5-16.

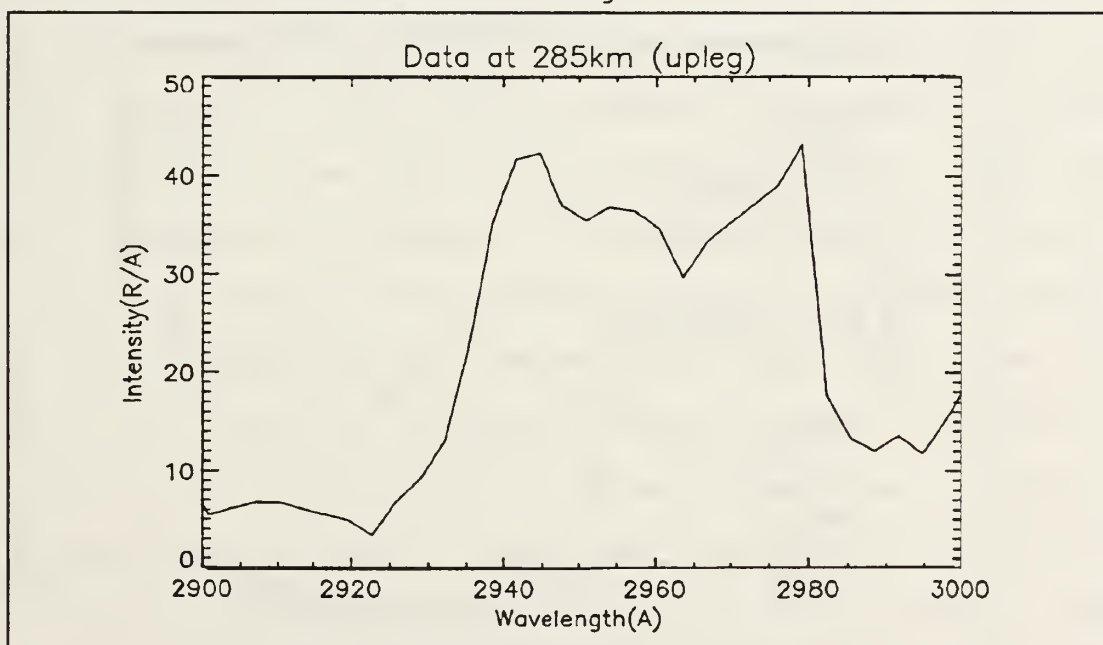


Figure 5-16 Averaged spectrum for 285km. The peak at 2940 $\text{\AA}$  is VK(0,7), the peak at 2980 $\text{\AA}$  is due to OI 2972 $\text{\AA}$ , and the feature at 2955 $\text{\AA}$  is unidentified.

### c. Temperature Profile

In addition to the column density profile, intensity profiles, and fits of model spectra to data, a temperature profile also was determined. The temperatures described by Mack (1991) were used as initial guesses. Several of the temperatures at the lowest altitudes were increased during fitting to improve the match of synthetic spectra to data. The resultant temperature profile is shown in Figure 5-17. The temperatures determined by the fitting procedure are all considerably hotter than predicted by MSIS. In particular, the asymptotic temperature is 400° hotter. This is possibly due to a magnetic storm which occurred about three hours prior to launch.

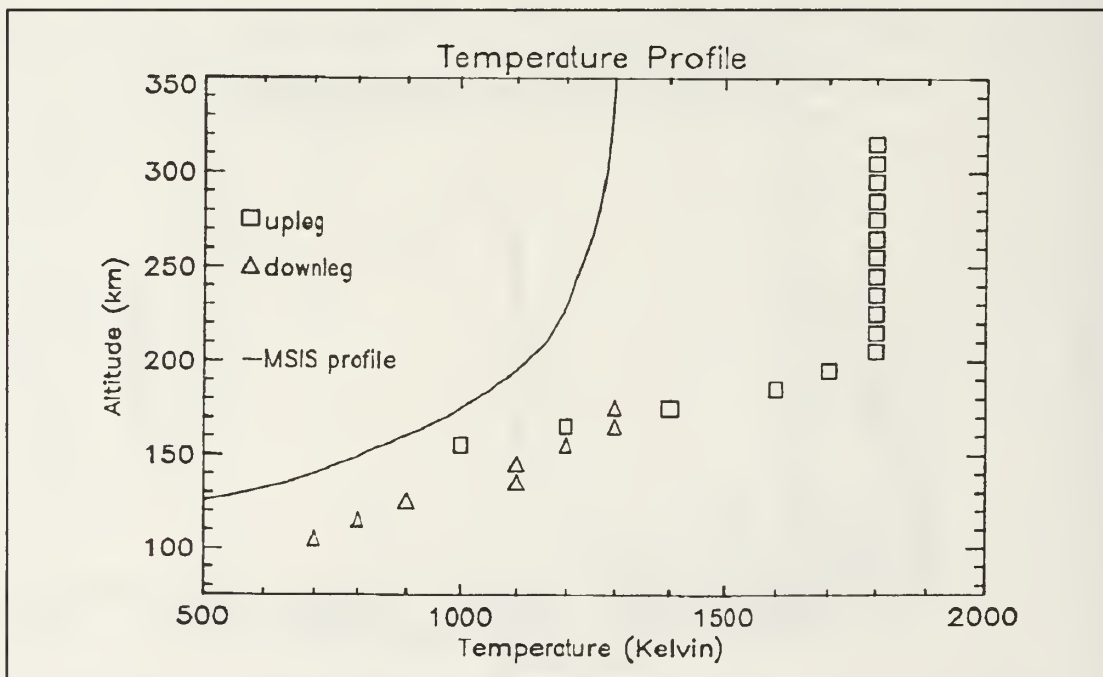


Figure 5-17 The temperatures used by the analysis are indicated by symbols. The solid line is the MSIS temperature profile for the day of the launch.

## VI. CONCLUSIONS

### A. SUMMARY OF FINDINGS

Thermospheric dayglow data from a rocket-borne spectrograph were analyzed in this study. Computer synthesized spectra were created for the  $N_2$  Lyman-Birge-Hopfield and Vegard-Kaplan bands; NO  $\gamma$ ,  $\delta$ , and  $\epsilon$  bands; OI 2972Å, OII 2470Å, and OIII 2853Å atomic lines; and NII 2143Å doublet feature. A spectrum of other possible atomic emissions and a background factor were also considered in the fit. These synthetic models were fitted to the observed data, then the scaling factors were used to determine an intensity profile (column density profile in the case of nitric oxide).

The intensity and column density profiles obtained were within 10-20% of the values acquired by simpler fitting routines in all cases except the OI 2972Å emission. Thus the analysis supports the concept of fitting of just one feature to arrive at density and intensity profiles. A relationship was noted between VK and LBH emissions that would seem to support the theory of quenching of the nitrogen VK system. The data above roughly 3000Å could not be modelled without a  $N_2$  Second Positive synthetic spectrum. The loss of datapoints was a major detriment in fitting the OI 2972Å emission, as there were two data dropouts where a peak was expected. The

temperature profile which best fit the data was higher at low altitudes than previous analysis had predicted.

#### B. TOPICS FOR FURTHER INVESTIGATION

With another launch scheduled for March 1992, further spectral analysis of the March 1990 data is imprudent. Contemplating the prospective data, a synthetic spectrum for the N<sub>2</sub> Second Positive would enhance the analysis. It is expected that there will be no problem with data dropouts on the next flight (Quint, 1991), so a repeat of this analysis (with the new data) will greatly improve the accuracy of fitting of the OI emission and possibly show that it can be accurately fitted over a limited wavelength range.

The quenching of VK below 200km should be paralleled by the density of the quenching agent, as well as a rise in emissions corresponding to the relaxation of the quenching agent from its excited state. The quenching phenomenon showed promise for rewarding study, but was not the subject of this thesis.

Looking toward the future, the MUSTANG will be part of an operational satellite in the late 1990's, providing a constant flow of data for analysis. Considering the numerous new mathematical theories for computer network calculations, there may be a method better suited for fitting large quantities of data than the GRIDLS routine. A modification to the fitting programs to place less stringent requirements on the initial

programs to place less stringent requirements on the initial guess and to provide a more formal check for global minimum would greatly improve the effectiveness of the existing routine. Additionally, automation of the analysis, including derivation of the electron density profile, would certainly add to the viability of MUSTANG as a provider of geophysical parameters for national defense agencies.

## APPENDIX A

The following table shows the unshifted and shifted array elements of data, and their corresponding wavelengths.

Record: [mustang]m90_avg/um90_avg		
Entry # (pixel) Shifted	Entry # (pixel) Unshifted	Wavelength Å
0	0	1,798.00
1	1	1,801.13
2	2	1,804.27
3	3	1,807.40
4	4	1,810.53
5	5	1,813.67
6	6	1,816.80
7	7	1,819.93
8	8	1,823.06
9	9	1,826.20
10	10	1,829.33
11	11	1,832.46
12	12	1,835.60
13	13	1,838.73
14	14	1,841.86
15	15	1,845.00
16		1,848.13
17	16	1,851.26
18	17	1,854.39
19	18	1,857.53
20	19	1,860.66
21	20	1,863.79
22	21	1,866.93
23	22	1,870.06
24	23	1,873.19
25	24	1,876.33
26	25	1,879.46
27	26	1,882.59

28	27	1,885.72
29	28	1,888.86
30	29	1,891.99
31	30	1,895.12
32	31	1,898.26
33		1,901.39
34	32	1,904.52
35	33	1,907.66
36	34	1,910.79
37	35	1,913.92
38	36	1,917.05
39	37	1,920.19
40	38	1,923.32
41	39	1,926.45
42	40	1,929.59
43	41	1,932.72
44	42	1,935.85
45	43	1,938.99
46	44	1,942.12
47	45	1,945.25
48	46	1,948.38
49	47	1,951.52
50		1,954.65
51	48	1,957.78
52	49	1,960.92
53	50	1,964.05
54	51	1,967.18
55	52	1,970.32
56	53	1,973.45
57	54	1,976.58
58	55	1,979.71
59	56	1,982.85
60	57	1,985.98
61	58	1,989.11
62	59	1,992.25
63	60	1,995.38
64	61	1,998.51

65	62	2,001.65
66	63	2,004.78
67		2,007.91
68	64	2,011.04
69	65	2,014.18
70	66	2,017.31
71	67	2,020.44
72	68	2,023.58
73	69	2,026.71
74	70	2,029.84
75	71	2,032.98
76	72	2,036.11
77	73	2,039.24
78	74	2,042.37
79	75	2,045.51
80	76	2,048.64
81	77	2,051.77
82	78	2,054.91
83	79	2,058.04
84		2,061.17
85		2,064.31
86	80	2,067.44
87	81	2,070.57
88	82	2,073.70
89	83	2,076.84
90	84	2,079.97
91	85	2,083.10
92	86	2,086.24
93	87	2,089.37
94	88	2,092.50
95	89	2,095.64
96	90	2,098.77
97	91	2,101.90
98	92	2,105.03
99	93	2,108.17
100	94	2,111.30
101		2,114.43

102		2,117.57
103	95	2,120.70
104	96	2,123.83
105	97	2,126.97
106	98	2,130.10
107	99	2,133.23
108	100	2,136.36
109	101	2,139.50
110	102	2,142.63
111	103	2,145.76
112	104	2,148.90
113	105	2,152.03
114	106	2,155.16
115	107	2,158.30
116	108	2,161.43
117	109	2,164.56
118	110	2,167.69
119		2,170.83
120	111	2,173.96
121	112	2,177.09
122	113	2,180.23
123	114	2,183.36
124	115	2,186.49
125	116	2,189.63

126	117	2,192.758
127	118	2,195.891
128	119	2,199.024
129	120	2,202.157
130	121	2,205.290
131	122	2,208.423
132	123	2,211.556
133	124	2,214.689
134	125	2,217.822
135	126	2,220.955
136		2,224.088

137	127	2,227.221
138	128	2,230.354
139	129	2,233.487
140	130	2,236.620
141	131	2,239.753
142	132	2,242.886
143	133	2,246.019
144	134	2,249.152
145	135	2,252.285
146	136	2,255.418
147	137	2,258.551
148	138	2,261.684
149	139	2,264.817
150	140	2,267.950
151	141	2,271.083
152	142	2,274.216
153		2,277.349
154	143	2,280.482
155	144	2,283.615
156	145	2,286.748
157	146	2,289.881
158	147	2,293.014
159	148	2,296.147
160	149	2,299.280
161	150	2,302.413
162	151	2,305.546
163	152	2,308.679
164	153	2,311.812
165	154	2,314.945
166	155	2,318.078
167	156	2,321.211
168	157	2,324.344
169	158	2,327.477
170		2,330.610
171	159	2,333.743
172	160	2,336.876
173	161	2,340.009

174	162	2,343.142
175	163	2,346.275
176	164	2,349.408
177	165	2,352.541
178	166	2,355.674
179	167	2,358.807
180	168	2,361.940
181	169	2,365.073
182	170	2,368.206
183	171	2,371.339
184	172	2,374.472
185	173	2,377.605
186	174	2,380.738
187		2,383.871
188	175	2,387.004
189	176	2,390.137
190	177	2,393.270
191	178	2,396.403
192	179	2,399.536
193	180	2,402.669
194	181	2,405.802
195	182	2,408.935
196	183	2,412.068
197	184	2,415.201
198	185	2,418.334
199	186	2,421.467
200	187	2,424.600
201	188	2,427.733
202	189	2,430.866
203	190	2,433.999
204		2,437.132
205	191	2,440.265
206	192	2,443.398
207	193	2,446.531
208	194	2,449.664
209	195	2,452.797
210	196	2,455.930

211	197	2,459.063
212	198	2,462.196
213	199	2,465.329
214	200	2,468.462
215	201	2,471.595
216	202	2,474.728
217	203	2,477.861
218	204	2,480.994
219	205	2,484.127
220	206	2,487.260
221		2,490.393
222	207	2,493.526
223	208	2,496.659
224	209	2,499.792
225	210	2,502.925
226	211	2,506.058
227	212	2,509.191
228	213	2,512.324
229	214	2,515.457
230	215	2,518.590
231	216	2,521.723
232	217	2,524.856
233	218	2,527.989
234	219	2,531.122
235	220	2,534.255
236	221	2,537.388
237	222	2,540.521
238		2,543.654
239		2,546.787
240	223	2,549.920
241	224	2,553.053
242	225	2,556.186
243	226	2,559.319
244	227	2,562.452
245	228	2,565.585
246	229	2,568.718
247	230	2,571.851

248	231	2,574.984
249	232	2,578.117
250	233	2,581.250
251	234	2,584.383
252	235	2,587.516
253	236	2,590.649

254	237	2,593.782
255	238	2,596.915
256		2,600.048
257	239	2,603.181
258	240	2,606.314
259	241	2,609.447
260	242	2,612.580
261	243	2,615.713
262	244	2,618.846
263	245	2,621.979
264	246	2,625.112
265	247	2,628.245
266	248	2,631.378
267	249	2,634.511
268	250	2,637.644
269	251	2,640.777
270	252	2,643.910
271	253	2,647.043
272		2,650.176
273	254	2,653.309
274	255	2,656.442
275	256	2,659.575
276	257	2,662.708
277	258	2,665.841
278	259	2,668.974
279	260	2,672.107
280	261	2,675.240
281	262	2,678.373
282	263	2,681.506
283	264	2,684.639

284	265	2,687.772
285	266	2,690.905
286	267	2,694.038
287	268	2,697.171
288	269	2,700.304
289		2,703.437
290	270	2,706.570
291	271	2,709.703
292	272	2,712.836
293	273	2,715.969
294	274	2,719.102
295	275	2,722.235
296	276	2,725.368
297	277	2,728.501
298	278	2,731.634
299	279	2,734.767
300	280	2,737.900
301	281	2,741.033
302	282	2,744.166
303	283	2,747.299
304	284	2,750.432
305	285	2,753.565
306		2,756.698
307	286	2,759.831
308	287	2,762.964
309	288	2,766.097
310	289	2,769.230
311	290	2,772.363
312	291	2,775.496
313	292	2,778.629
314	293	2,781.762
315	294	2,784.895
316	295	2,788.028
317	296	2,791.161
318	297	2,794.294
319	298	2,797.427
320	299	2,800.560

321	300	2,803.693
322	301	2,806.826
323		2,809.959
324	302	2,813.092
325	303	2,816.225
326	304	2,819.358
327	305	2,822.491
328	306	2,825.624
329	307	2,828.757
330	308	2,831.890
331	309	2,835.023
332	310	2,838.156
333	311	2,841.289
334	312	2,844.422
335	313	2,847.555
336	314	2,850.688
337	315	2,853.821
338	316	2,856.954
339	317	2,860.087
340		2,863.220
341	318	2,866.353
342	319	2,869.486
343	320	2,872.619
344	321	2,875.752
345	322	2,878.885
346	323	2,882.018
347	324	2,885.151
348	325	2,888.284
349	326	2,891.417
350	327	2,894.550
351	328	2,897.683
352	329	2,900.816
353	330	2,903.949
354	331	2,907.082
355	332	2,910.215
356	333	2,913.348
357		2,916.481

358	334	2,919.614
359	335	2,922.747
360	336	2,925.880
361	337	2,929.013
362	338	2,932.146
363	339	2,935.279
364	340	2,938.412
365	341	2,941.545
366	342	2,944.678
367	343	2,947.811
368	344	2,950.944
369	345	2,954.077
370	346	2,957.210
371	347	2,960.343
372	348	2,963.476
373	349	2,966.609
374		2,969.742
375		2,972.875
376	350	2,976.008
377	351	2,979.141
378	352	2,982.274

379	353	2,985.407
380	354	2,988.540
381	355	2,991.673
382	356	2,994.806
383	357	2,997.939
384	358	3,001.072
385	359	3,004.205
386	360	3,007.338
387	361	3,010.471
388	362	3,013.604
389	363	3,016.737
390	364	3,019.870
391	365	3,023.003

392		3,026.136
393	366	3,029.269
394	367	3,032.402
395	368	3,035.535
396	369	3,038.668
397	370	3,041.801
398	371	3,044.934
399	372	3,048.067
400	373	3,051.200
401	374	3,054.333
402	375	3,057.466
403	376	3,060.599
404	377	3,063.732
405	378	3,066.865
406	379	3,069.998
407	380	3,073.131
408	381	3,076.264
409		3,079.397
410	382	3,082.530
411	383	3,085.663
412	384	3,088.796
413	385	3,091.929
414	386	3,095.062
415	387	3,098.195
416	388	3,101.328
417	389	3,104.461
418	390	3,107.594
419	391	3,110.727
420	392	3,113.860
421	393	3,116.993
422	394	3,120.126
423	395	3,123.259
424	396	3,126.392
425	397	3,129.525
426		3,132.658
427	398	3,135.791
428	399	3,138.924

429	400	3,142.057
430	401	3,145.190
431	402	3,148.323
432	403	3,151.456
433	404	3,154.589
434	405	3,157.722
435	406	3,160.855
436	407	3,163.988
437	408	3,167.121
438	409	3,170.254
439	410	3,173.387
440	411	3,176.520
441	412	3,179.653
442	413	3,182.786
443		3,185.919
444	414	3,189.052
445	415	3,192.185
446	416	3,195.318
447	417	3,198.451
448	418	3,201.584
449	419	3,204.717
450	420	3,207.850
451	421	3,210.983
452	422	3,214.116
453	423	3,217.249
454	424	3,220.382
455	425	3,223.515
456	426	3,226.648
457	427	3,229.781
458	428	3,232.914
459	429	3,236.047
460		3,239.180
461	430	3,242.313
462	431	3,245.446
463	432	3,248.579
464	433	3,251.712
465	434	3,254.845

466	435	3,257.978
467	436	3,261.111
468	437	3,264.244
469	438	3,267.377
470	439	3,270.510
471	440	3,273.643
472	441	3,276.776
473	442	3,279.909
474	443	3,283.042
475	444	3,286.175
476	445	3,289.308
477		3,292.441
478	446	3,295.574
479	447	3,298.707
480	448	3,301.840
481	449	3,304.973
482	450	3,308.106
483	451	3,311.239
484	452	3,314.372
485	453	3,317.505
486	454	3,320.638
487	455	3,323.771
488	456	3,326.904
489	457	3,330.037
490	458	3,333.170
491	459	3,336.303
492	460	3,339.436
493	461	3,342.569
494		3,345.702
495	462	3,348.835
496	463	3,351.968
497	464	3,355.101
498	465	3,358.234
499	466	3,361.367
500	467	3,364.500
501	468	3,367.633
502	469	3,370.766

503	470	3,373.899
504	471	3,377.032
505	472	3,380.165
506	473	3,383.298
507	474	3,386.431
508	475	3,389.564
509	476	3,392.697
510	477	3,395.830
511		3,398.963

## APPENDIX B

Appendix B contains the least squares fitting program and its subroutines. Additionally, the synthetic spectrum generation routines are given.

;Walden,1991, modified from Mack,1991

@getfunc

@fchisqr

pro nimpfit\_all

; This program fits data for the 1800 to 3400A range with models of the  
; NO gamma, delta, and epsilon bands, N2 LBH emissions, N2 Vegard-  
; Kaplan bands, oxygen emissions at 2470, 2972, & 2853A, N+ doublet  
; at 2143A, various atomic emissions, and the background level  
; through an iterative process. It uses gridls.pro, getfunc.pro, and  
; fchisqr.pro as subprograms; it uses parameter.dat as an in/out file;  
; and it writes the fit by altitude to nimpfit\_all.dat. The subprograms  
; utilize synthetic spectra which are stored in allvk.dat, all\_lbh.dat,  
; nii\_2143doub.dat, nodlt.dat, nogammack.dat, noeps.dat, oiii\_2853.dat  
; oii\_2470.dat, oi\_2972.dat, and otherspec.dat.

parameter.dat - file of parameters- records have 25 elements each  
record#- contents

0 - temperature  
1 - altitude record number (1 through 25;1-17 up,18-25 down)  
2 - chi squared of the fit  
3 - scale factor for O 2972A emission, in Rayleighs(intensity)  
4 - sigma for O scale factor  
5 - scale factor for O+ 2470A emission, in Rayleighs  
6 - sigma for O+ scale factor  
7 - scale factor for O++ 2853A emission, in Rayleighs  
8 - sigma for O++ scale factor  
9 - scale factor for the N2 LBH bands  
10 - sigma for LBH scale factor  
11 - scale factor for the NO gamma, delta, and epsilon bands, in  
molecules per square centimeter (column density)  
12 - sigma for NO scale factor  
13 - scale factor for the N2 V-K bands  
14 - sigma for VK scale factor  
15 - scale factor for N+ 2143A emission, in Rayleighs  
16 - sigma for N+ doublet scale factor  
17 - scale factor for synthetic atomics spectrum, in Rayleighs  
18 - sigma for atomic spectrum  
19 - scale factor for the background, in Rayleighs per Angstrom  
20 - sigma for background scale factor  
21 - altitudes in kilometers

para - array((2\*nterms)+2) in same order as record order in file

a - array(nterms+1) of temp followed by scale factors

yfit - 512 element array of best fit

start- first record number

stop - last record number

openr,30,['mustang]m90\_int.dat' ;open data file  
aa=assoc(30,fltarr(512))

openu,31,'nimpfit\_all.dat' ;open file to save yfit  
bb=assoc(31,fltarr(512))

openu,32,'parameter.dat' ;open parameter file  
pp=assoc(32,fltarr(25))

openr,33,['walden.datafix]m90\_domwt.dat'  
dd=assoc(33,fltarr(512))

```

start=0
stop=511
npts=(stop-start)+1
nterms = 9
para=fltarr(2*nterms+3)
a=fltarr(nterms+1)

for i=0,24 do begin
    for j=0,(2*nterms)+2 do begin
        hold=pp(j)
        para(j)=hold(i)
    endfor
    alt=para(1)
    count=0
    a(0)=para(0)
    for j=3,(2*nterms)+1,+2 do begin
        count=count+1
        a(count)=para(j)
    endfor
    y=aa(start:stop,alt)
;
;deltaa is step size for estimations, cannot be zero, first element is dummy
h=a
for j=1,nterms do begin
    h(j)=a(j)
    if (h(j) eq 0.0) then h(j)=1000.00
endfor
deltaa=h/10.

mode=1
weights=dd(alt)
;
gridls,y,weights,npts,nterms,mode,a,deltaa,sigmaa,yfit,chisqr,start,stop
bb(alt)=yfit
;
count=0
para(2)=chisqr
for j=3,(2*nterms)+1,+2 do begin
    count=count+1
    para(j)=a(count)
    para(j+1)=sigmaa(count)
endfor
for j=0,(2*nterms)+2 do begin
    hold=pp(j)
    hold(i)=para(j)
    pp(j)=hold
endfor
;
print,'alt=',alt,'a=',a,'chisqr=',chisqr
endfor
;
close,30
close,31
close,32
close,33
return
end
@gridls

```

```

;Walden,1991 modified from Mack,1991
function getfunc,a
; This function computes the synthetic spectrum from 1800 to 3400 A
; for given scaling factors.
;           INPUTS
; a - 9-D array of parameters
; a(0) - temperature at altitude of interest
; a(1) - scale factor for O emission @ 2972
; a(2) - scale factor for O+ emission @ 2470
; a(3) - scale factor for O++ emission @ 2853
; a(4) - scale factor for N2 LBH bands
; a(5) - scale factor for the sum of NO gamma, delta,
; and epsilon bands
; a(6) - scale factor for N2 Vegard-Kaplan bands
; a(7) - scale factor for N2 doublet emission @2143
; a(8) - scale factor for "Other Atomics" spectrum
; a(9) - scale factor for background .

; GETfunc returns an array of 511 points to be compared to the
; experimentally recorded profile from 1800 to 3400 A.

; LBH - The N2 LBH bands convolved with the slit function
; NOSYN - The sum of the NO gamma, delta, and epsilon bands convolved
; with the slit function
; VK - The N2 V-K bands convolved with the slit function
; OI - The OI emission @ 2972 A convolved with the slit function
; OII - The OII emission @ 2470 A convolved with the slit function
; OIII - The OIII emission @ 2853 A convolved with the slit function
; N2 - The N2 emission @2143 A convolved with the slit function
; AT - The spectrum of possible atomic emissions

openr,20,'ALL_LBH.DAT'
rr=assoc(20,fltarr(512))
LBH=rr(a(0)/100)

openr,21,'NOGAMMACK.DAT'
ss=assoc(21,fltarr(512))
NOGAM=ss(a(0)/100)

openr,22,'NODLT.DAT'
tt=assoc(22,fltarr(512))
NODLT=tt(a(0)/100)

openr,23,'NOEPS.DAT'
uu=assoc(23,fltarr(512))
NOEPS=uu(a(0)/100)

openr,24,'ALLVK.DAT'
vv=assoc(24,fltarr(512))
VK=vv(a(0)/100)

openr,25,'OI_2972.DAT'
ww=assoc(25,fltarr(512))
OI=ww(0)

openr,26,'OII_2470.DAT'
xx=assoc(26,fltarr(512))
OII=xx(0)

openr,27,'OIII_2853.DAT'

```

```

yy=assoc(27,fltarr(512))
OIII=yy(0)

openr,28,'NII_2143DOUB.DAT'
zz=assoc(28,fltarr(512))
N2=zz(1)

openr,29,'otherspec.dat'
atsp=assoc(29,fltarr(512))
AT=atsp(1)

NOSYN = NOGAM + .25*NODLT + NOEPS ;25% flourescent efficiency of
;delta band

getfunc = a(4)*LBH + a(5)*NOSYN/3.133e6 + a(6)*VK + a(1)*OI $
+ a(2)*OII + a(3)*OIII + a(7)*N2 +a(8)*AT + a(9)/3.133
;background is divided by wavelength bin so that
;scale factor is absolute intensity, NOSYN is divided
;by 3.133e6 for same reason

;
close,20
close,21
close,22
close,23
close,24
close,25
close,26
close,27
close,28
close,29

;
return,getfunc
end

```

```

;Mack,1991
function fchisqr,y,weights,npts,free,mode,yfit,start,stop
;      This function evaluates the reduced chi squared
;      for a fit to the data.
;      Adapted from Bevington, pg 194.
;      INPUTS
;      y      - array of data points
;      weights- array of weightings based on sdom's of data points
;      npts   - number of data points being fit
;      free    - number of degrees of freedom
;      mode   - determines method of weighting the fit
;                  +1 instrumental weighting(sdom weights)
;                  0 no weighting
;                  -1 statistical weighting
;      yfit   - array of fitted points
;      start  - first record element to be fit
;      stop   - last record element to be fit

count=0
chisqr=0.

if mode eq 0 then wt=1.
if mode gt 0 then wt=weights
if mode lt 0 then wt=1./abs(y)

for i=start,stop do begin
    chisqr=chisqr + wt(i)*(y(count)-yfit(count))^2
    count=count + 1
endfor
fchisqr=chisqr/free
return,fchisqr
end

```

```

;Walden,1991
pro lbhcalc,wl,int,slit          ;Calculates synthetic lbh spectra at temps
  openu,10,'all_lbh.dat'          ; from 100 to 2000 deg for wavelengths from
  lbh=assoc(10,fltarr(512))      ; 1800 to 3400 A. Results are convolved with
                                  ; MUSTANG instrument slit function.

wl=indgen(512)*3.133 + 1798

openr,11,['walden]slit.dat'
sl=assoc(11,fltarr(11))
slit=sl(1)

i=0
for t=100,2000,100 do begin
  i=i+1                         ; Wavelength
  int=wl*0                         ; variables for tweaking individual transitions
  int1=wl*0
  int2=wl*0
  int3=wl*0
  int4=wl*0
  int5=wl*0
  int6=wl*0
  int7=wl*0
  int8=wl*0
  int9=wl*0
  int10=wl*0
  lbhsyn,t,4,9,wl,int      ; 1801.0
  lbhsyn,t,0,6,wl,int      ; 1804.6
  lbhsyn,t,5,10,wl,int     ; 1817.9
  lbhsyn,t,1,7,wl,int10   ; 1820.8
  int=int+int10*1.7
  lbhsyn,t,6,11,wl,int     ; 1835.0
  lbhsyn,t,2,8,wl,int     ; 1837.2
  lbhsyn,t,3,9,wl,int1     ; 1853.8
  int=int+int1*1.203
  lbhsyn,t,4,10,wl,int     ; 1870.8
  lbhsyn,t,0,7,wl,int     ; 1877.7
  lbhsyn,t,5,11,wl,int2   ; 1887.9
  int=int+int2*1.4
  lbhsyn,t,1,8,wl,int3     ; 1894.2
  int=int+int3*1.3
  lbhsyn,t,6,12,wl,int     ; 1905.4
  lbhsyn,t,2,9,wl,int     ; 1910.9
  lbhsyn,t,3,10,wl,int4   ; 1927.8
  int=int+int4*.8
  lbhsyn,t,4,11,wl,int5   ; 1945.0
  int=int+int5*.9
  lbhsyn,t,0,8,wl,int     ; 1955.9
  lbhsyn,t,5,12,wl,int6   ; 1962.4
  int=int+int6*.757
  lbhsyn,t,1,9,wl,int     ; 1972.6
  lbhsyn,t,6,13,wl,int     ; 1980.1
  lbhsyn,t,2,10,wl,int     ; 1989.6
  lbhsyn,t,3,11,wl,int7   ; 2006.8
  int=int+int7*.8
  lbhsyn,t,4,12,wl,int8   ; 2024.2
  int=int+int8*.9
  lbhsyn,t,0,9,wl,int     ; 2040
  lbhsyn,t,5,13,wl,int9   ; 2041.9

```

```

int=int+int9*1.2
lbhsyn,t,1,10,wl,int ; 2056.6
lbhsyn,t,6,14,wl,int ; 2059.8
lbhsyn,t,2,11,wl,int ; 2073.8
lbhsyn,t,3,12,wl,int ; 2091.2
lbhsyn,t,4,13,wl,int ; 2108.8
lbhsyn,t,5,14,wl,int ; 2126.7
lbhsyn,t,0,10,wl,int ; 2130
lbhsyn,t,6,15,wl,int ; 2144.0
lbhsyn,t,1,11,wl,int ; 2147
lbhsyn,t,2,12,wl,int ; 2164
lbhsyn,t,3,13,wl,int ; 2181.1
lbhsyn,t,4,14,wl,int ; 2198.7
lbhsyn,t,5,15,wl,int ; 2217
lbhsyn,t,0,11,wl,int ; 2227
lbhsyn,t,6,16,wl,int ; 2235
lbhsyn,t,1,12,wl,int ; 2244
lbhsyn,t,2,13,wl,int ; 2261
lbhsyn,t,3,14,wl,int ; 2279
lbhsyn,t,4,15,wl,int ; 2297
lbhsyn,t,5,16,wl,int ; 2314
lbhsyn,t,6,17,wl,int ; 2332
lbhsyn,t,1,13,wl,int ; 2349
lbhsyn,t,2,14,wl,int ; 2366
lbhsyn,t,3,15,wl,int ; 2384
lbhsyn,t,4,16,wl,int ; 2401
lbhsyn,t,5,17,wl,int ; 2419
lbhsyn,t,6,18,wl,int ; 2437
lbhsyn,t,2,15,wl,int ; 2479
lbhsyn,t,3,16,wl,int ; 2496
lbhsyn,t,4,17,wl,int ; 2514
lbhsyn,t,5,18,wl,int ; 2531
lbhsyn,t,6,19,wl,int ; 2549
lbhsyn,t,4,18,wl,int ; 2636
lbhsyn,t,5,19,wl,int ; 2653
lbhsyn,t,6,20,wl,int ; 2670
lbhsyn,t,6,21,wl,int ; 2801

print,total(int)
spec=convol(int,slit)
lbh(i)=spec/total(spec)
endfor

close,10
close,11

return
nd
[SYNSPEC]LBHSYN

```

```

;Walden,1991
pro allvkcalc,wl,int,slit
openr,1,['WALDEN]slit.dat'
openu,3,'allvk.dat'
sl=assoc(1,fltarr(11))
slit=sl(1)
vk=assoc(3,fltarr(512))
wl=indgen(512)*3.133 +1798
i=0
for t=100,2000,100 do begin
  i=i+1

  int=wl*0
  int1=wl*0
  int2=wl*0
  int3=wl*0
  int4=wl*0
  int5=wl*0
  int6=wl*0
  int7=wl*0
  int8=wl*0
  int9=wl*0
  int10=wl*0
  int11=wl*0
  int12=wl*0
  int13=wl*0
  int14=wl*0
  int15=wl*0
  int16=wl*0
  int17=wl*0
  int18=wl*0
  int19=wl*0
  int20=wl*0
  int21=wl*0
  int22=wl*0
  int23=wl*0
  int24=wl*0
  int25=wl*0
  int26=wl*0
  int27=wl*0
  int28=wl*0

; these variables provide a means of tweaking
; individual transitions

```

This section calculates the transitions' band systems, summing each one into the total spectrum.

TRANSITION

WL

vkSyn,t,6,1,wl,int	; 1798
vkSyn,t,4,0,wl,int	; 1808
vkSyn,t,13,5,wl,int	; 1823
vkSyn,t,11,4,wl,int	; 1824
vkSyn,t,9,3,wl,int	; 1827
vkSyn,t,7,2,wl,int	; 1833
vkSyn,t,5,1,wl,int	; 1841
vkSyn,t,3,0,wl,int	; 1853
vkSyn,t,12,5,wl,int	; 1860
vkSyn,t,10,4,wl,int	; 1863
vkSyn,t,8,3,wl,int	; 1868
vkSyn,t,6,2,wl,int	; 1876
vkSyn,t,4,1,wl,int	; 1887
vkSyn,t,13,6,wl,int	; 1899

```

vksyn,t,11,5,wl,int ; 1900
vksyn,t,2,0,wl,int ; 1901
vksyn,t,9,4,wl,int ; 1905
vksyn,t,7,3,wl,int ; 1912
vksyn,t,5,2,wl,int ; 1923
vksyn,t,3,1,wl,int ; 1936
vksyn,t,12,6,wl,int ; 1939
vksyn,t,10,5,wl,int ; 1943
vksyn,t,8,4,wl,int ; 1950
vksyn,t,1,0,wl,int1 ; 1954
int=int+int1*1.5
vksyn,t,6,3,wl,int ; 1960
vksyn,t,4,2,wl,int ; 1973
vksyn,t,13,7,wl,int ; 1980
vksyn,t,11,6,wl,int ; 1983
vksyn,t,9,5,wl,int ; 1989
vksyn,t,2,1,wl,int ; 1990
vksyn,t,7,4,wl,int ; 1998
vksyn,t,0,0,wl,int2 ; 2010
int=int+int2*2.6
vksyn,t,5,3,wl,int ; 2011
vksyn,t,12,7,wl,int ; 2024
vksyn,t,3,2,wl,int ; 2027
vksyn,t,10,6,wl,int ; 2029
vksyn,t,8,5,wl,int ; 2038
vksyn,t,1,1,wl,int3 ; 2047
int=int+int3*1.5
vksyn,t,6,4,wl,int ; 2050
vksyn,t,4,3,wl,int ; 2065
vksyn,t,13,8,wl,int ; 2067
vksyn,t,11,7,wl,int ; 2071
vksyn,t,9,6,wl,int ; 2079
vksyn,t,2,2,wl,int ; 2085
vksyn,t,7,5,wl,int ; 2090
vksyn,t,5,4,wl,int ; 2106
vksyn,t,0,1,wl,int4 ; 2109
int=int+int4*2.6
vksyn,t,12,8,wl,int ; 2115
vksyn,t,10,7,wl,int ; 2122
vksyn,t,3,3,wl,int ; 2125
vksyn,t,8,6,wl,int ; 2133
vksyn,t,6,5,wl,int ; 2147
vksyn,t,1,2,wl,int5 ; 2148
int=int+int5*1.5
vksyn,t,13,9,wl,int ; 2161
vksyn,t,4,4,wl,int ; 2166
vksyn,t,11,8,wl,int ; 2167
vksyn,t,9,7,wl,int ; 2177
vksyn,t,2,3,wl,int ; 2189
vksyn,t,7,6,wl,int ; 2191
vksyn,t,5,5,wl,int ; 2209
vksyn,t,12,9,wl,int ; 2213
vksyn,t,0,2,wl,int6 ; 2216
int=int+int6*2.6
vksyn,t,10,8,wl,int ; 2222
vksyn,t,3,4,wl,int ; 2231
vksyn,t,8,7,wl,int ; 2236
vksyn,t,6,6,wl,int ; 2253
vksyn,t,1,3,wl,int7 ; 2258
int=int+int7*1.5

```

vksyn,t,13,10,wl,int	; 2262
vksyn,t,11,9,wl,int	; 2270
vksyn,t,4,5,wl,int	; 2275
vksyn,t,9,8,wl,int	; 2282
vksyn,t,7,7,wl,int	; 2299
vksyn,t,2,4,wl,int	; 2302
vksyn,t,12,10,wl,int	; 2320
vksyn,t,5,6,wl,int	; 2321
vksyn,t,10,9,wl,int	; 2331
vksyn,t,0,3,wl,int8	; 2334
int=int+int8*2.6	
vksyn,t,3,5,wl,int	; 2347
vksyn,t,8,8,wl,int	; 2347
vksyn,t,6,7,wl,int	; 2368
vksyn,t,13,11,wl,int	; 2372
vksyn,t,1,4,wl,int9	; 2379
int=int+int9*1.5	
vksyn,t,11,10,wl,int	; 2382
vksyn,t,4,6,wl,int	; 2394
vksyn,t,9,9,wl,int	; 2397
vksyn,t,7,8,wl,int	; 2417
vksyn,t,2,5,wl,int	; 2425
vksyn,t,12,11,wl,int	; 2435
vksyn,t,5,7,wl,int	; 2443
vksyn,t,10,10,wl,int	; 2449
vksyn,t,0,4,wl,int10	; 2463
int=int+int10*2.6	
vksyn,t,8,9,wl,int	; 2469
vksyn,t,3,6,wl,int	; 2474
vksyn,t,13,12,wl,int	; 2490
vksyn,t,6,8,wl,int	; 2494
vksyn,t,11,11,wl,int	; 2504
vksyn,t,1,5,wl,int11	; 2511
int=int+int11*1.5	
vksyn,t,9,10,wl,int	; 2522
vksyn,t,4,7,wl,int	; 2524
vksyn,t,7,9,wl,int	; 2547
vksyn,t,2,6,wl,int	; 2561
vksyn,t,12,12,wl,int	; 2561
vksyn,t,5,8,wl,int	; 2577
vksyn,t,10,11,wl,int	; 2578
vksyn,t,8,10,wl,int	; 2602
vksyn,t,0,5,wl,int12	; 2605
int=int+int12*2.6	
vksyn,t,3,7,wl,int	; 2613
vksyn,t,13,13,wl,int	; 2620
vksyn,t,6,9,wl,int13	; 2632
int=int+int13*.83	
vksyn,t,11,12,wl,int	; 2637
vksyn,t,1,6,wl,int14	; 2657
int=int+int14*1.5	
vksyn,t,9,11,wl,int	; 2659
vksyn,t,4,8,wl,int15	; 2668
int=int+int15*.67	
vksyn,t,7,10,wl,int16	; 2689
int=int+int16*.6	
vksyn,t,12,13,wl,int	; 2698
vksyn,t,2,7,wl,int	; 2711
vksyn,t,10,12,wl,int	; 2719
vksyn,t,5,9,wl,int	; 2724

vksyn,t,8,11,wl,int	; 2748
vksyn,t,13,14,wl,int	; 2761
vksyn,t,0,6,wl,int17	; 2762
int=int+int17*2.6	
vksyn,t,3,8,wl,int	; 2767
vksyn,t,11,13,wl,int18	; 2782
int=int+int18*.7	
vksyn,t,6,10,wl,int	; 2783
vksyn,t,9,12,wl,int	; 2810
vksyn,t,1,7,wl,int19	; 2818
int=int+int19*1.5	
vksyn,t,4,9,wl,int	; 2826
vksyn,t,7,11,wl,int	; 2845
vksyn,t,12,14,wl,int20	; 2848
int=int+int20*.67	
vksyn,t,10,13,wl,int	; 2875
vksyn,t,2,8,wl,int21	; 2877
int=int+int21*.67	
vksyn,t,5,10,wl,int22	; 2887
int=int+int22*.5	
vksyn,t,8,12,wl,int23	; 2909
int=int+int23*.5	
vksyn,t,13,15,wl,int	; 2916
vksyn,t,0,7,wl,int24	; 2937
int=int+int24*2.6	
vksyn,t,3,9,wl,int	; 2938
vksyn,t,11,14,wl,int	; 2942
vksyn,t,6,11,wl,int	; 2951
vksyn,t,9,13,wl,int	; 2976
vksyn,t,1,8,wl,int25	; 2998
int=int+int25*1.5	
vksyn,t,4,10,wl,int	; 3002
vksyn,t,12,15,wl,int	; 3013
vksyn,t,7,12,wl,int	; 3017
vksyn,t,10,14,wl,int	; 3046
vksyn,t,2,9,wl,int	; 3062
vksyn,t,5,11,wl,int	; 3068
vksyn,t,13,16,wl,int	; 3087
vksyn,t,8,13,wl,int	; 3087
vksyn,t,11,15,wl,int	; 3119
vksyn,t,3,10,wl,int	; 3128
vksyn,t,0,8,wl,int26	; 3133
int=int+int26*2.6	
vksyn,t,6,12,wl,int	; 3137
vksyn,t,9,14,wl,int	; 3159
vksyn,t,12,16,wl,int	; 3196
vksyn,t,4,11,wl,int	; 3198
vksyn,t,1,9,wl,int27	; 3200
int=int+int27*1.5	
vksyn,t,7,13,wl,int	; 3210
vksyn,t,10,15,wl,int	; 3235
vksyn,t,2,10,wl,int	; 3269
vksyn,t,5,12,wl,int	; 3270
vksyn,t,13,17,wl,int	; 3276
vksyn,t,8,14,wl,int	; 3285
vksyn,t,11,16,wl,int	; 3315
vksyn,t,3,11,wl,int	; 3342
vksyn,t,6,13,wl,int	; 3345
vksyn,t,0,9,wl,int28	; 3353
int=int+int28*2.6	

```
vk$yn,t,9,15,wl,int           ; 3364
vk$yn,t,12,17,wl,int           ; 3399
vk(i)=convol(int,slit)

endfor
close,1
close,3
return
end
@[synspec]vk$yn
```

```
;Walden,1991
PRO NODLTCALC,WL,INT,SLIT
```

```
OPENU,10,'NODLT.DAT'
DLT=ASSOC(10,FLTARR(512))
WL=INDGEN(512)*3.133 + 1798
```

```
;This procedure calculates synthetic
; nitric oxide delta band spectra
; at temps from 100 to 2000 deg and
; convolves results with MUSTANG instru-
; ment slit function.
```

```
OPENR,11,'[WALDEN]SLIT.DAT'
SL=ASSOC(11,FLTARR(11))
SLIT=SL(1)
```

```
I=0
FOR T=100,2000,100 DO BEGIN
  I=I+1                                ; Wavelength
  INT=WL*0
  DELSYN,T,0,0,WL,INT      ; 1909.8
  DELSYN,T,0,1,WL,INT      ; 1980.5
  DELSYN,T,0,2,WL,INT      ; 2055.9
  DELSYN,T,0,3,WL,INT      ; 2134.8
  DELSYN,T,0,4,WL,INT      ; 2219.6
  DELSYN,T,0,5,WL,INT      ; 2310.1
  DELSYN,T,0,6,WL,INT      ; 2407.6
  DELSYN,T,0,7,WL,INT      ; 2509
  DELSYN,T,0,8,WL,INT      ; 2620
  DELSYN,T,0,9,WL,INT      ; 2739
  DELSYN,T,0,10,WL,INT     ; 2866
  DELSYN,T,0,11,WL,INT     ; 3003
  DELSYN,T,0,12,WL,INT     ; 3152
  DELSYN,T,0,13,WL,INT     ; 3313
  DELSYN,T,0,14,WL,INT     ; 3488

  DLT(I)=CONVOL(INT,SLIT)

ENDFOR

CLOSE,10
CLOSE,11

RETURN
END
?SYNSPEC]DELSYN
```

Walden, 1991

This program derives the synthetic spectrum using tweaking factors first determined by Mack(1991) for 1800-2100A, and extended the full range of the MUSTANG data.

RO NOGAMCALC,WL,INT,SLIT

```
OPENU,10,'NOGAM.DAT'
GAM=ASSOC(10,FLTARR(512))
WL=INDGEN(512)*3.133 + 1798
;This procedure calculates synthetic
; nitric oxide gamma band spectra
; at temps from 100 to 2000 deg and
; convolves results with MUSTANG instru-
; ment slit function.

OPENR,11,'[WALDEN]SLIT.DAT'
SL=ASSOC(11,FLTARR(11))
SLIT=SL(1)

I=0
FOR T=100,2000,100 DO BEGIN
  I=I+1
  ;These variables allow for the adjusting of
  ;individual transition's probability
  INT=WL*0
  INT1=WL*0
  INT2=WL*0
  INT3=WL*0
  INT4=WL*0
  INT5=WL*0
  INT6=WL*0
  INT7=WL*0
  INT8=WL*0
  INT9=WL*0
  INT10=WL*0.
  INT11=WL*0.
  INT12=WL*0.
  INT13=WL*0.
  INT14=WL*0.
  INT15=WL*0.
  INT16=WL*0.
  INT17=WL*0.
  INT18=WL*0.
  INT19=WL*0.
  INT20=WL*0.
  INT21=WL*0.
  INT22=WL*0.
  INT23=WL*0.
  This section calculates the spectrum from each transition's band
system.
  Transition          WL
  GAMSYN,T,3,0,WL,INT      ; 1956.1
  GAMSYN,T,3,1,WL,INT      ; 2029.8
  GAMSYN,T,2,0,WL,INT9      ; 2046.5
  INT=INT+INT9*.75
  GAMSYN,T,3,2,WL,INT      ; 2108.5
  GAMSYN,T,2,1,WL,INT      ; 2128.4
  GAMSYN,T,1,0,WL,INT1      ; 2148.1
  INT=INT+INT1*1.125
  GAMSYN,T,3,3,WL,INT      ; 2192.8
  GAMSYN,T,2,2,WL,INT2      ; 2215.4
```

```

INT=INT+INT2*1.26
GAMSYN,T,1,1,WL,INT3      ; 2238.3
INT=INT+INT3*1.3
GAMSYN,T,0,0,WL,INT4      ; 2261.8
INT=INT+INT4*1.2
GAMSYN,T,3,4,WL,INT       ; 2283.0
GAMSYN,T,2,3,WL,INT5      ; 2308.5
INT=INT+INT5*1.6
GAMSYN,T,1,2,WL,INT10     ; 2335
INT=INT+INT10*1.8
GAMSYN,T,0,1,WL,INT6      ; 2362.2
INT=INT+INT6*1.2
GAMSYN,T,3,5,WL,INT       ; 2378.8
GAMSYN,T,2,4,WL,INT       ; 2409
GAMSYN,T,1,3,WL,INT7      ; 2438.6
INT=INT+INT7*1.6
GAMSYN,T,0,2,WL,INT8      ; 2470.1
INT=INT+INT8*1.2
GAMSYN,T,3,6,WL,INT       ; 2481.2
GAMSYN,T,2,5,WL,INT       ; 2516.4
GAMSYN,T,1,4,WL,INT17     ; 2550.3
INT=INT+INT17*1.3
GAMSYN,T,0,3,WL,INT11     ; 2586.3
INT=INT+INT11*1.2
GAMSYN,T,3,7,WL,INT       ; 2591
GAMSYN,T,2,6,WL,INT       ; 2629.9
GAMSYN,T,1,5,WL,INT12     ; 2670.1
INT=INT+INT12*1.3
GAMSYN,T,3,8,WL,INT       ; 2709
GAMSYN,T,0,4,WL,INT13     ; 2712.0
INT=INT+INT13*1.2
GAMSYN,T,2,7,WL,INT       ; 2753.6
GAMSYN,T,1,6,WL,INT14     ; 2800.0
INT=INT+INT14*1.3
GAMSYN,T,3,9,WL,INT       ; 2836
GAMSYN,T,0,5,WL,INT15     ; 2848.2
INT=INT+INT15*1.2
GAMSYN,T,2,8,WL,INT       ; 2888.2
GAMSYN,T,1,7,WL,INT16     ; 2940.5
INT=INT+INT16*1.3
GAMSYN,T,3,10,WL,INT      ; 2973
GAMSYN,T,0,6,WL,INT18     ; 2997.6
INT=INT+INT18*1.2
GAMSYN,T,2,9,WL,INT       ; 3044.3
GAMSYN,T,1,8,WL,INT19     ; 3112.4
INT=INT+INT19*1.3
GAMSYN,T,3,11,WL,INT      ; 3120.6
GAMSYN,T,0,7,WL,INT20     ; 3170.7
INT=INT+INT20*1.2
GAMSYN,T,2,10,WL,INT      ; 3201.1
GAMSYN,T,1,9,WL,INT21     ; 3278.5
INT=INT+INT21*1.3
GAMSYN,T,3,12,WL,INT      ; 3303.0
GAMSYN,T,2,11,WL,INT      ; 3361
GAMSYN,T,0,8,WL,INT22     ; 3375.5
INT=INT+INT22*1.2
GAMSYN,T,3,13,WL,INT      ; 3456
GAMSYN,T,1,10,WL,INT23     ; 3458.5
INT=INT+INT23*1.3

```

```
GAM( I )=CONVOL( INT,SLIT )
ENDFOR
CLOSE,10
CLOSE,11
RETURN
END
@[SYNSPEC]GAMSYN
```

;Walden,1991  
PRO NOEPS CALC

```
OPENU,1,'NOEPS.DAT'  
EPS=ASSOC(1,FLTARR(512))
```

;This procedure calculates synthetic  
; nitric oxide epsilon band spectra  
; at temps from 100 to 2000 deg and  
; convolves results with MUSTANG instr-  
; ment slit function, where EPS(1)  
; corresponds to T=100,etc. It uses  
; scale factors determined by Bosserman  
; except for (0,1), which Bosserman  
; used .84 to tweak

```
WL=INDGEN(512)*3.133 + 1798
```

```
OPENR,2,['WALDEN]SLIT.DAT'  
SL=ASSOC(2,FLTARR(11))  
SLIT=SL(1)
```

```
I=0  
FOR T=100,2000,100 DO BEGIN  
    I=I+1  
    INT=WL*0  
    INT1=WL*0  
    INT2=WL*0  
    INT3=WL*0  
    INT4=WL*0  
    EPSSYN,T,1,0,WL,INT      ; 1799.6  
    EPSSYN,T,2,2,WL,INT      ; 1849.5  
    EPSSYN,T,1,1,WL,INT      ; 1863.2  
    EPSSYN,T,0,0,WL,INT1     ; 1876.6  
    INT=INT+INT1*.63  
    EPSSYN,T,2,3,WL,INT      ; 1918  
    EPSSYN,T,1,2,WL,INT      ; 1932.3  
    EPSSYN,T,0,1,WL,INT2     ; 1945.0  
    INT=INT+INT2*.90  
    EPSSYN,T,1,3,WL,INT      ; 1998.6  
    EPSSYN,T,0,2,WL,INT3     ; 2017.5  
    INT=INT+INT3*1.03  
    EPSSYN,T,1,4,WL,INT      ; 2073.0  
    EPSSYN,T,0,3,WL,INT4     ; 2094.5  
    INT=INT+INT4*1.11  
    EPSSYN,T,1,5,WL,INT      ; 2157.5  
    EPSSYN,T,0,4,WL,INT      ; 2176.1  
    EPSSYN,T,2,8,WL,INT      ; 2294.0  
    EPSSYN,T,2,9,WL,INT      ; 2385.0
```

```
EPS(I)=CONVOL(INT,SLIT)
```

```
ENDFOR
```

```
CLOSE,2  
CLOSE,1
```

```
ETURN  
ND  
[synspec]EPSSYN
```

```
;Walden,1991
pro OI_2972calc          ;This program creates a synthetic model for a
                           ; neutral atomic oxygen emission

openu,1,'OI_2972.dat'
dat=assoc(1,fltarr(512))

openr,2,['walden]slit.dat'
sl=assoc(2,fltarr(11))
slit=sl(4)                 ; adjusts wl to 2972 vice 2972.875

hold=fltarr(512)

hold=indgen(512)*0.0
hold(375)=1.0

dat(0)=convol(hold,slit)/3.133 ;spectra=1/wl bin so that scale factor is
                           ;absolute intensity

close,2
close,1

return
end
```

```

;Walden,1991
pro OII_2470calc
openu,1,'OII 2470.dat'
dat=assoc(1,fltarr(512))

openr,2,['walden]slit.dat'
sl=assoc(2,fltarr(11))
slit=sl(1)                                ;this makes wl centered @ 2968.5A

hold=fltarr(512)

hold=indgen(512)*0.0
hold(214)=1.0

dat(0)=convol(hold,slit)/3.133           ;spectra is 1/wl bin so scale factor
                                              ;is absolute intensity

close,2
close,1

return
end

```

```
;Walden,1991
;This program creates a synthetic model for the O++ atomic emission @ 2853A.
pro OIII_2853calc

openu,1,'OIII_2853.dat'
dat=assoc(1,fltarr(512))

openr,2,['walden]slit.dat'
sl=assoc(2,fltarr(11))
slit=sl(1)

hold=fltarr(512)

hold=indgen(512)*0.0
hold(337)=1.0

spike=convol(hold,slit)
dat(0)=spike/total(spike)/3.133 ;dat(0) is regular convolved spike
spike(338:510)=spike(339:511) ;dat(1) is spike with adjustment for apparent
; dropped point in data.
dat(1)=(spike/total(spike))/3.133

close,2
close,1

return
end
```

```

;Walden,1991
;This program calculates a synthetic spectrum for the NII doublet
;with the ratio based on the findings of Bcsela and Sharp (1989)
pro NII_doubcalc
    openu,1,'NII 2143doub.dat'
    nii=assoc(1,fltarr(512))

    openr,2,['walden]slit.dat'
    sl=assoc(2,fltarr(11))

    hold=fltarr(512)
    hold(109)=.58           ;2139.68A line
    int1=convol(hold,sl(1)) ;wl is in center of pixel

    hold2=fltarr(512)
    hold2(110)=1.0          ;2143.55 line
    int2=convol(hold2,sl(3));wl is 1/4 to the right of center of pixel

    int=int1+int2
    nii(1)=(int/total(int))/3.133
                                ;total of spectral area is 1/wl bin, so
                                ;scale factor will be the absolute intensity

close,2
close,1
return
end

```

```

;Walden,1991
;This program creates a synthetic spectrum of atomic emissions observed in
;the March 1990 MUSTANG data.
pro otherspec

openr,1,['walden]slit.dat'
slit=assoc(1,fltarr(11))

openu,2,'otherspec.dat'
spect=assoc(2,fltarr(512))

spec=fltarr(512)
numlines=20
;number of contributing atomics
;wavelengths determined from Bureau of Standards
;listing of atomic emissions and NASA listing of atomic
;emissions

;      Wavelength          Species      Pixel
;      1846.0            NIII        15
;      2182.6            OII         123
;      2190.6            OII         125
;      2337.8            ARII        172
;      2384.6            OIV         187
;      2445.6            OII         207
;      2490.3            NII         221
;      2509.9            NII         227
;      2665.8            OIII        277
;      2709.8            NII         291
;      2741.3            OII         301
;      2885.3            NII         347
;      2973.6,2974.6,     NII multiplet 375-377
;      2975.7,2975.9,
;      2976.9,2977.3,
;      2978.4,2978.6

pix=[15,123,125,172,187,207,221,227,277,291,301,347,$
     375,375,376,376,376,376,377,377]

int=[10,2,1,10,9,3,3,4,5,6,4,4,2,3,3,4,4,4,4,5,5]
slno=[3,4,3,3,4,4,1,3,1,1,1,1,3,2,4,1,3,2,4,4]

for i=0,numlines-1 do begin
    blank=fltarr(512)
    blank(pix(i))=.1*int(i)
    impulse=convol(blank,slit(slno(i)))
    spec=spec+impulse
endfor

spect(0)=indgen(512)*3.133+1798
spect(1)=(spec/total(spec))/3.133      ;so that scale factor is absolute int.

close,2
close,1
return
end

```

## APPENDIX C

Appendix C is the programs used to determine the standard deviations of the means(sdoms) for the data. The sdoms are used to determine the weighting factors for the fitting routine by the program titled "weights2," which is also included.

```

;Walden,1991
pro m90sdev,alt,index1,index2

;This procedure calculates the std.dev and std dev of the mean
;for the averaged spectra.
;Inputs consist of the requested altitude (1-25) and its corresponding
;beginning and ending index numbers.
;Outputs are the SDOM (unshifted and shifted) and are written to
;um90_sdom.dat and m90_sdom.dat, respectively

navg=0
st=''
sigma=dblarr(512)
sigmam=dblarr(512)

openr,1,'dub0:[clayton]mustang_raw.dat'
dat=assoc(1,intarr(512))                                ;opens the raw data file

openr,2,['mustang]um90_avg.dat'
avg=assoc(2,fltarr(512))                                ;opens the averaged spectrum file
; (unshifted version)

openu,3,['mustang]um90_sdm.dat'                         ;opens the file to write SDOM into
sdom=assoc(3,fltarr(512))

n=index2-index1
for j=0,n do begin
  print,index1+j
  print,'Do you want to include this record'
  print,'Type <CR> for yes, N for no.'
  read,st
  if st eq 'n' then goto,label1
  sigma=sigma + (dat(index1+j)-avg(alt))^2
  navg=navg+1
  label1:dummy=0
endfor
free=navg-1
sigma=sqrt(sigma/free)
sigmam=sigma/sqrt(navg)
sdom(alt)=sigmam

lose,1
lose,2
lose,3

return
nd

```

```
;Walden,1991
pro weights2
```

```
;This program checks for values where the detector saturated, and gives
;weights based on the deviations of the mean being equal to the data at
;those points. It also gives a small weight factor to those elements
;corresponding to nitrogen second positive wavelengths (sets sdom equal to
;largest data value in N2 2nd pos bands). Since sdom was given value of data at
;dropped points, it gives small weights to dropped values (with the exception
;of 2972A)
```

```
openr,1,['mustang]m90_intsdm.dat'
dom=assoc(1,fltarr(512))
```

```
openr,2,['mustang]m90_int.dat'
dat=assoc(2,fltarr(512))
```

```
openu,3,'m90_domwt.dat'
domwt=assoc(3,fltarr(512))
```

```
openr,4,['mack]mack_cal.dat'
ss=assoc(4,fltarr(512))
sens=ss(22)
```

```
openr,5,['mustang]m90_avg.dat'
dd=assoc(5,fltarr(512))
```

```
big=1800                                ;approx N2 2nd pos largest datapoint value
holddom=fltarr(512)
holddomwt=fltarr(512)
holddat=fltarr(512)
sat=900.00/sens
```

```
for i=1,25 do begin
    holddom=dom(i)
    holddat=dat(i)
    for j=0,511 do begin
;if detector was saturated, make sdom equal to data value
        if (holddat(j) gt sat(j)) then holddom(j)=holddat(j)
;if wavelength is in N2 2nd pos, make sdom equal to big      wavelength
if (j eq 277) or (j eq 278) or (j eq 279) then holddom(j)=big ;2669
if (j eq 318) or (j eq 319) or (j eq 320) then holddom(j)=big ;2796
if (j eq 322) or (j eq 323) or (j eq 324) then holddom(j)=big ;2811
if (j eq 362) or (j eq 363) or (j eq 364) then holddom(j)=big ;2934
if (j eq 368) or (j eq 369) or (j eq 370) then holddom(j)=big ;2953
if (j eq 374) or (j eq 375) or (j eq 376) then holddom(j)=big ;2973
if (j eq 409) or (j eq 410) or (j eq 411) then holddom(j)=big ;3083
if (j eq 417) or (j eq 418) or (j eq 419) then holddom(j)=big ;3107
if (j eq 425) or (j eq 426) or (j eq 427) then holddom(j)=big ;3132
if (j eq 433) or (j eq 434) or (j eq 435) then holddom(j)=big ;3157
if (j eq 461) or (j eq 462) or (j eq 463) then holddom(j)=big ;3244
if (j eq 470) or (j eq 471) or (j eq 472) then holddom(j)=big ;3274
if (j eq 480) or (j eq 481) or (j eq 482) then holddom(j)=big ;3305
if (j eq 490) or (j eq 491) or (j eq 492) then holddom(j)=big ;3337
if (j eq 501) or (j eq 502) or (j eq 503) then holddom(j)=big ;3370
```

```
f (j gt 493) then holddom(j)=big ;last spike
```

```
now give weights their values
```

```
    if holddom(j) eq 0. then holddomwt(j)=1.
```

```

        if holddom(j) ne 0. then holddomwt(j)=1./holddom(j)^2
    endfor
;Correct for where low value of data point at dropped word gives false
;high weight to point by giving dropped points 1/10 the maximum weight
;of any other point
;(except for 2972A -pixels 371 to 376 and 2850A -333 to 336).
dropped=where(dd(i) eq -1.)
hold=holddomwt
hold(dropped)=0.0
holddomwt(dropped)=.1*max(hold)
;    holddomwt(371:376)=max(hold)
;    holddomwt(333:336)=max(hold)
;assign weight to file m90_domwt.dat
domwt(i)=holddomwt
endfor
close,1
close,2
close,3
close,4
close,5
return
end

```

```

;Walden,1991
;This program shifts the MUSTANG data array according to dropped pixels, as
;input in the procedure shiftarray.
pro shiftdata

    openr,1,['mustang]um90_avg.dat'
    mm=assoc(1,fltarr(512))

    openu,2,['mustang]m90_avg.dat'
    dd=assoc(2,fltarr(512))

    openr,3,['mustang]um90_sdm.dat'
    uu=assoc(3,fltarr(512))

    openu,4,['mustang]m90_sdm.dat'
    ss=assoc(4,fltarr(512))

    wl=indgen(512)*3.133+1798

    dd(0)=wl
    ss(0)=wl

    for i=1,25 do begin
        shiftarray,mm(i),hold1
        dd(i)=hold1
        shiftarray,uu(i),hold2
        ss(i)=hold2
    endfor

    close,4
    close,3
    close,2
    close,1

    return
end

```

```
;Walden,1991
;This program shifts an array of data according to the "drop" array of
;pixels.
pro shiftarray,inarr,outarr

drop=[462,446,430,414,398,382,366,350,350,334,318,302,286,270,254,239,223,223,$
      207,191,175,159,143,127,111,95,95,80,80,64,48,32,16]

ndrops=n_elements(drop)
outarr=inarr
length=n_elements(inarr)

for i=0,ndrops-1 do begin
;      This section is to put a -1 in dropped values and shift as required.
      outarr(drop(i)+1)=outarr(drop(i):length-2)
      outarr(drop(i))=-1.0
endfor

return
end
```

```

;Walden,1991
;This program takes the MUSTANG data from the averaged, shifted records
;and puts in the appropriate average, and adjusts for instrument response.
pro average

    openr,1,['mustang]m90_avg.dat'
    mm=assoc(1,fltarr(512))

    openr,2,['mustang]m90_sdm.dat'
    ss=assoc(2,fltarr(512))

    openu,3,['mustang]m90_int.dat'
    dat=assoc(3,fltarr(512))

    openu,4,['mustang]m90_intsdm.dat'
    dev=assoc(4,fltarr(512))

    openr,5,['mack]mack_cal.dat'
    sen=assoc(5,fltarr(512))
    sens=sen(22)
boolean=fltarr(512)
dat(0)=mm(0)
dev(0)=ss(0)

for i=1,25 do begin
;get array of where dropped words are
    points=mm(i)
    index=where(points eq -1.0)
;correct for sensitivity
    points=points/sens
;assign average for dropped data values
    points(index)=(points(index+1)+points(index-1))/2.
;correct averages for double drops
    boolean(index)=1
    double=where(boolean*shift(boolean,-1))
    points(double)=(2*points(double-1)+points(double+2))/3.
    points(double+1)=(points(double-1)+2*points(double+2))/3.
;assign value of data to dropped word sdom's
    errors=ss(i)
    errors(index)=points(index)
;zero first six elements
    points(0:5)=0.0
    errors(0:5)=0.0
assign data to m90_int.dat
    dat(i)=points
correct for sensitivity and assign sdom to m90_intsdm.dat
    dev(i)=errors/sens
endfor

close,5
close,4
lose,3
lose,2
lose,1

eturn
nd

```

```
;Walden,1991
pro units

openr,1,['mustang]m90_avg.dat' ;reads out avg spectra, shifted
a=assoc(1,fltarr(512))

openr,4,['mustang]m90_sdm.dat' ;reads out SDOMs, shifted
c=assoc(4,fltarr(512))

openr,2,['mack]mack_cal.dat' ;calibration to correct units to intensity
b=assoc(2,fltarr(512))
sens=b(22)

openw,3,['mustang]m90_int.dat',512*4 ;file to accept corrected values
int=assoc(3,fltarr(512))

openw,5,['mustang]m90_intsdm.dat',512*4
intdom=assoc(5,fltarr(512))

for i=1,25 do begin
    int(i) = a(i)/sens
    intdom(i)=c(i)/sens
endfor

close,1
close,2
close,3
close,4
close,5

return
end
```

```
;Walden,1991
;This program assigns zeros to the first six values of an array of 512.
pro zerosix, fname

openu,1, fname
a=assoc(1,fltarr(512))

temp=fltarr(512)

for i=1,25 do begin
    temp=a(i)
    temp(0:5)=0.0
    a(i)=temp
endfor

close,1
return
end
```

## APPENDIX D

Appendix D shows the programs used to convert the scale factors obtained from the fitting routine to absolute intensities. The equations were derived from Barth (1965).

The equation used for converting the scale factor to intensity for the VK(0,5) band is:

$$I_{0,5} = VKCALC(0,5) * SF(alt),$$

where  $I_{0,5}$  is the band intensity in Rayleighs,  $VKCALC(0,5)$  is the total intensity of the synthetic VK(0,5) band in Rayleighs, and  $SF(alt)$  is the VK scale factor for the altitude desired. The factor  $VKCALC$  is just the area under the synthetic spectrum curve for the transition and is obtained using the IDL command  $TOTAL()$  and multiplying by wavelength bin size, as seen in the program VK\_ABSINT.

The conversion for the LBH scale factor included all bands, and is performed in the program LBH\_ABSINT and the subroutine INTENCALC. The basic equation for this program, derived from equations (4) & (8) of Barth (1965) is given by:

$$I_{LBH} = \frac{LBHCALC(j, k) \sum_{allv''} q_{j, v''} v_{j, v''}^3}{v_{j, k}^3 q_{j, 0} q_{j, k}},$$

where  $I_{LBH}$  is the total intensity of LBH emissions in Rayleighs,  $LBHCALC(j, k)$  is the area under the synthetic spectrum curve for a transition band  $(j, k)$ ,  $q_{j, k}$  is the Franck-

Condon factor for the  $(j, k)$  band, and  $\nu$  is the corresponding frequency for each transition. The summation over  $v''$  is to include all possible upper states. The result of this equation was essentially the same for any  $(j, k)$ . This thesis utilized the  $(4, 12)$  transition.

```

;Walden,1991
;This program converts the scale factor from the nimpfit_all routine into
;an absolute intensity for a particular transition band of Vegard-Kaplan.
;Stored in vk_absint.dat, the values are for the (0,5) transition in record 1,
;the (0,6) in record 3, and the (1,8) in record 5.
pro vk_absint
    openr,10,'finalpara.dat'
    p=assoc(10,fltarr(25))
    temp=p(0)
    alt=p(21)
    vksf=p(13)
    delvksf=p(14)

    openu,11,'vk_absint.dat'
    dat=assoc(11,fltarr(25))
    dat(0)=alt

    wl=indgen(512)*3.133+1798
    hold=fltarr(25)
    errhold=fltarr(25)

    for run=2,6,+2 do begin
        if (run eq 2) then begin ;F-C factors are not currently used
            v1=0 ;in the determination of intensity,
            v2=5 ;but are included for future use
        ; q1=5.9e-4 ;F-C factor for (0,0)
        ; q2=1.69e-1 ;F-C factor for (0,5)
        twk=2.6
        endif
        if (run eq 4) then begin
            v1=0
            v2=6
            q1=5.9e-4 ;F-C factor for (0,0)
            q2=1.89e-1 ;F-C factor for (0,6)
            twk=2.6
        endif
        if (run eq 6) then begin
            v1=1
            v2=8
            q1=3.32e-3 ;F-C factor for (1,0)
            q2=7.87e-2 ;F-C factor for (1,8)
            twk=1.5
        endif
        for a=0,24 do begin
            int=indgen(512)*0.0
            vksyn,temp(a),v1,v2,wl,int
            int=int*twk
            hold(a)=total(int)*3.133*vksf(a)
            errhold(a)=total(int)*3.133*delvksf(a)
        endfor
        dat(run-1)=hold
        dat(run)=errhold
    endfor
lose,10
lose,11

eturn
nd
[synspec]vksyn

```

```

;Walden,1991
pro lbh_absint
; This program determines the absolute intensity of LBH emissions based
; on the fits of intensity to three different transition bands (the results were
; basically equal in Walden's analysis). Stored in record 1 of lbh_absint.dat
; is based on th (2,9), record 3 is the (4,12), record 5 is (3,10).-
    openr,10,'finalpara.dat'
    p=assoc(10,fltarr(25))
    temp=p(0)
    lbhsf=p(9)
    dellbhsf=p(10)
    alt=p(21)

    openr,11,'lbh_tots.dat'
    t=assoc(11,fltarr(20))
    lbhtotint=t(0)

    openu,12,'lbh_absint.dat'
    i=assoc(12,fltarr(25))
    i(0)=alt

    hold=fltarr(25)
    errhold=fltarr(25)

for run=1,3 do begin
    if (run eq 1) then begin
    v1=2
    v2=9
    endif
    if (run eq 2) then begin
    v1=4
    v2=12
    endif
    if (run eq 3) then begin
    v1=3
    v2=10
    endif
    for a=0,24 do begin
        intencalc,temp(a),v1,v2,bandint
        intlbh=bandint*3.133*lbhsf(a)/lbhtotint((temp(a)/100)-1)
        errintlbh=bandint*3.133*dellbhsf(a)/lbhtotint((temp(a)/100)-1)
        hold(a)=intlbh
        errhold(a)=errintlbh
    endfor
    i(2*run-1)=hold          ;put absolute intensities in appropriate record
    i(2*run)=errhold         ;put errors in correct record
endfor

:close,10
:close,11
:close,12

return
nd
[synspec]lbhsyn

```

```

;Walden,1991
;This procedure is called by the lbh_absint program in order to determine
;the intensity under a particular "hump" (a transition band) in the LBH curve.
;The inputs v1 and v2 are the upper and lower states' vibrational levels
;for the transition to be determined. Intlbh returns the intensity value.
pro intencalc,T,v1,v2,intlbh

openr,1,'[synspec]frnkcondn.dat'
fc=assoc(1,fltarr(15,30))
lbhfc=fc(0)

openr,2,'[walden]lbhtrans_wl.dat'
wl=assoc(2,fltarr(15,30))
lbhw1=wl(0)

summa=0.0
wl=indgen(512)*3.133+1798
int=fltarr(512)
lbhfreq=fltarr(15,30)

for j=0,14 do begin
    for k=0,29 do begin
        if (lbhw1(j,k) ne 0) then lbhfreq(j,k)=2.997e8/lbhw1(j,k)
        if (lbhw1(j,k) eq 0) then lbhfreq(j,k)=0.0
    endfor
endfor

for i=0,29 do begin
    summa=summa+(lbhfreq(v1,i)^3)*lbhfc(v1,i)
endfor

lbhsyn,T,v1,v2,wl,int

intv1v2=total(int)

intlbh=intv1v2*summa/(lbhfreq(v1,v2)^3*lbhfc(v1,0)*lbhfc(v1,v2))

close,1
close,2
return
end
@[synspec]lbhsyn

```

## APPENDIX E

Appendix E contains plots of the final fits obtained, along with the program used to print them. The plots are divided into 400Å increments, from 1800Å to 3400Å, and are in order of increasing altitude. Each plot shows the fit versus data in the upper view, and a breakdown of the fit by major contributors in the second view.

```

;Walden,1991
pro plotapp,alt,xmin,xmax
;program plots data vs. fit and fit by
;parts in format used by Walden thesis
;for appendix. alt can be 1 to 25, xmin
;and xmax are presumed to be 1800-2200,
;2200-2600,2600-3000, or 3000-3400, so
;other combinations would need adjust-
;ments to the plot key

openr,1,'finalpara.dat'
para=assoc(1,fltarr(25))

height=para(21)

openr,2,['mustang]m90 intnh.dat'
d=assoc(2,fltarr(512)) ;data is in records d=1 to 25

openr,3,'finaltwk.dat'
f=assoc(3,fltarr(512)) ;fits are in records f=1 to 25

temp=para(0)
it=(temp(alt-1))/100

openr,4,'all_lbh.dat'
vk=assoc(4,fltarr(512))
pvk=para(13)

openr,5,'all_lbh.dat'
1bh=assoc(5,fltarr(512))
p1bh=para(9)

openr,6,'nodlt.dat'
dlt=assoc(6,fltarr(512))

openr,7,'noeps.dat'
eps=assoc(7,fltarr(512))

openr,8,'nogammack.dat'
gam=assoc(8,fltarr(512))

pno=para(11)

openr,9,'OIII_2853.dat'
oiii=assoc(9,fltarr(512))
poiii=para(7)

openr,10,'OII_2470.dat'
ooi=assoc(10,fltarr(512))
poii=para(5)

openr,11,'OI_2972.dat'
oi=assoc(11,fltarr(512))
poi=para(3)

openr,12,'NII_2143doub.dat'
n2=assoc(12,fltarr(512))
pn2=para(15)

w1=indgen(512)*3.133+1798.000

```

```

set_plot,'hp'
device,/portrait,/plotter_on_off
device,xoffset=1.27
device,yoffset=.635
device,xsize=17.78
device,ysize=24.13

;TOP OF PAGE--DATA AND FIT
set_xy,xmin,xmax
set_viewport,.18,.82,.59,.91

if (alt ge 18) then $
!mttitle='Data & Fit at '+strtrim((fix(height(alt-1))),2) +'km (downleg)'
if (alt lt 18) then $
!mttitle='Data & Fit at '+strtrim((fix(height(alt-1))),2) +'km (upleg)'

!xtitle='Wavelength(A)'
!ytitle='Intensity(R/A)'

dat=d(alt)
fit=f(alt)

!linetype=0
plot,wl,dat

!linetype=2
oplot,wl,fit

;KEY FOR TOP PLOT--xrange must be determined in terms of pixels so that
;yrange can be known for placing the key in the correct place on the graph
;case section does this for the ranges designated

case 1 of
(xmin eq 1800) and (xmax eq 2200): begin
    ldat=dat(0:129)
    lfit=fit(0:129)
    end
(xmin eq 2200) and (xmax eq 2600): begin
    ldat=dat(129:257)
    lfit=fit(129:257)
    end
(xmin eq 2600) and (xmax eq 3000): begin
    ldat=dat(257:384)
    lfit=fit(257:384)
    end
(xmin eq 3000) and (xmax eq 3400): begin
    ldat=dat(384:511)
    lfit=fit(384:511)
    end
else: begin
    ldat=dat
    lfit=fit
    end
endcase

;key will probably not be correct
;this section must be manually altered
;to concur with the wl range

;this section designates x and y coordinates for the sample lines in the key
xcoord1=[xmin+20,xmin+50]
xcoord2=[xmin+20,xmin+100]
xcoord3=[xmin+120,xmin+200]
ycoord1=[.96*max(ldat),.96*max(ldat)]

```

```

ycoord2=[.90*max(ldat),.90*max(ldat)]
ycoord3=[.84*max(ldat),.84*max(ldat)]
ycoord4=[.78*max(ldat),.78*max(ldat)]
ycoord5=[.72*max(ldat),.72*max(ldat)]
ycoord6=[.66*max(ldat),.66*max(ldat)]
ycoord7=[.60*max(ldat),.60*max(ldat)]

!linetype=0
oplot,xcoord1,ycoord1
!linetype=2
oplot,xcoord1,ycoord2
!linetype=0
xyouts,xmin+60,.995*ycoord1(0),'Data'
xyouts,xmin+60,.995*ycoord2(0),'Fit'

;BOTTOM OF PAGE--PLOT OF PARTS AND FIT

set_xy,xmin,xmax
set_viewport,.18,.82,.09,.41

!mtitle='Data and Fit by Parts'
!xtitle='Wavelength(A)'
!ytitle='Intensity(R/A)'

!linetype=0
plot,w1,dat
oplot,w1,dat
!linetype=1
oplot,w1,vk(it)*pvk(alt-1)
!linetype=2
oplot,w1,lbh(it)*plbh(alt-1)
!linetype=3
nitric=pno(alt-1)*(gam(it)+eps(it)+.25*dlt(it))/3.133e6
oplot,w1,nitric
!linetype=4
oplot,w1,oiii(0)*poiii(alt-1)
!linetype=5
oplot,w1,n2(1)*pn2(alt-1)
!linetype=5
oplot,w1,oii(0)*poii(alt-1)
!linetype=5
oplot,w1,oi(0)*poi(alt-1)

;key for bottom plot--x and y ranges from top plot used for locating key

case 1 of
(xmin eq 1800) and (xmax eq 2200): begin
    !linetype=0
    oplot,xcoord2,ycoord1
    oplot,xcoord2,ycoord1
    !linetype=3
    oplot,xcoord2,ycoord2
    !linetype=2
    oplot,xcoord2,ycoord3
    !linetype=5
    oplot,xcoord2,ycoord4
    !linetype=0
    xyouts,xmin+110,.995*ycoord1(0),'Data'
    xyouts,xmin+110,.995*ycoord2(0),'NO'

```

```

xyouts,xmin+110,.995*ycoord3(0),'LBH'
xyouts,xmin+110,.995*ycoord4(0),'NII doublet 2143A'
end
(xmin eq 2200) and (xmax eq 2600): begin
!linetype=0
oplot,xcoord2,ycoord1
oplot,xcoord2,ycoord1
!linetype=3
oplot,xcoord2,ycoord2
!linetype=2
oplot,xcoord2,ycoord3
!linetype=1
oplot,xcoord2,ycoord4
!linetype=5
oplot,xcoord2,ycoord5
!linetype=0
xyouts,xmin+110,.995*ycoord1(0),'Data'
xyouts,xmin+110,.995*ycoord2(0),'NO'
xyouts,xmin+110,.995*ycoord3(0),'LBH'
xyouts,xmin+110,.995*ycoord4(0),'VK'
xyouts,xmin+110,.995*ycoord5(0),'OII 2470A'
end
(xmin eq 2600) and (xmax eq 3000): begin
!linetype=0
oplot,xcoord3,ycoord1
oplot,xcoord3,ycoord1
!linetype=3
oplot,xcoord3,ycoord2
!linetype=1
oplot,xcoord3,ycoord3
!linetype=5
oplot,xcoord3,ycoord4
!linetype=4
oplot,xcoord3,ycoord5
!linetype=0
xyouts,xmin+210,.995*ycoord1(0),'Data'
xyouts,xmin+210,.995*ycoord2(0),'NO'
xyouts,xmin+210,.995*ycoord3(0),'VK'
xyouts,xmin+210,.995*ycoord4(0),'OI 2972A'
xyouts,xmin+210,.995*ycoord5(0),'OIII 2853A'
end
(xmin eq 3000) and (xmax eq 3400): begin
!linetype=0
oplot,xcoord2,ycoord1
oplot,xcoord2,ycoord1
!linetype=3
oplot,xcoord2,ycoord2
!linetype=1
oplot,xcoord2,ycoord3
!linetype=0
xyouts,xmin+110,.995*ycoord1(0),'Data'
xyouts,xmin+110,.995*ycoord2(0),'NO'
xyouts,xmin+110,.995*ycoord3(0),'VK'
end
else: dummy=0
endcase

;close,13
close,12
close,11

```

```
close,10
close,9
close,8
close,7
close,6
close,5
close,4
close,3
close,2
close,1
```

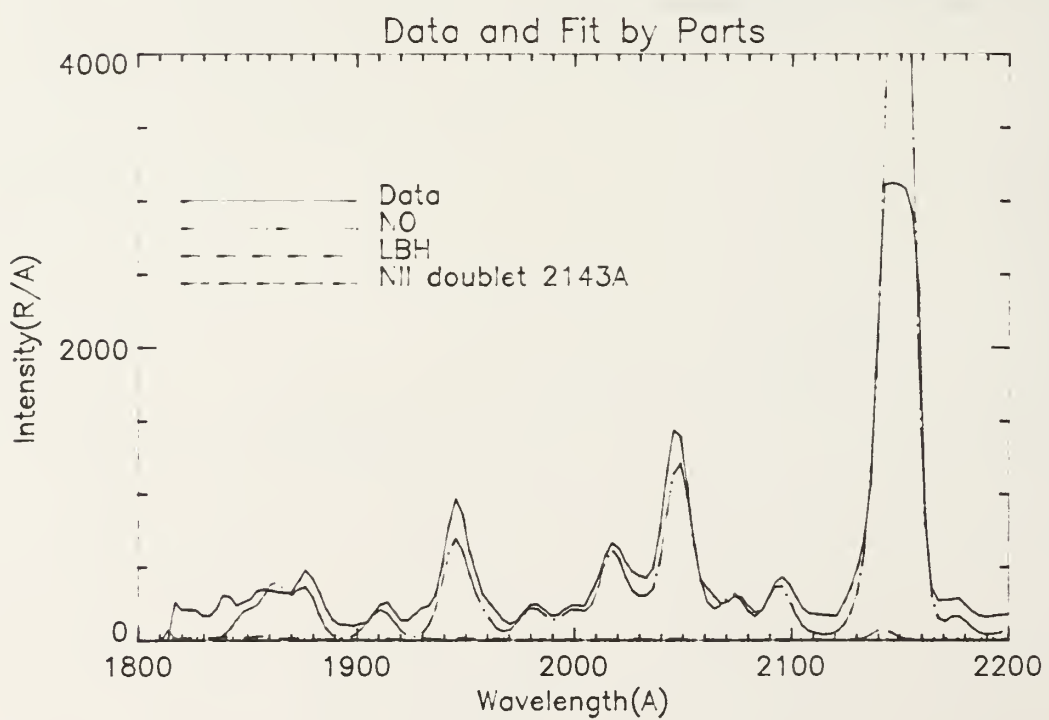
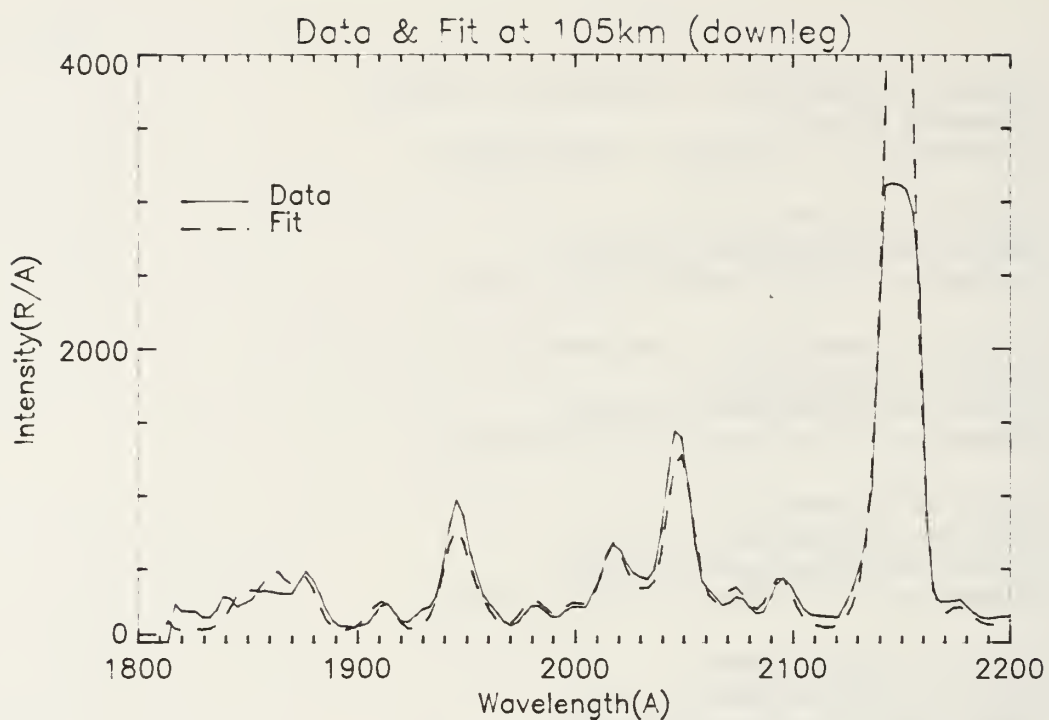
```
return
end
```

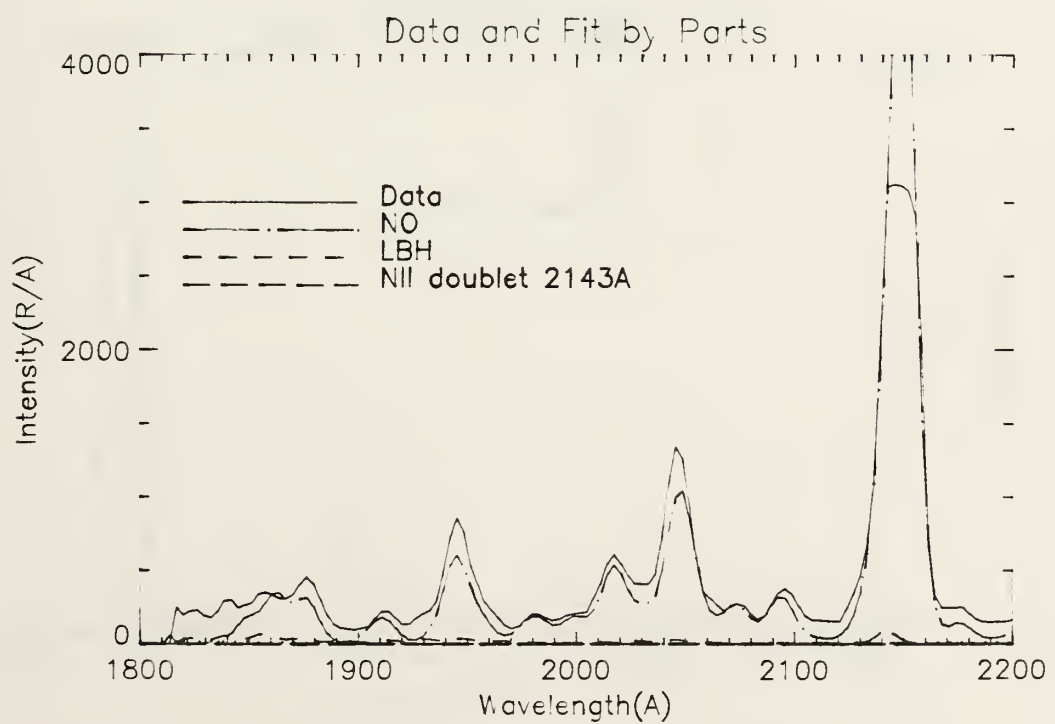
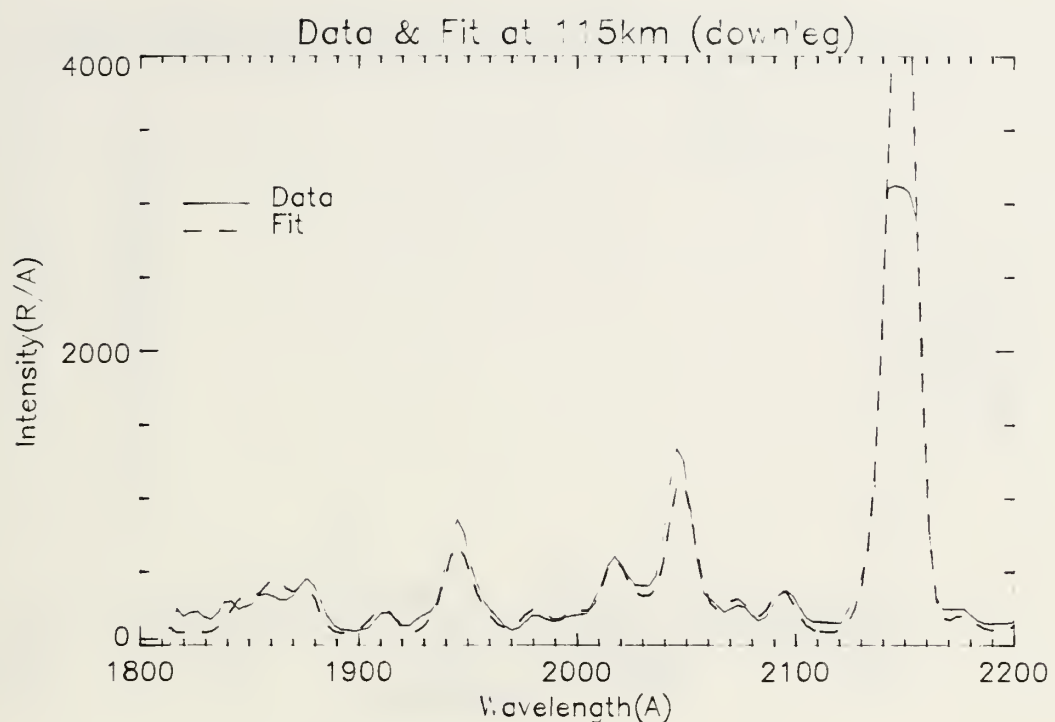


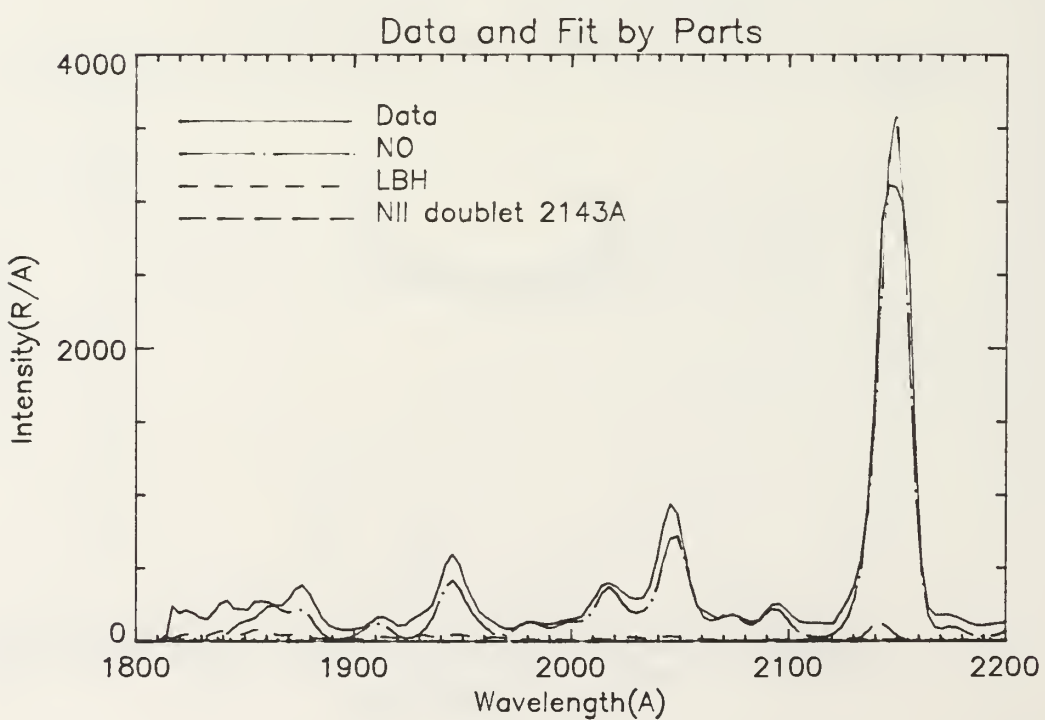
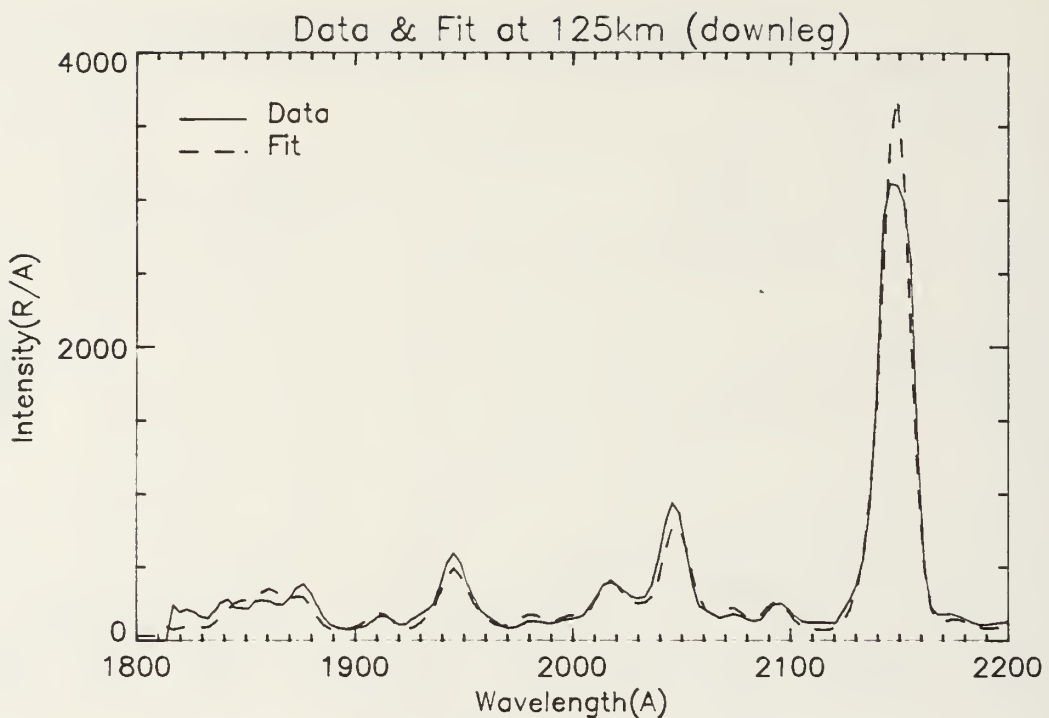
INITIAL DISTRIBUTION LIST

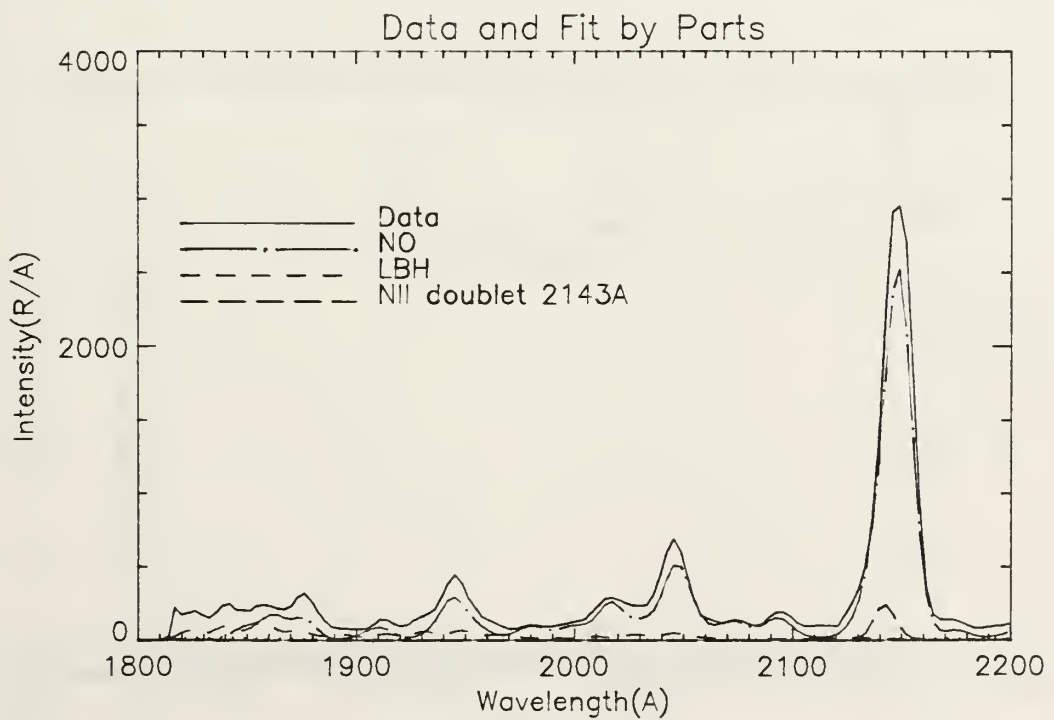
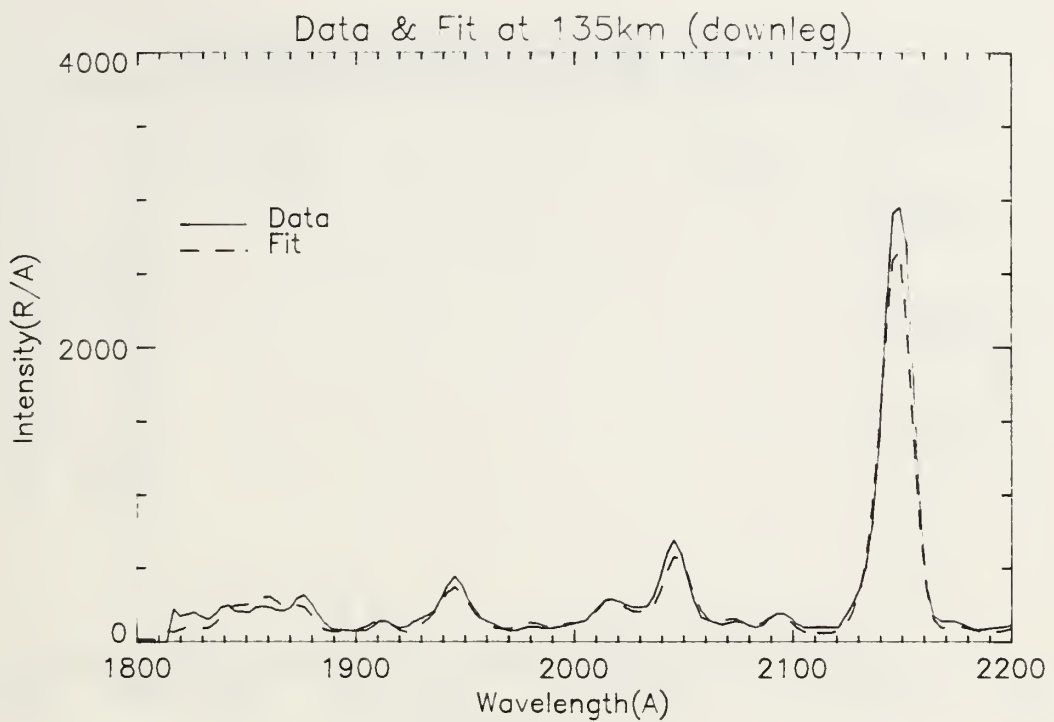
No. Copies

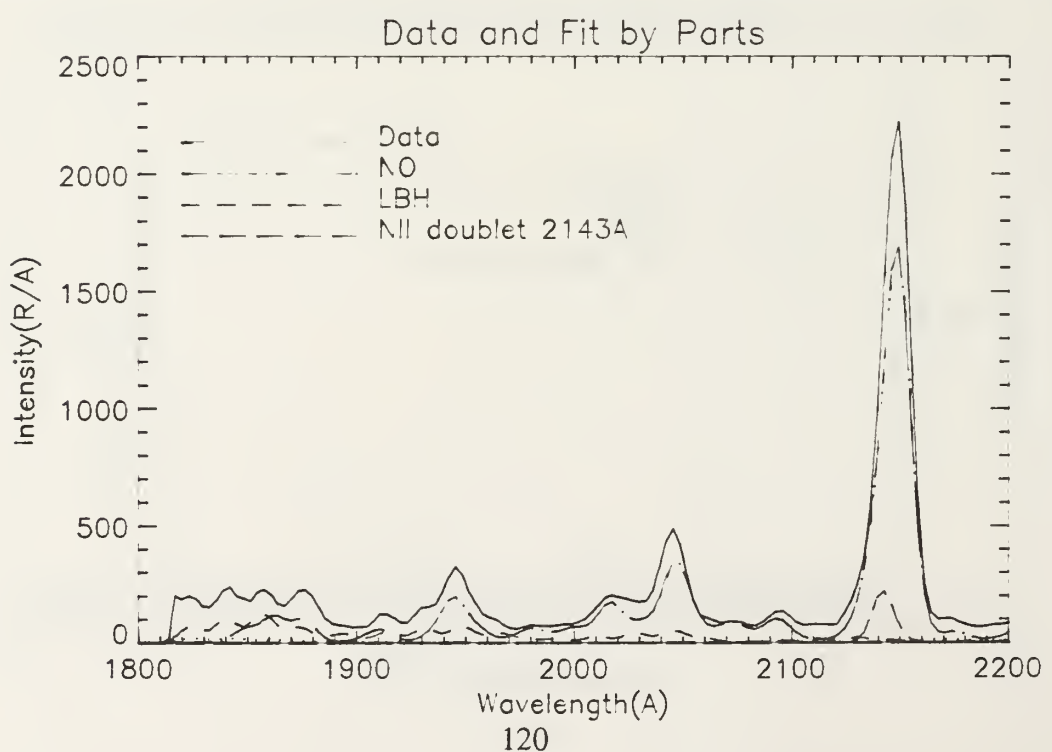
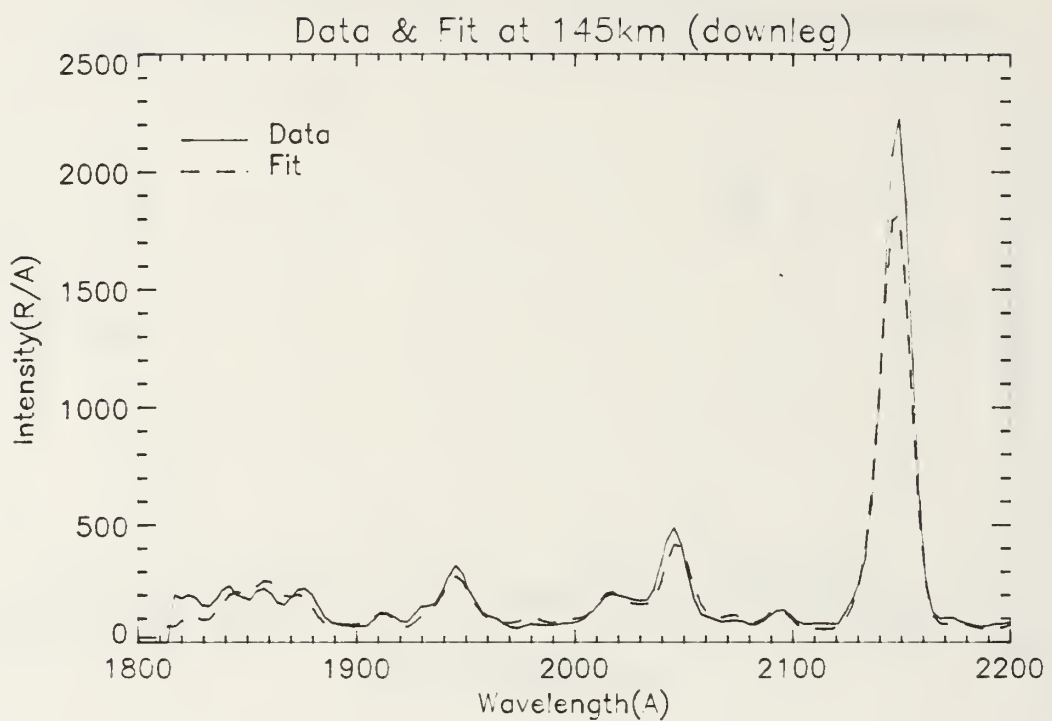
1.	Defense Technical Information Center Cameron Station Alexandria, Virginia 22394-6145	2
2.	Library, Code 0142 Naval Postgraduate School Monterey, California 93943-5002	2
3.	Dr. K.E. Woehler, Chairman 61 Physics Department Naval Postgraduate School Monterey, California 93943-5000	1
4.	Dr. D.D. Cleary Physics Department 61-C1 Naval Postgraduate School Monterey, California 93943-5000	5
5.	Dr. S. Gnanalingam Physics Department 61-Gm Naval Postgraduate School Monterey, California 93943-5000	1
6.	LT Billie S. Walden c/o Mr. J.W. Dickson, Jr. 3060 Shipley Street Kingsport, Tennessee 37664	2

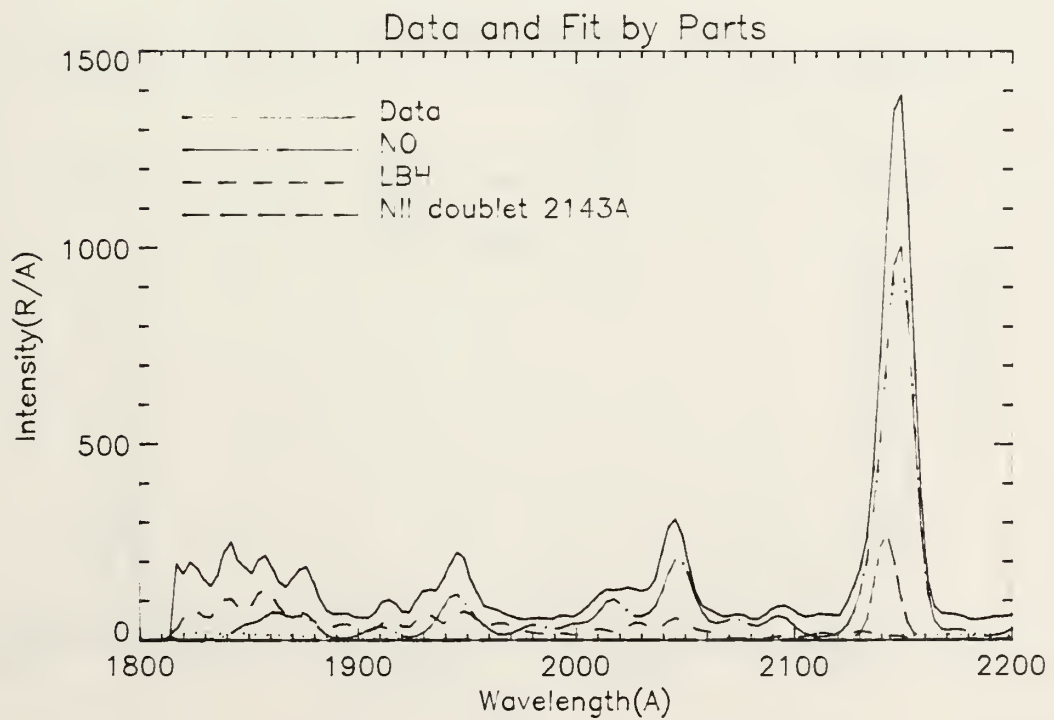
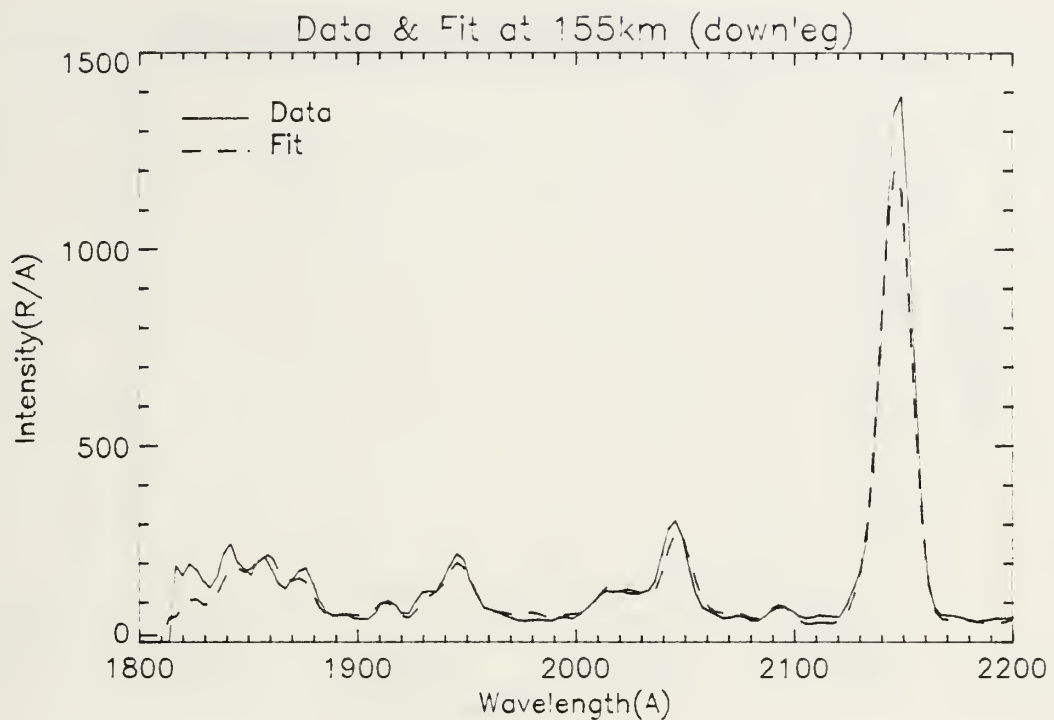


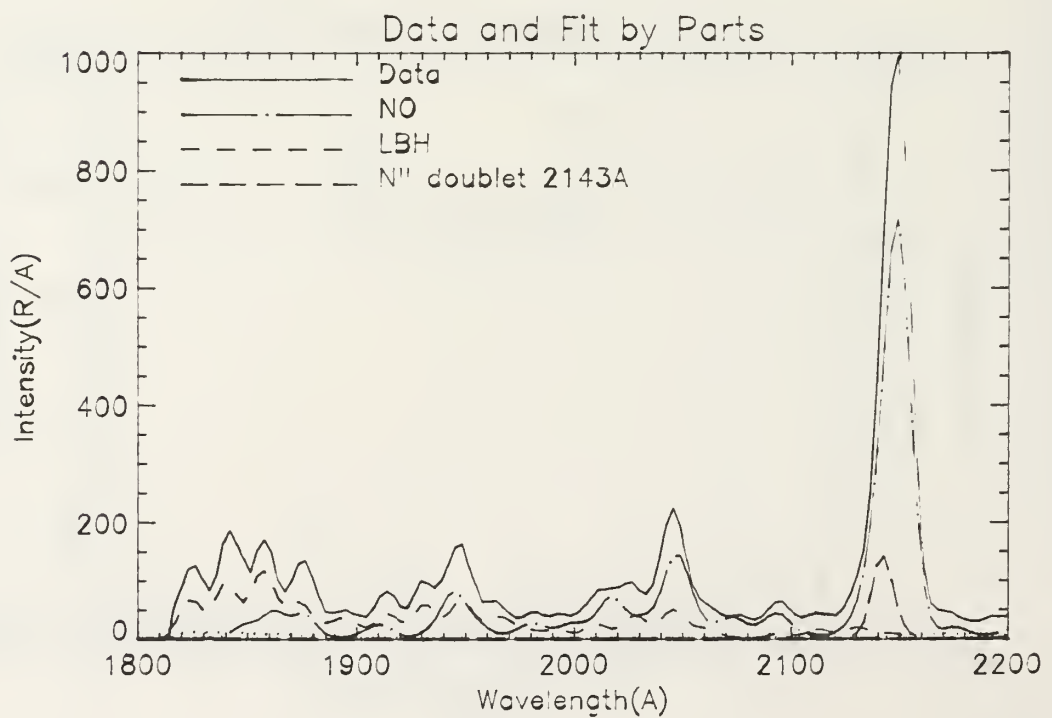
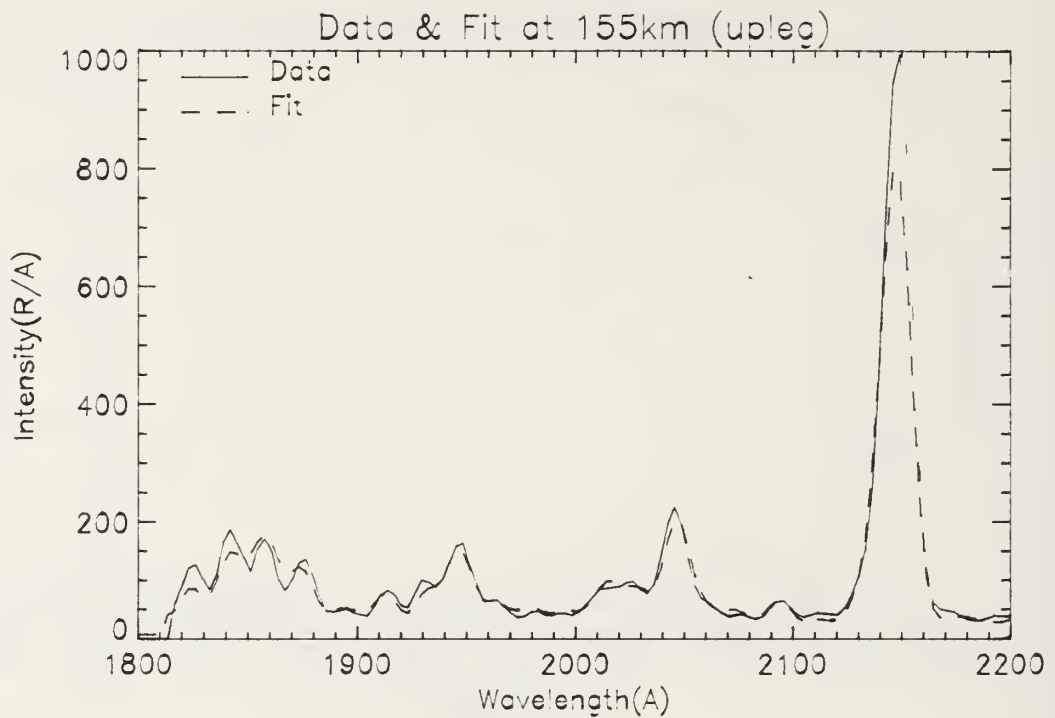


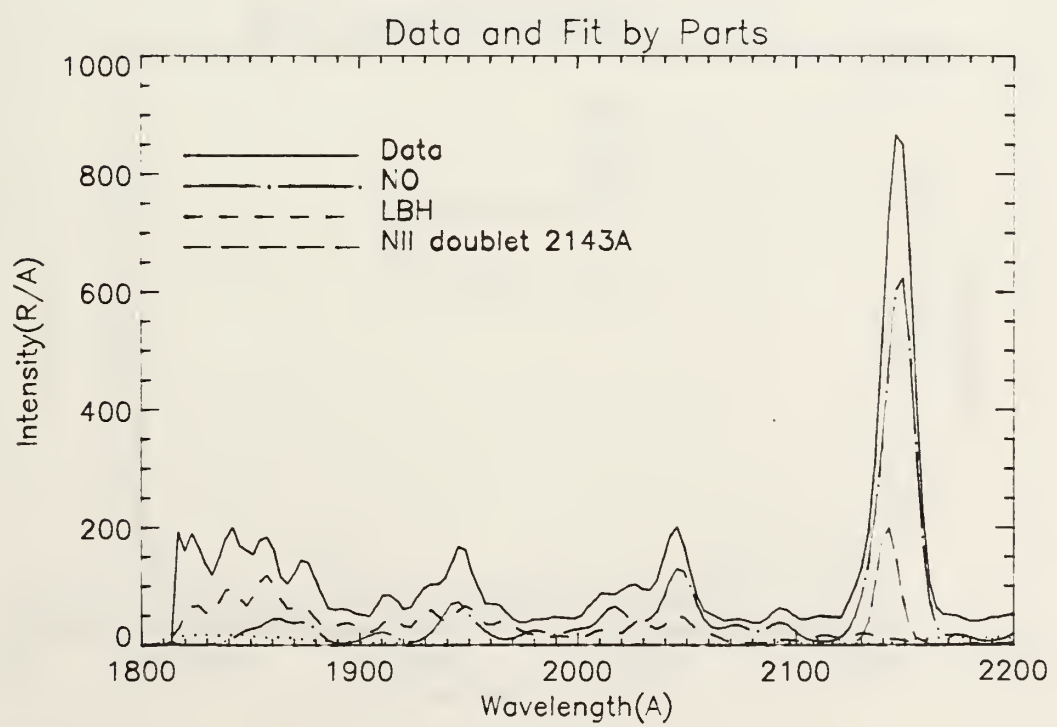
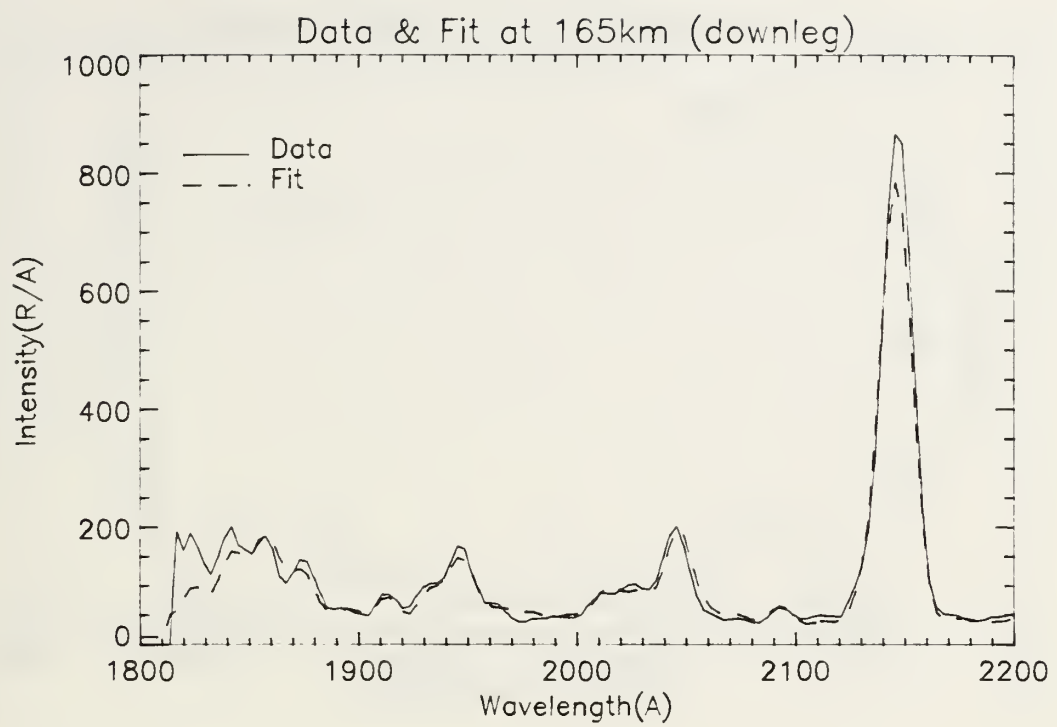


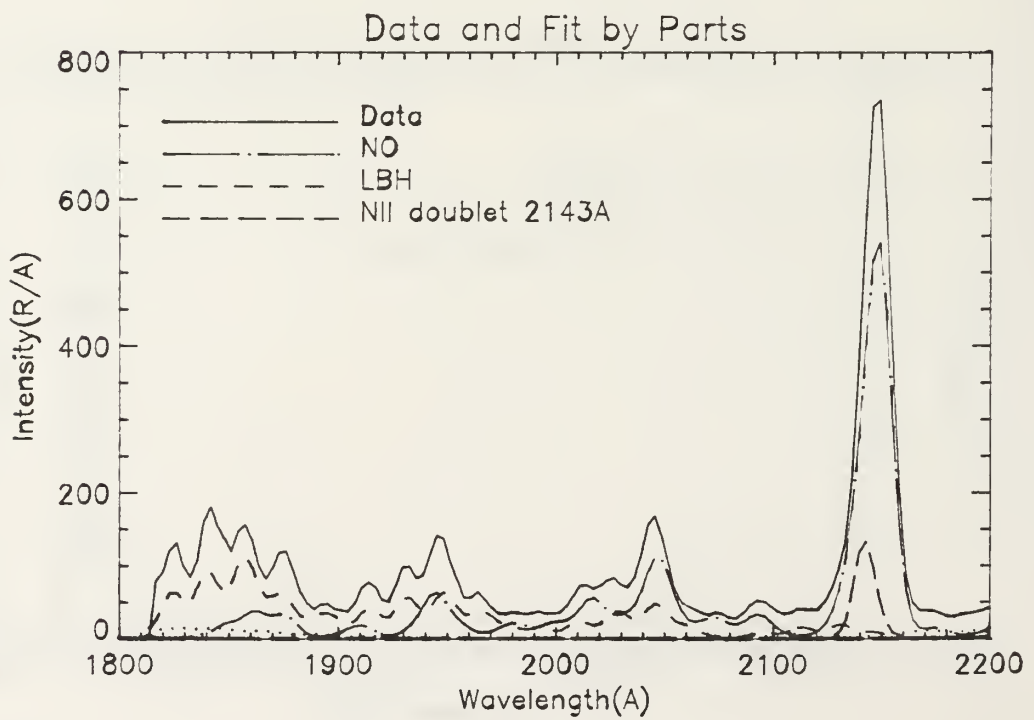
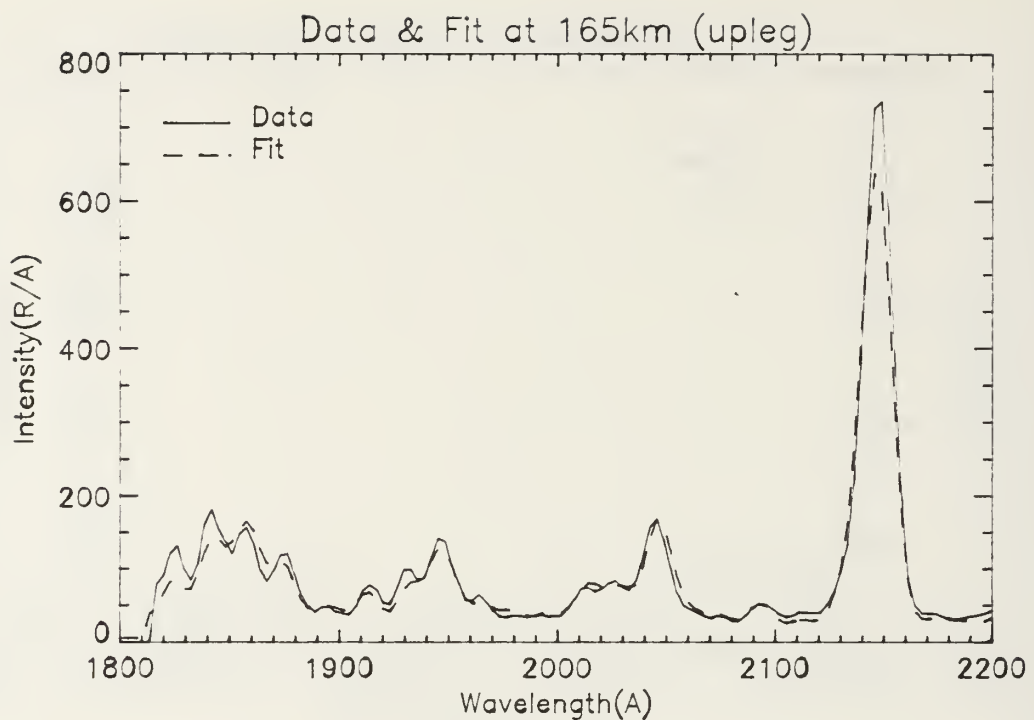


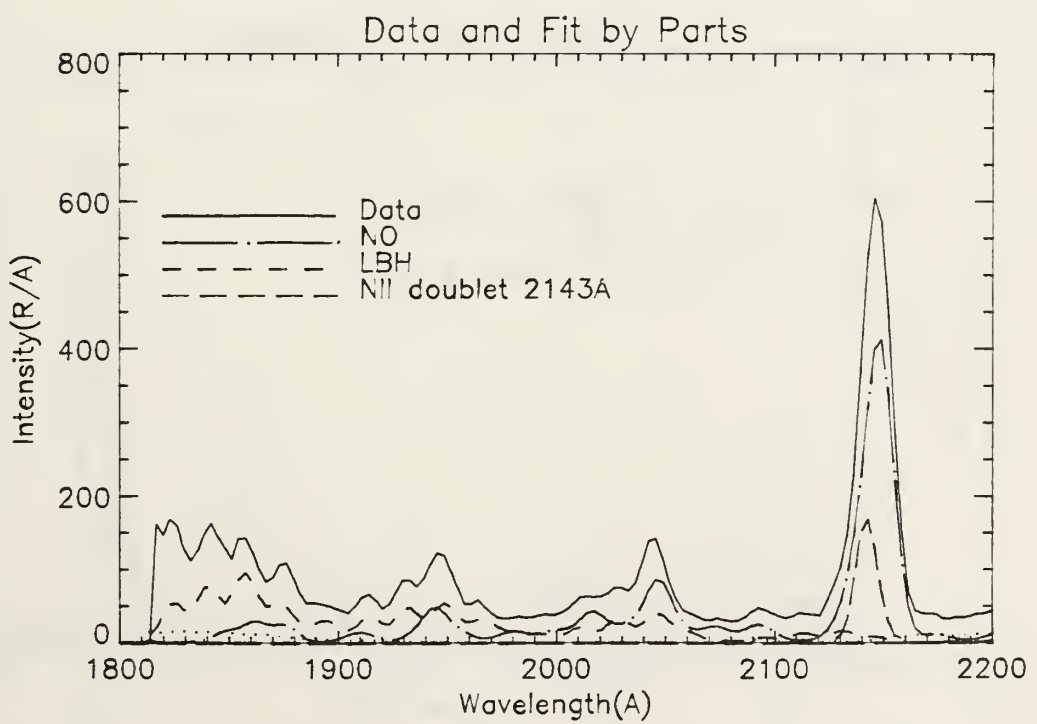
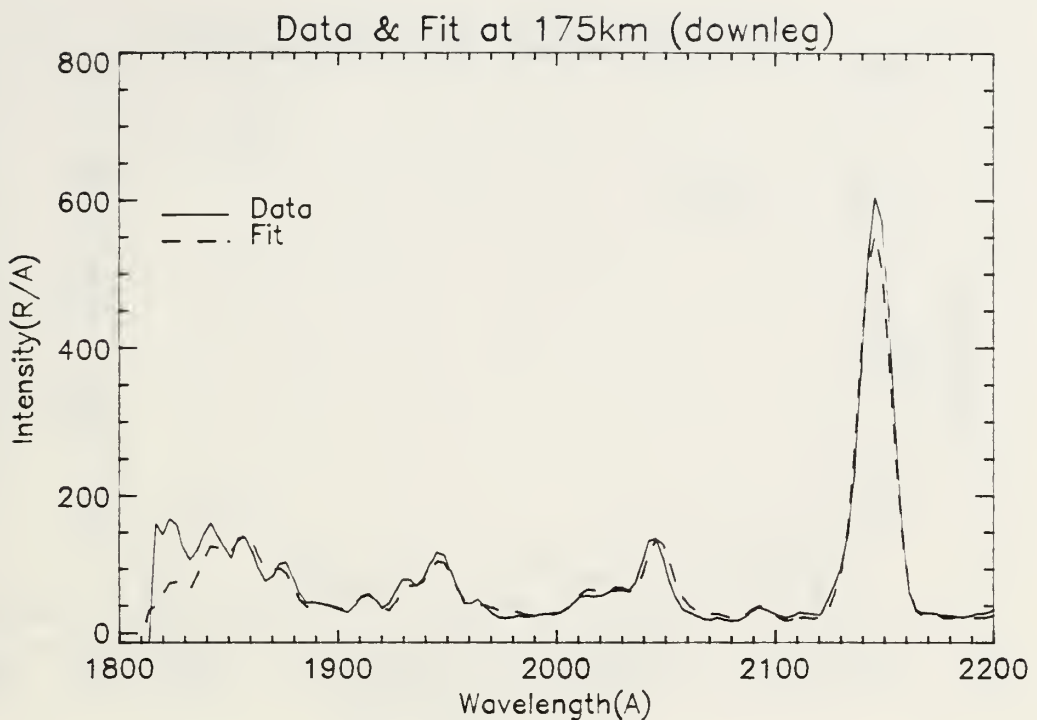


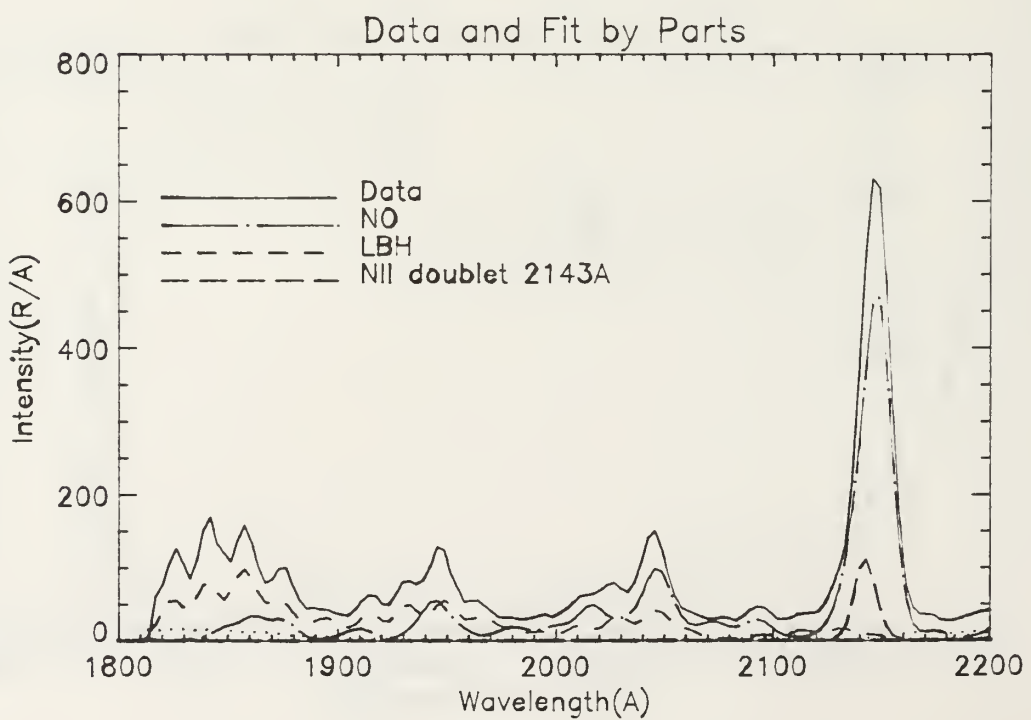
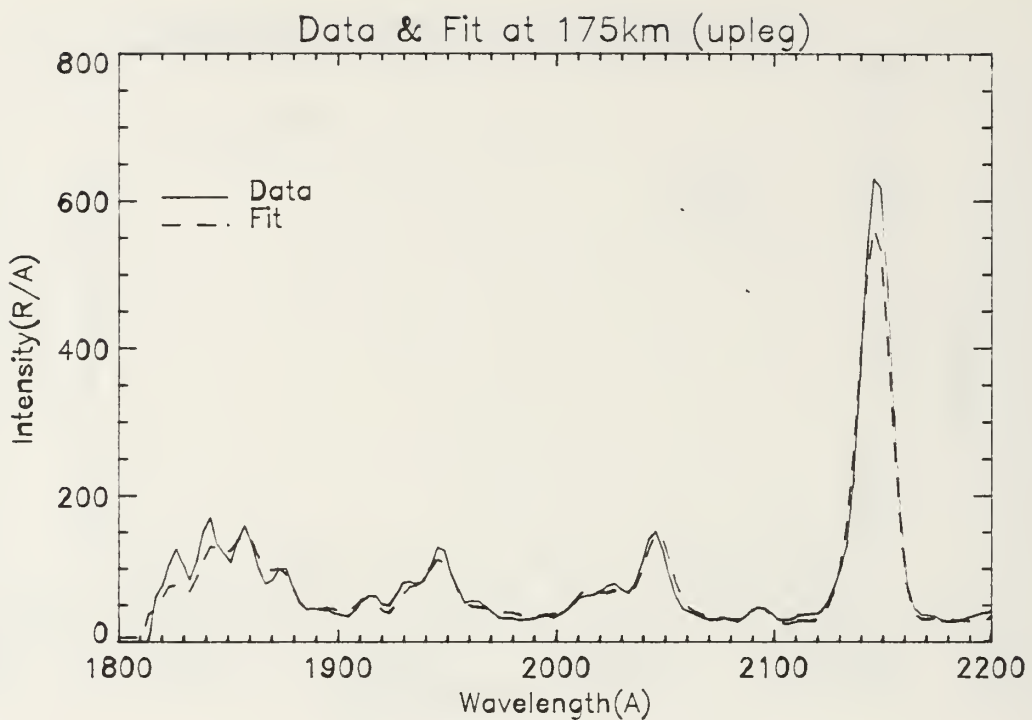


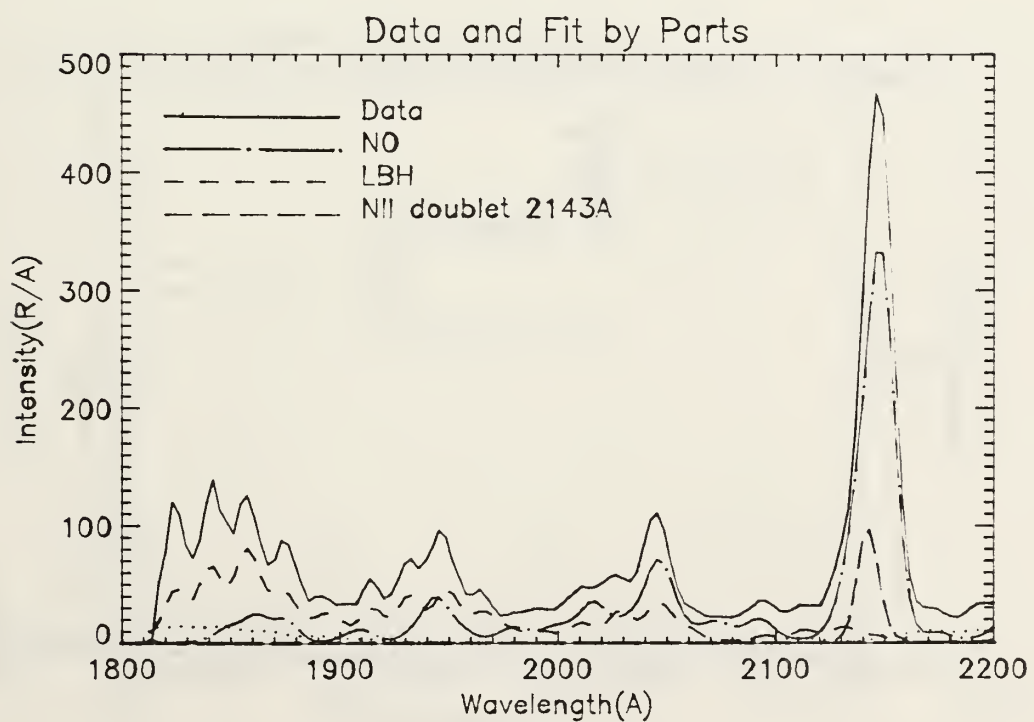
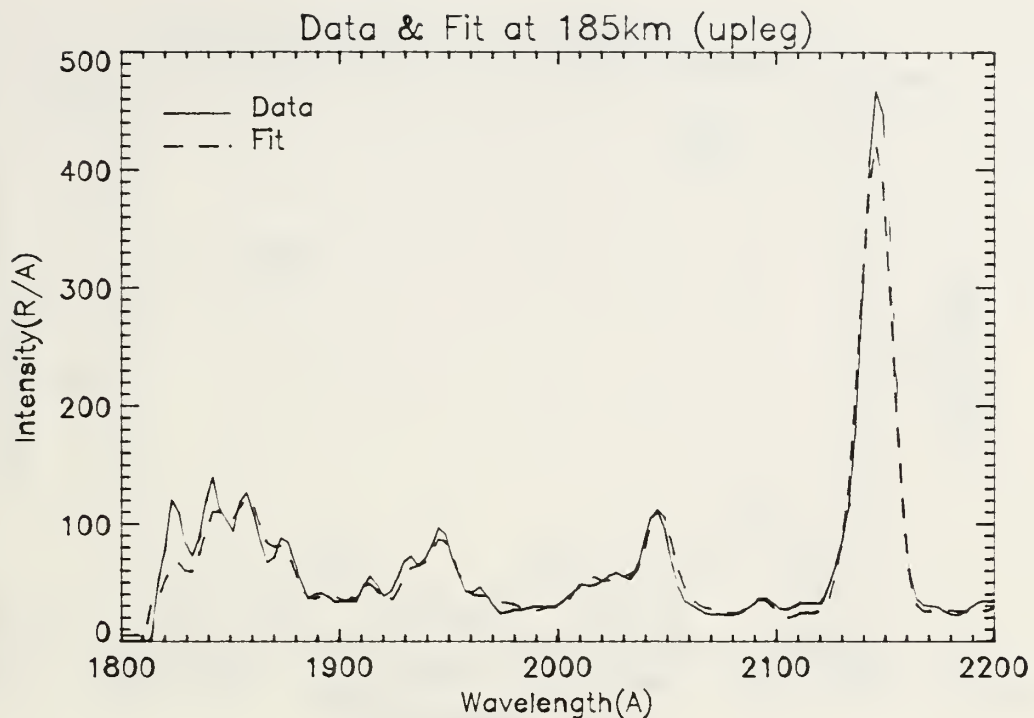


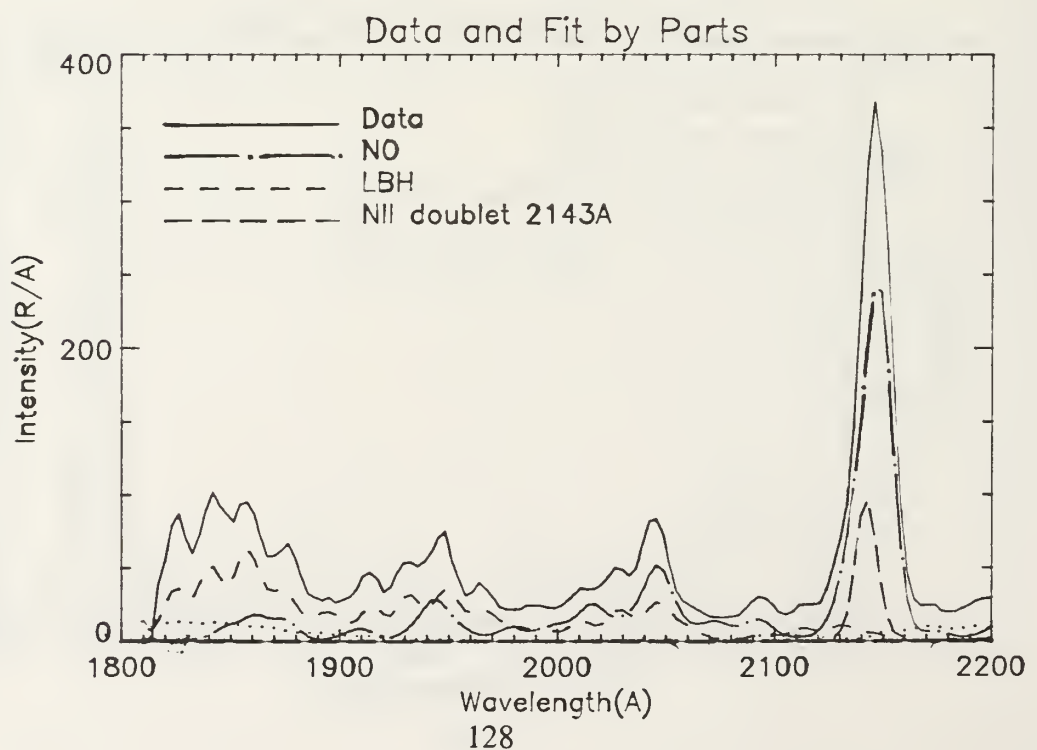
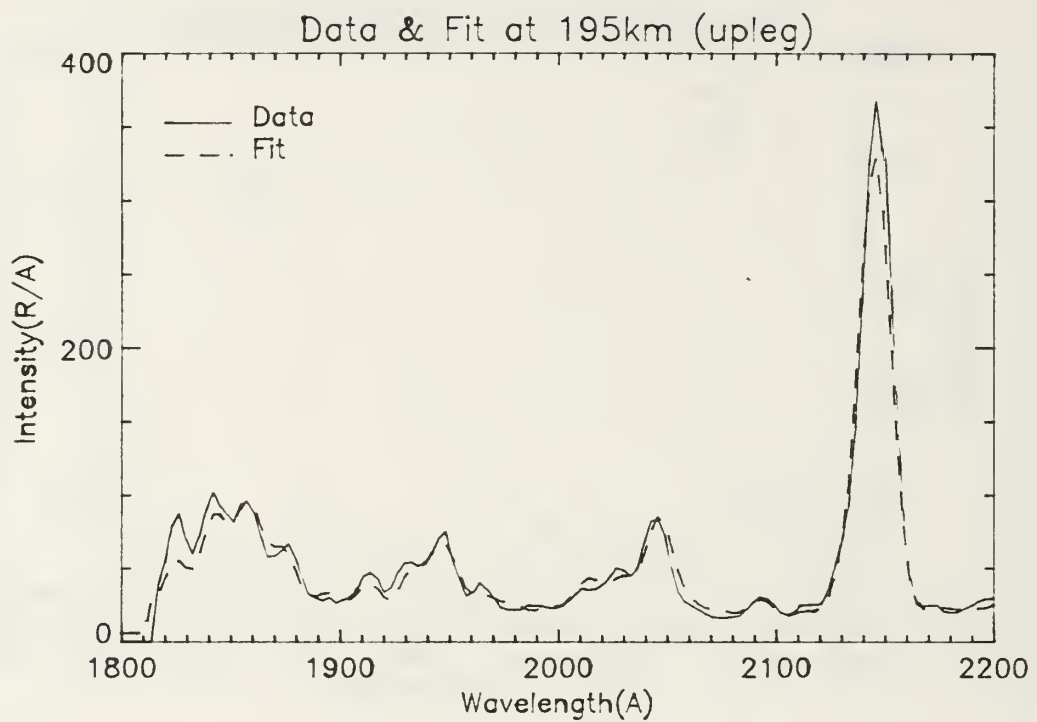


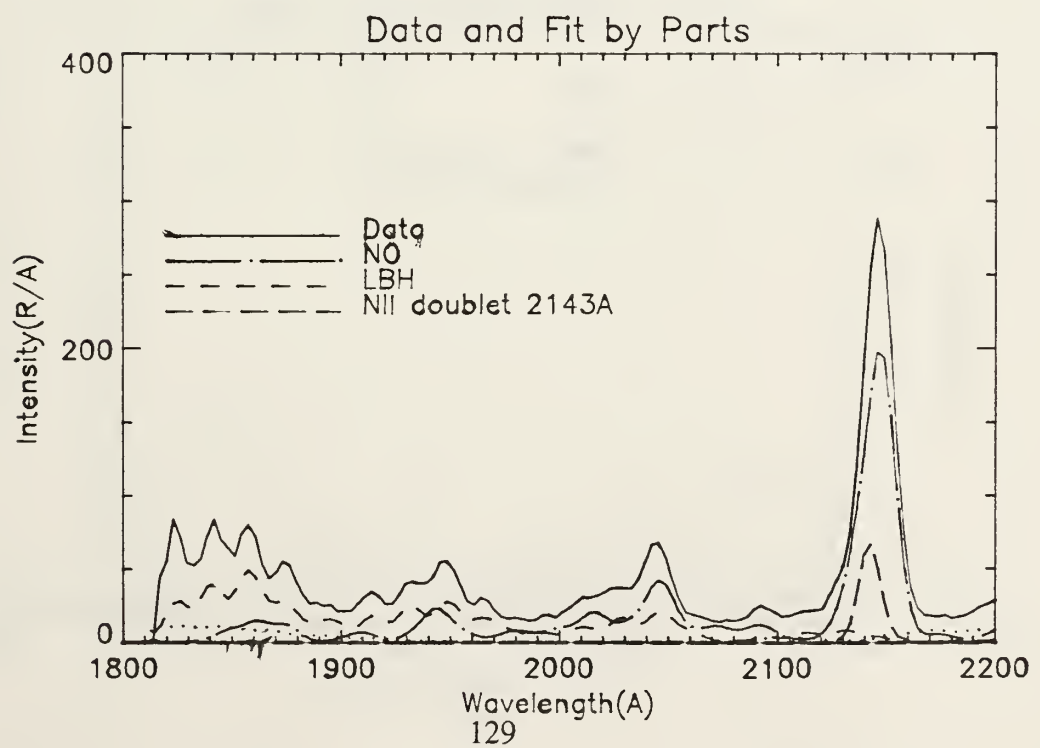
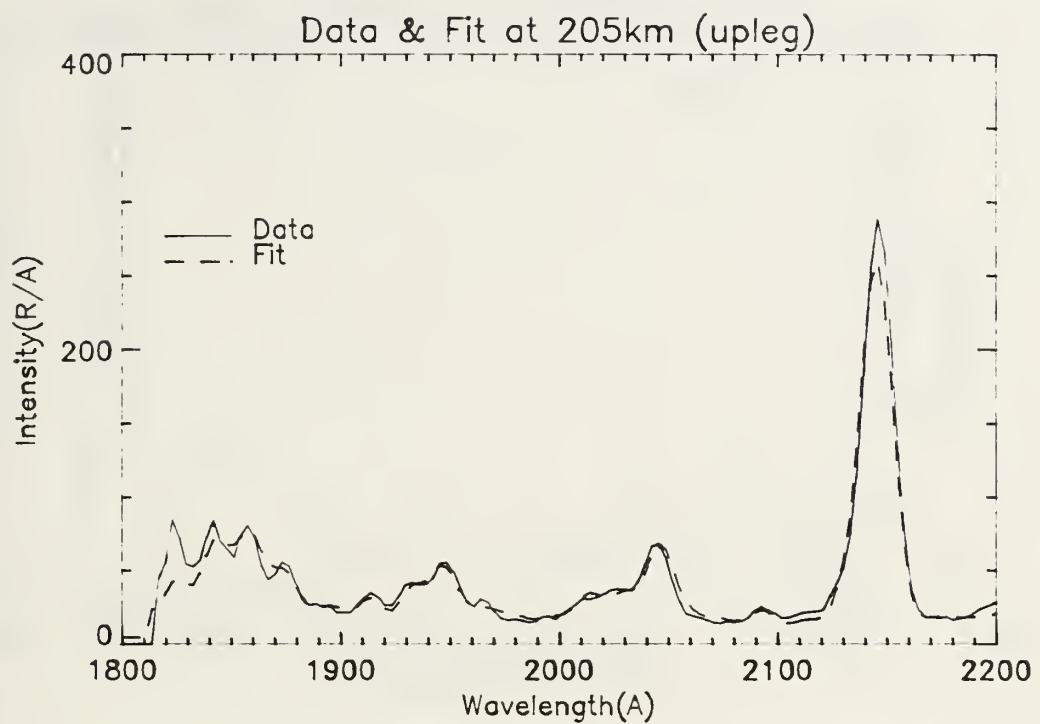


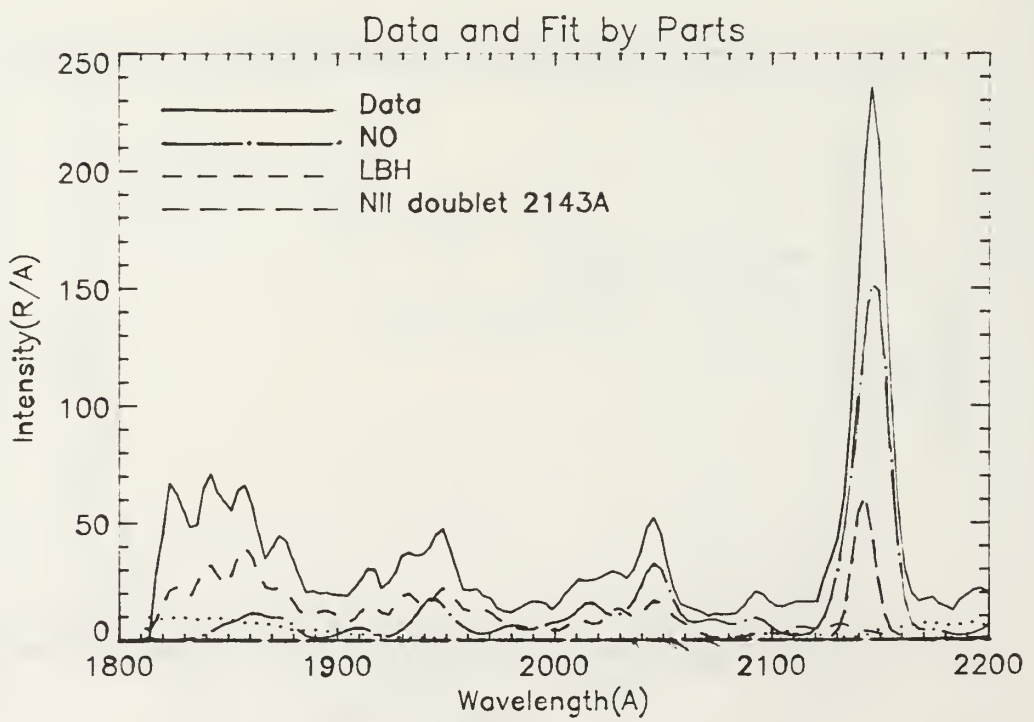
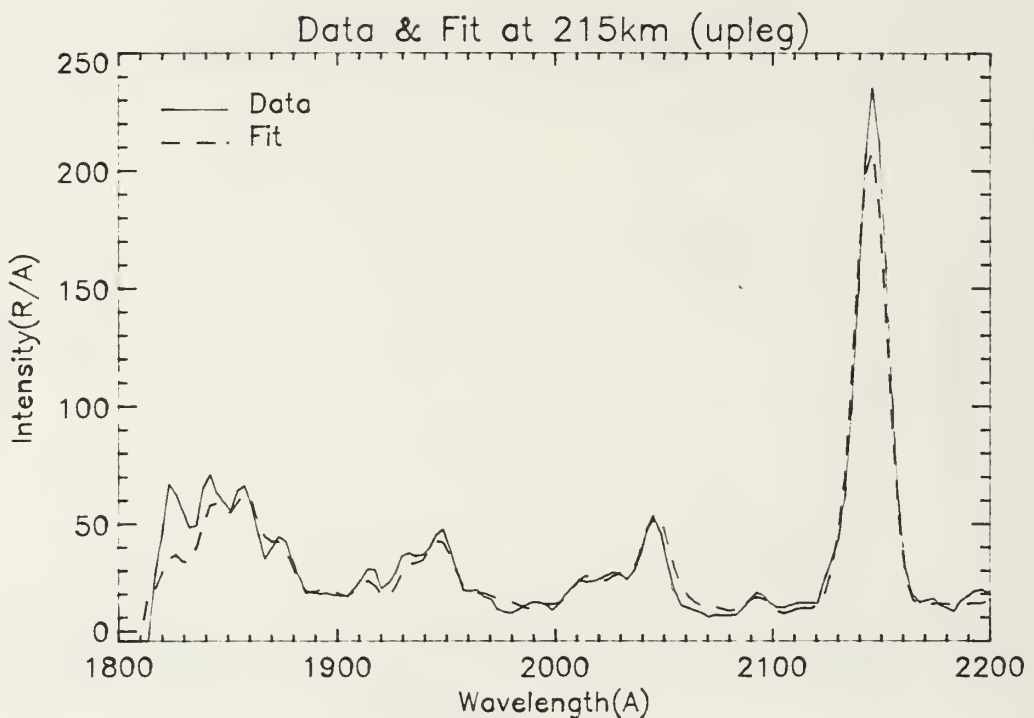


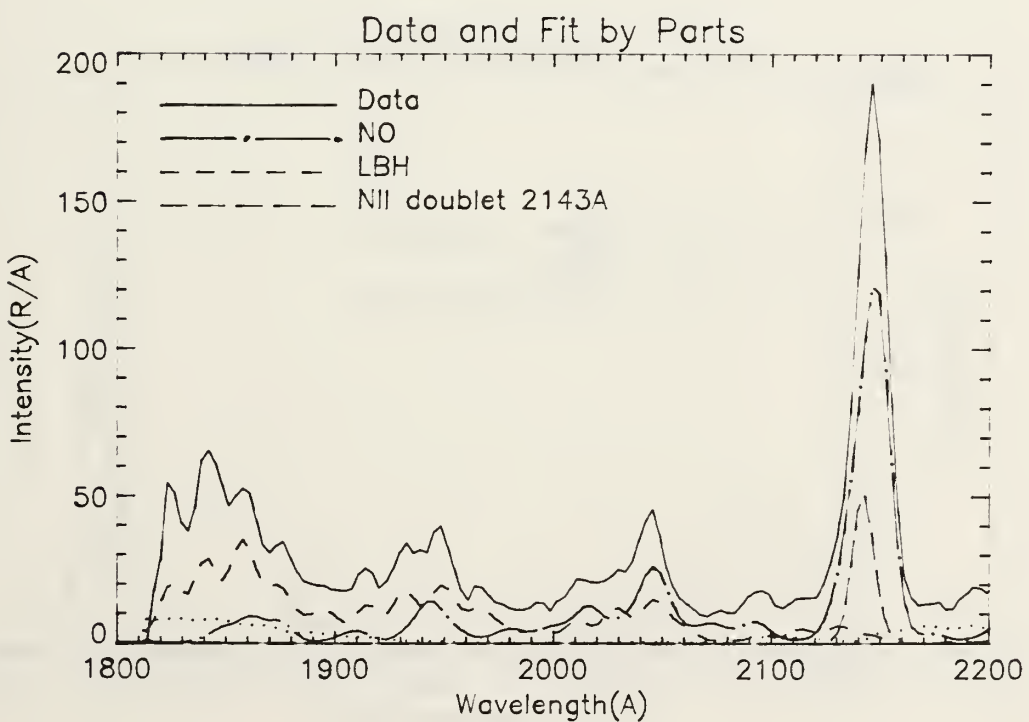
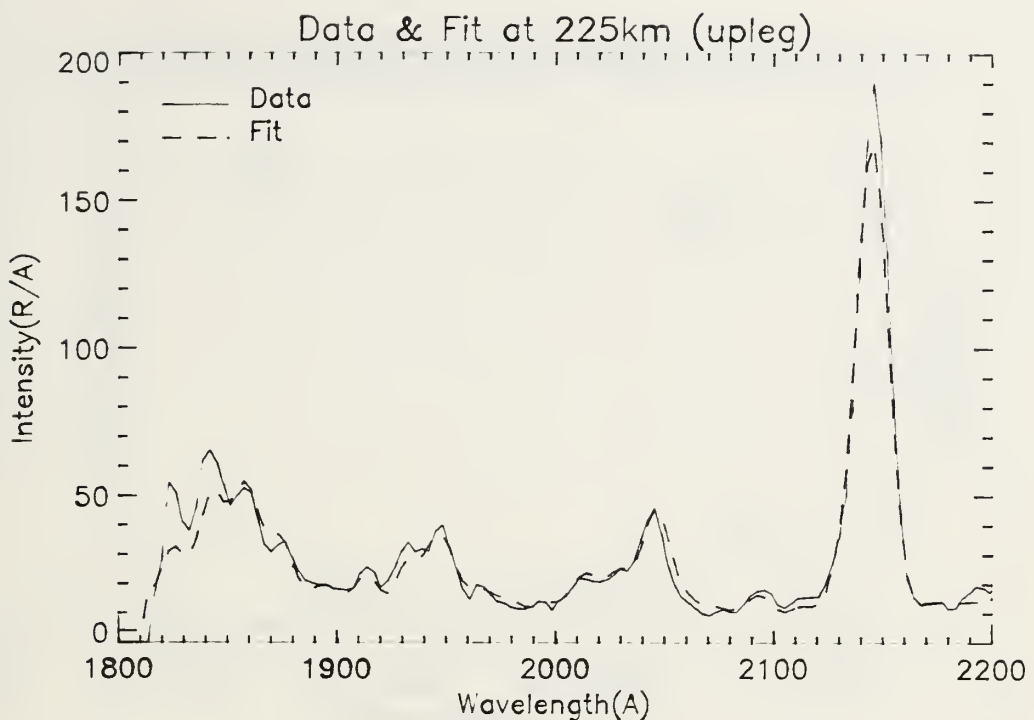


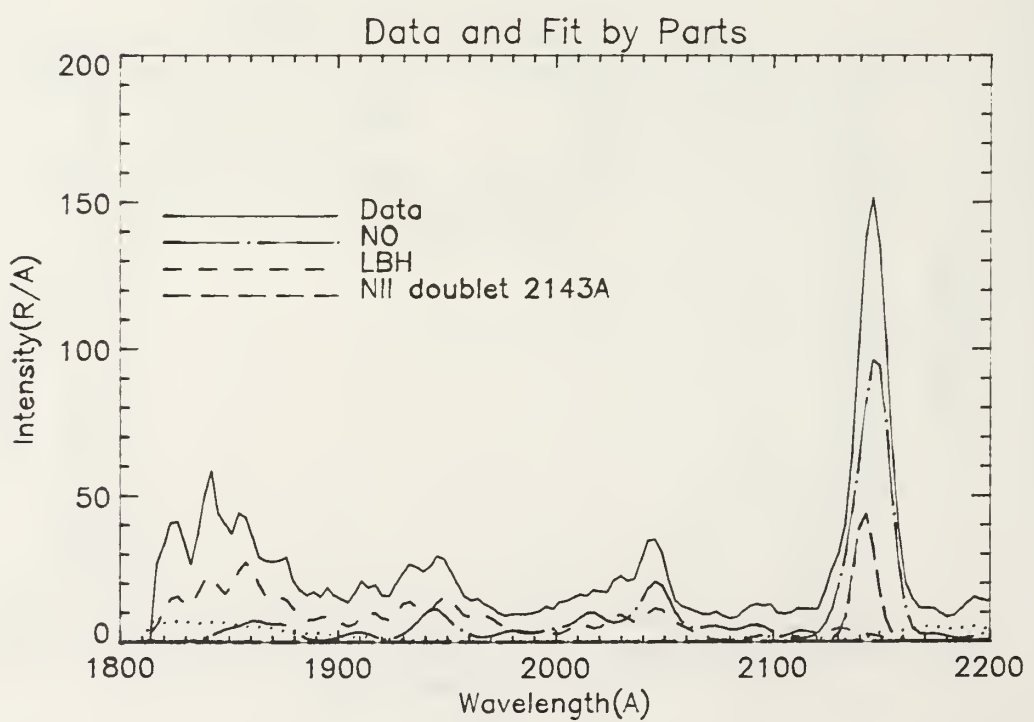
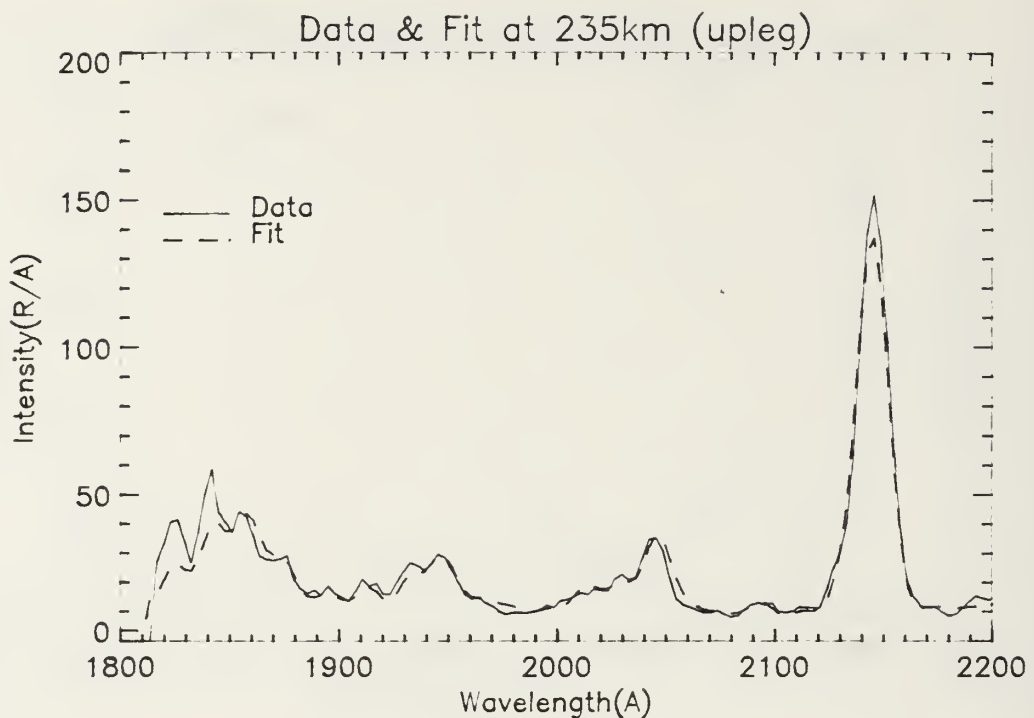


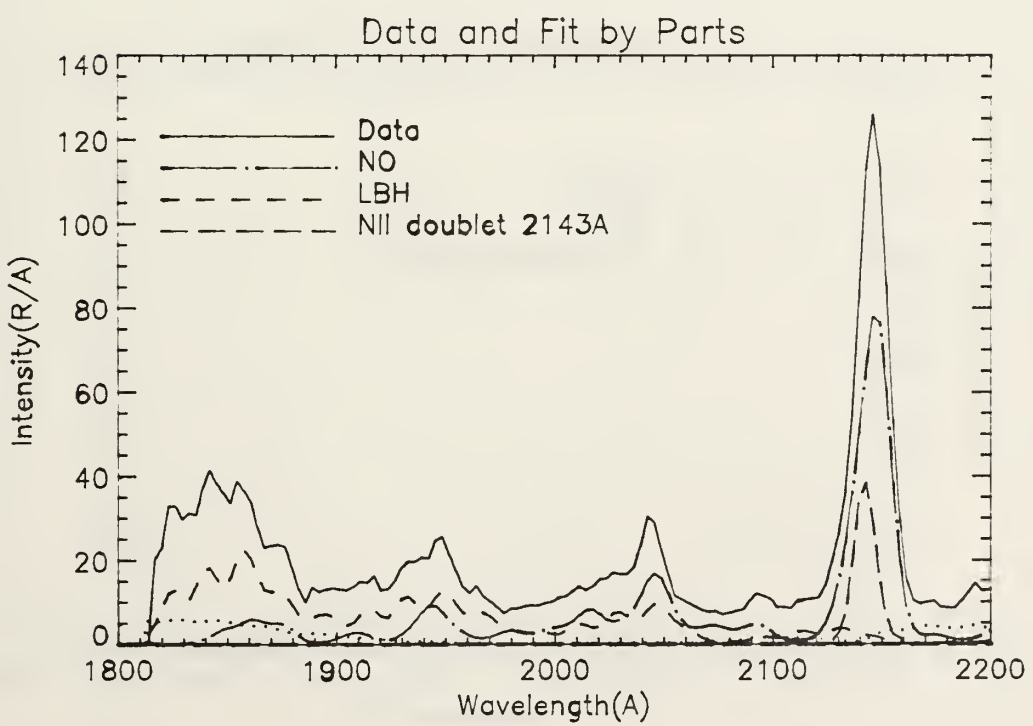
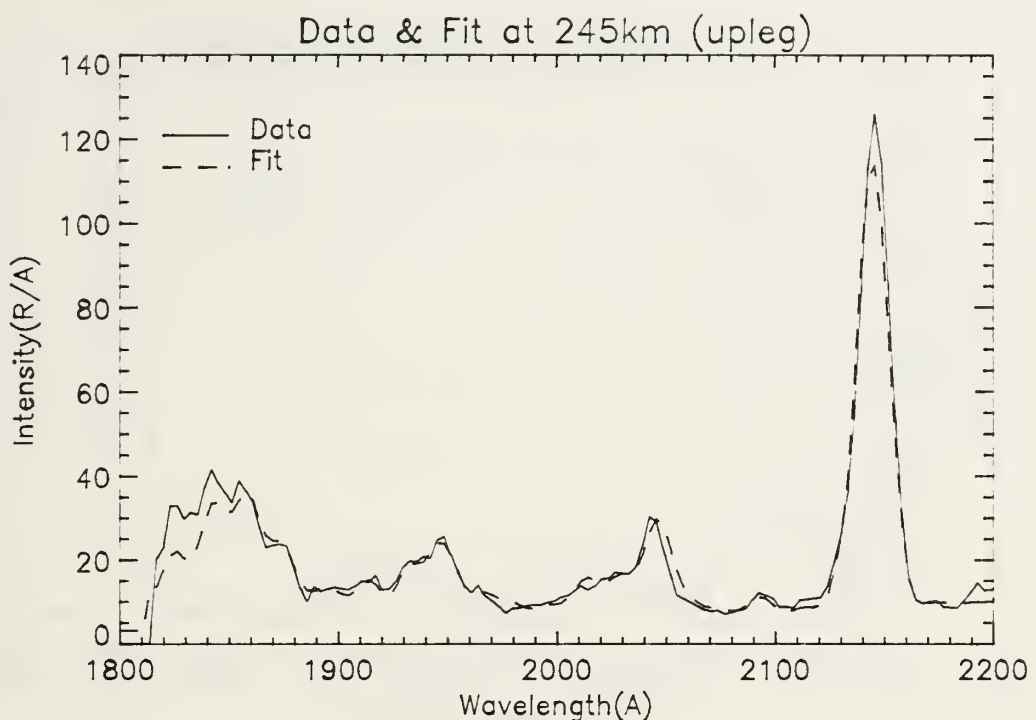


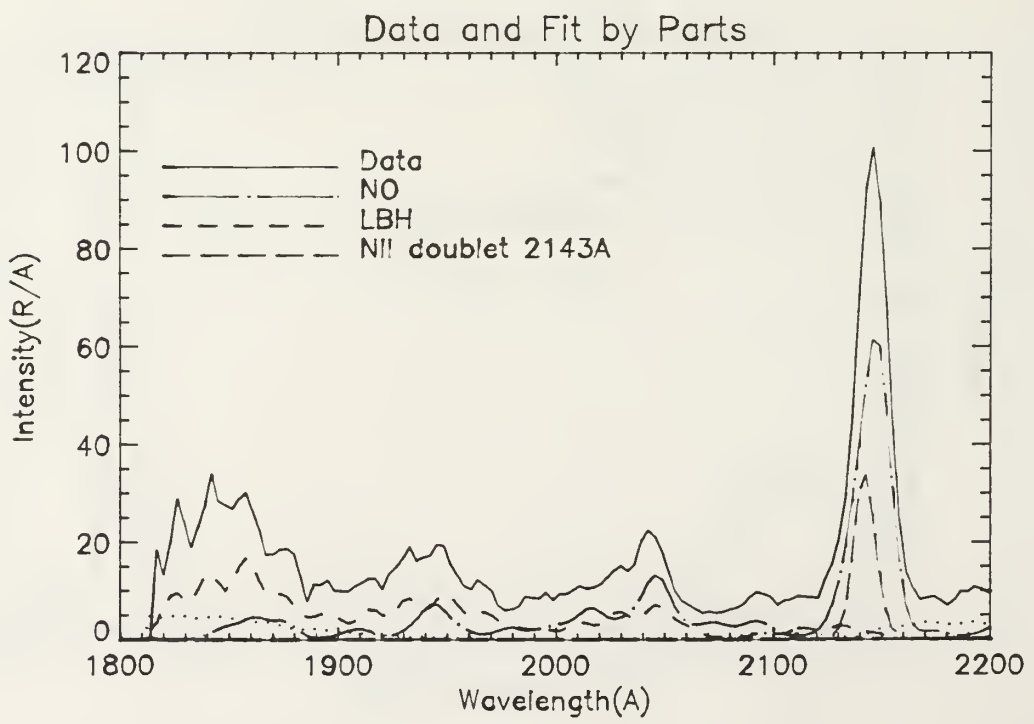
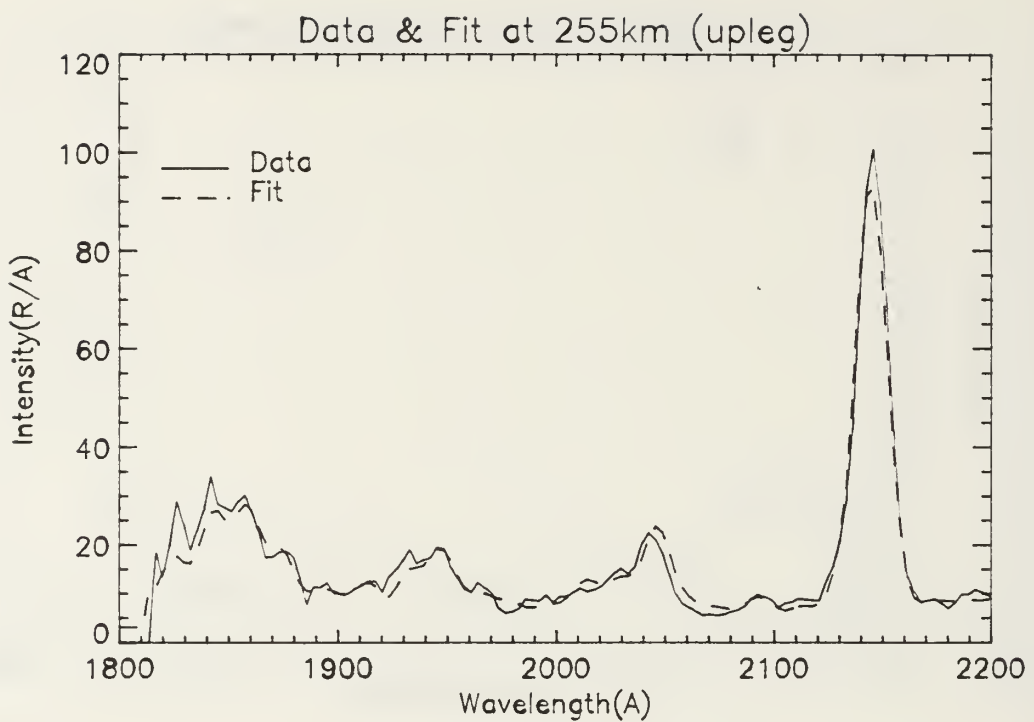


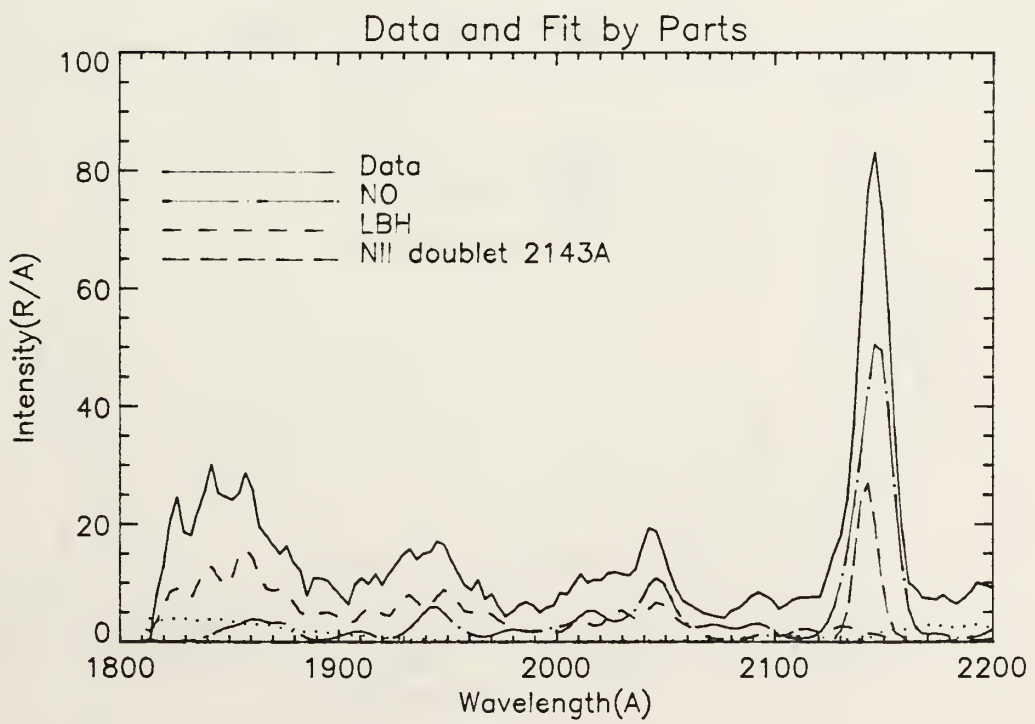
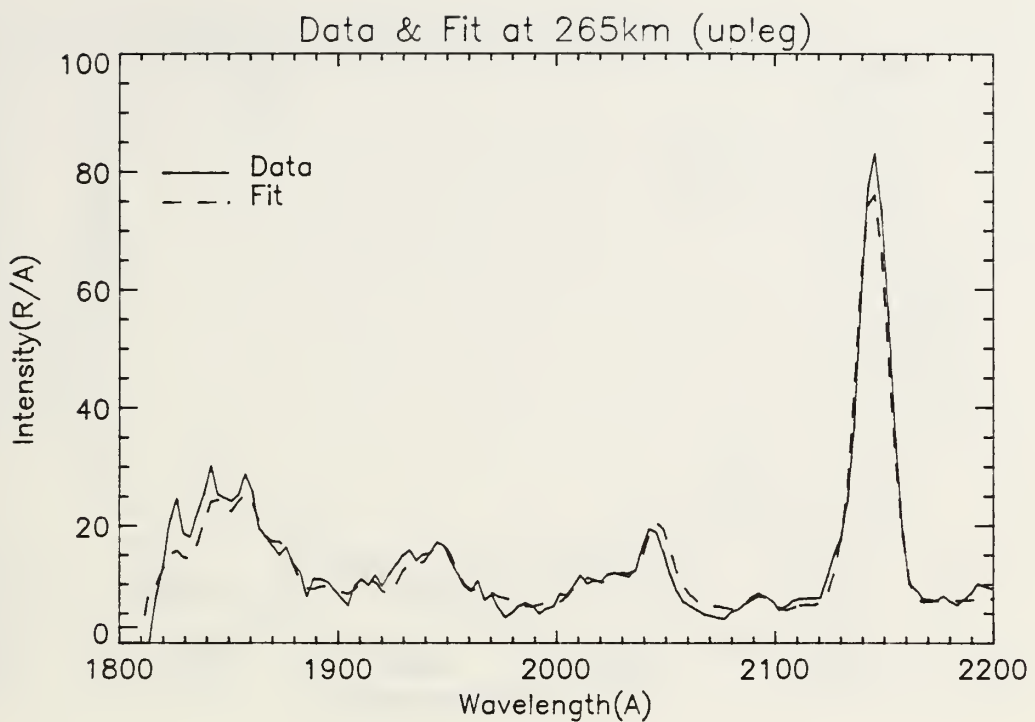


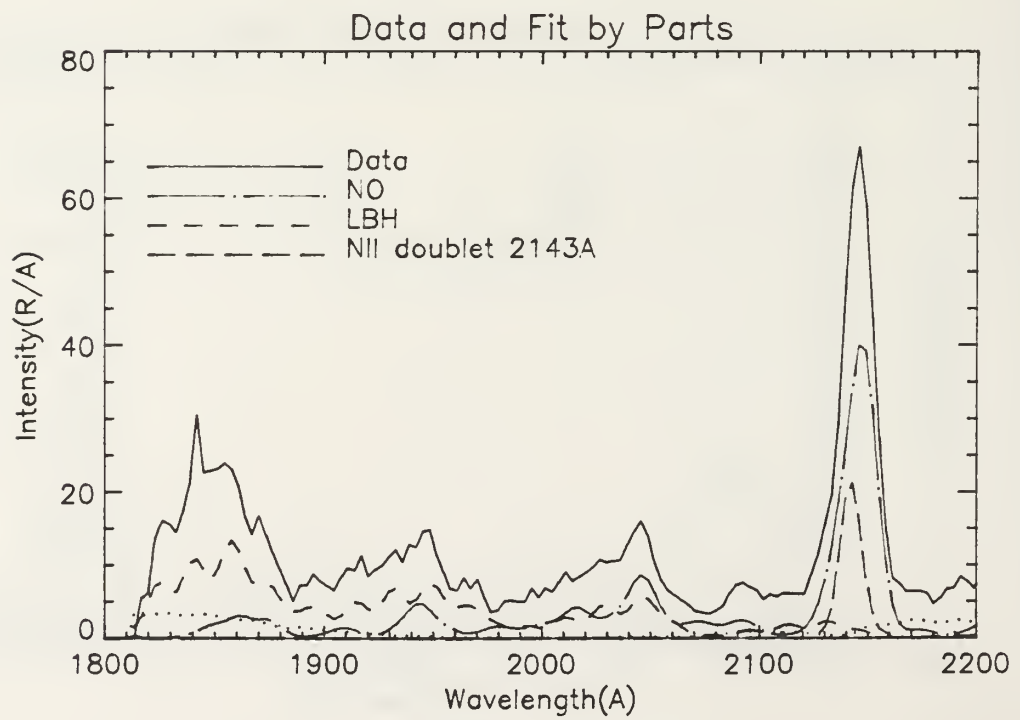
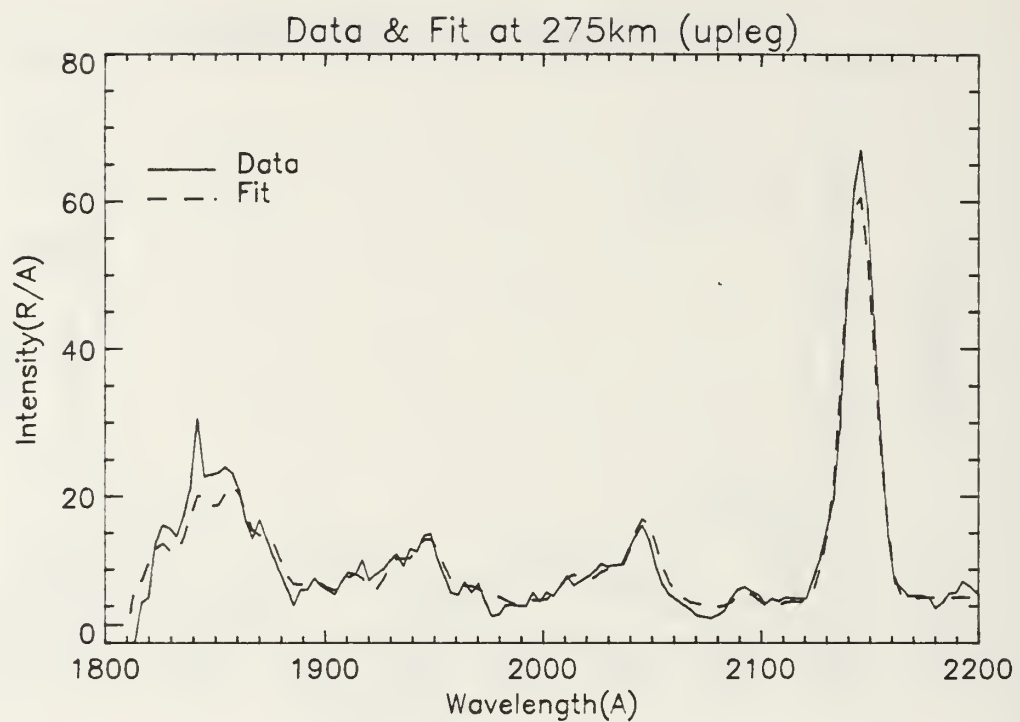


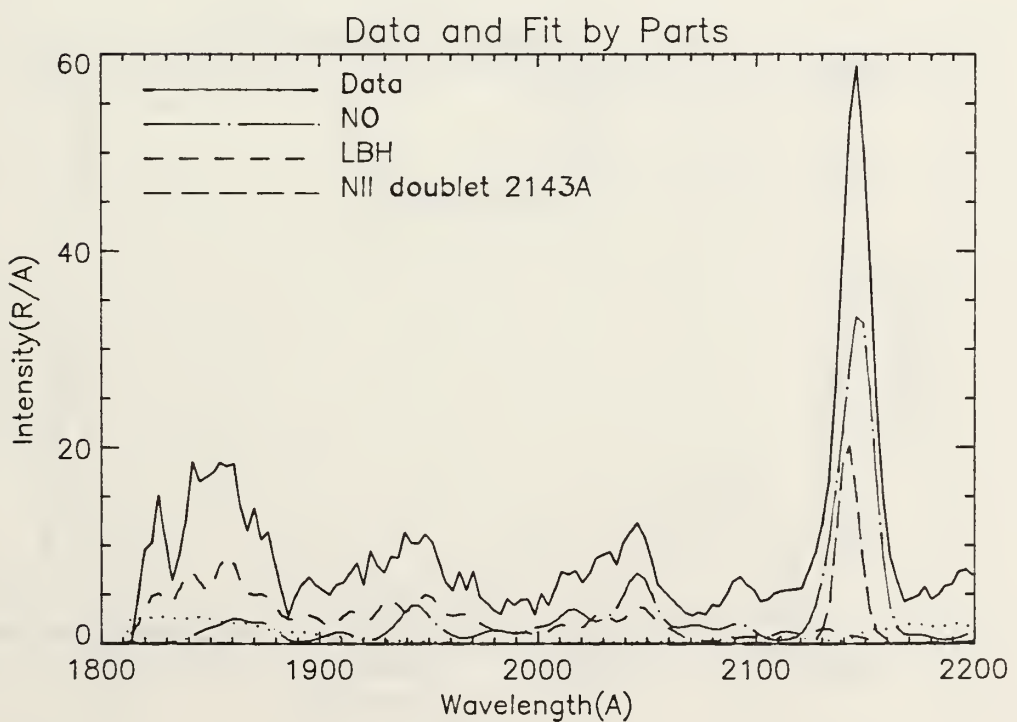
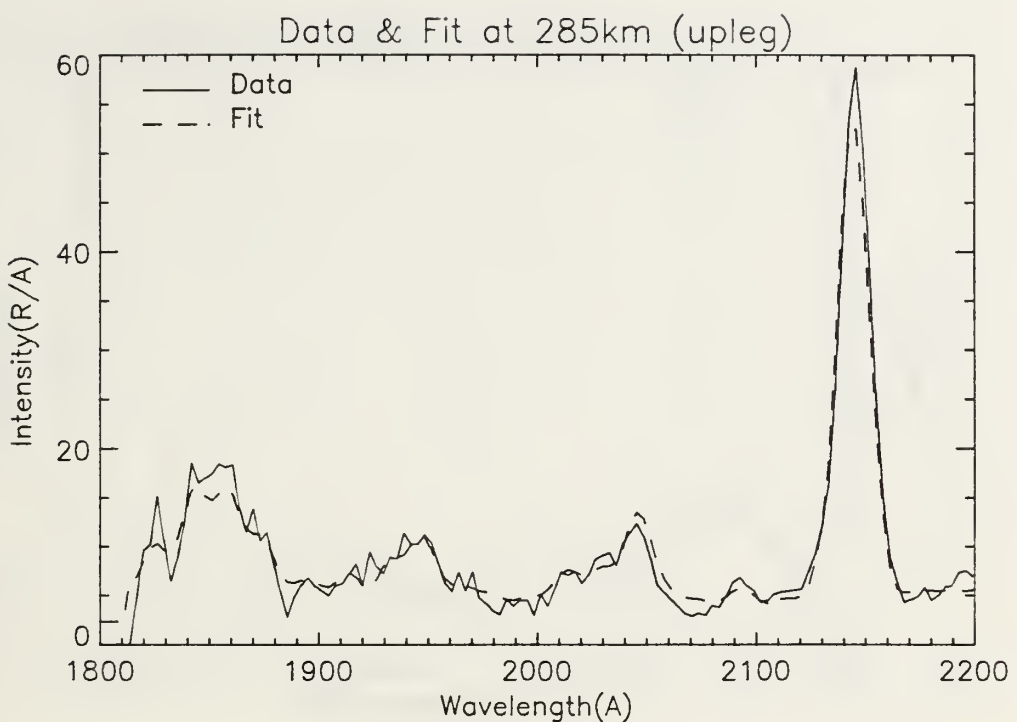


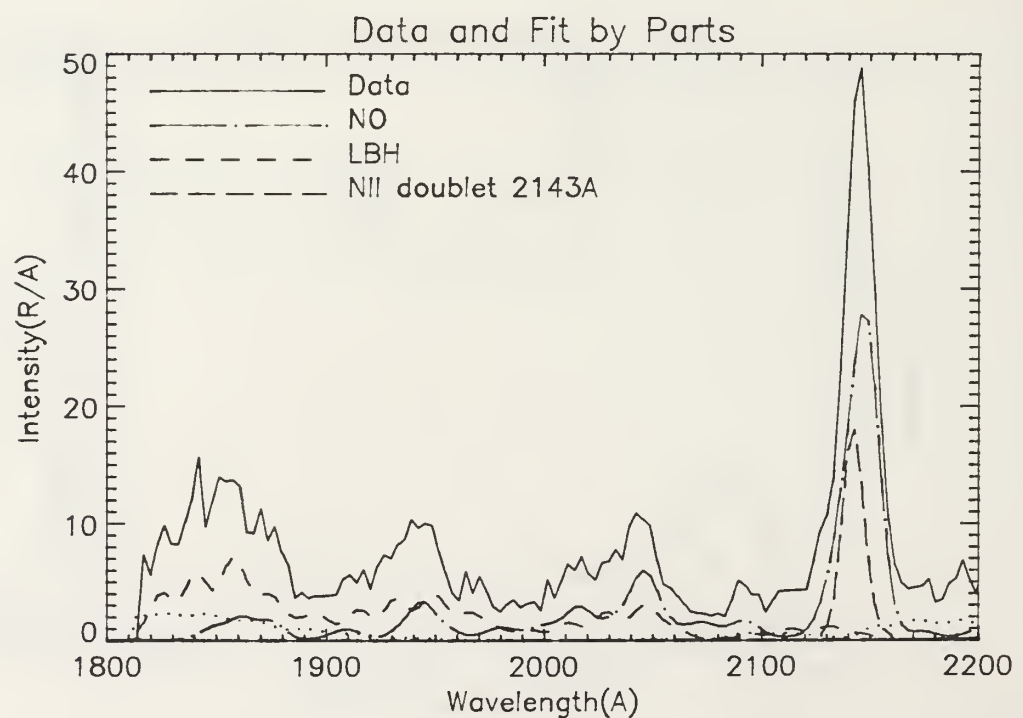
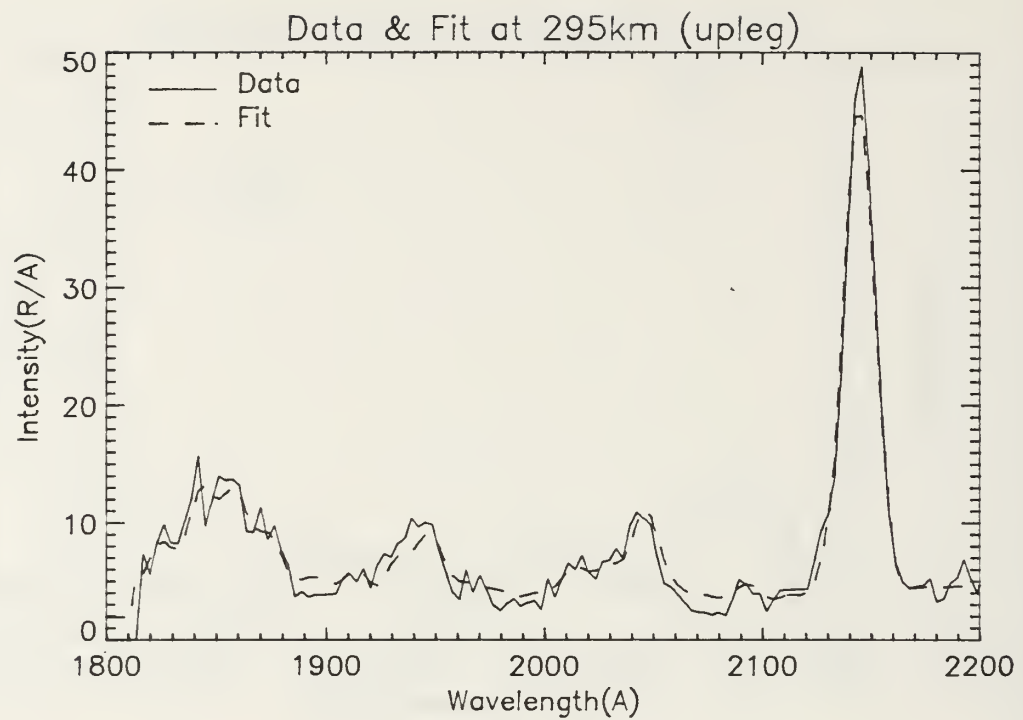


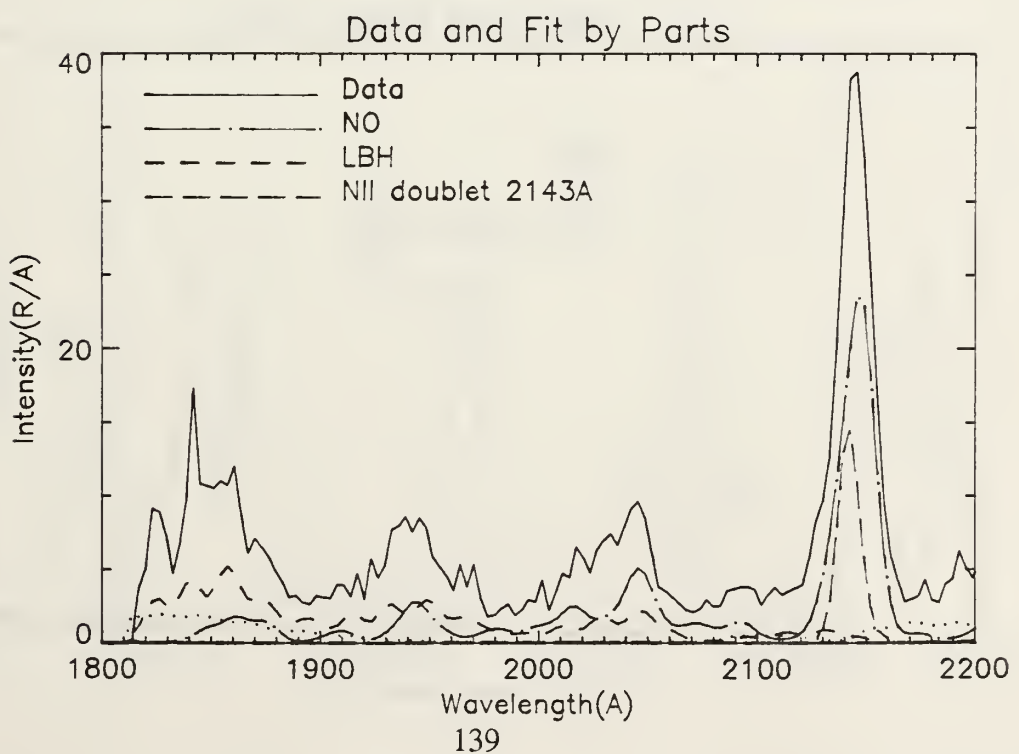
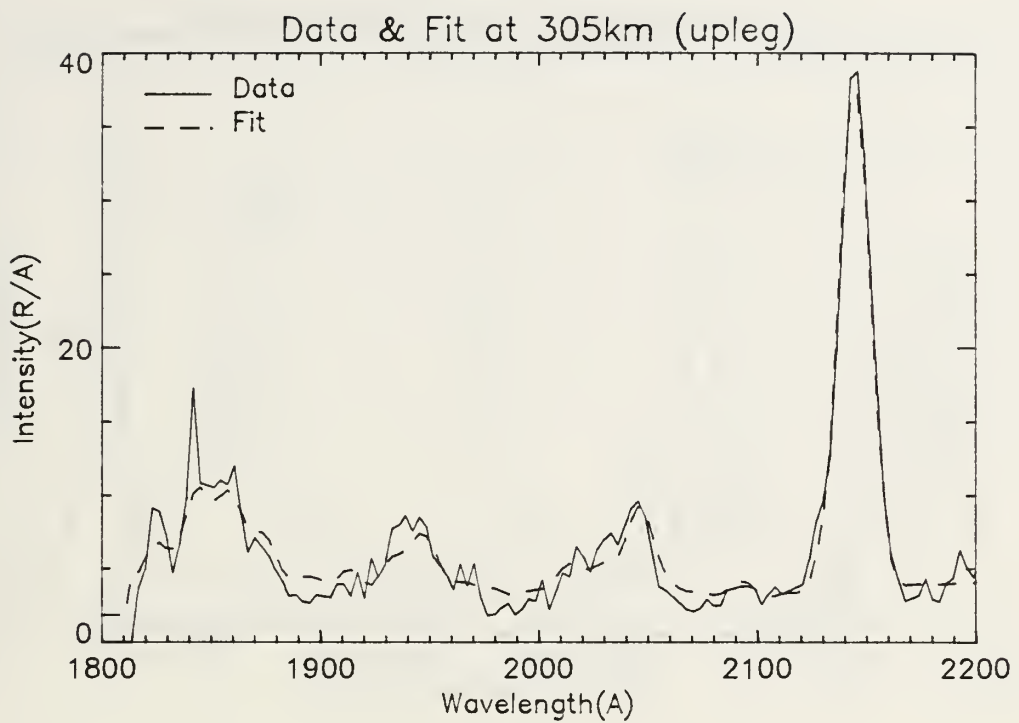


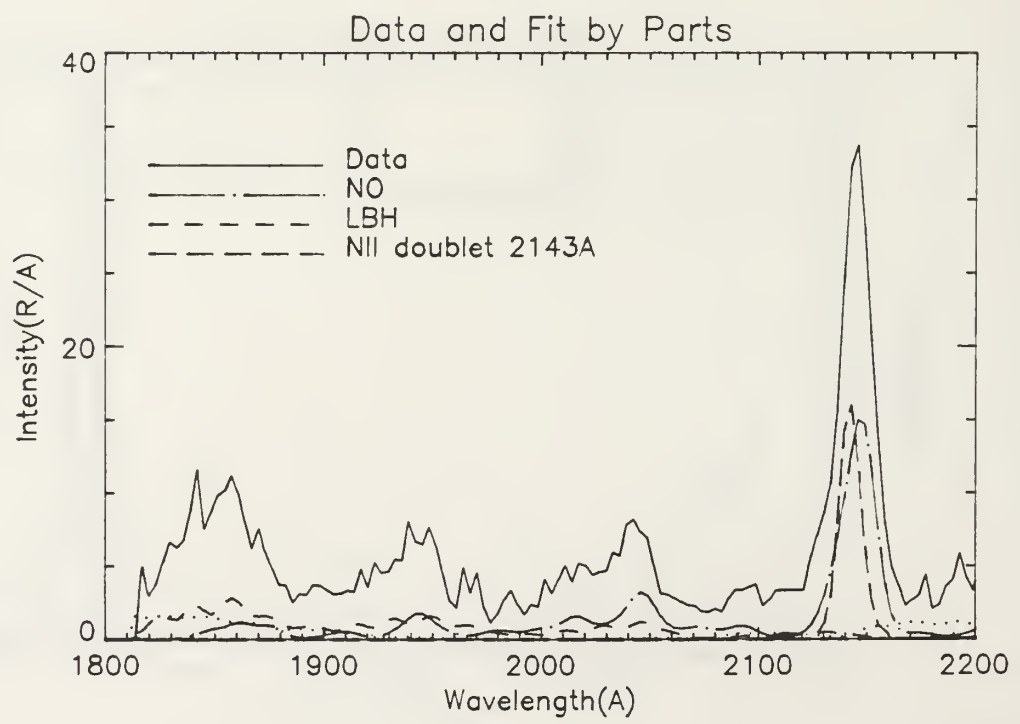
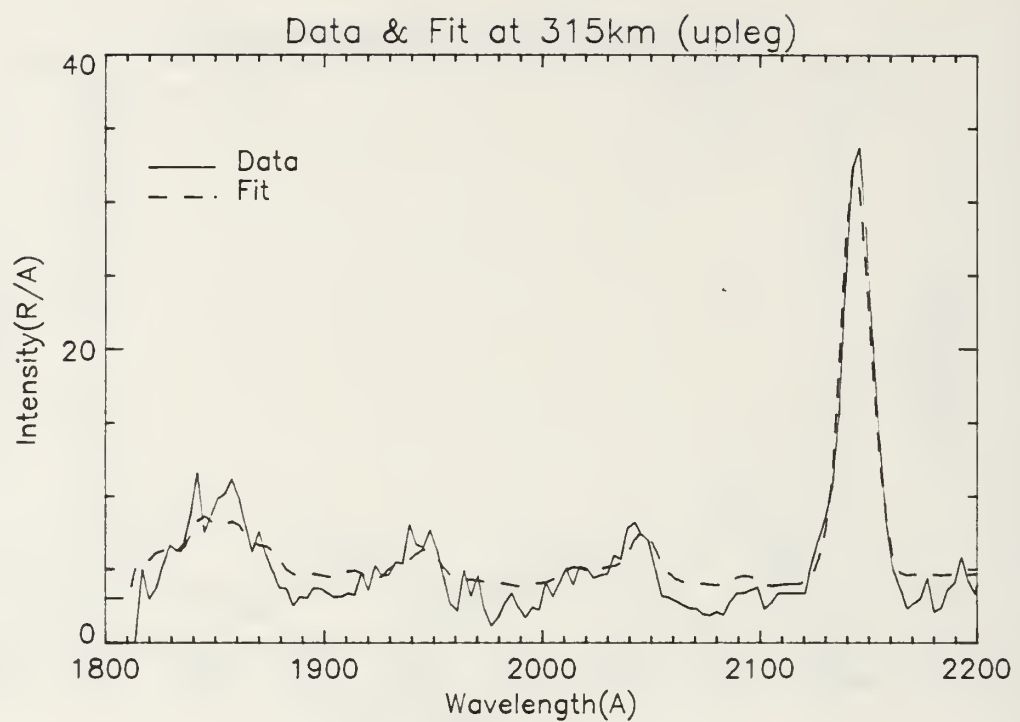


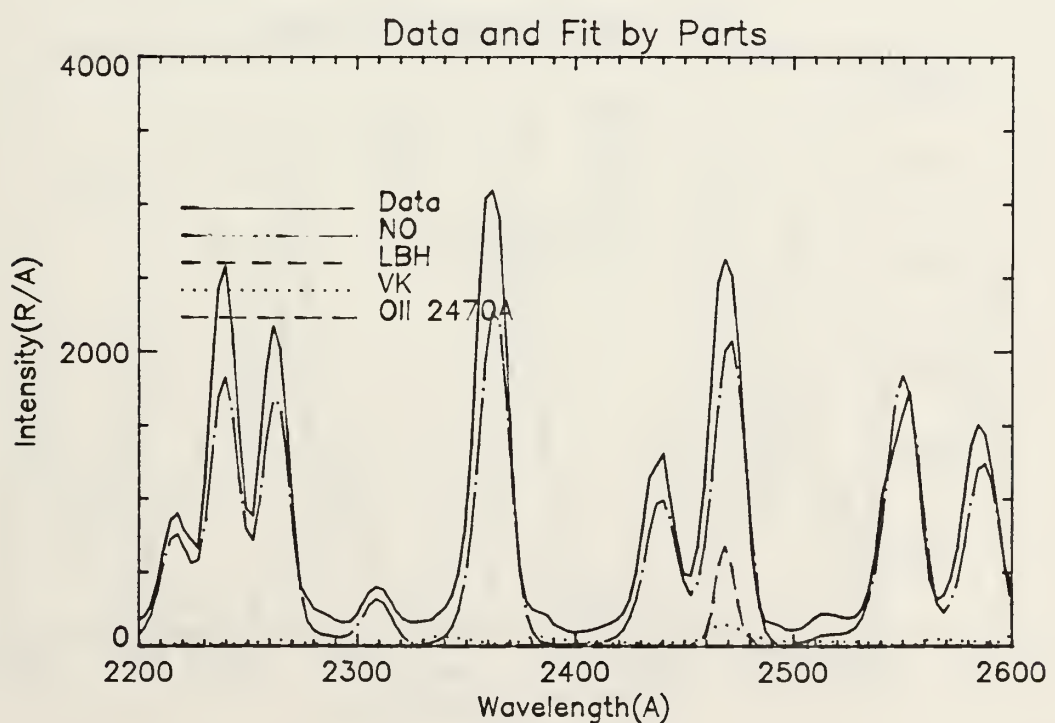
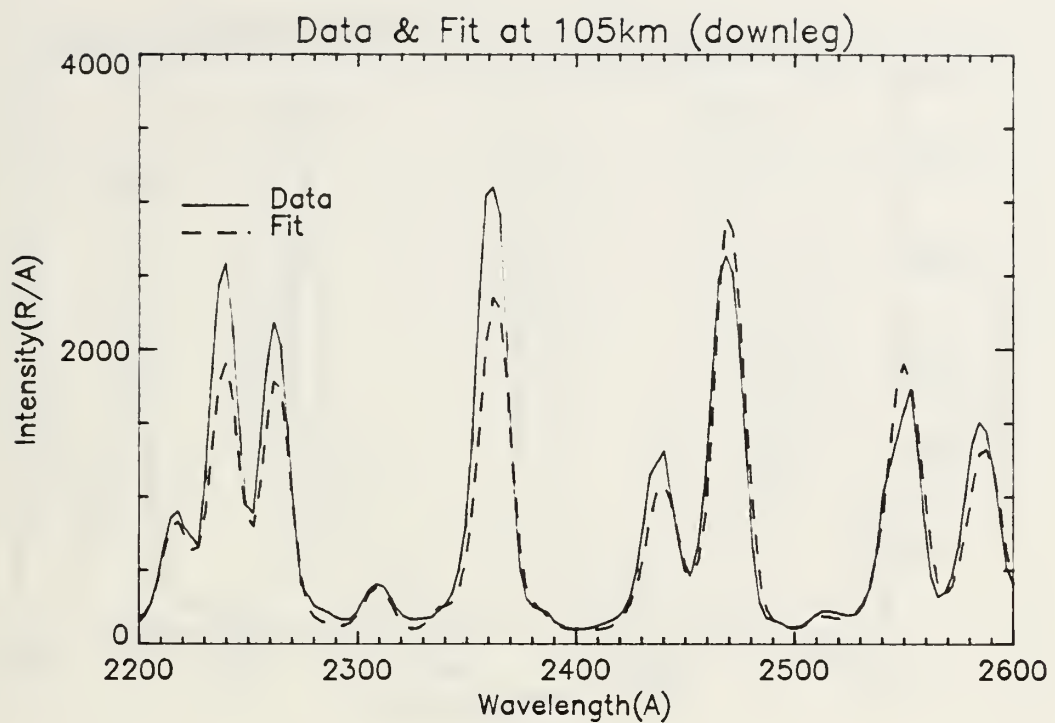


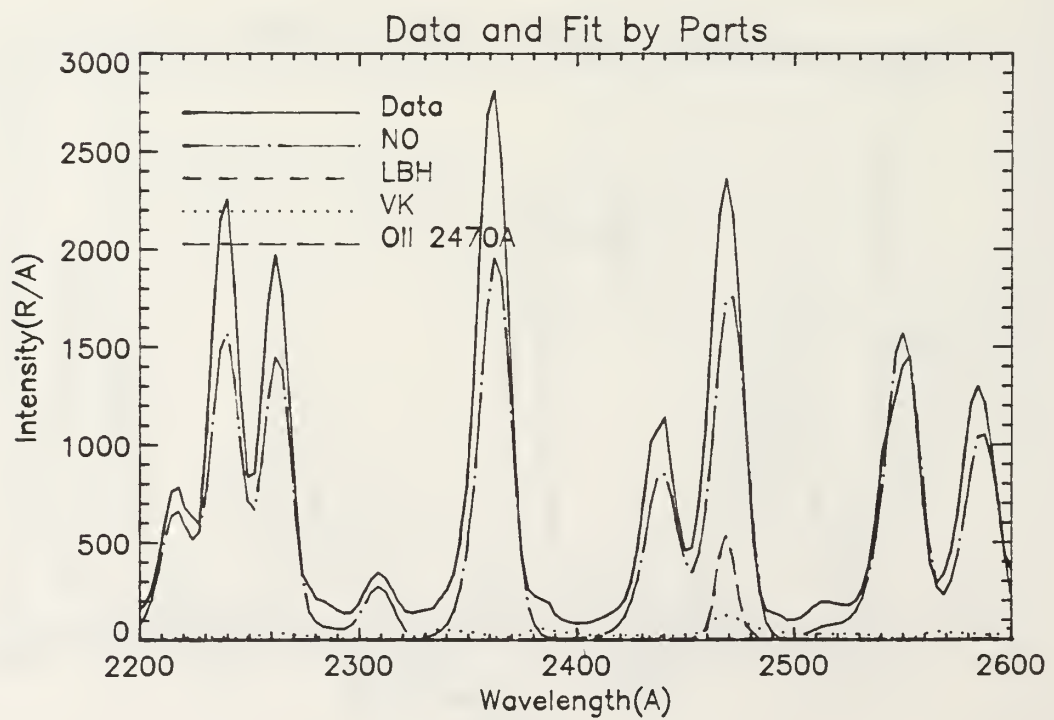
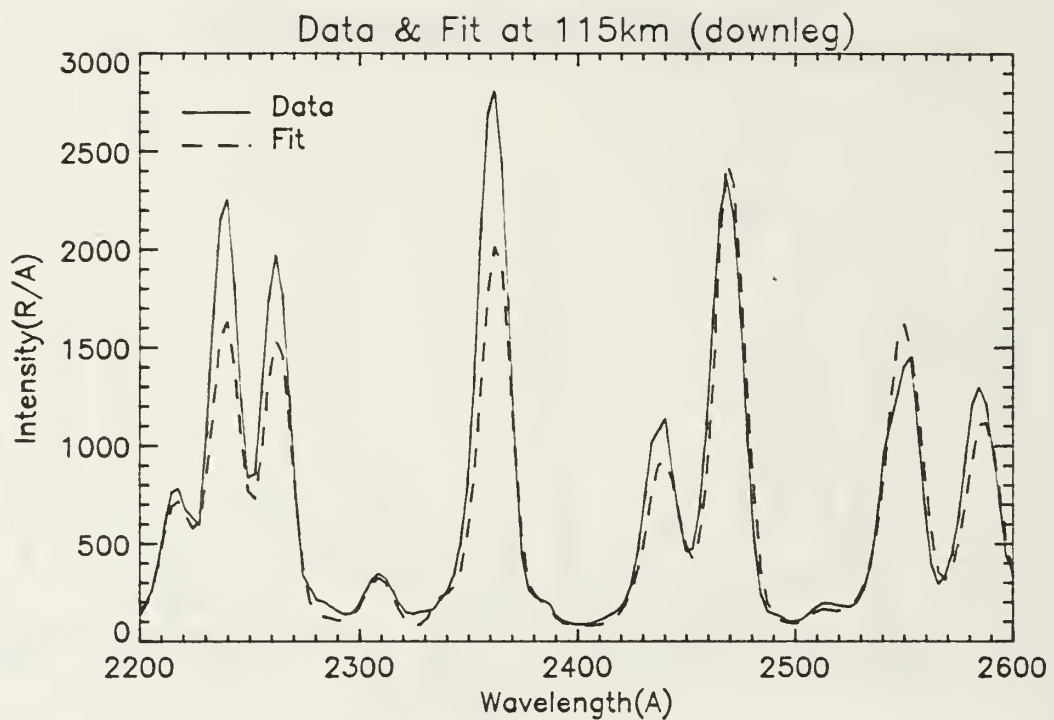


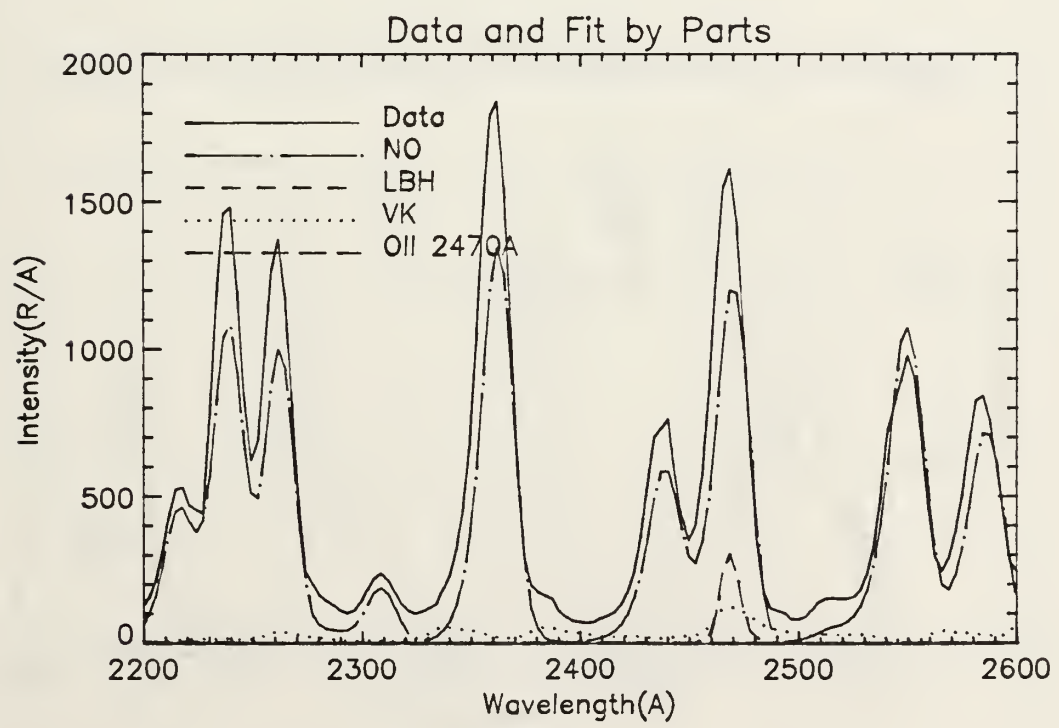
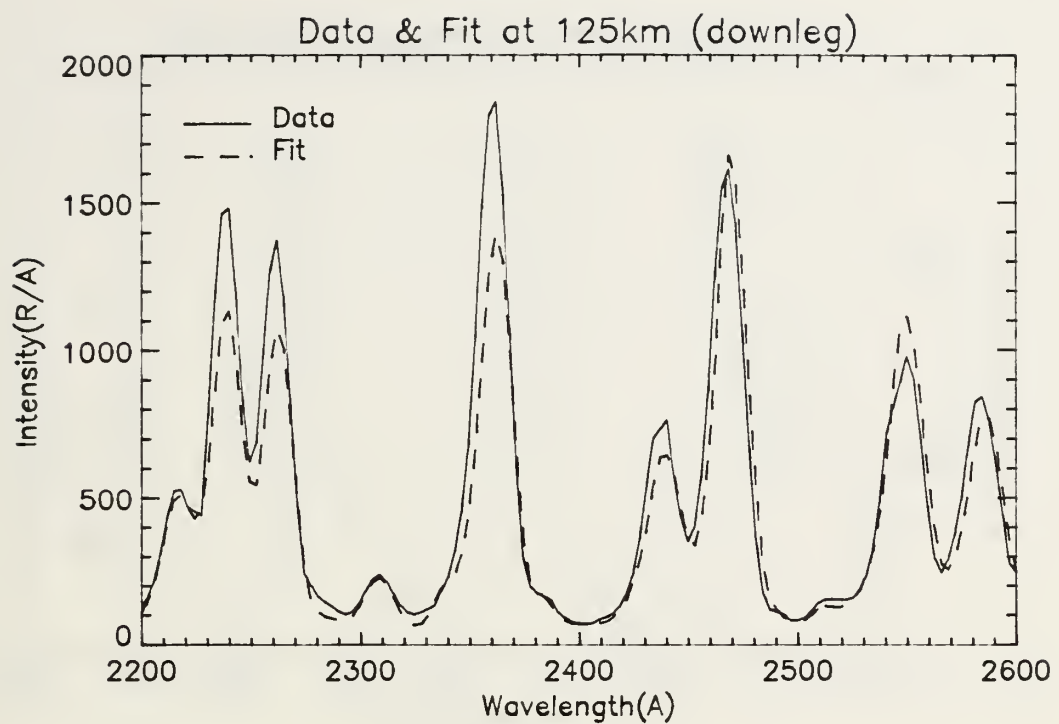


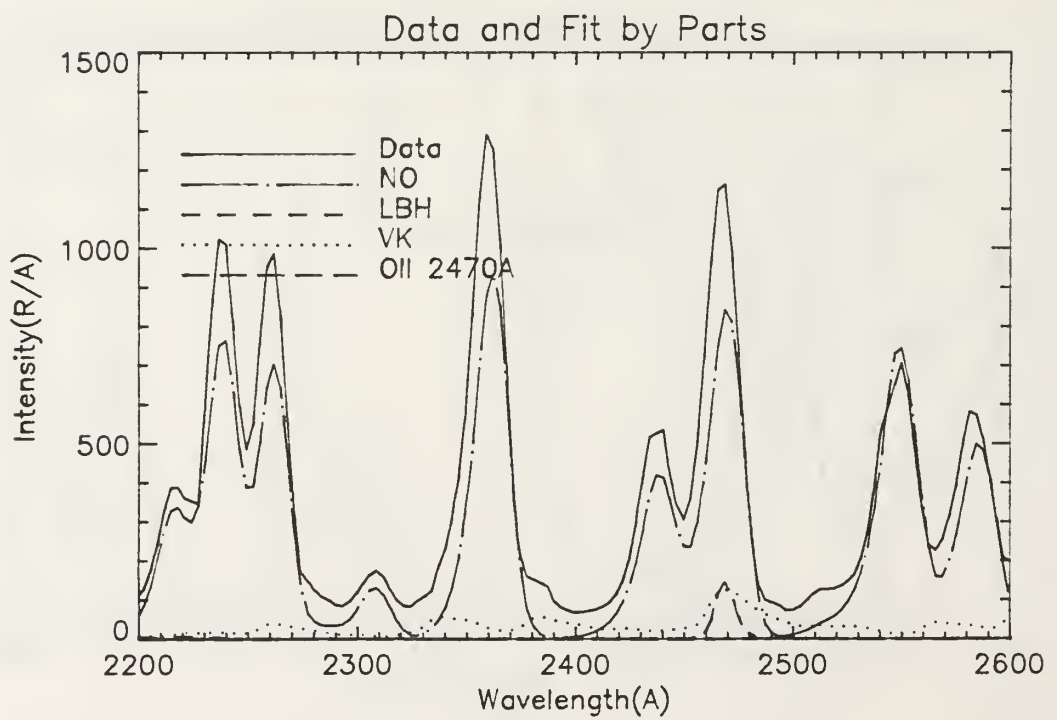
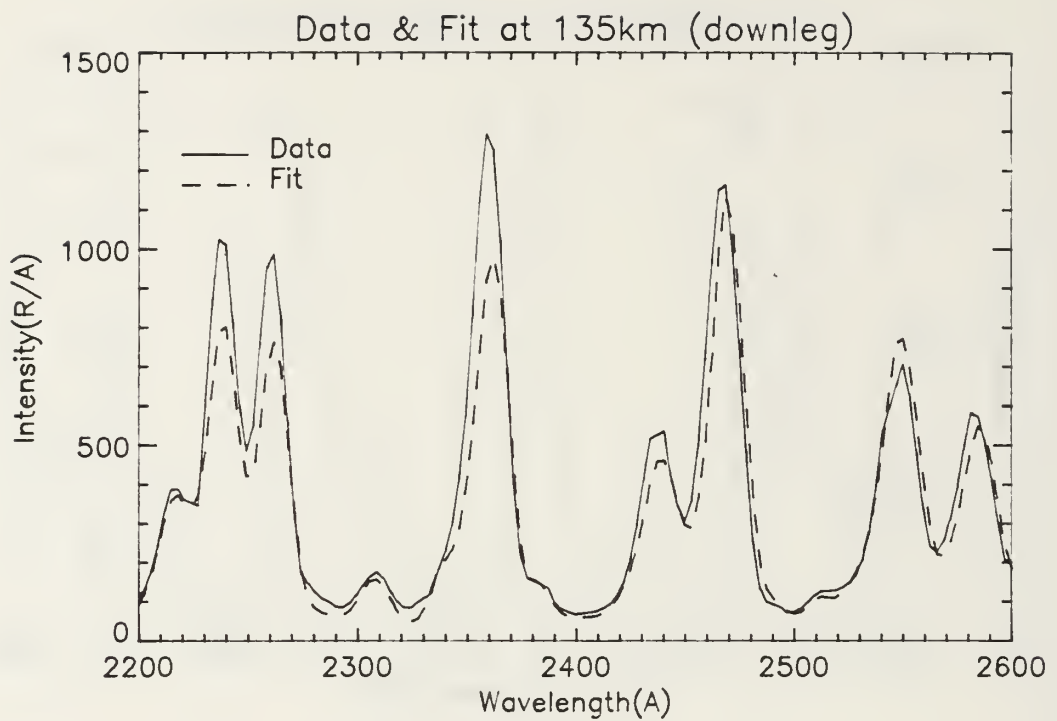


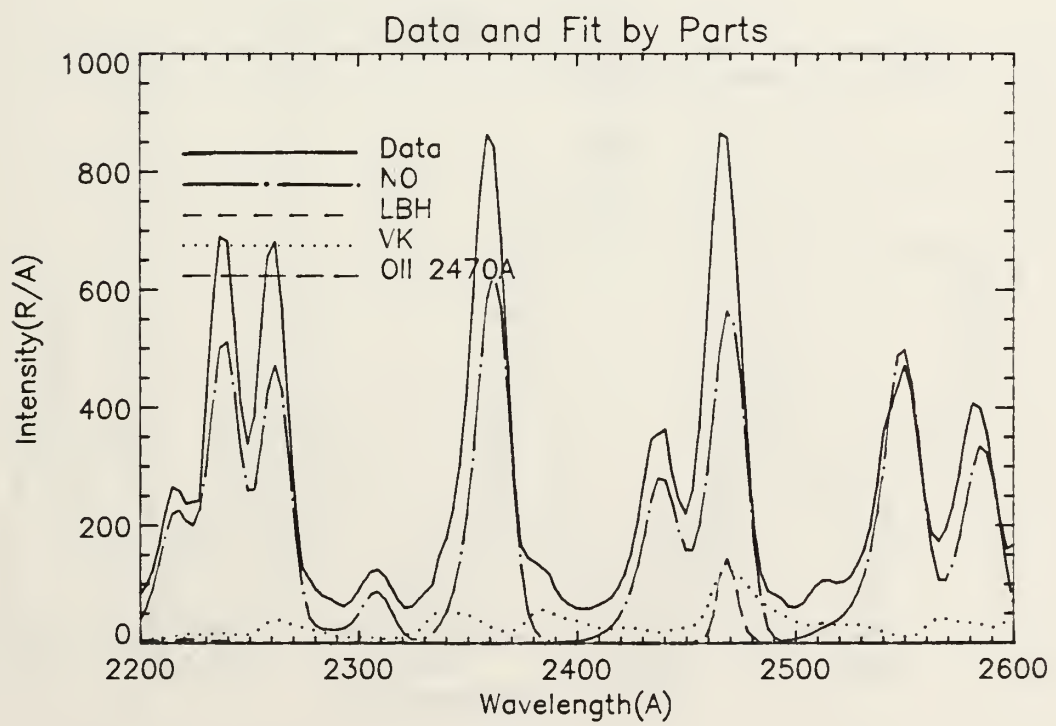
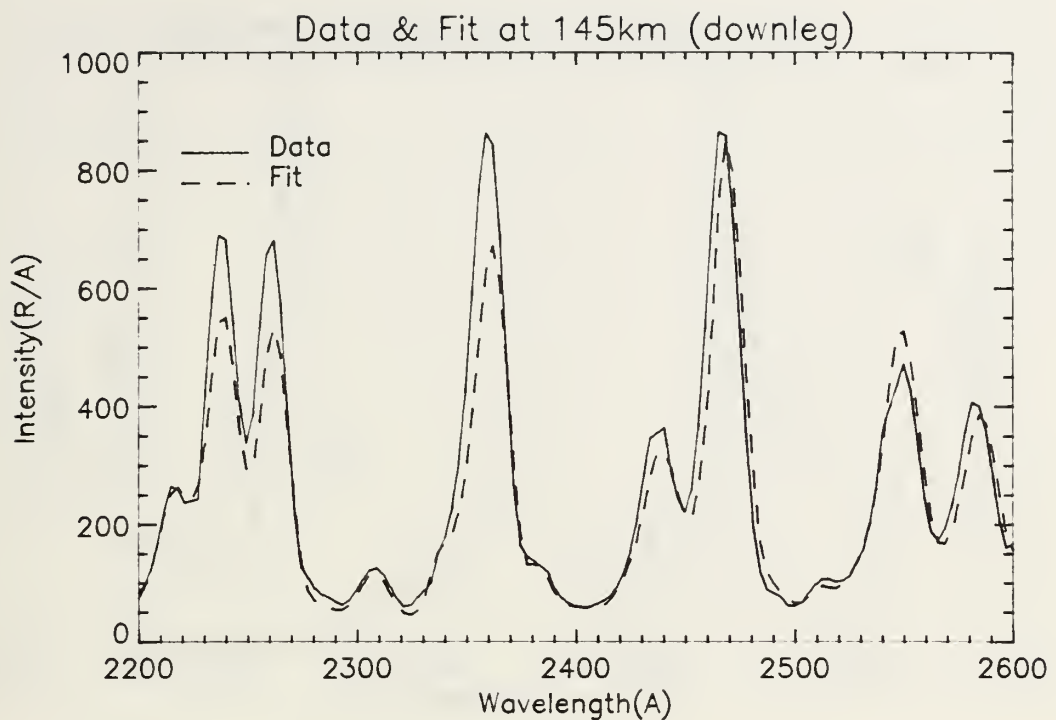


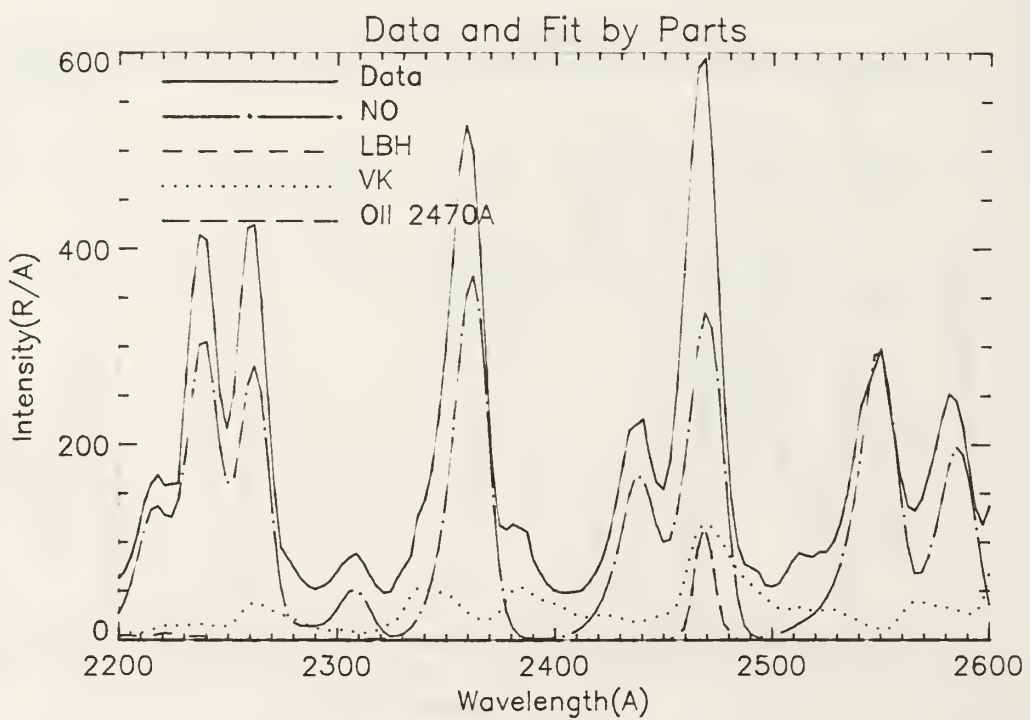
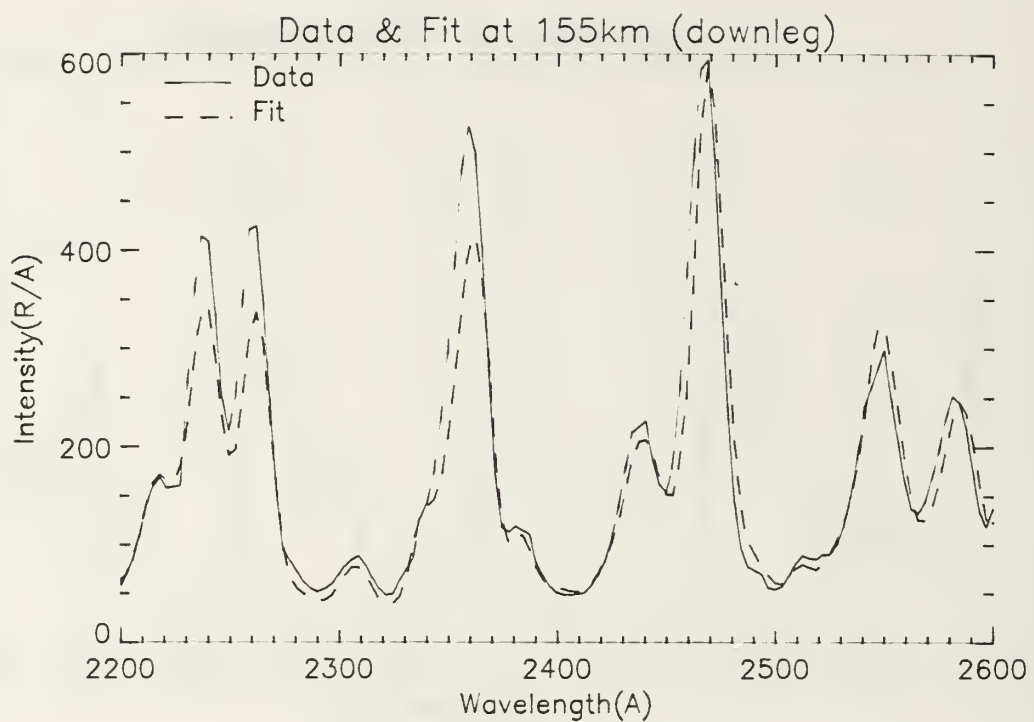


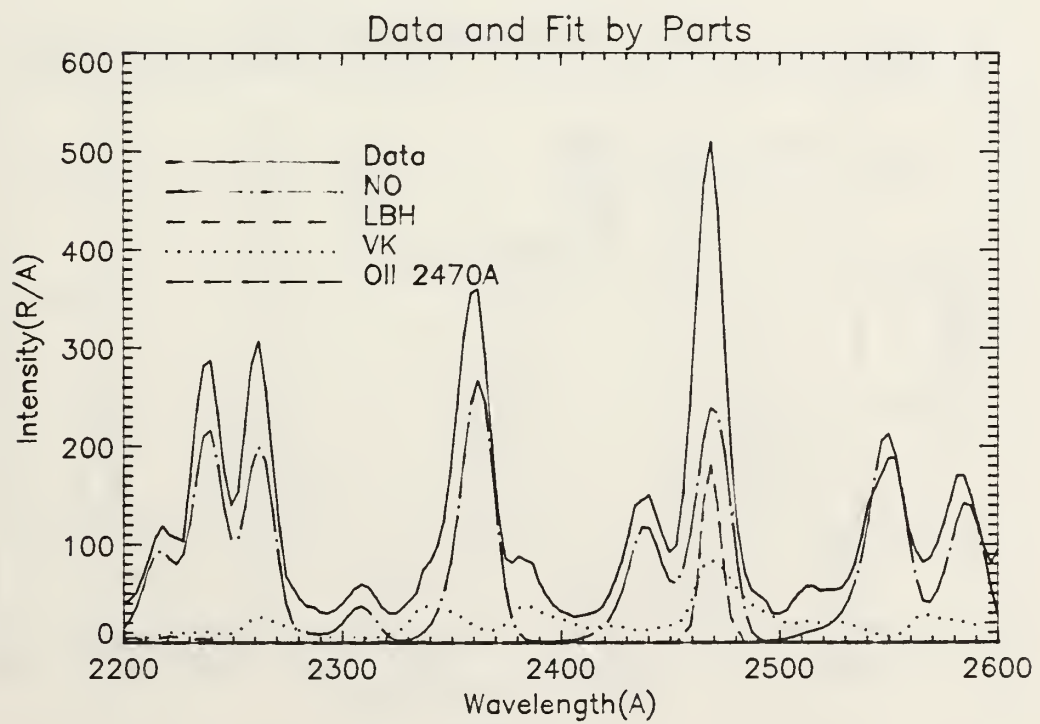
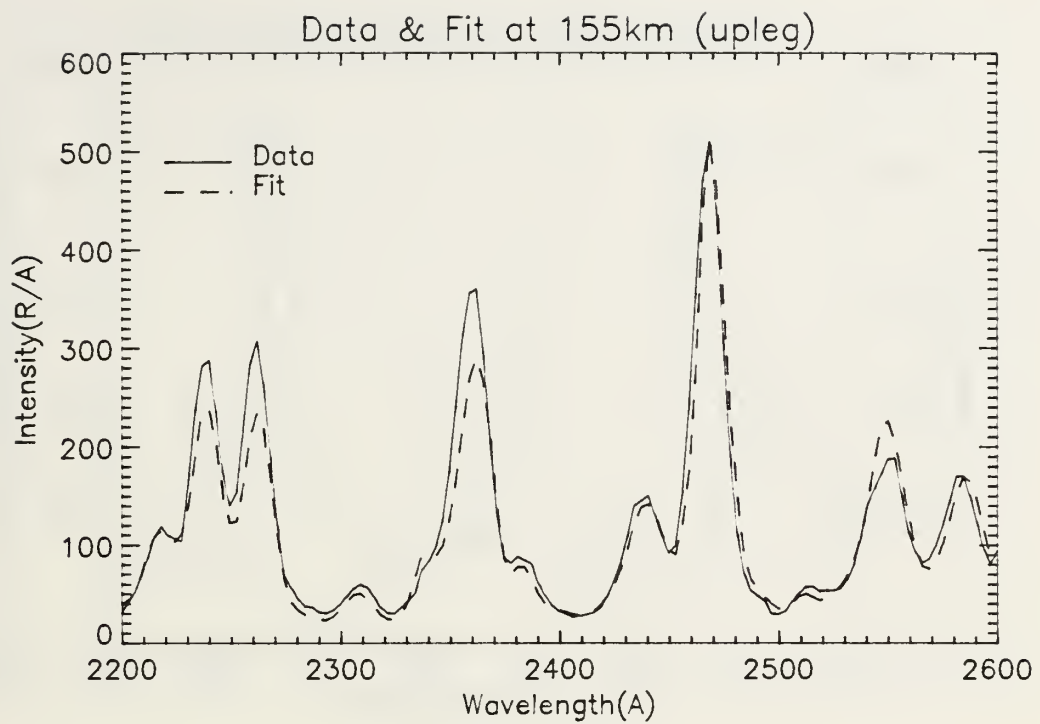


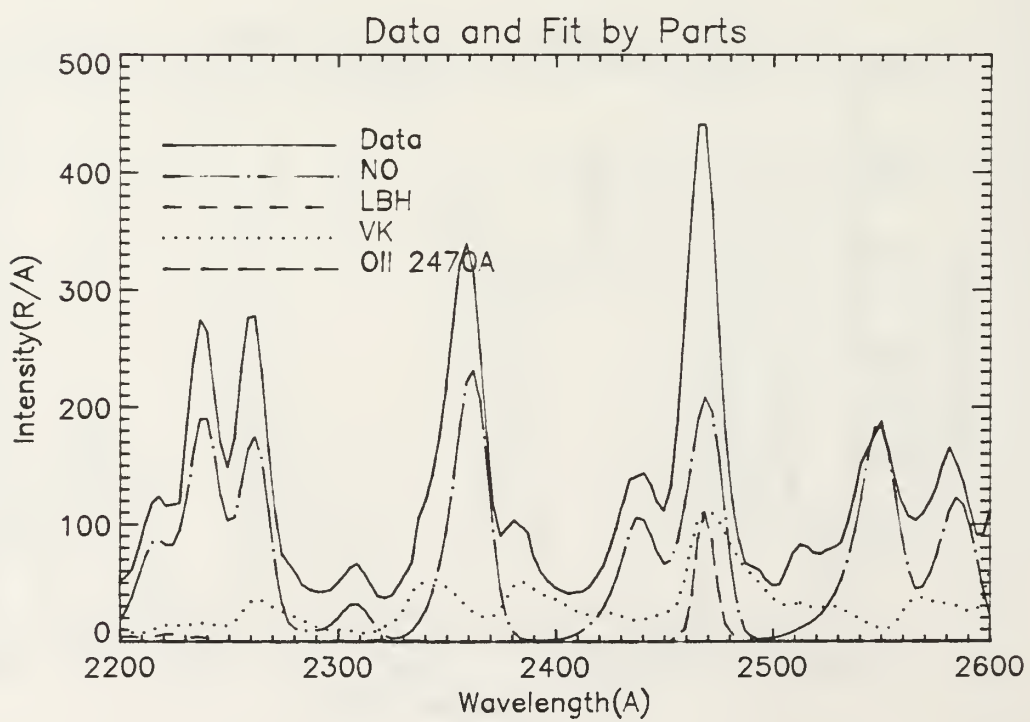
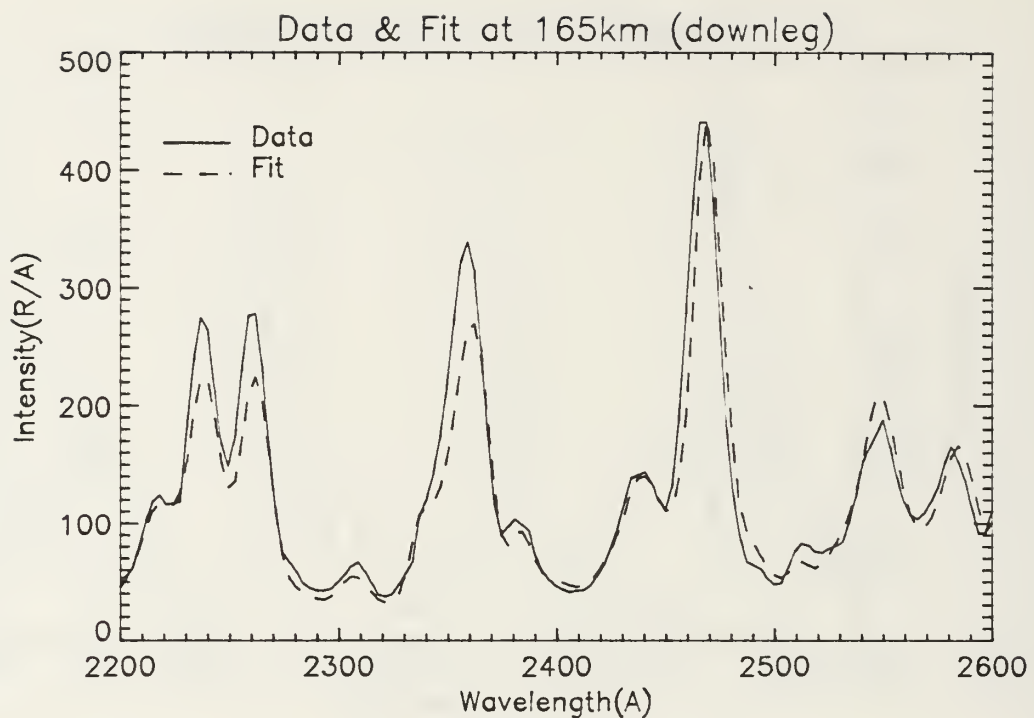


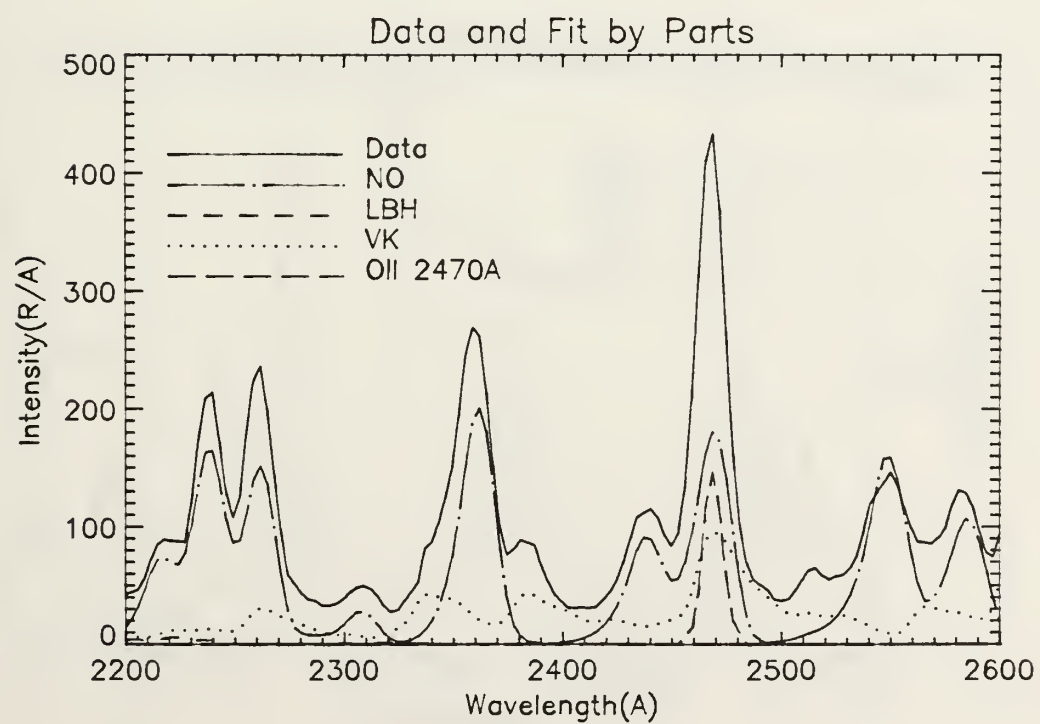
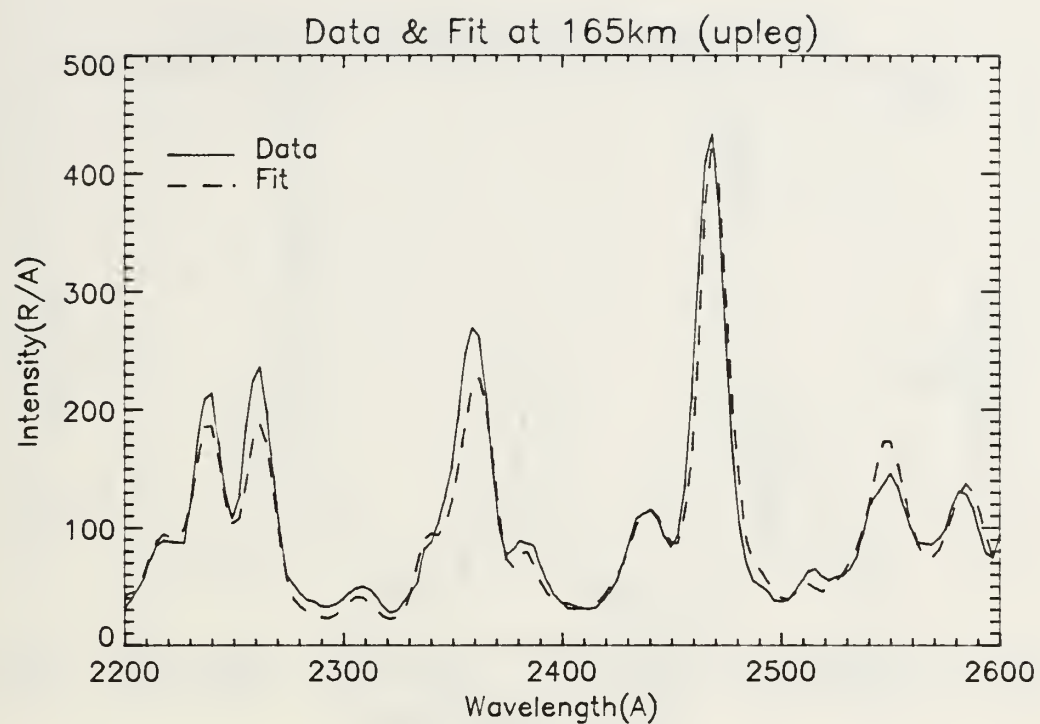


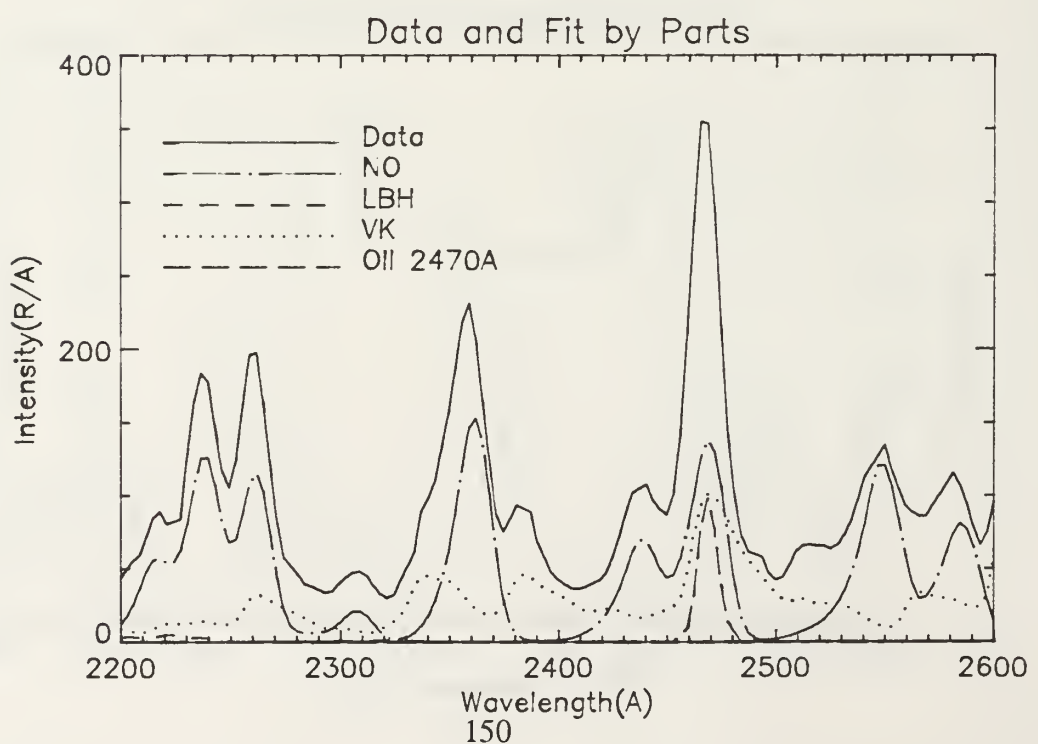
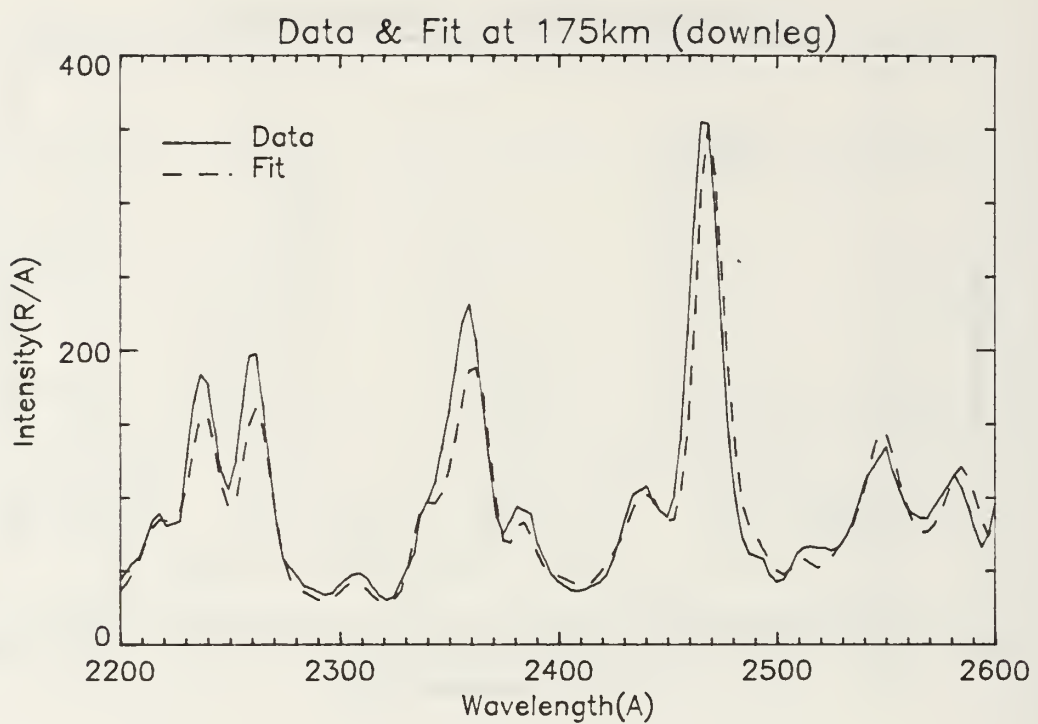


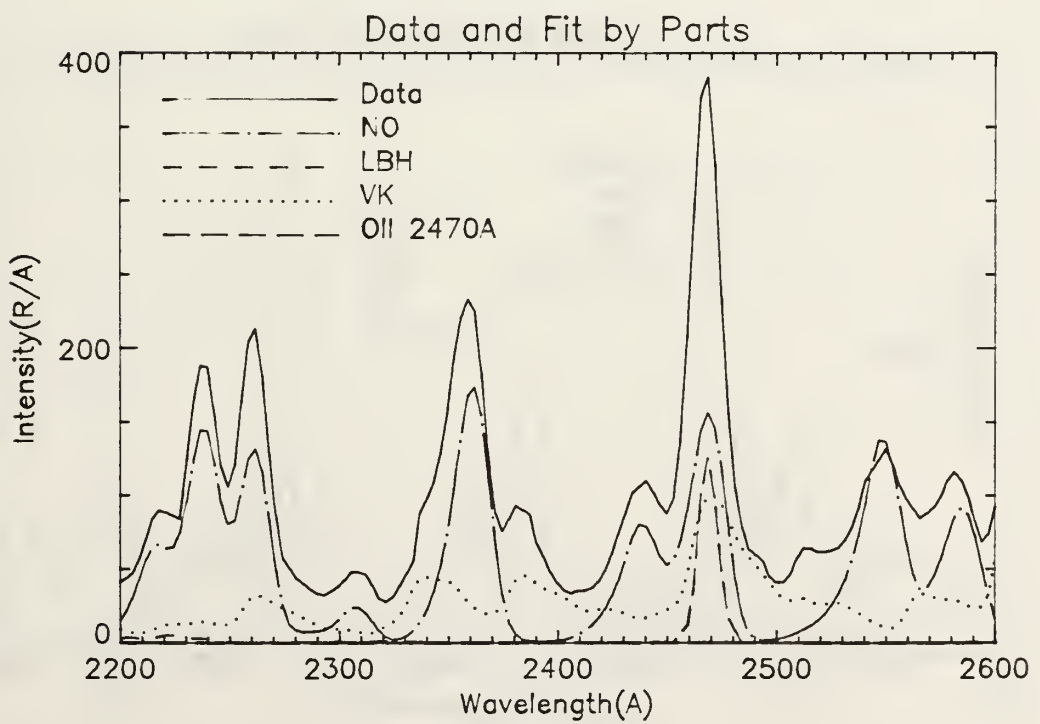
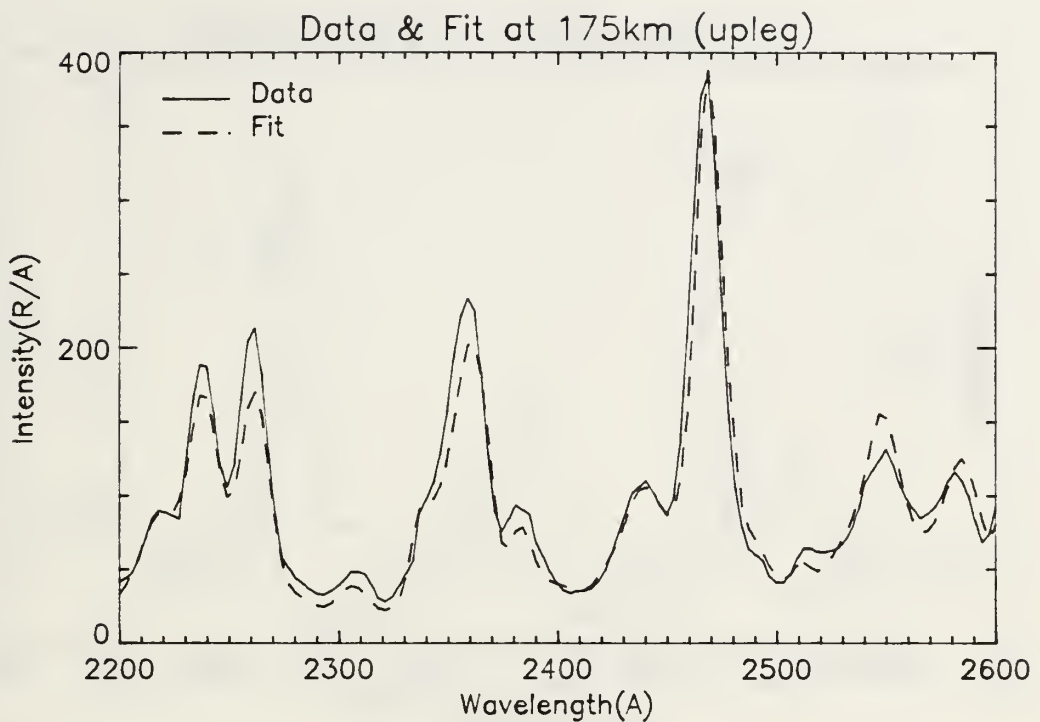


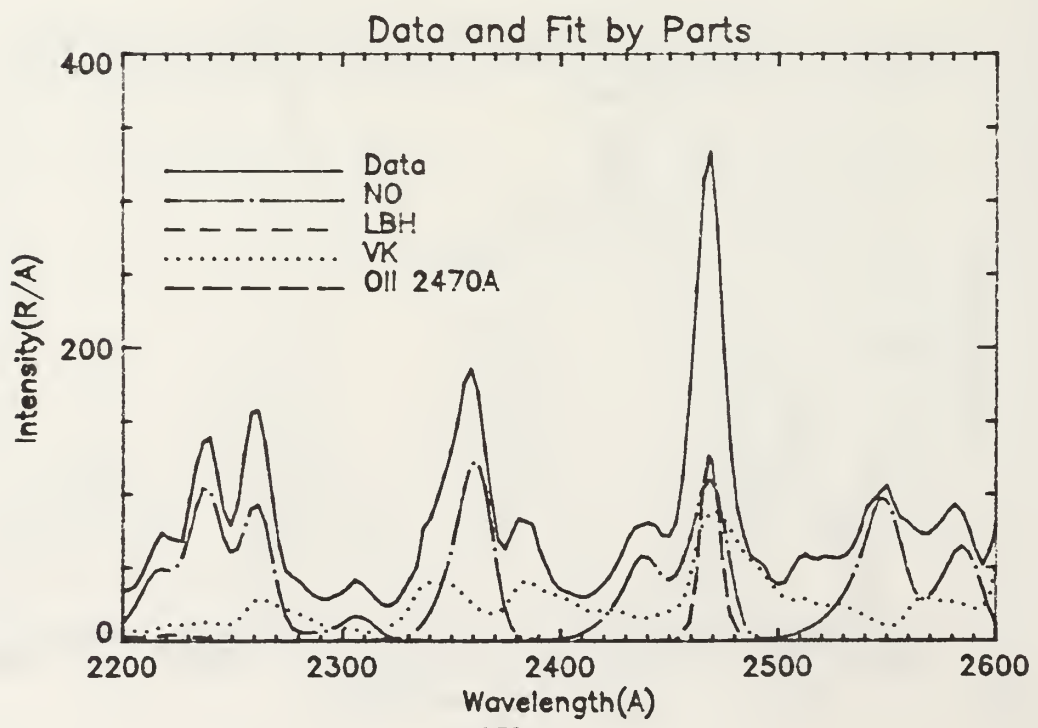
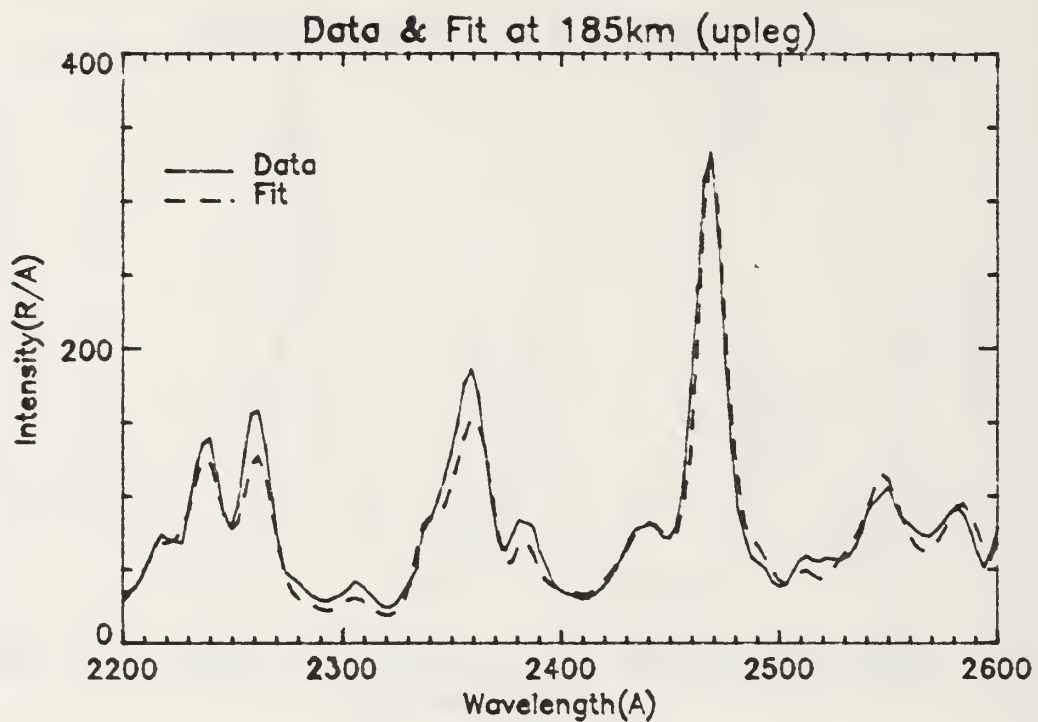


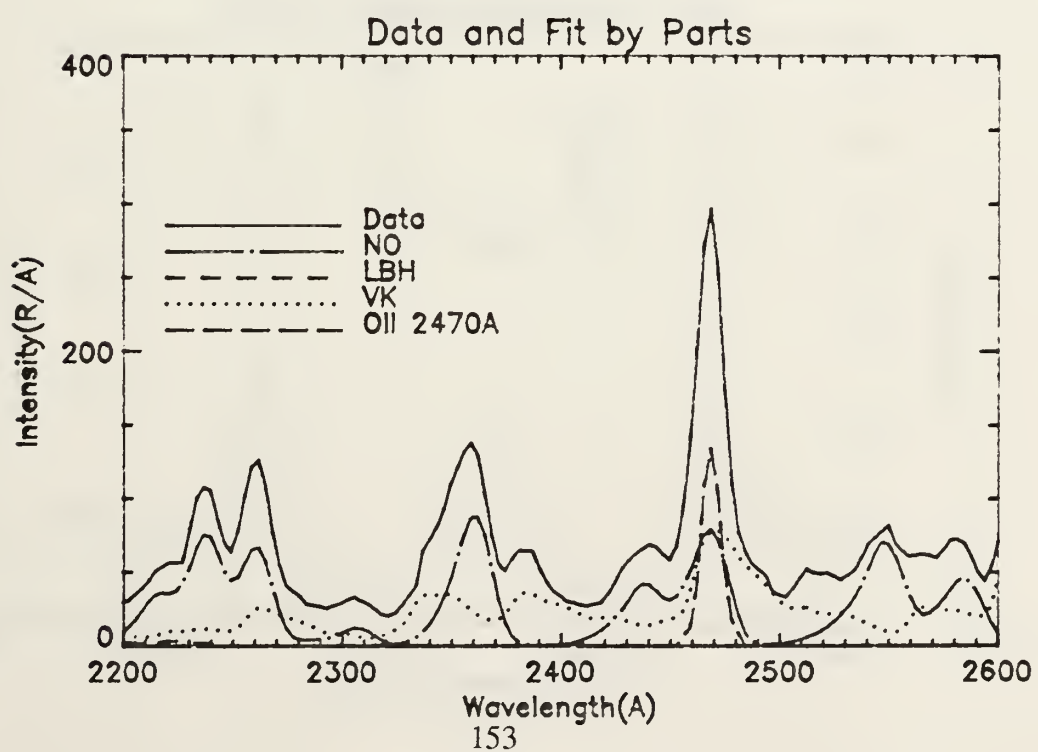
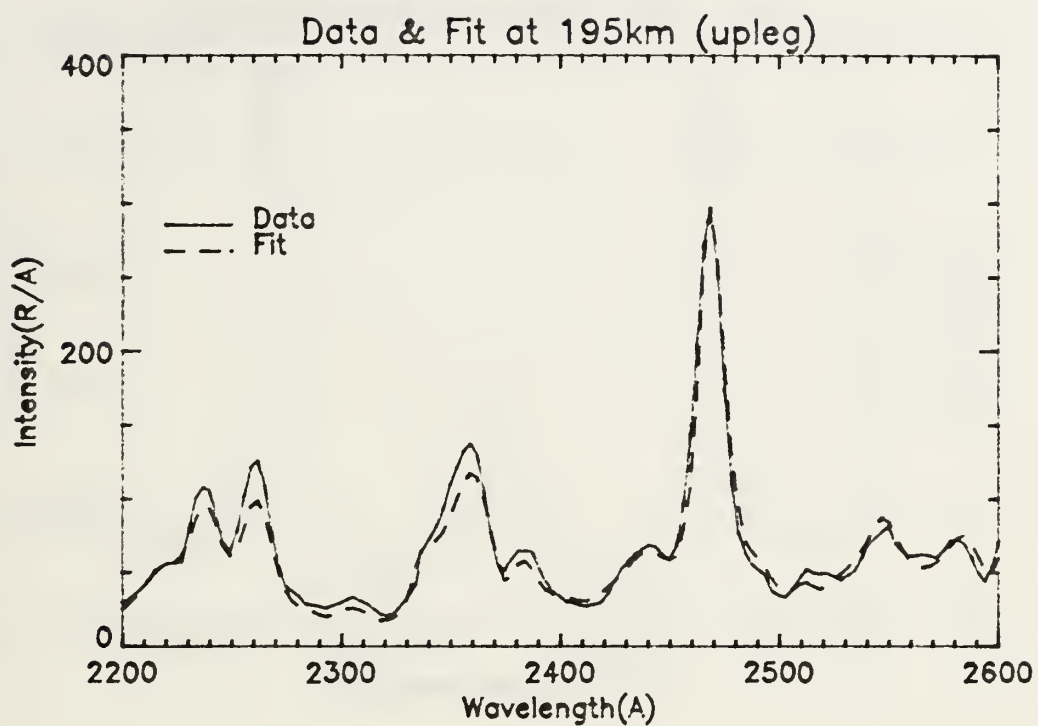


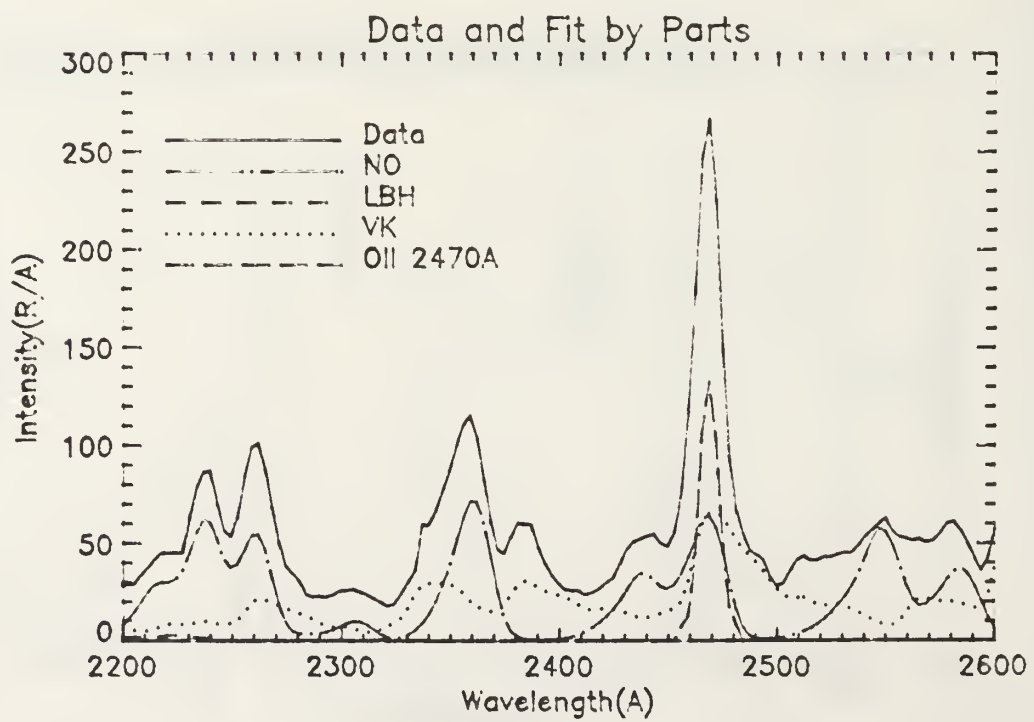
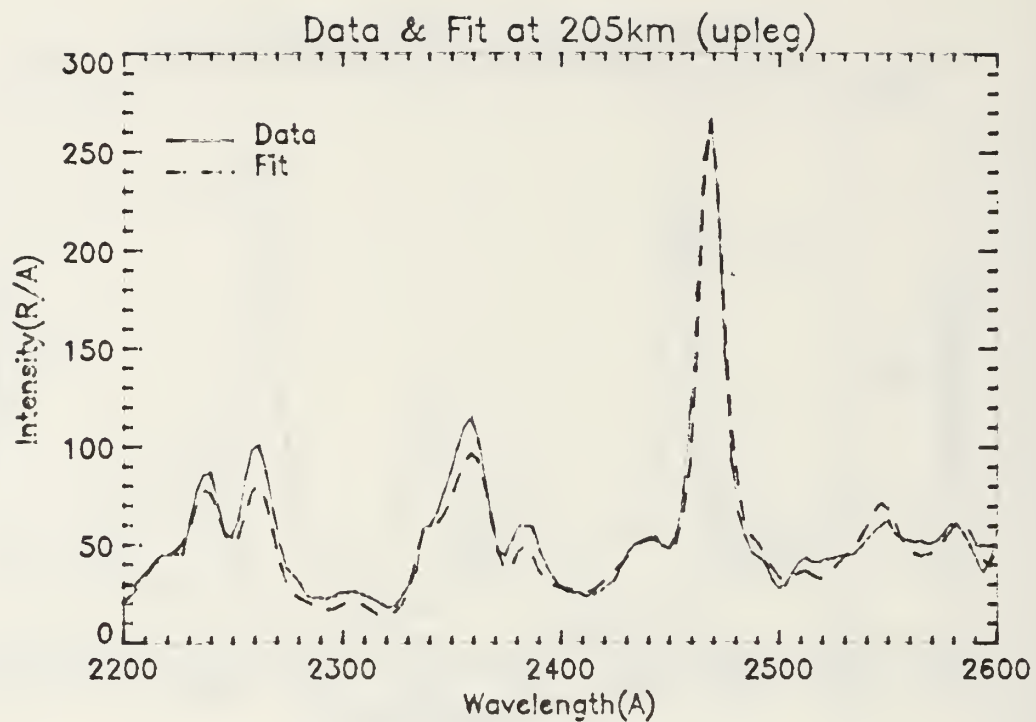


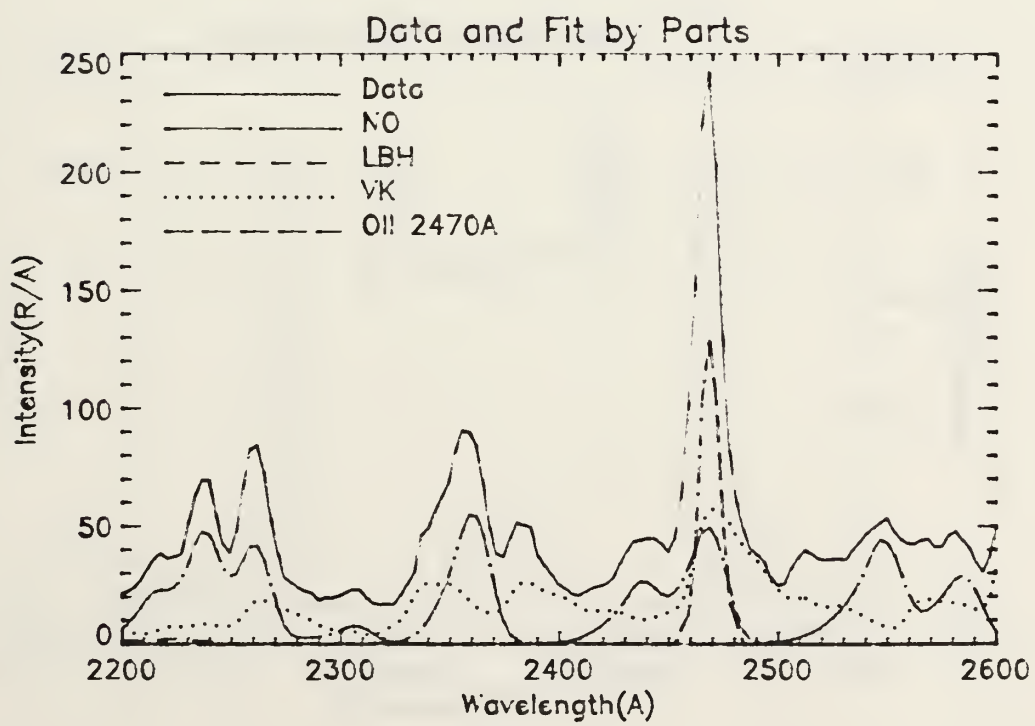
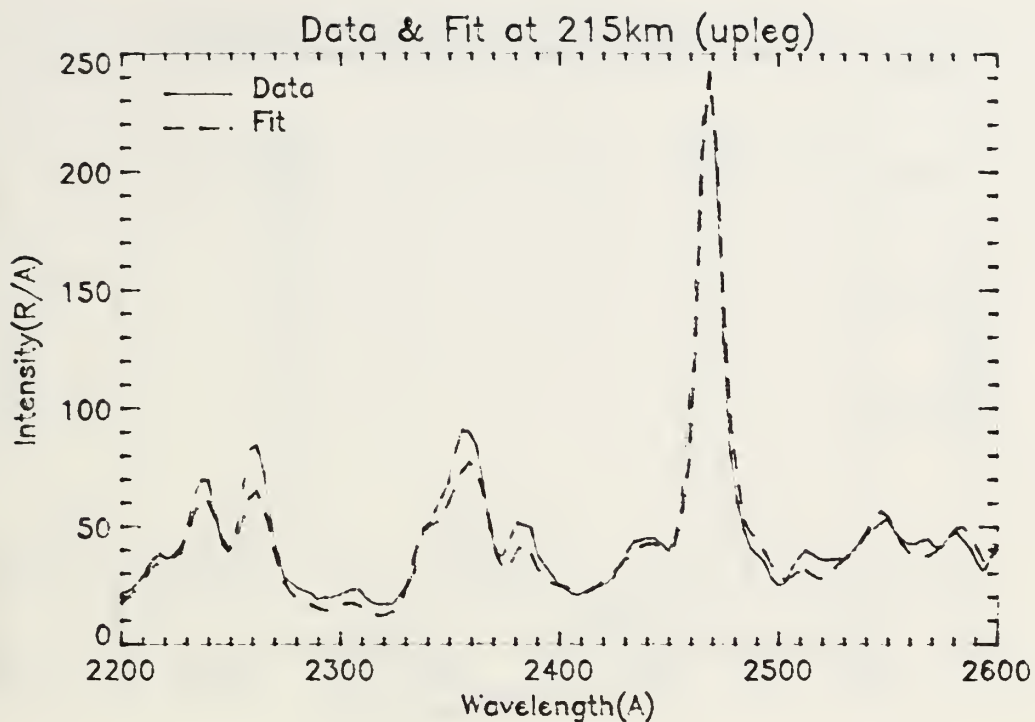


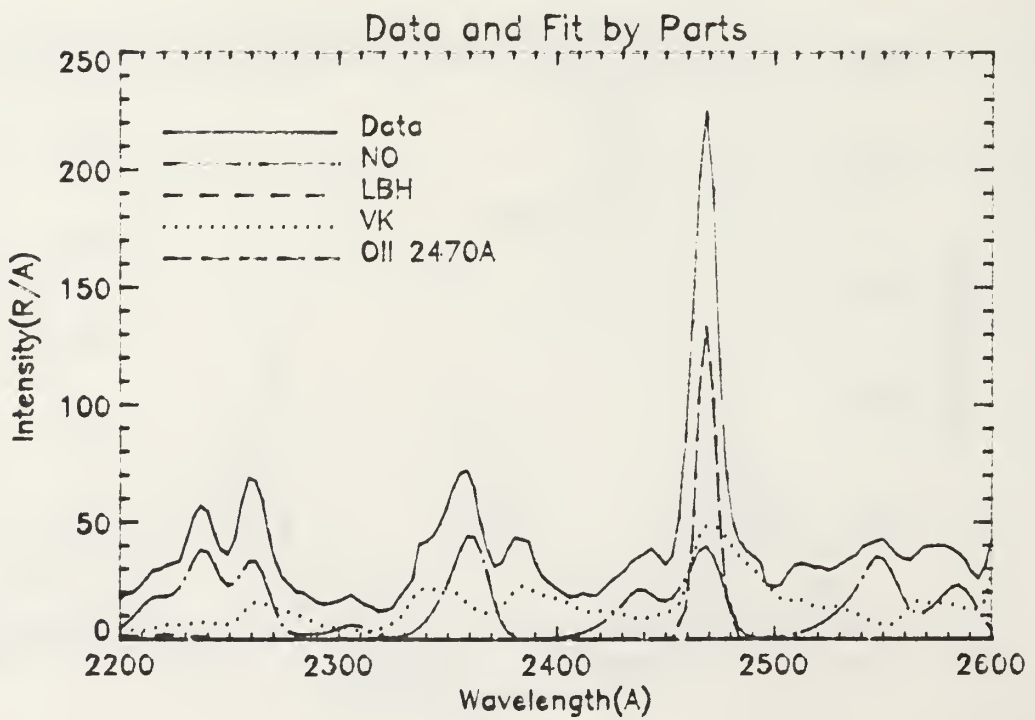
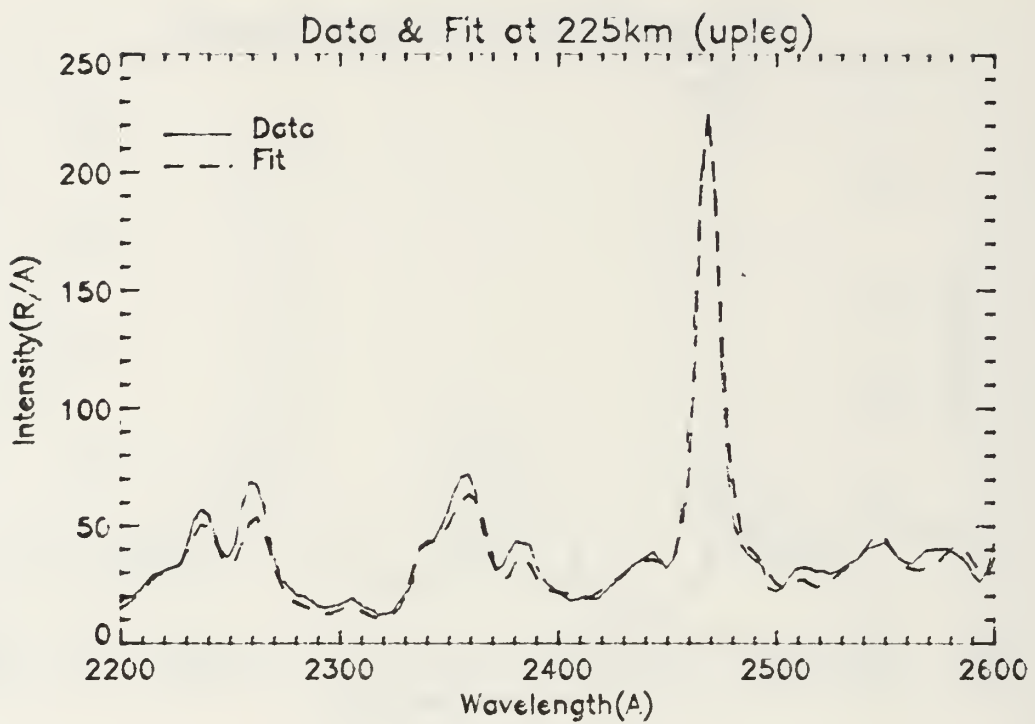


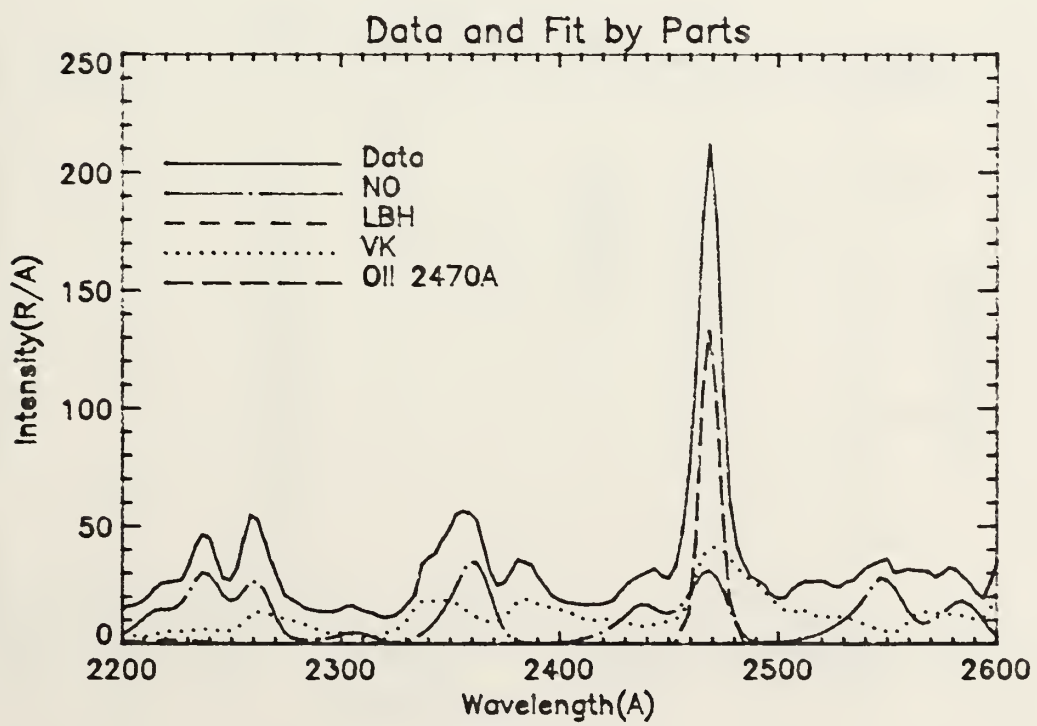
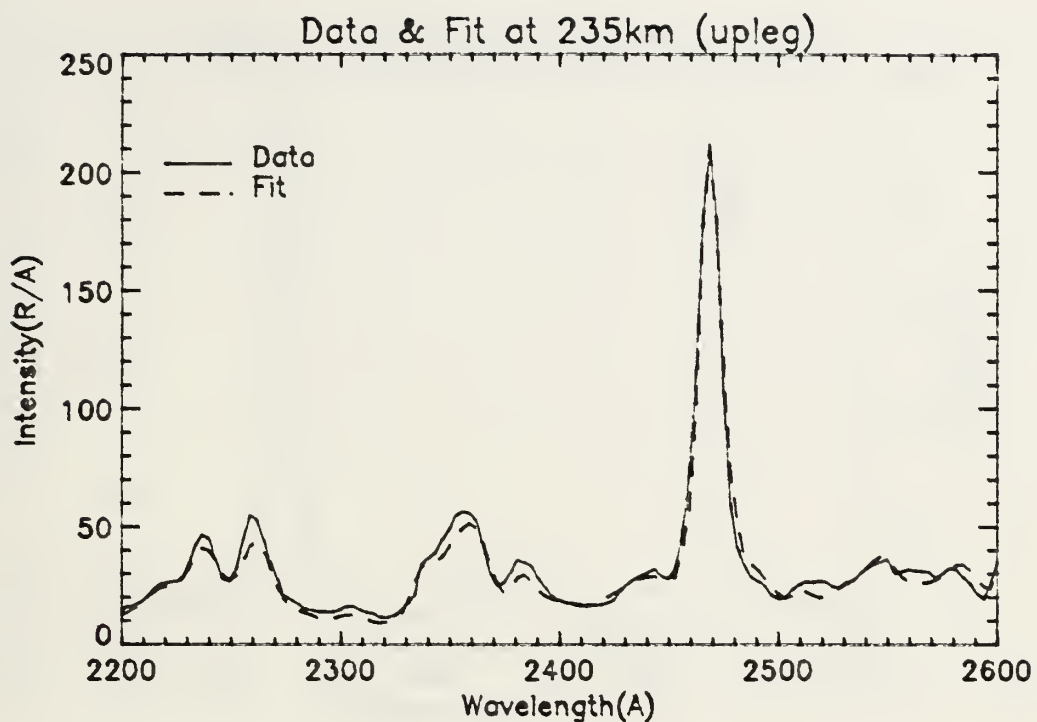


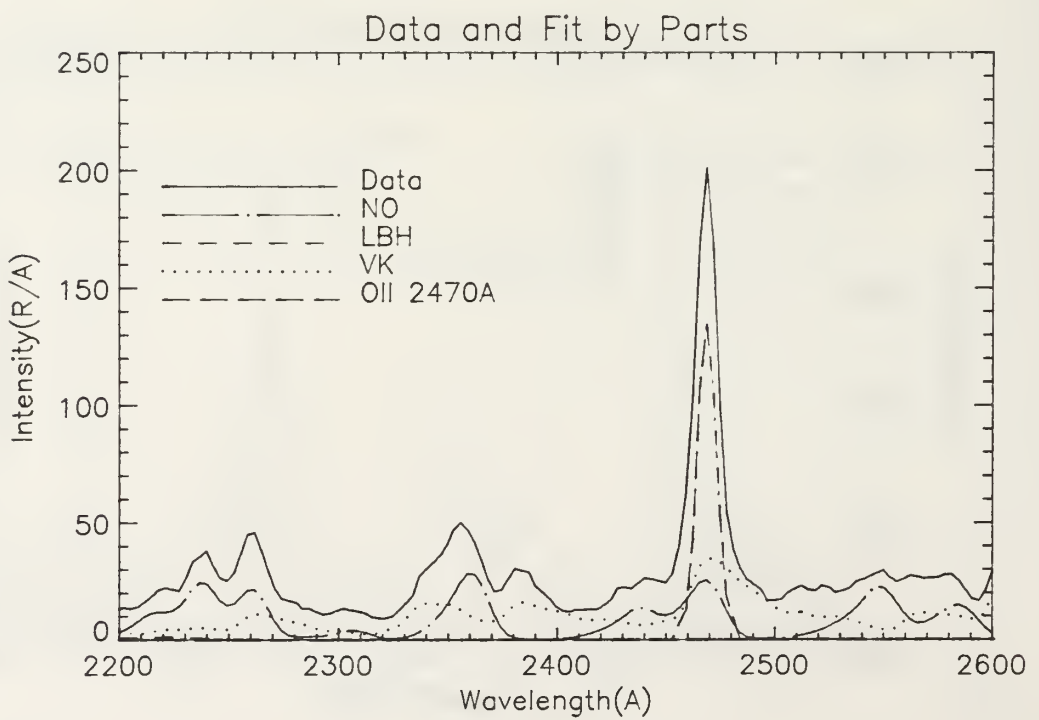
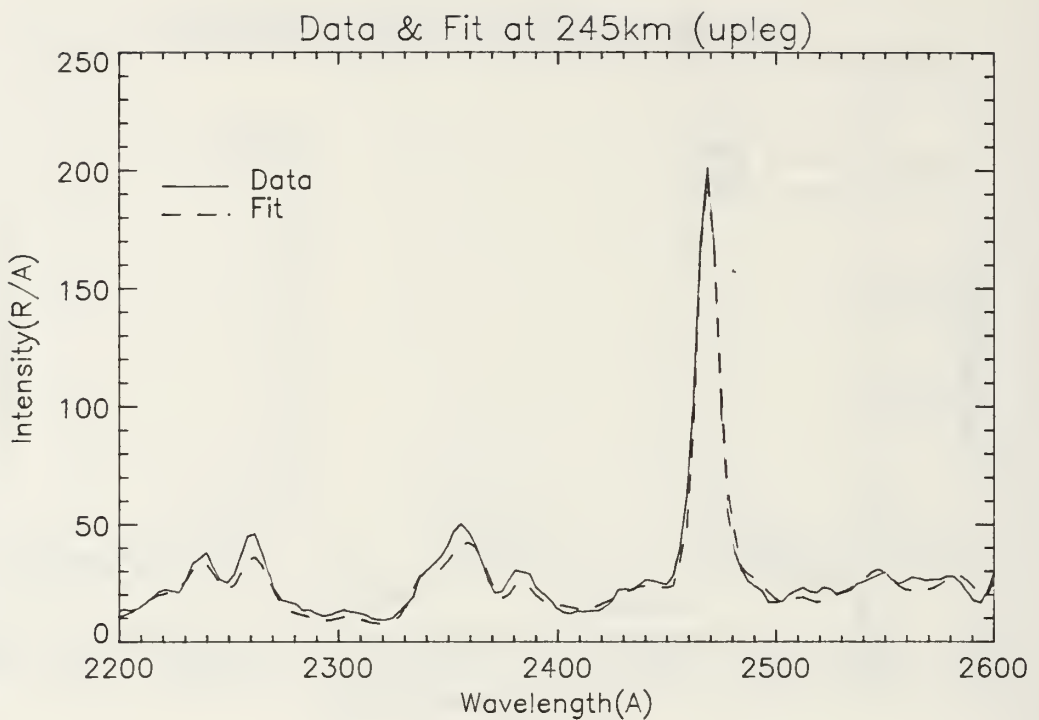


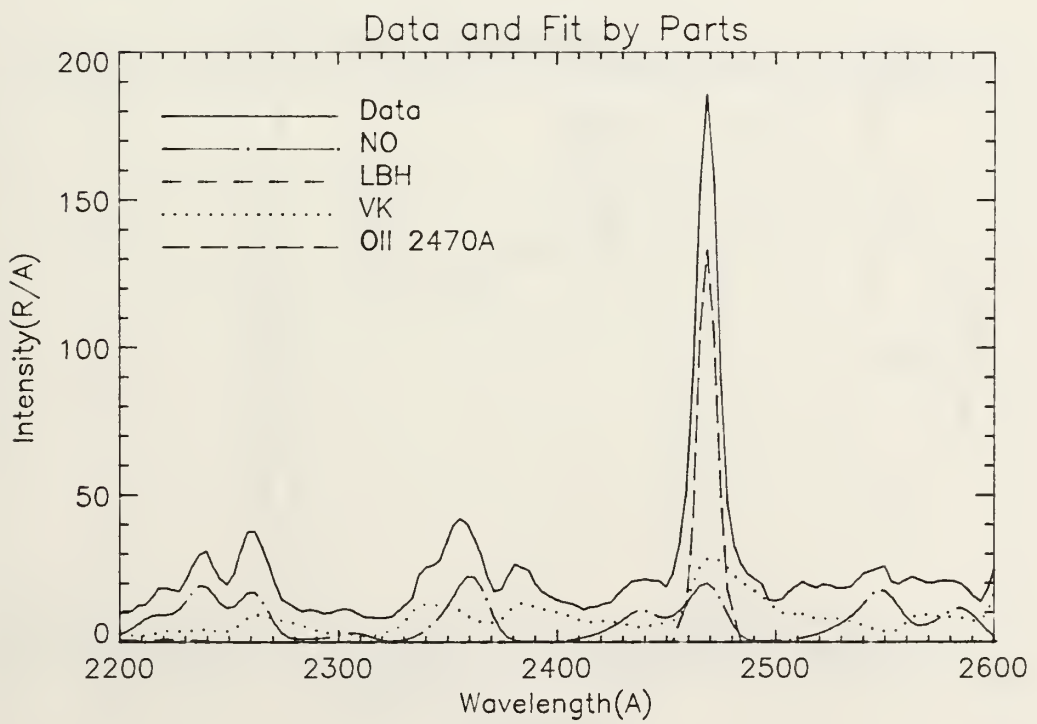
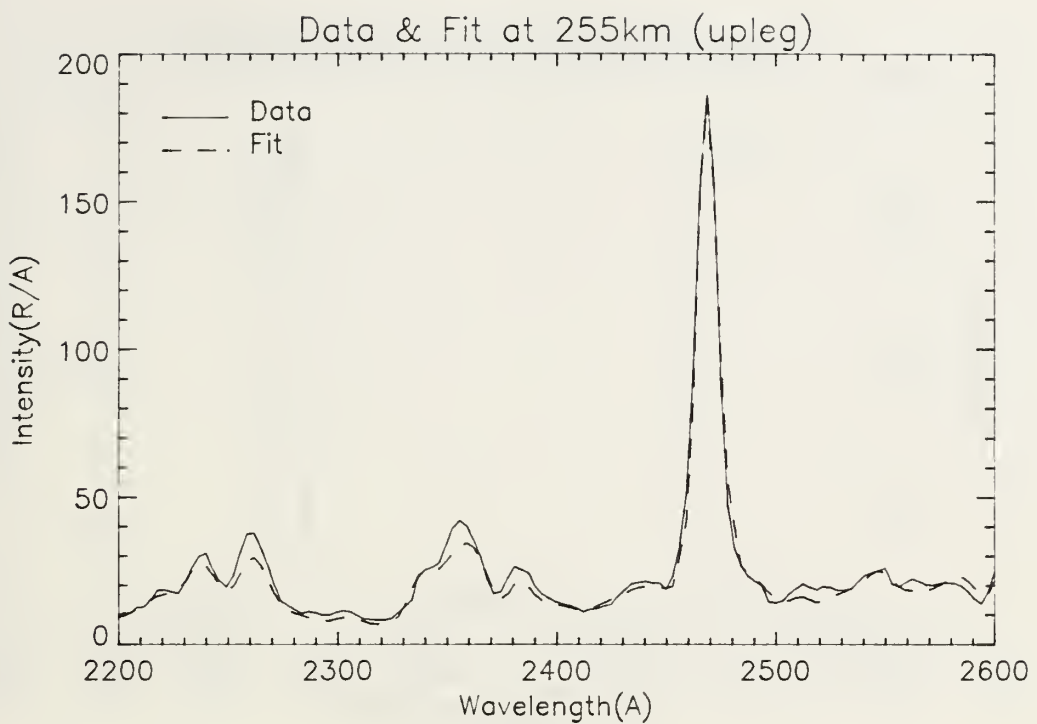


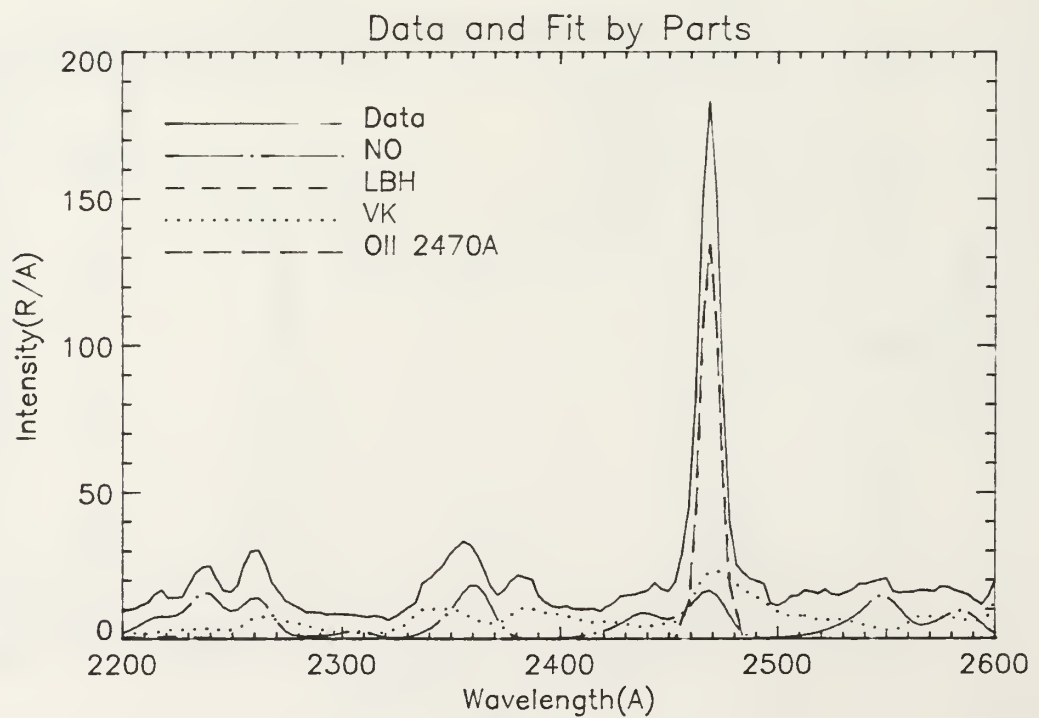
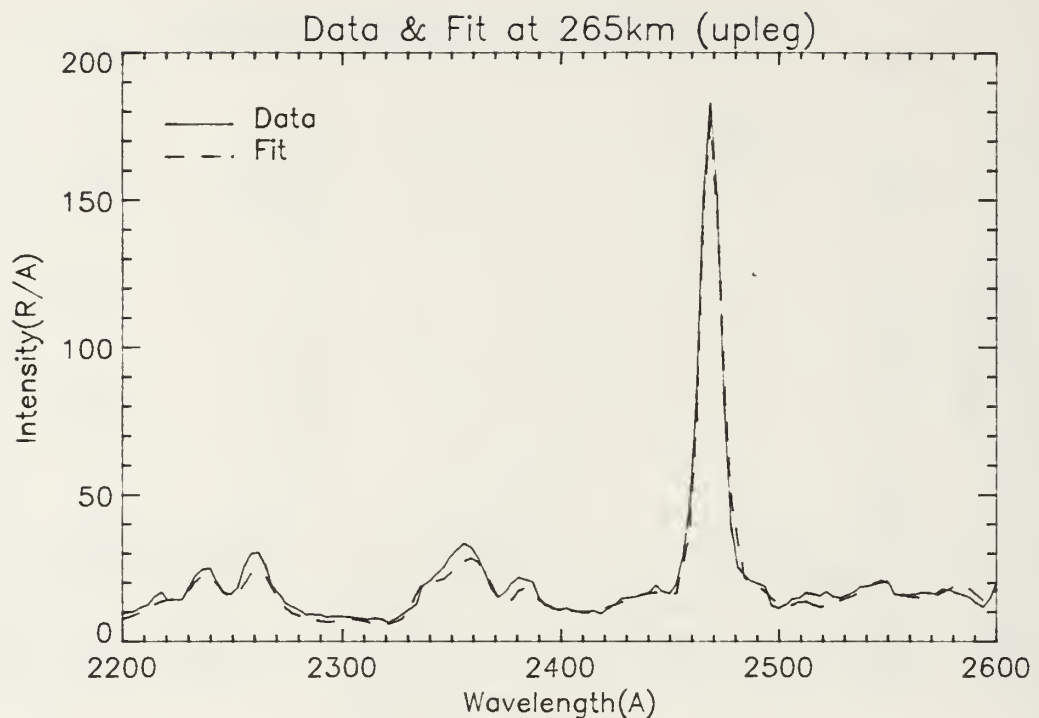


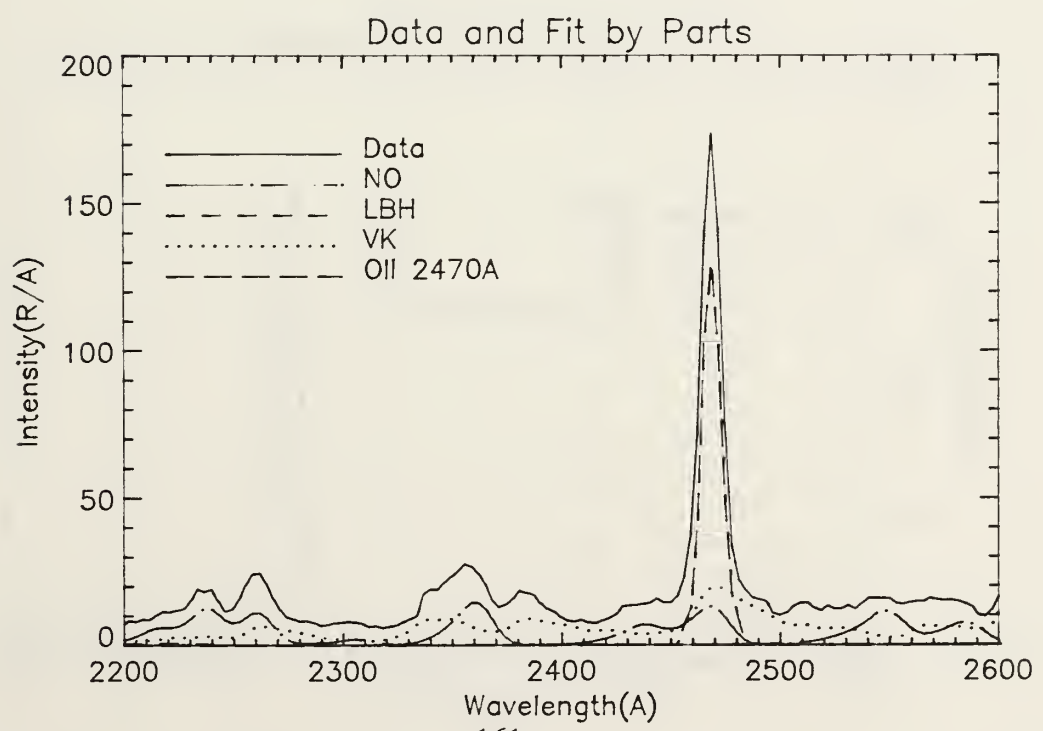
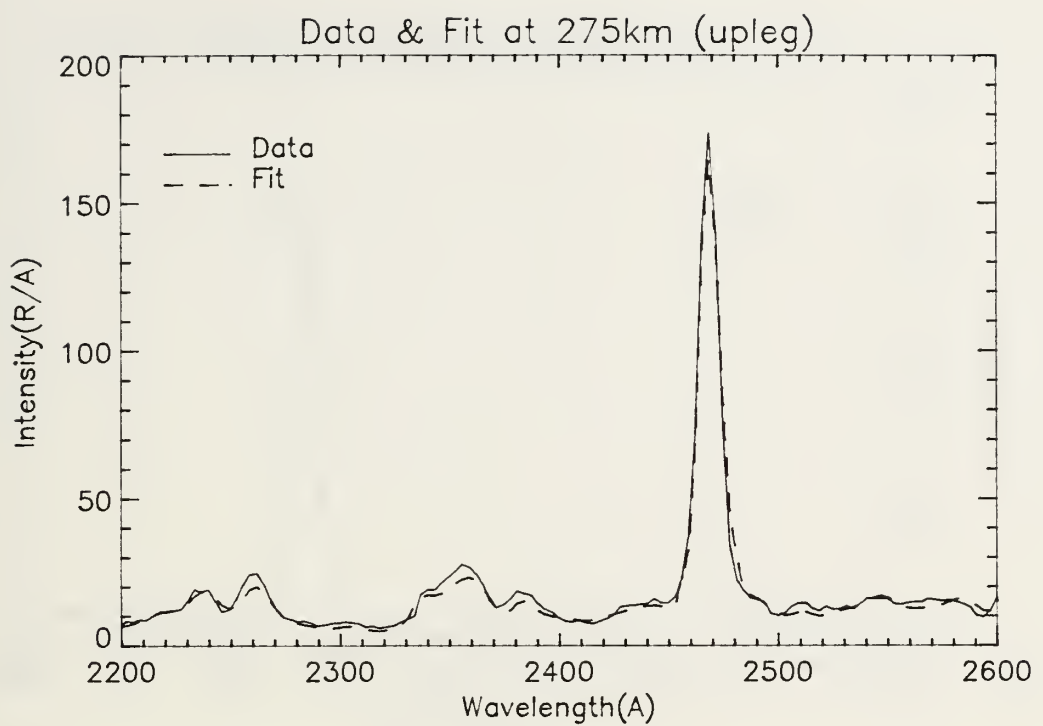


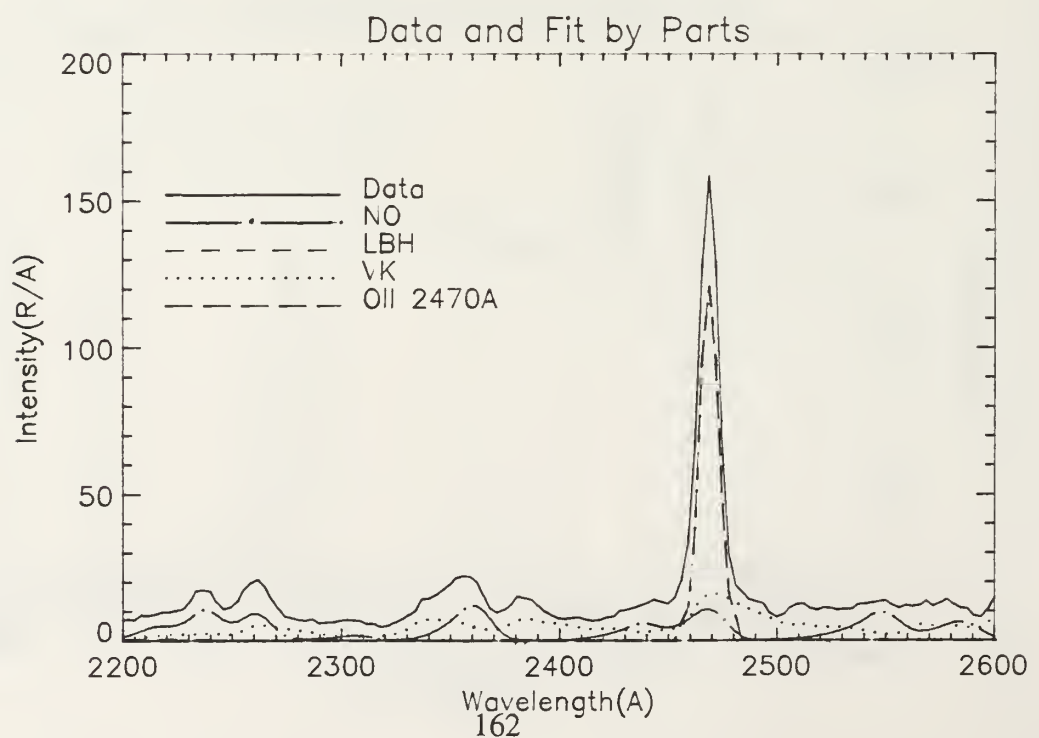
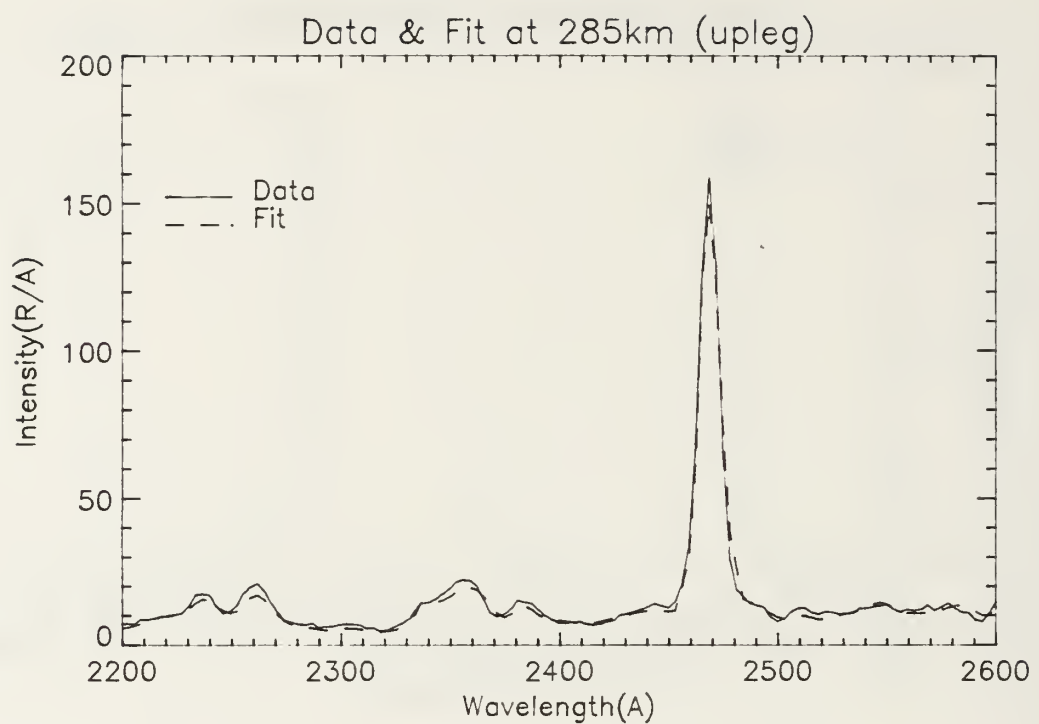


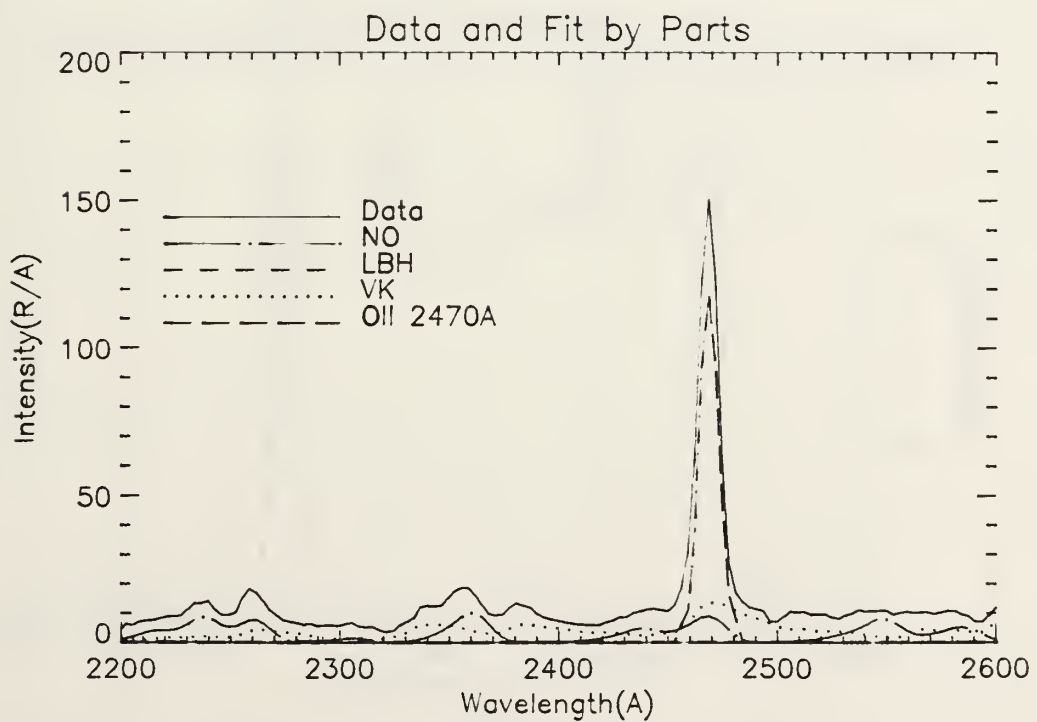
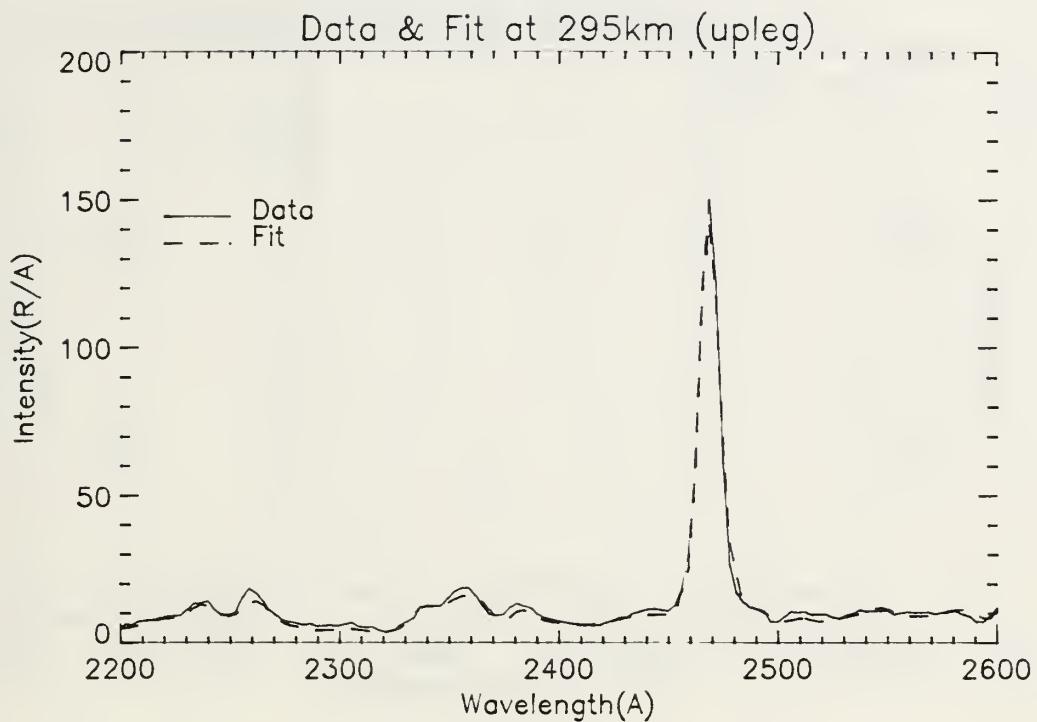


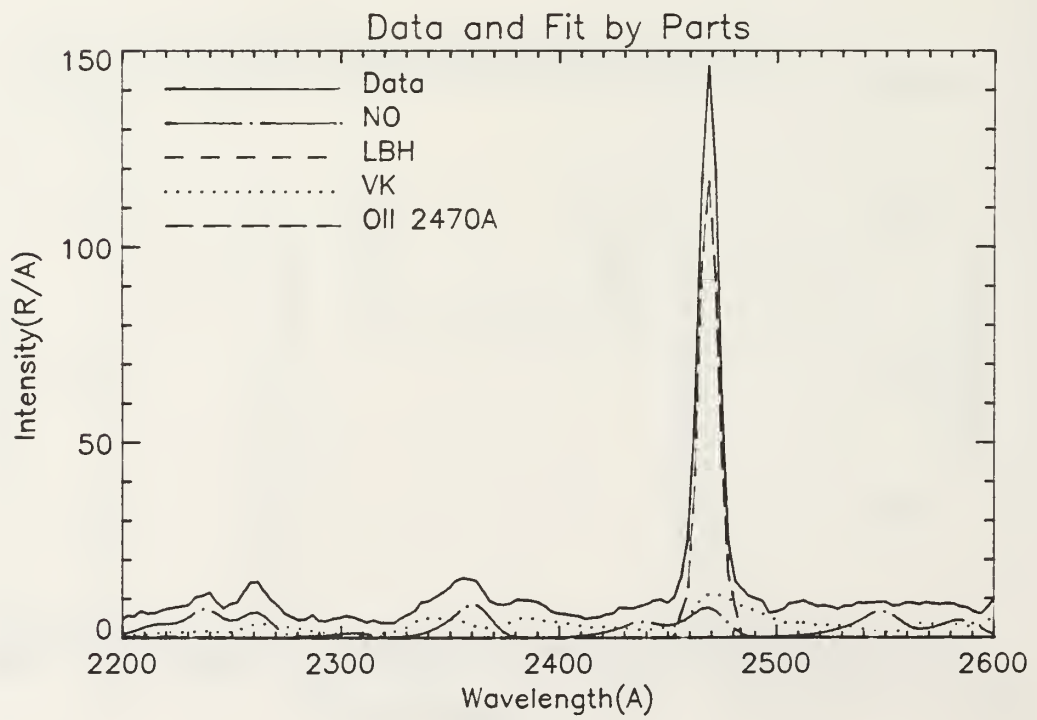
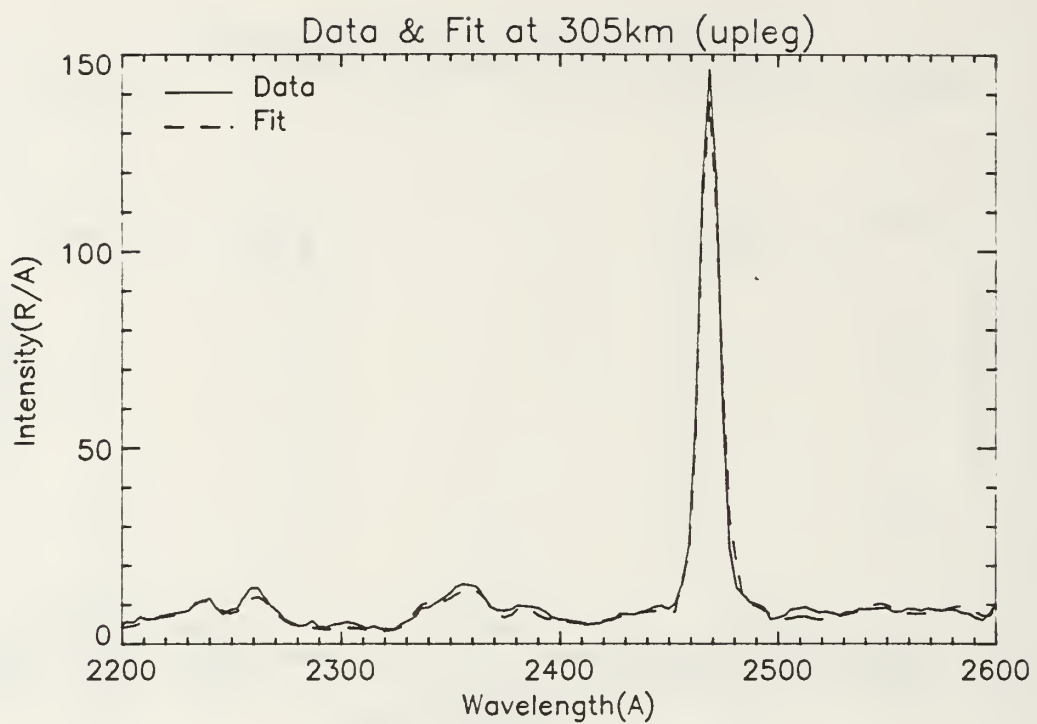


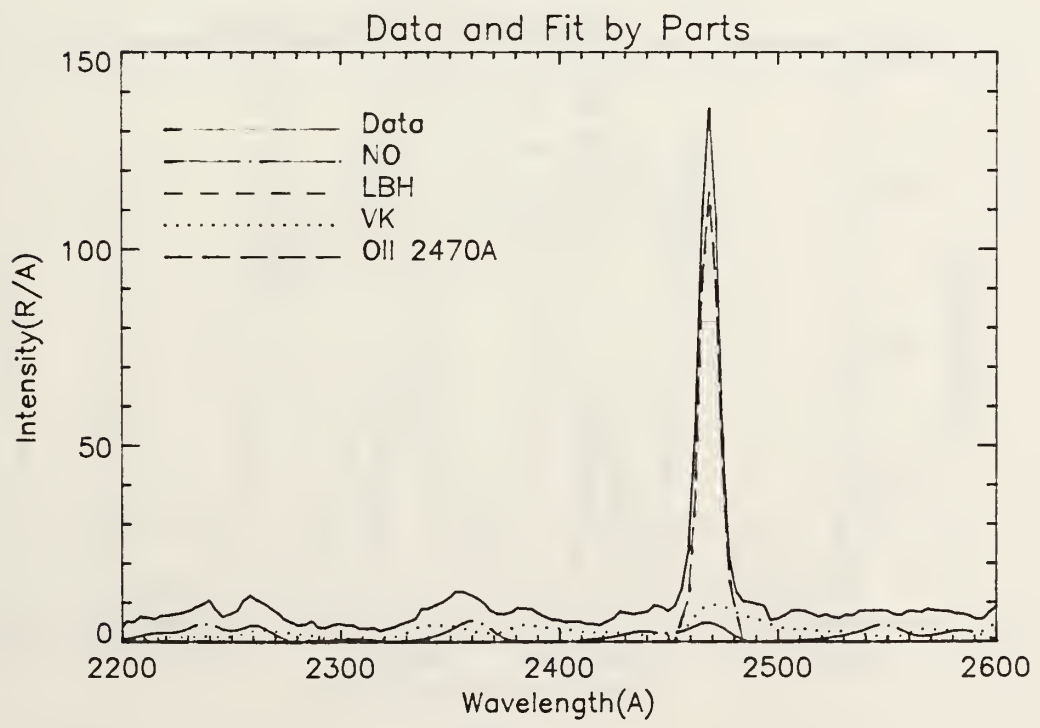
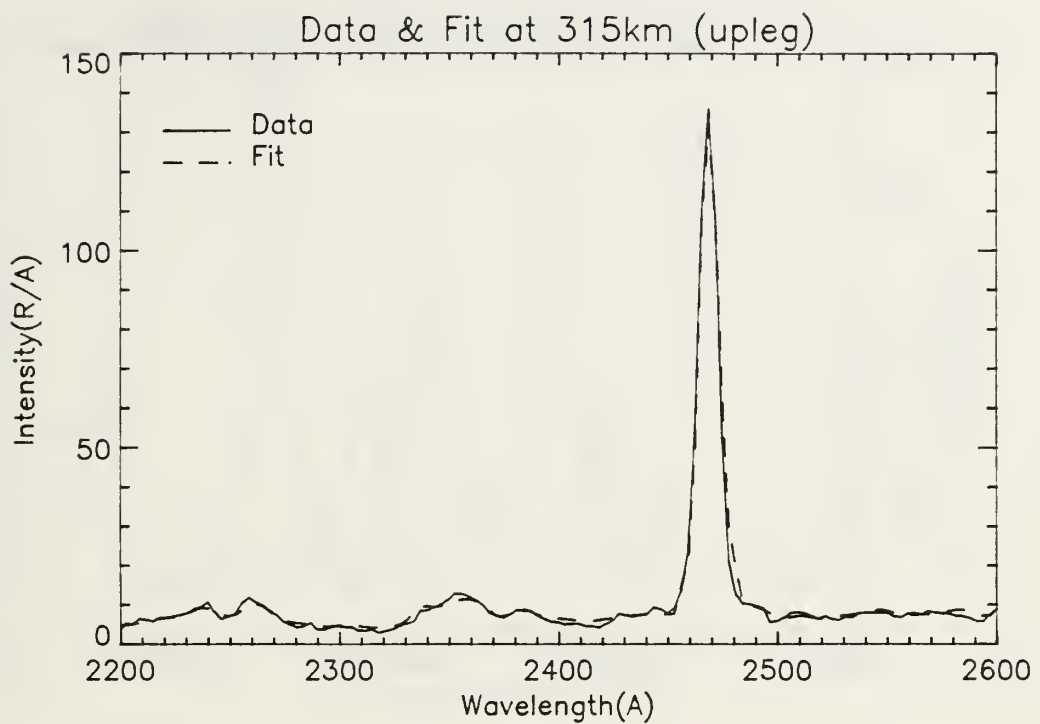


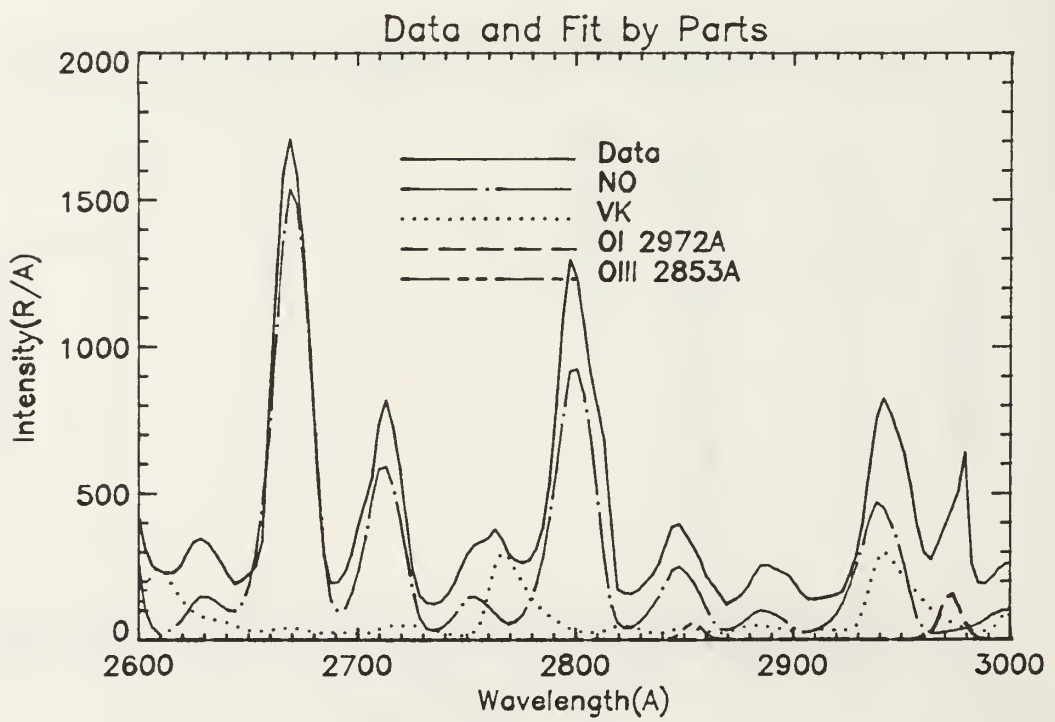
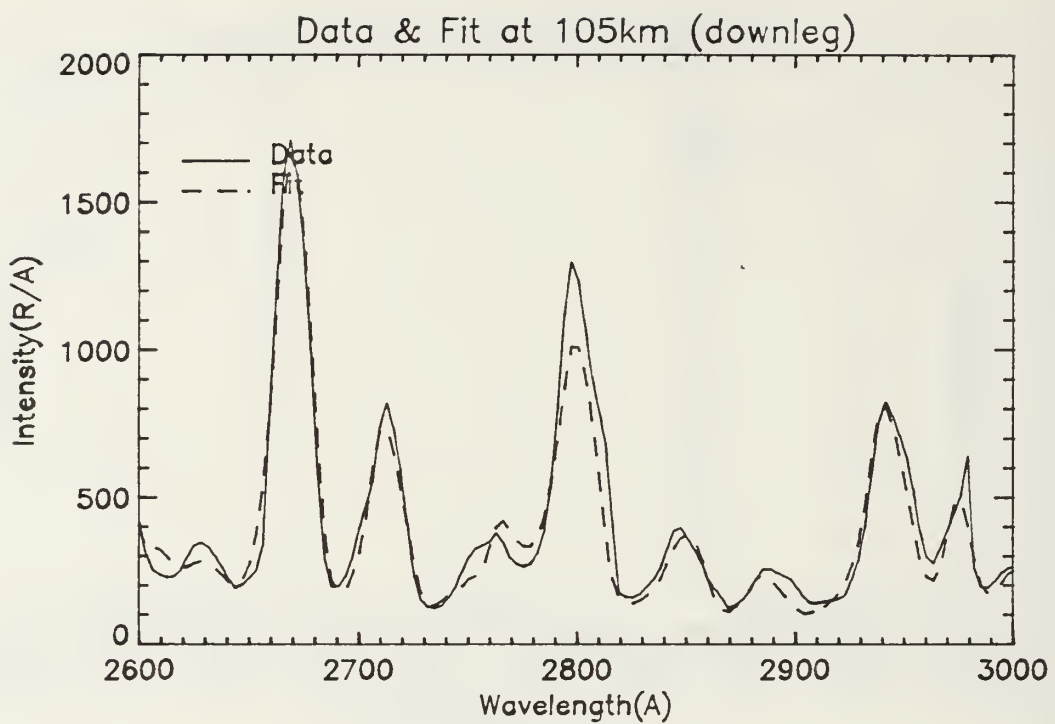


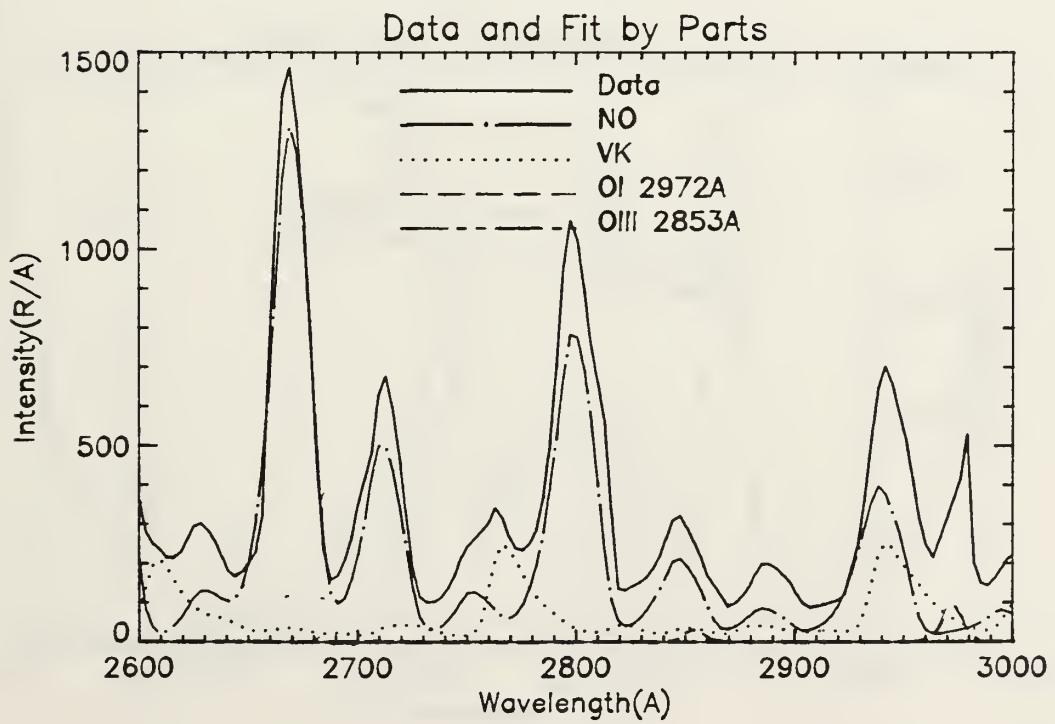
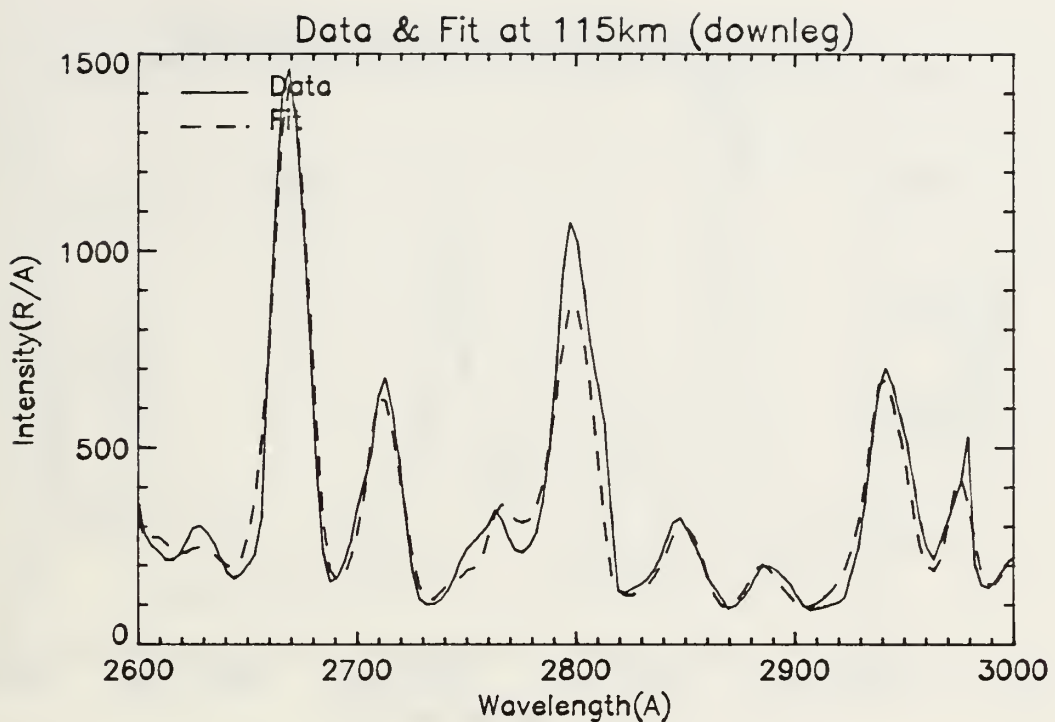


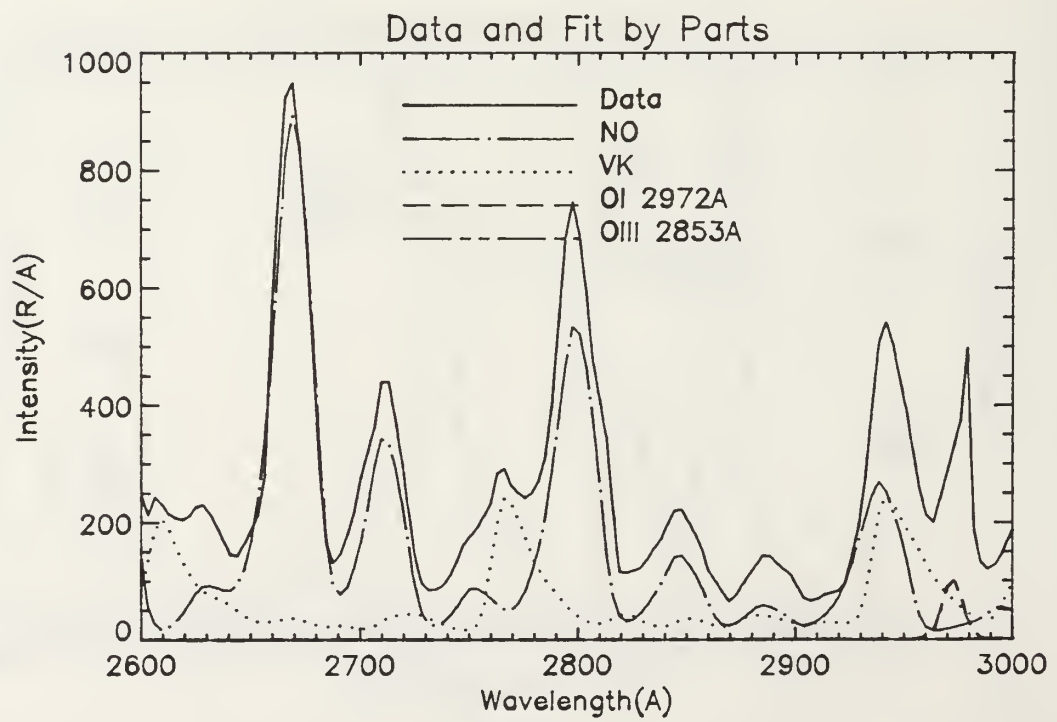
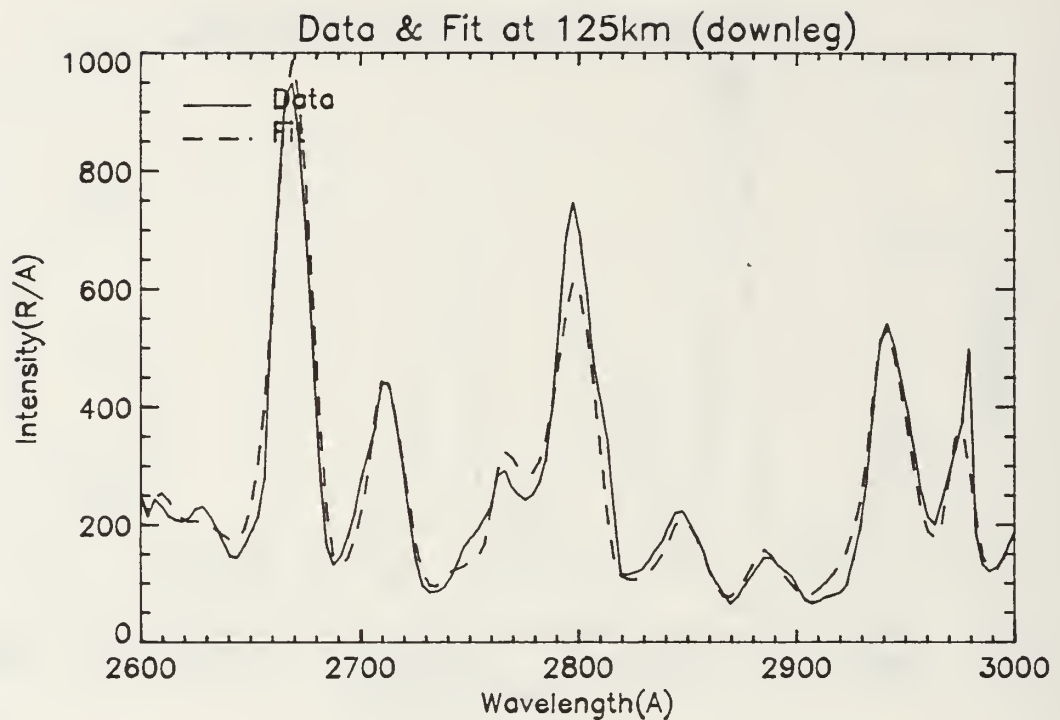


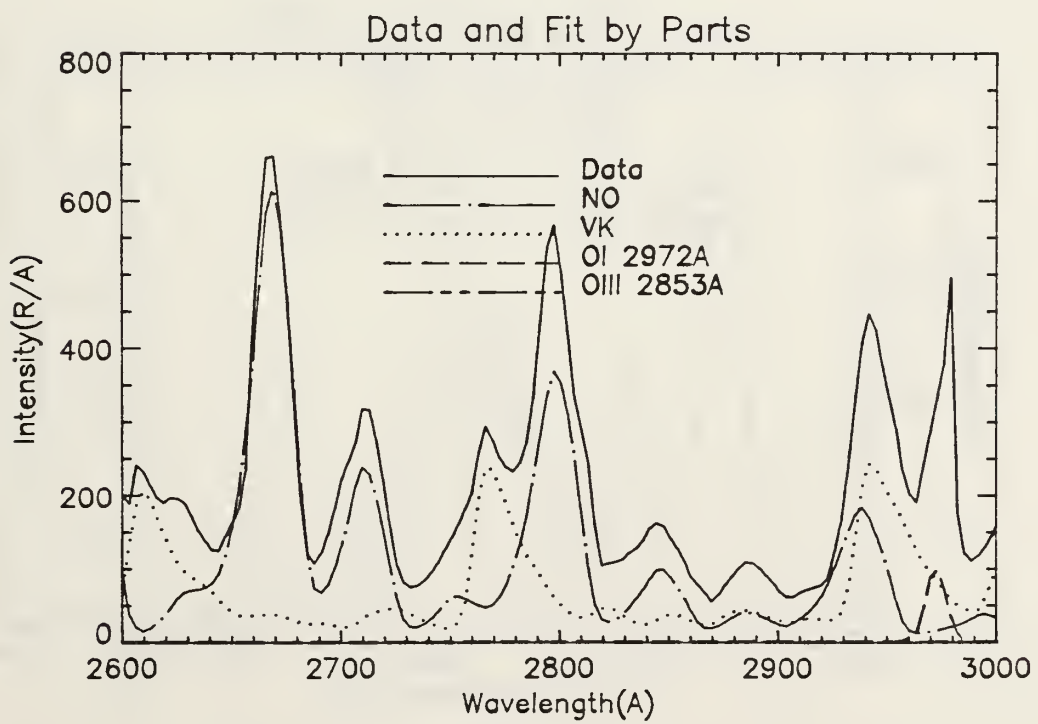
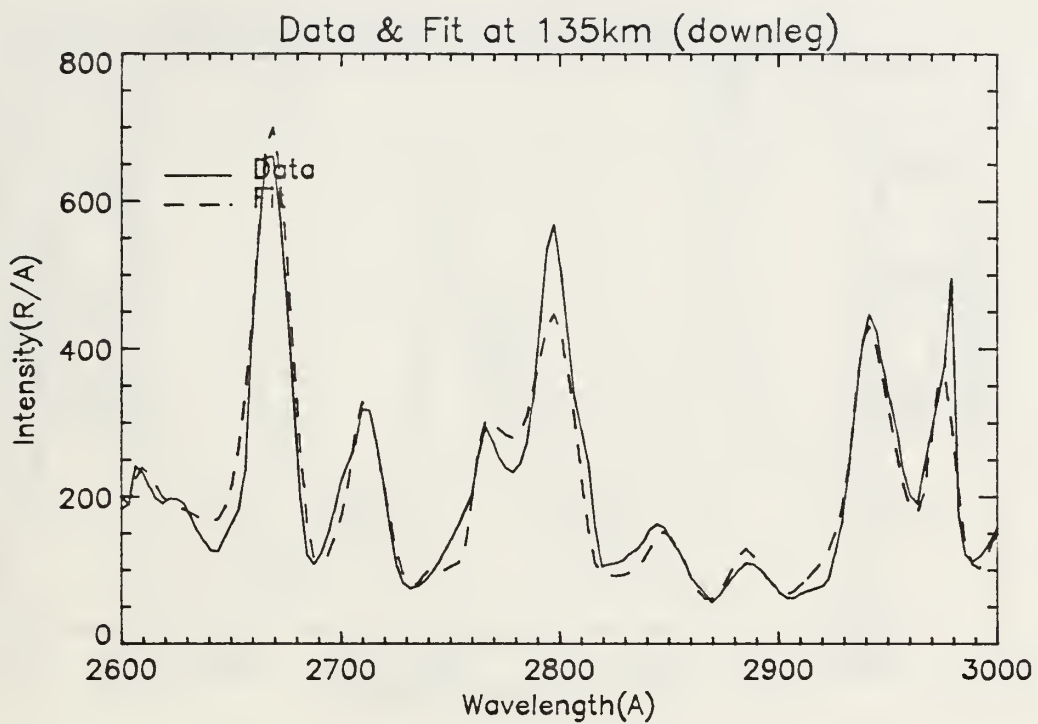


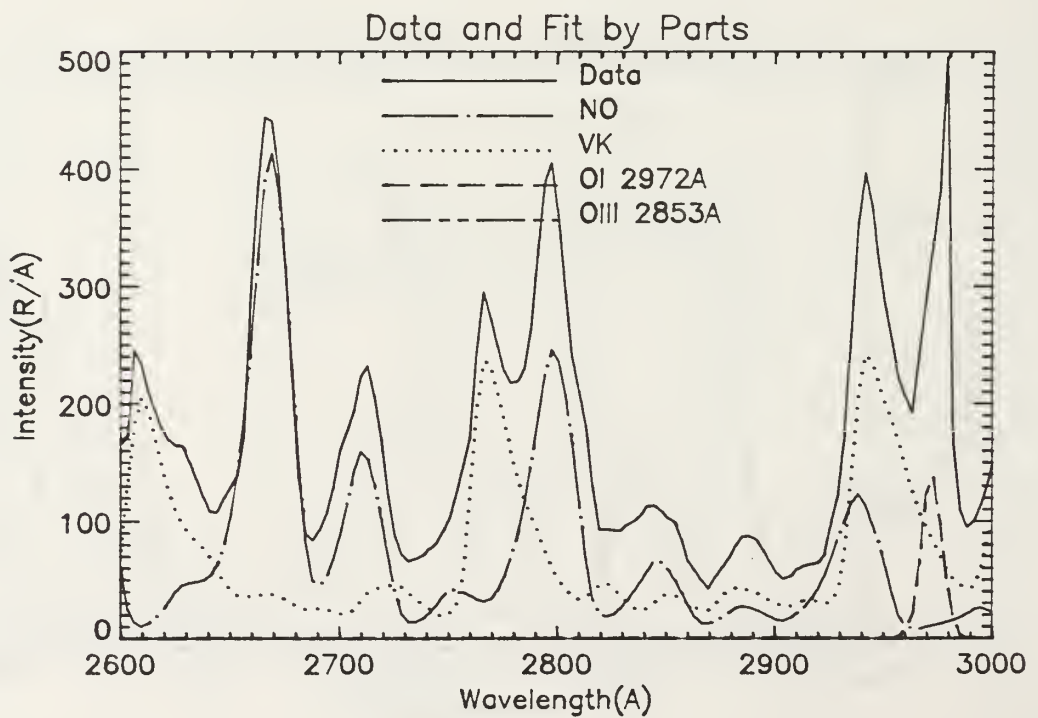
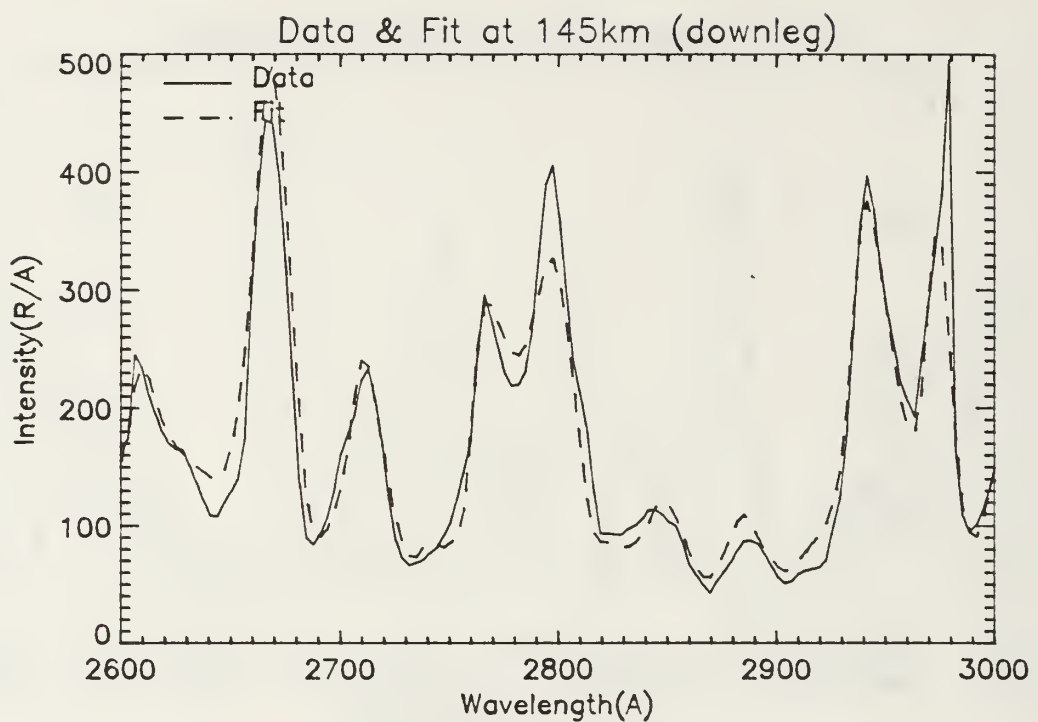


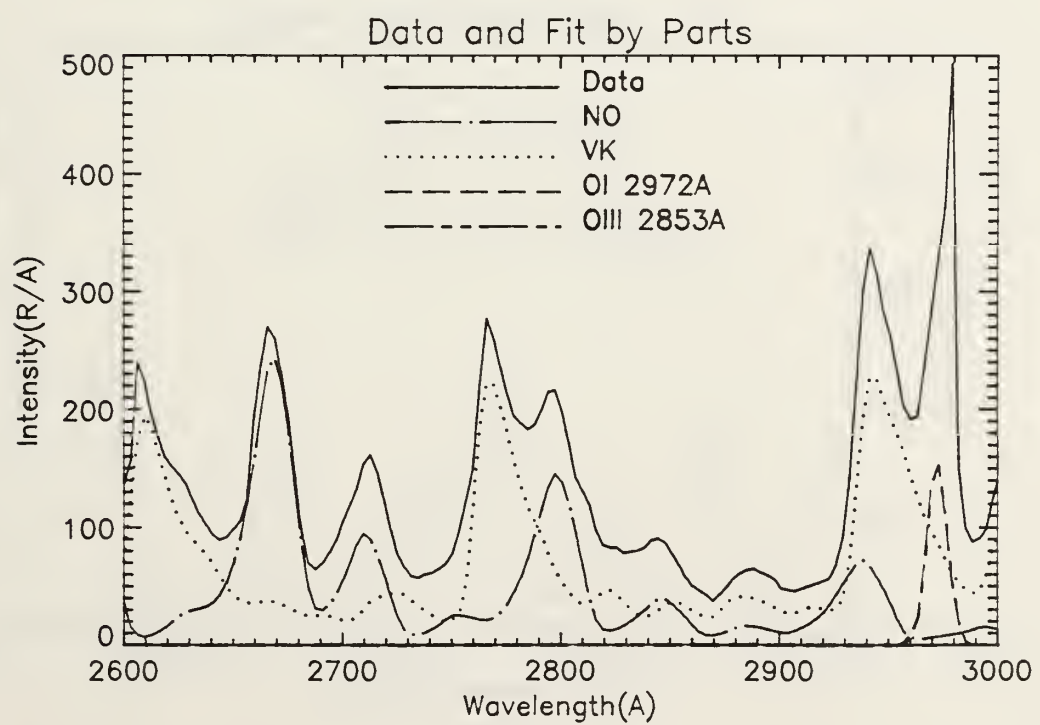
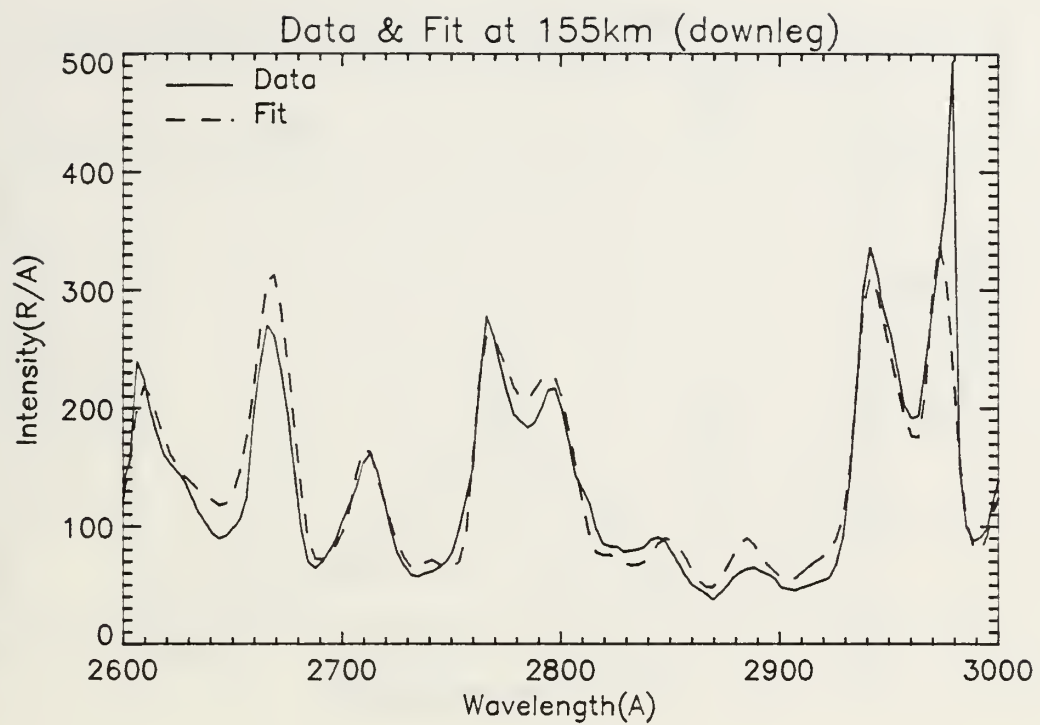


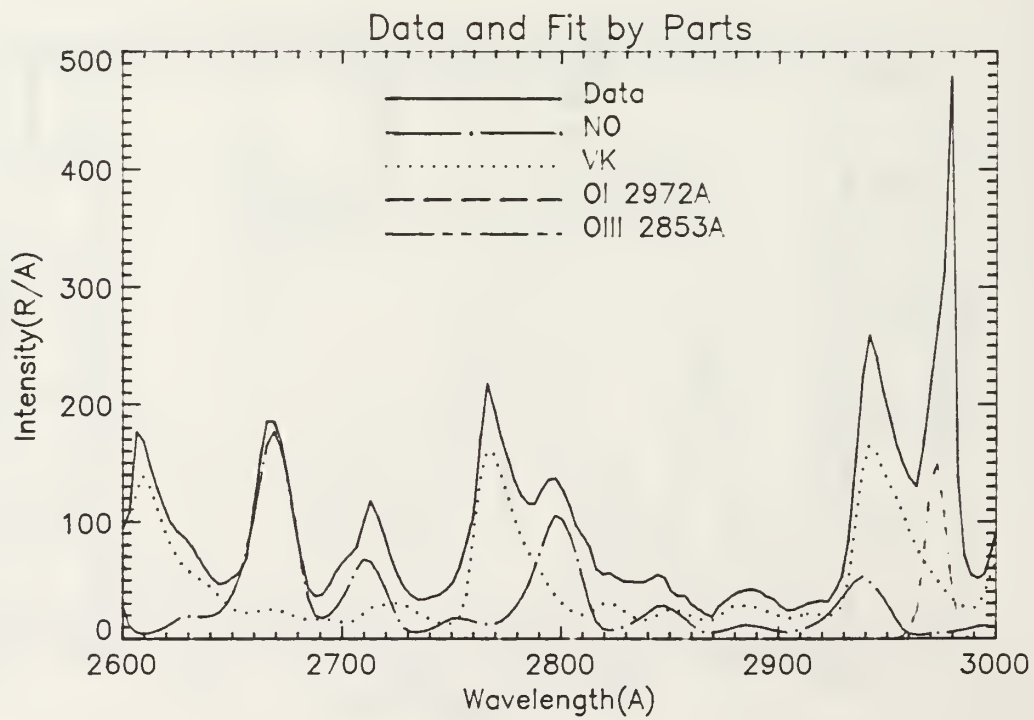
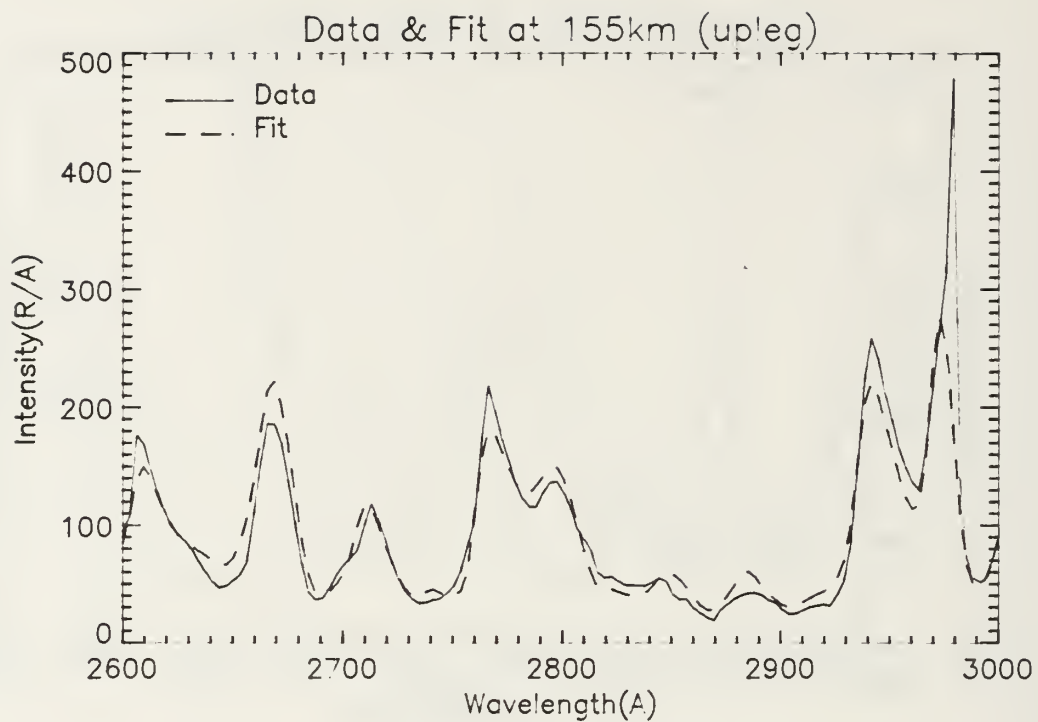


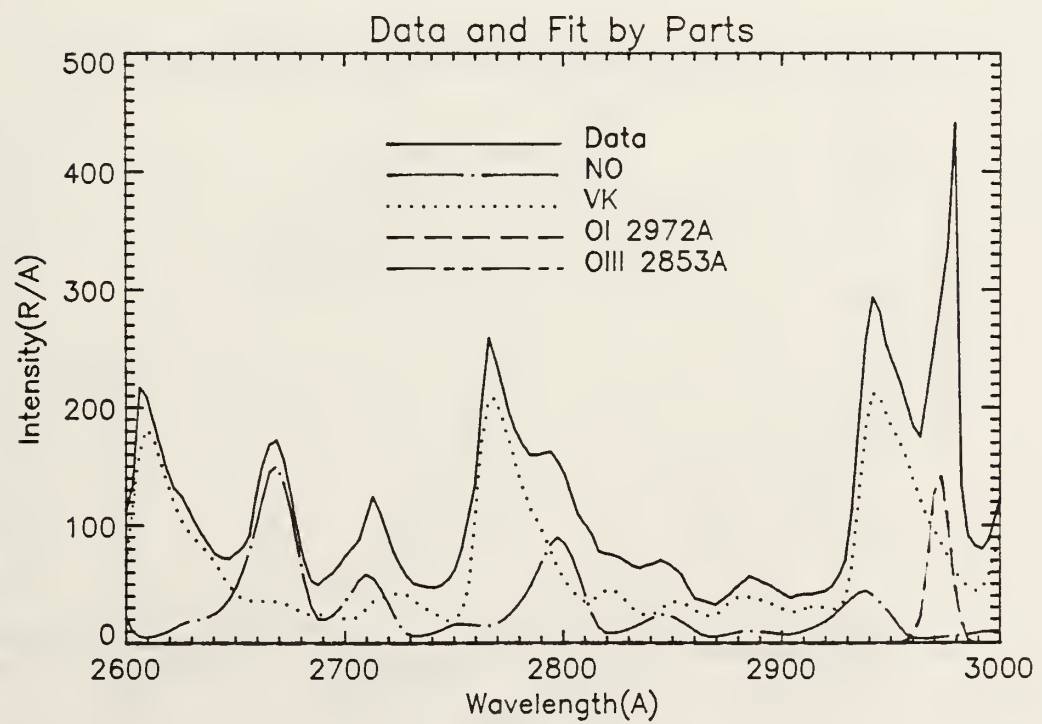
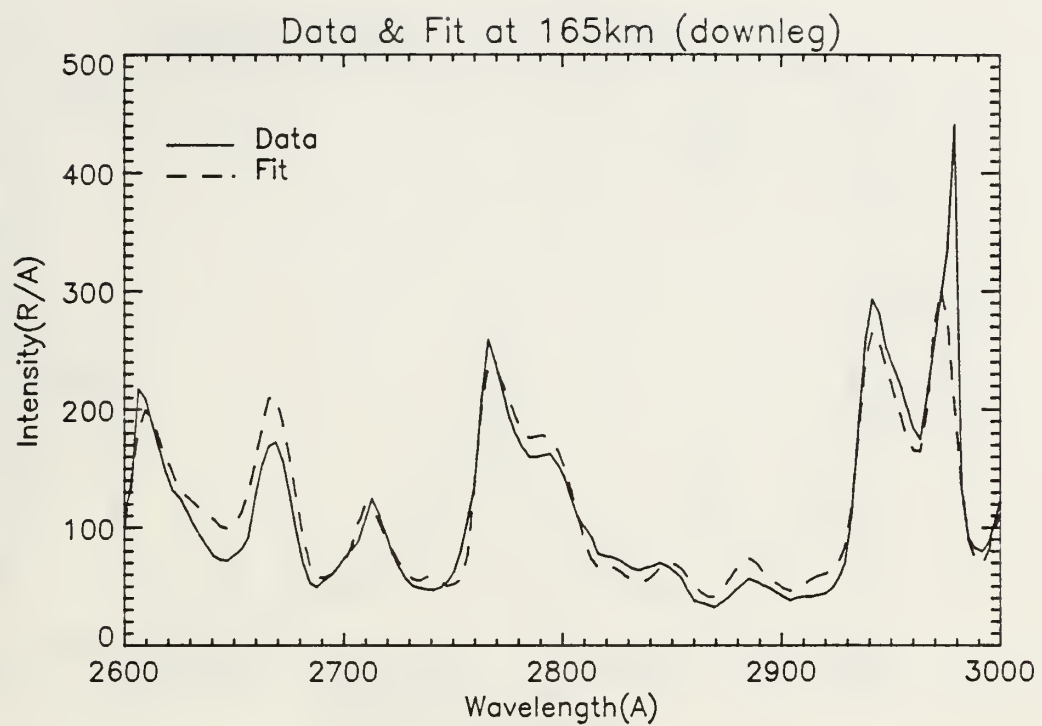


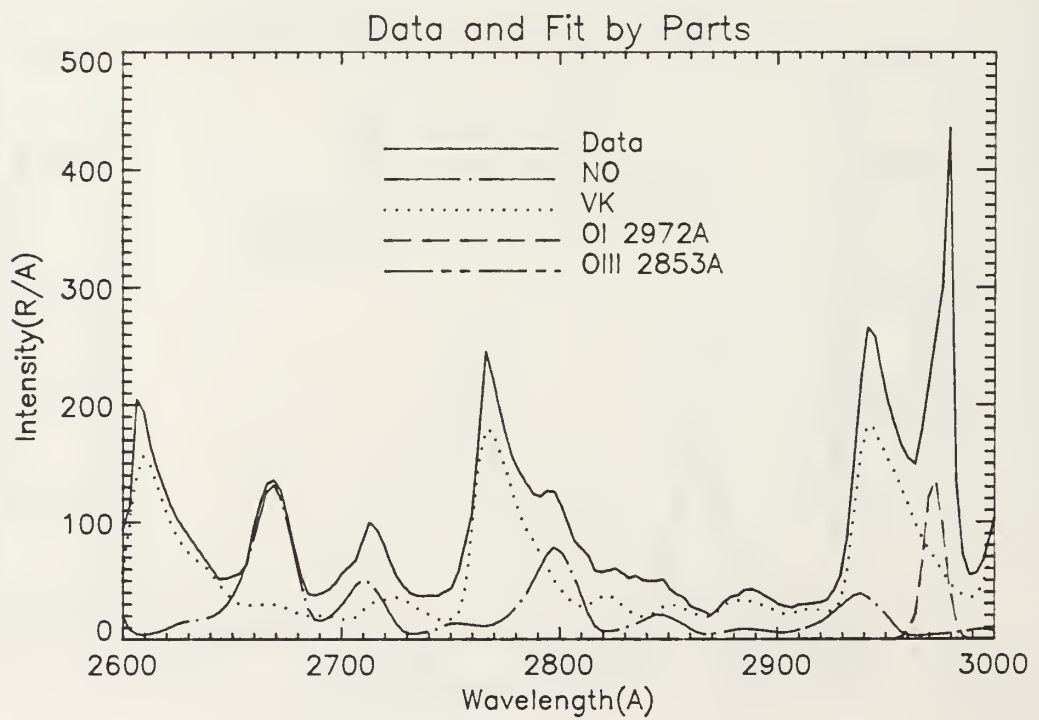
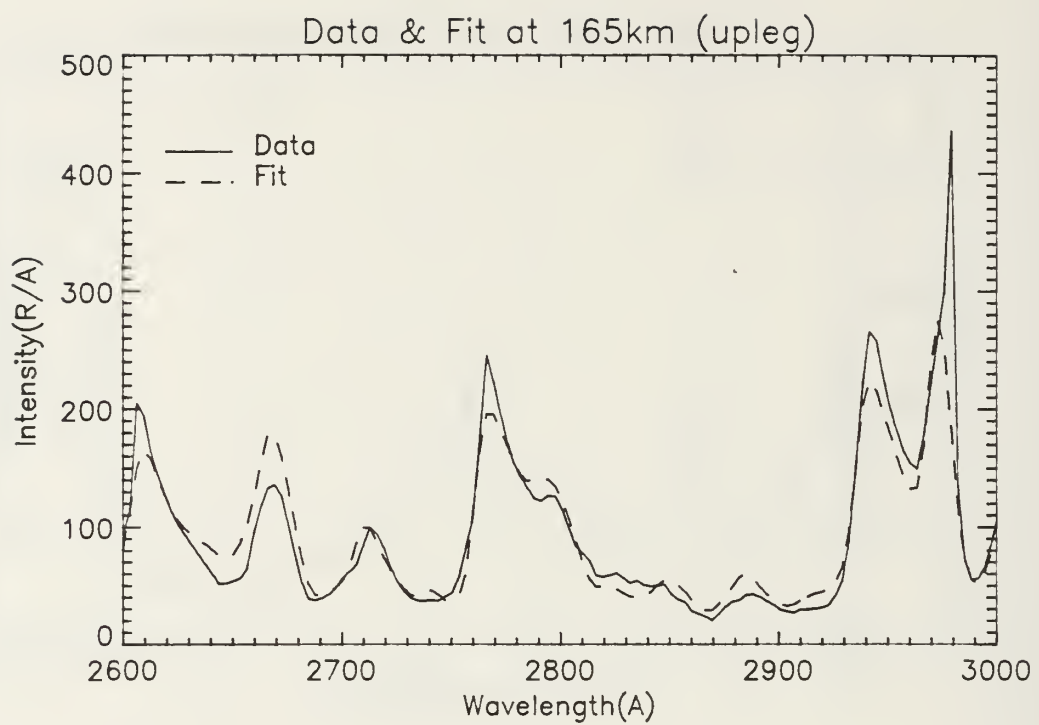


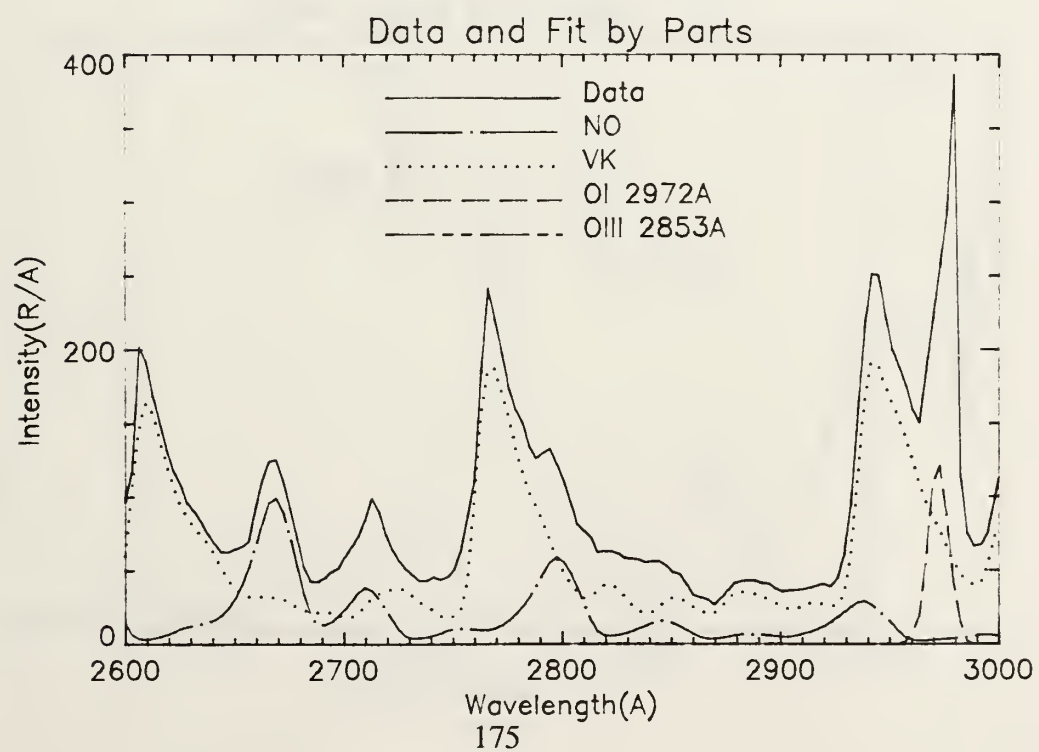
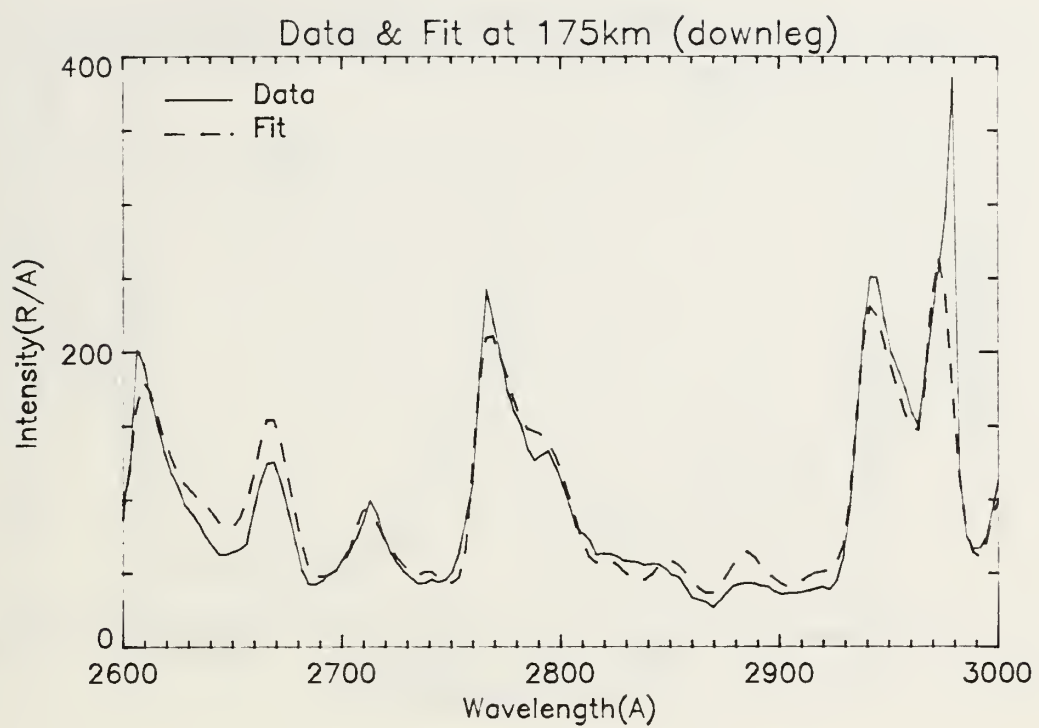


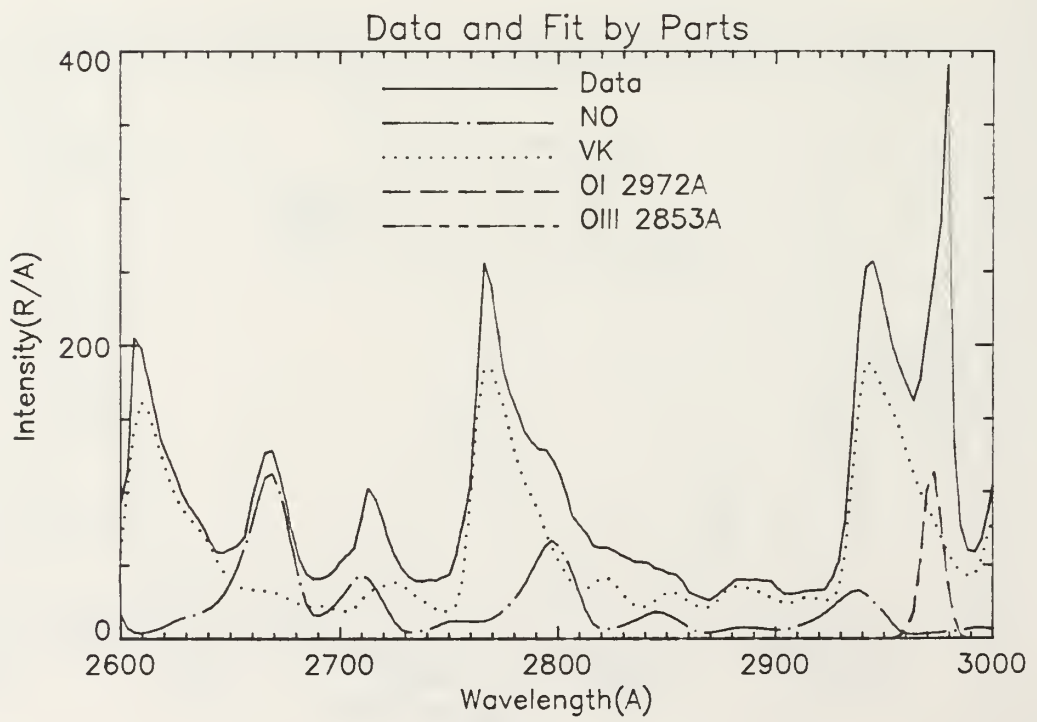
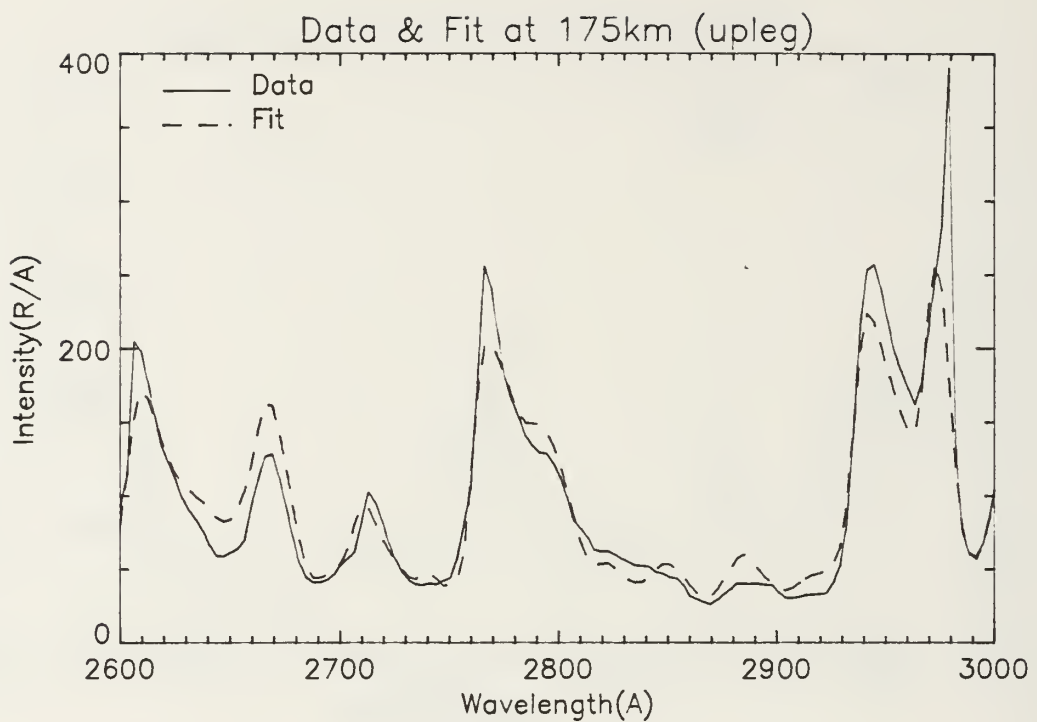


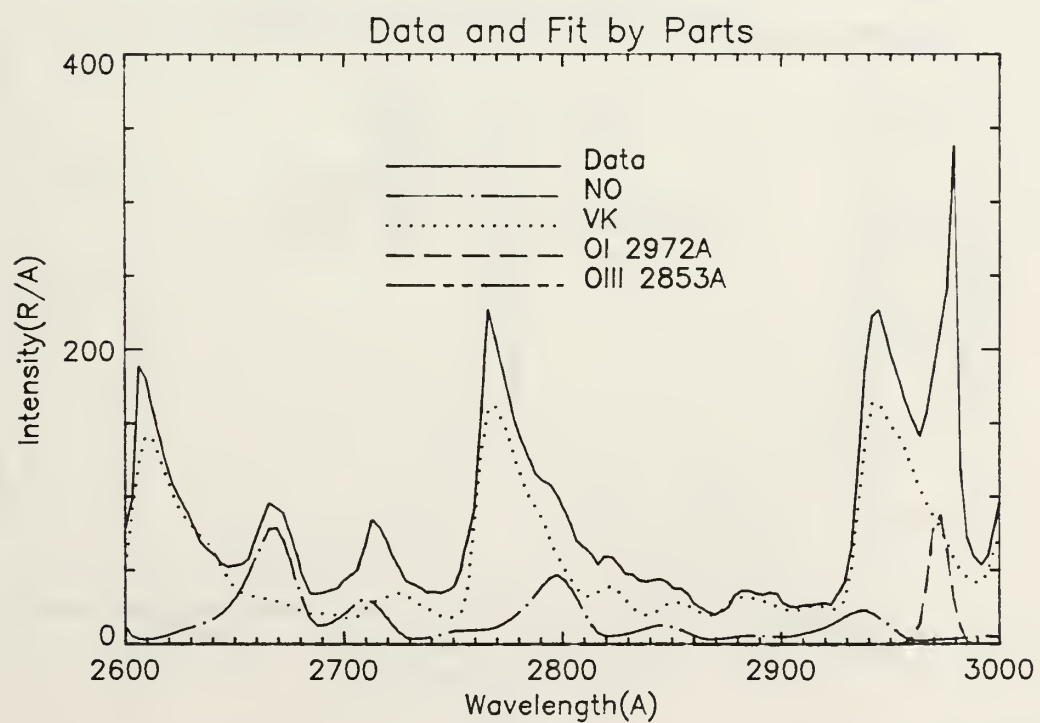
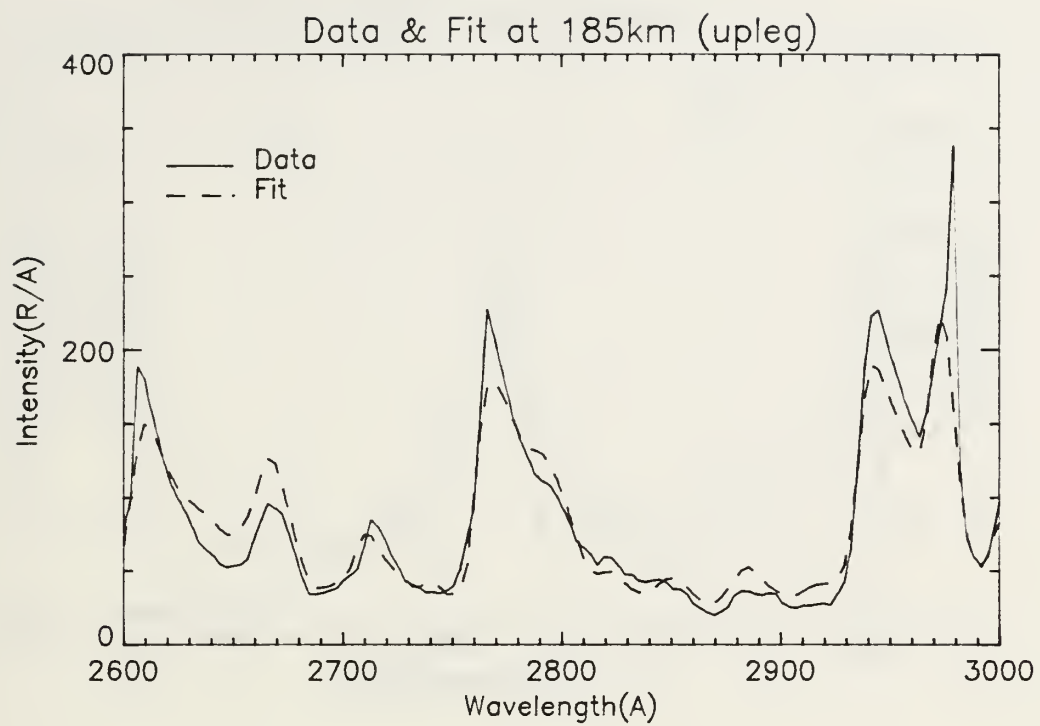


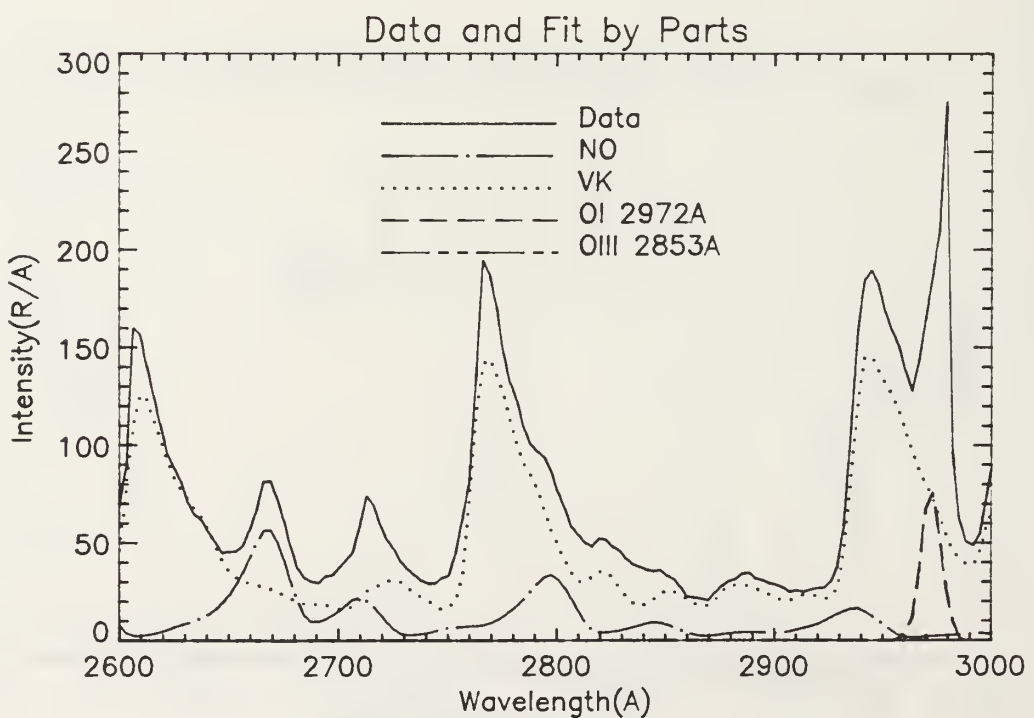
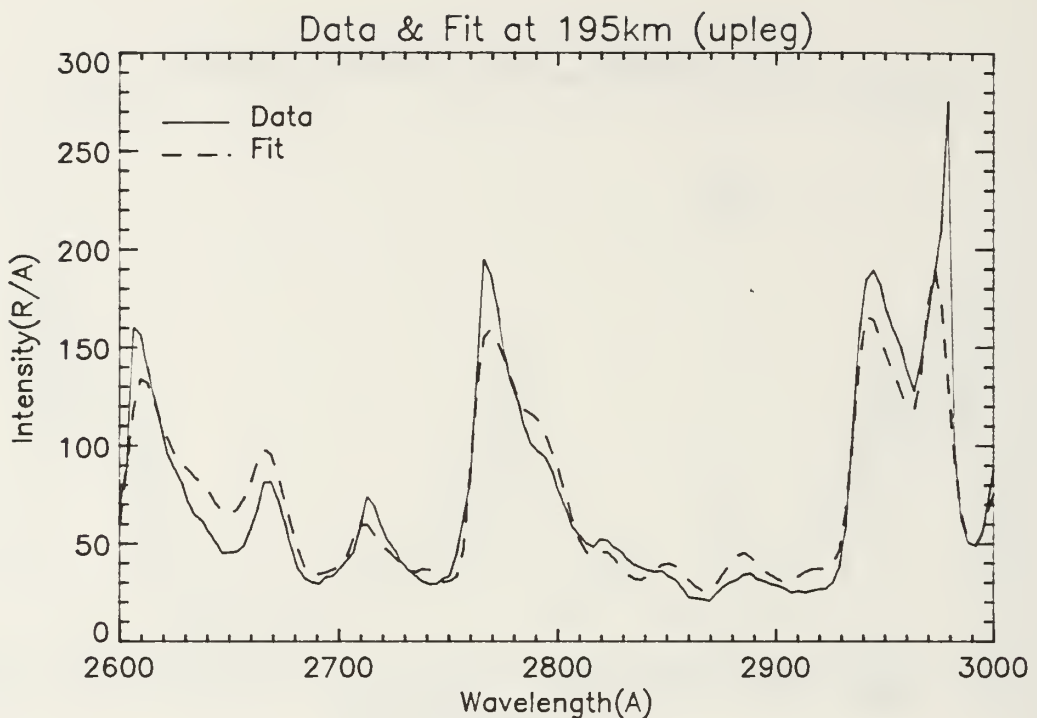


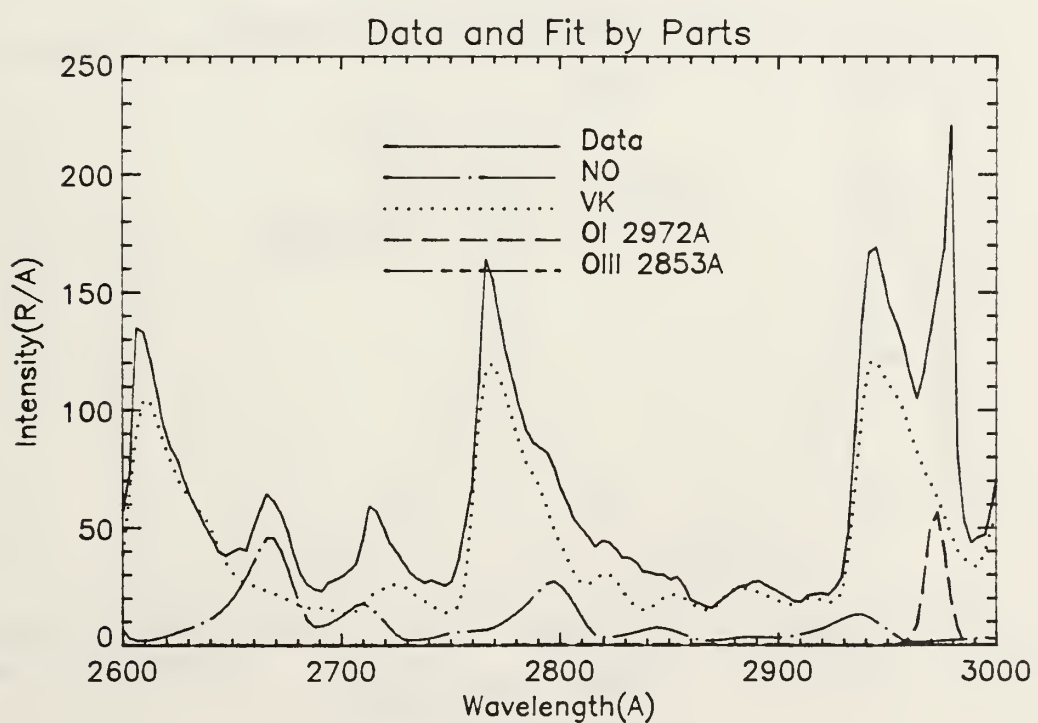
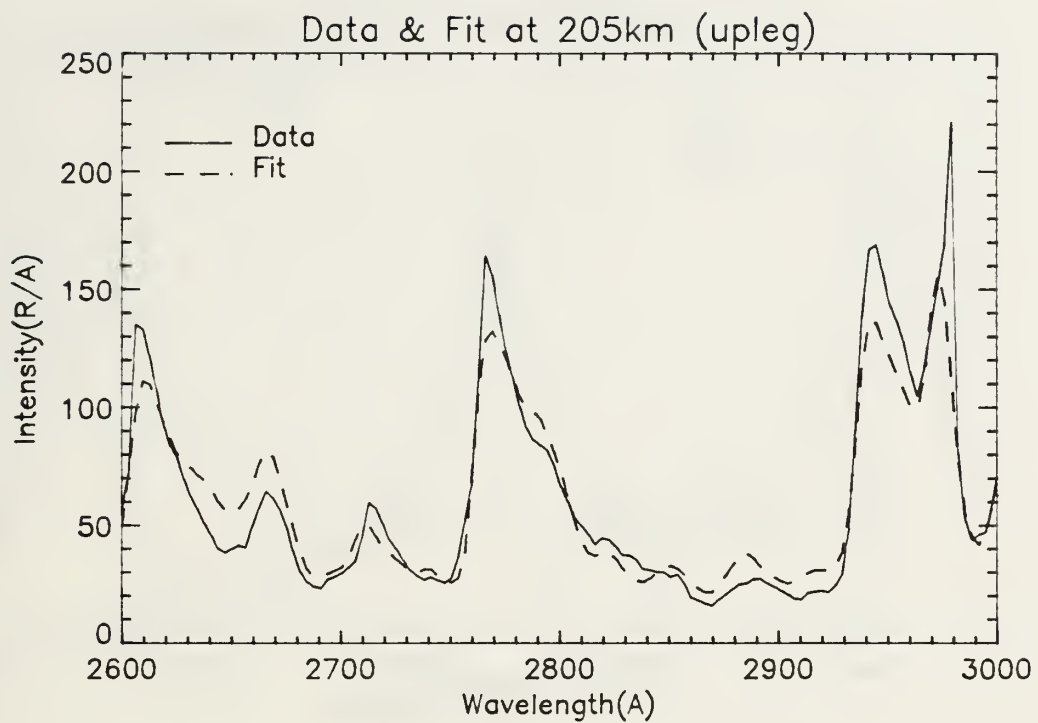


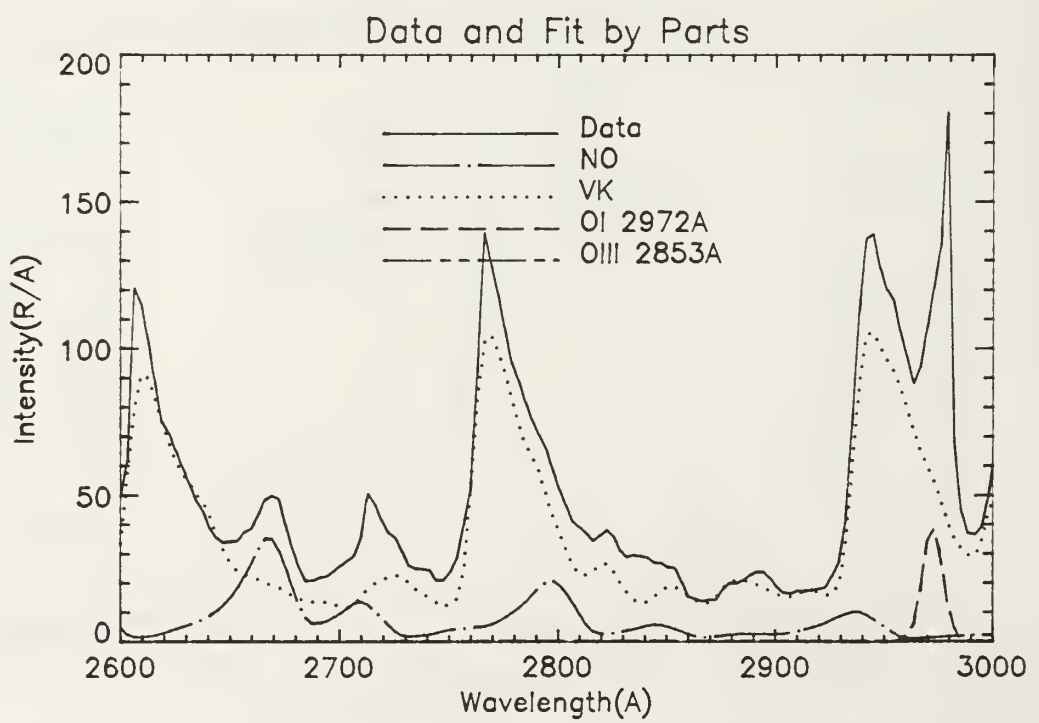
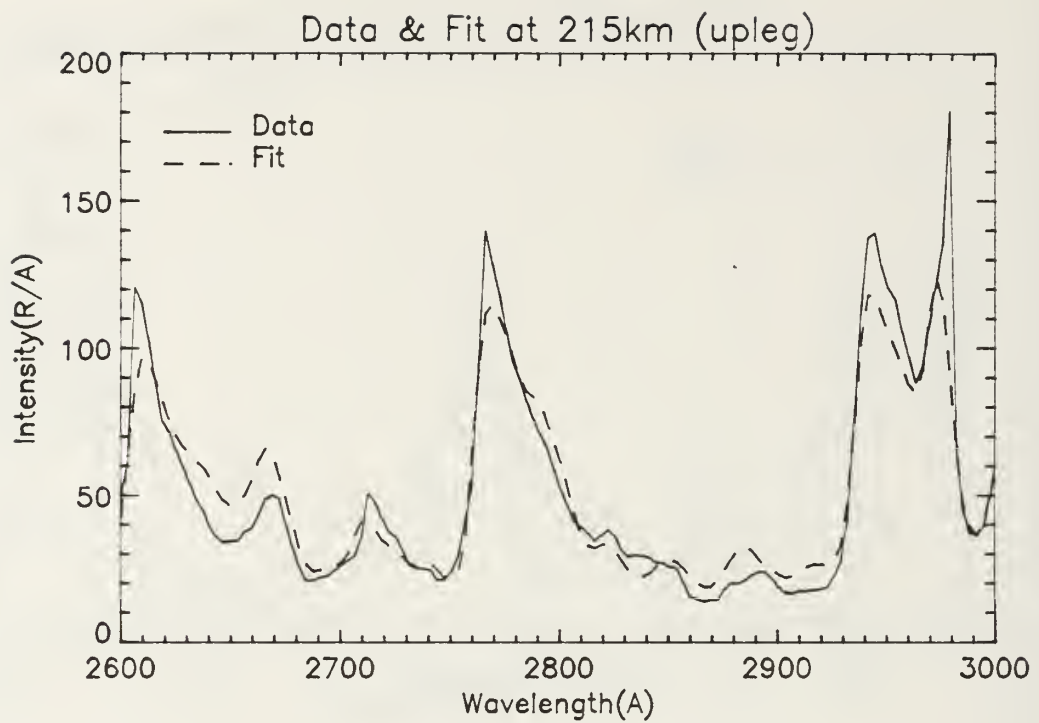


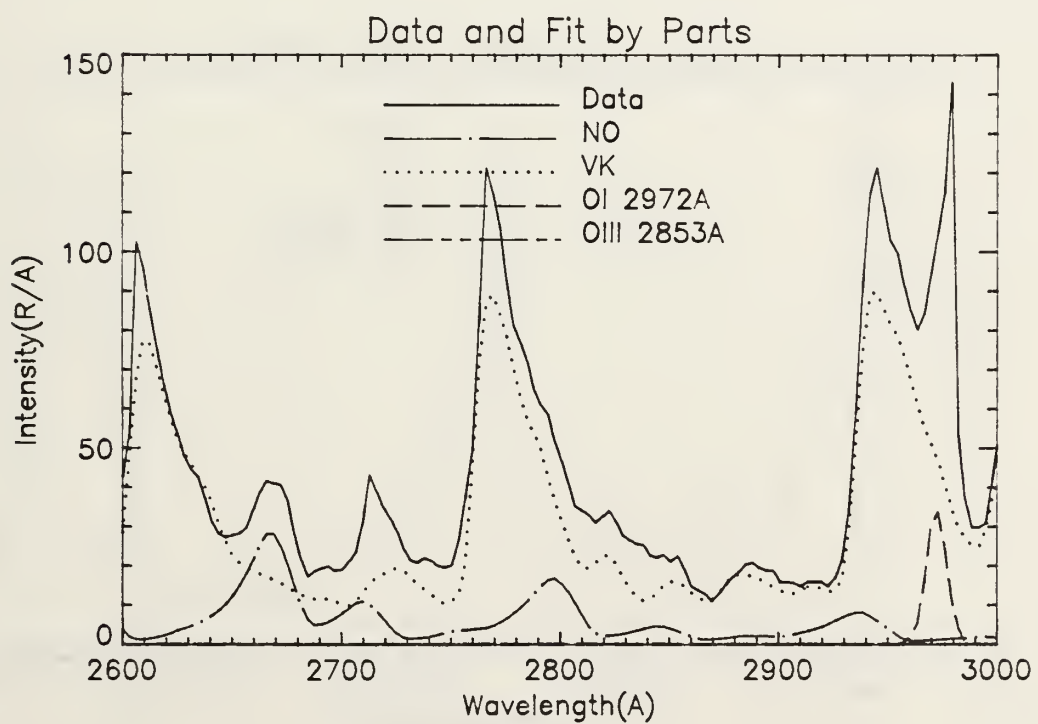
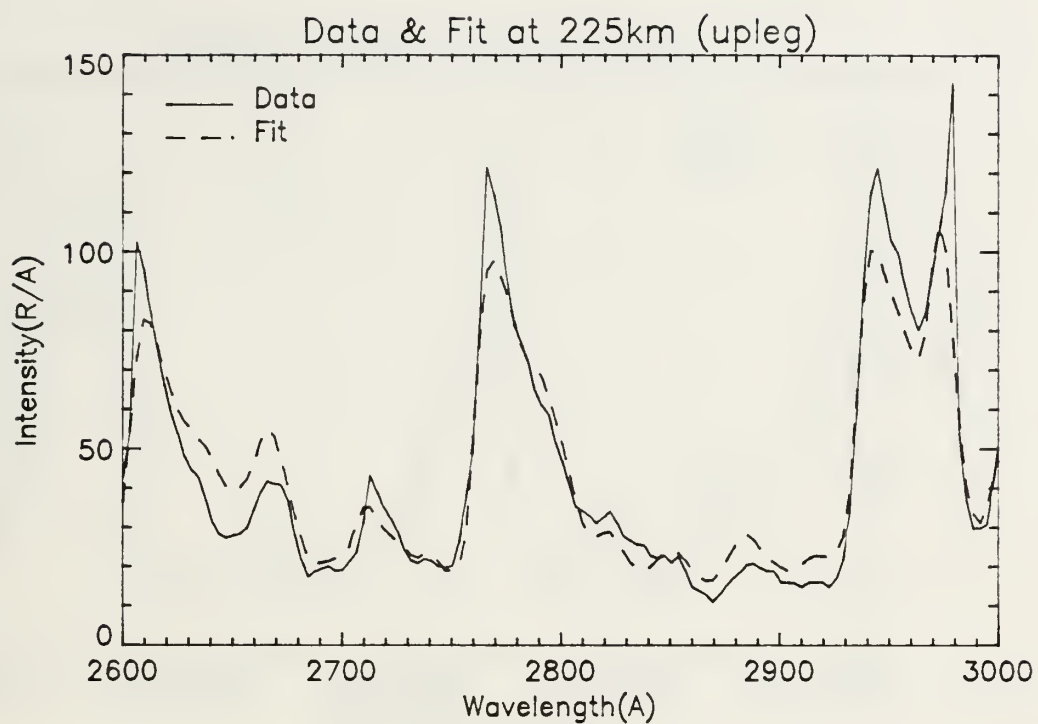


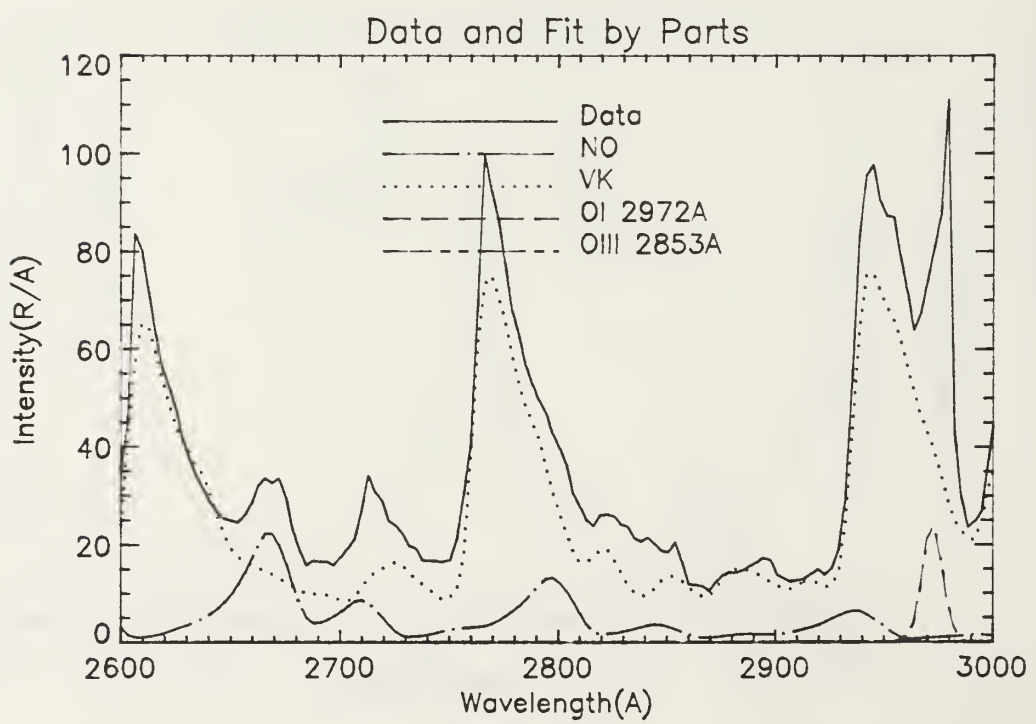
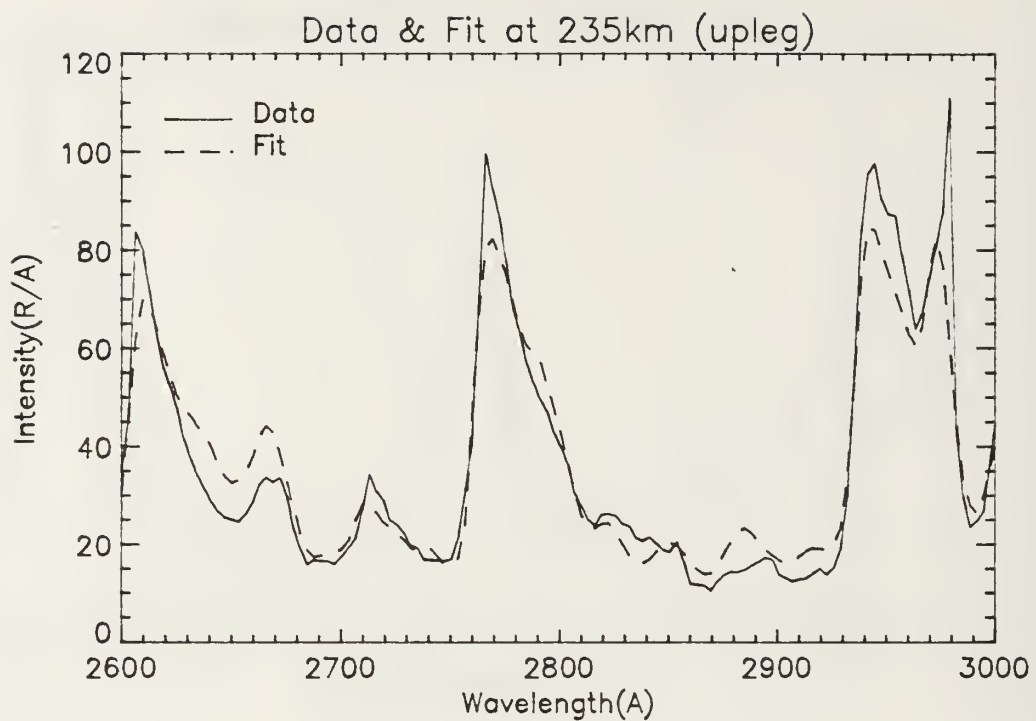


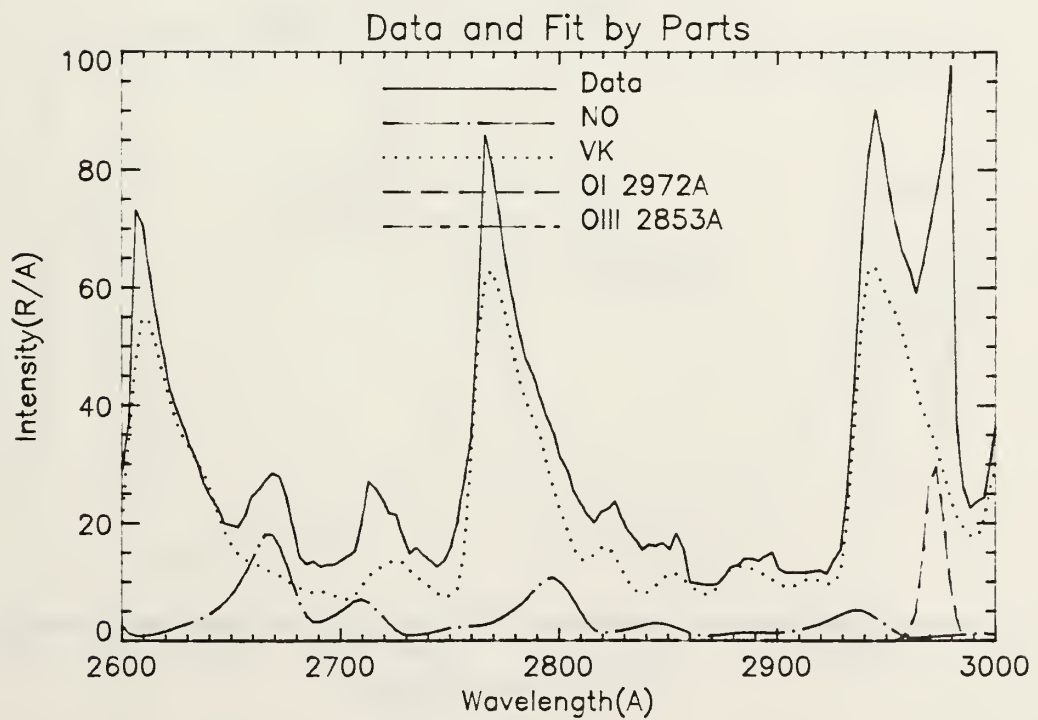
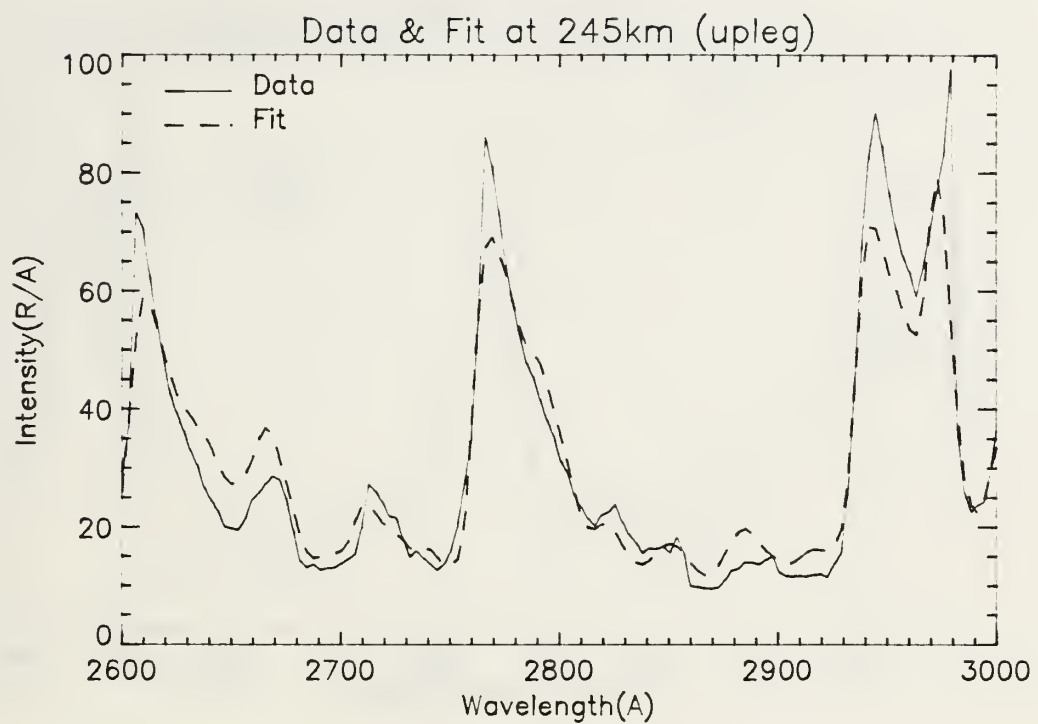


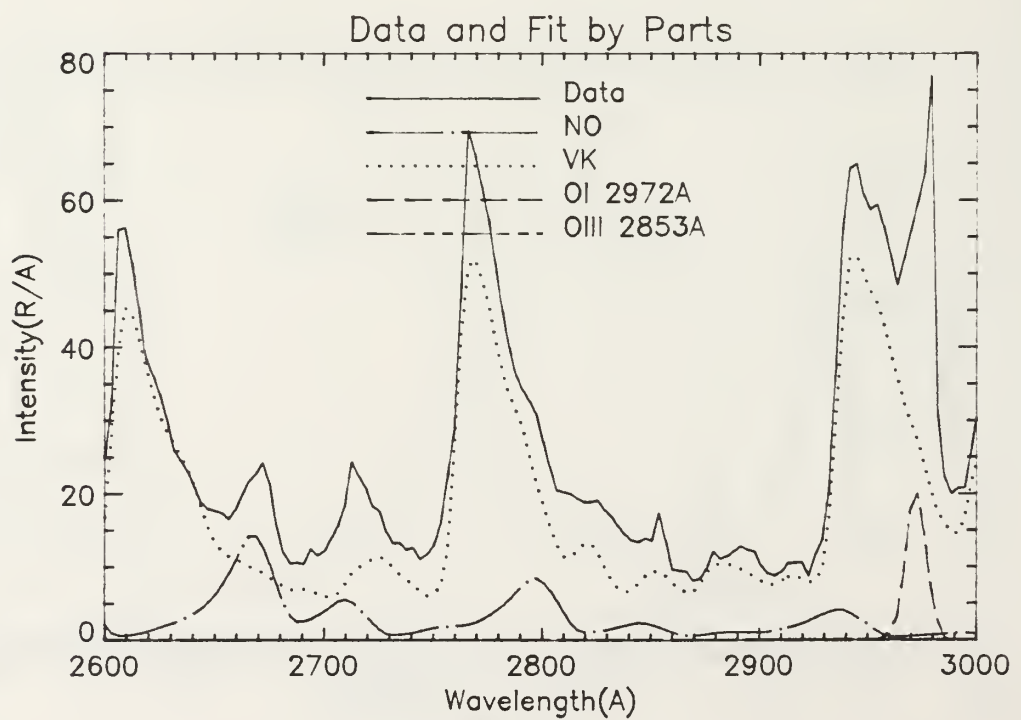
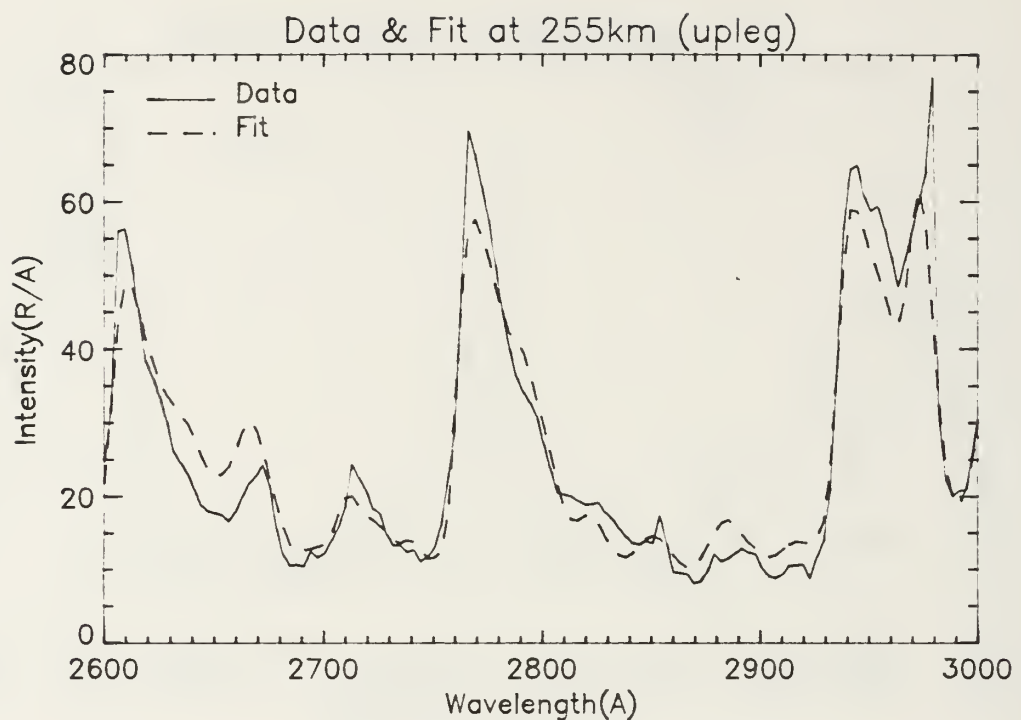


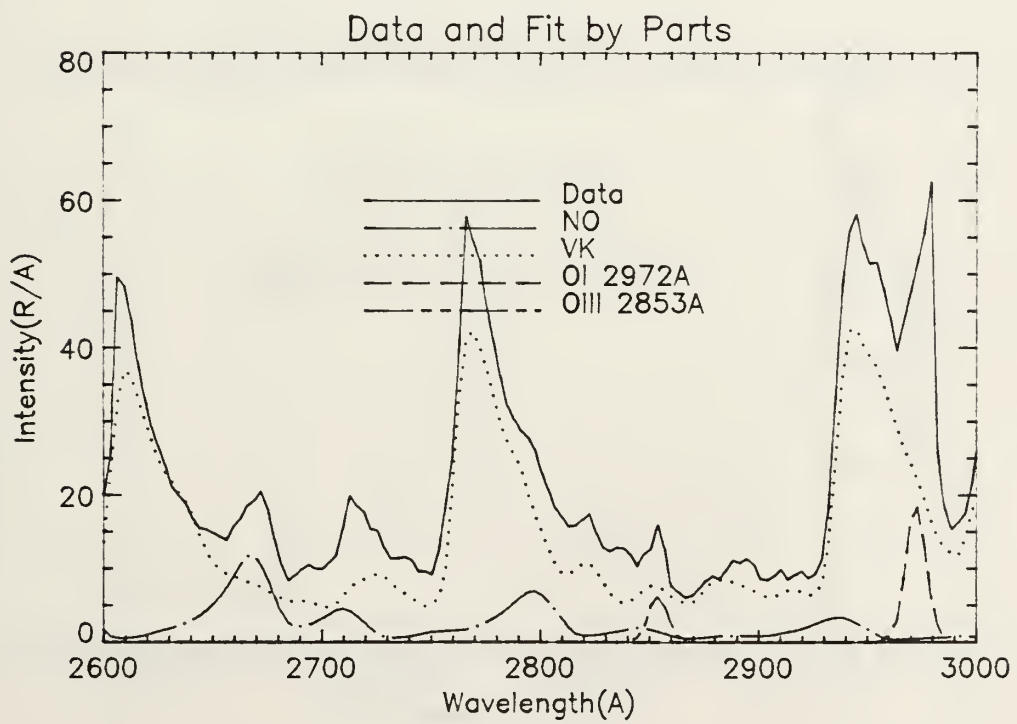
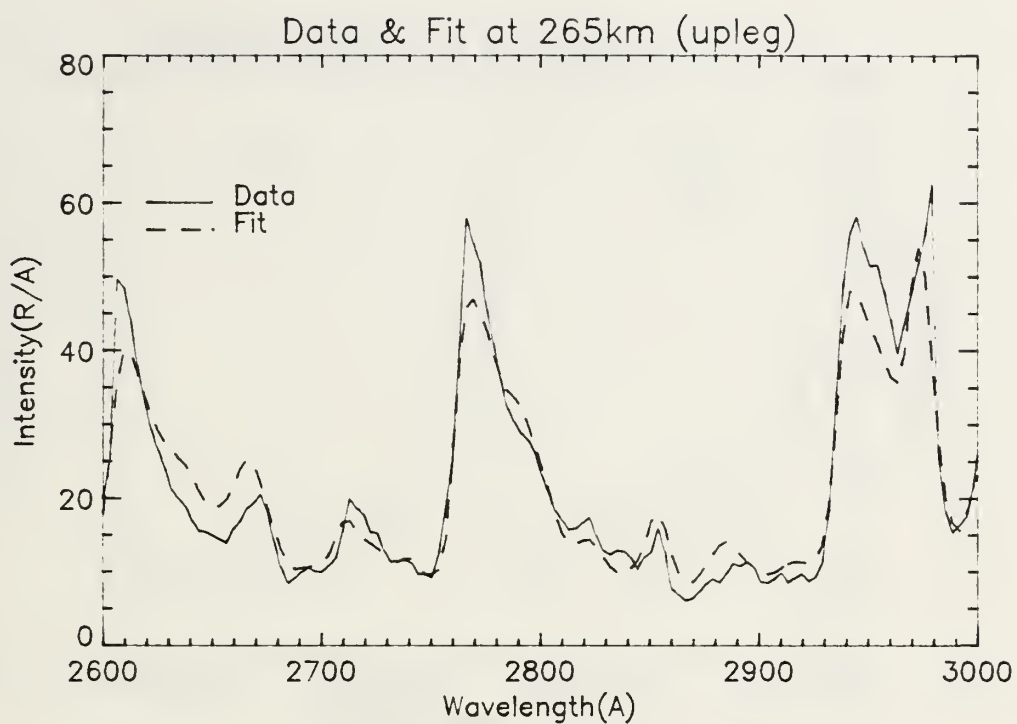


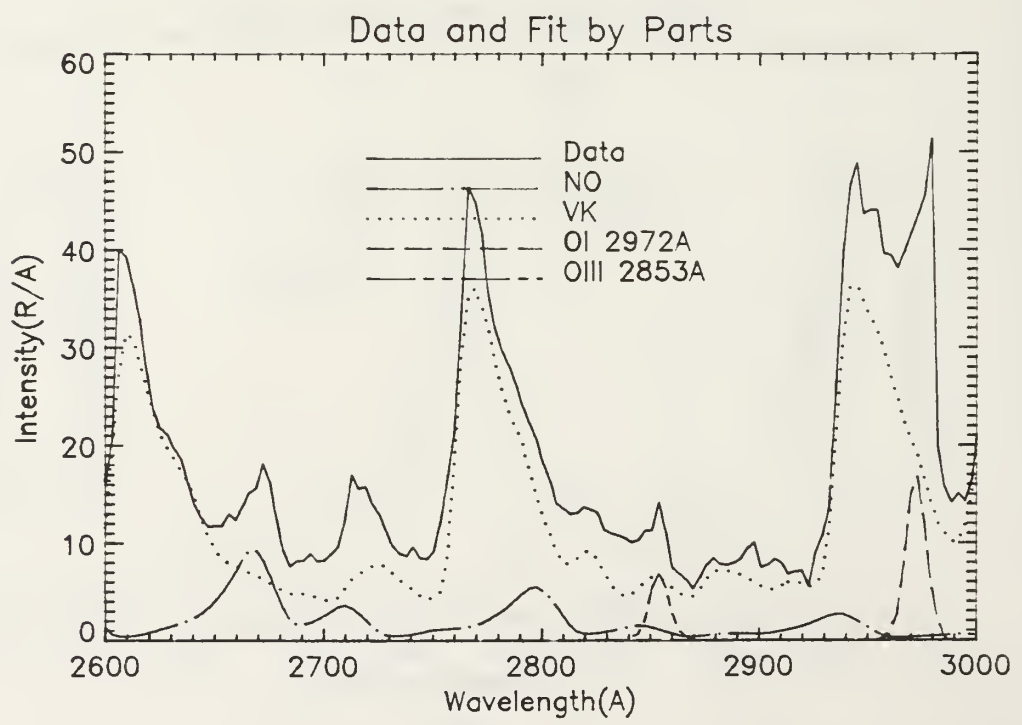
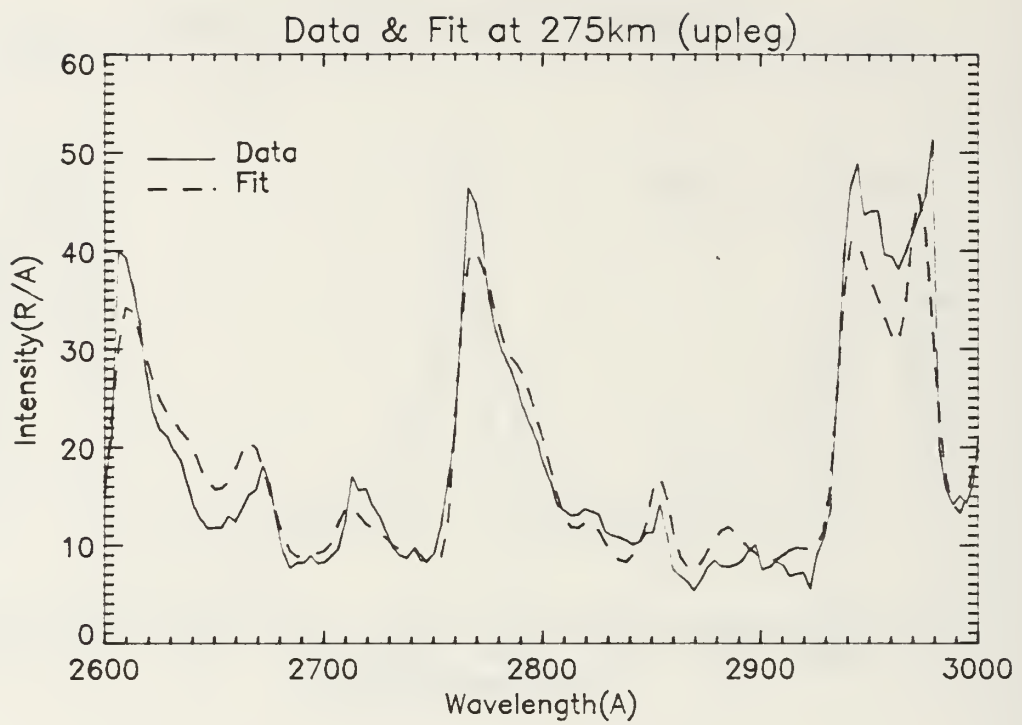


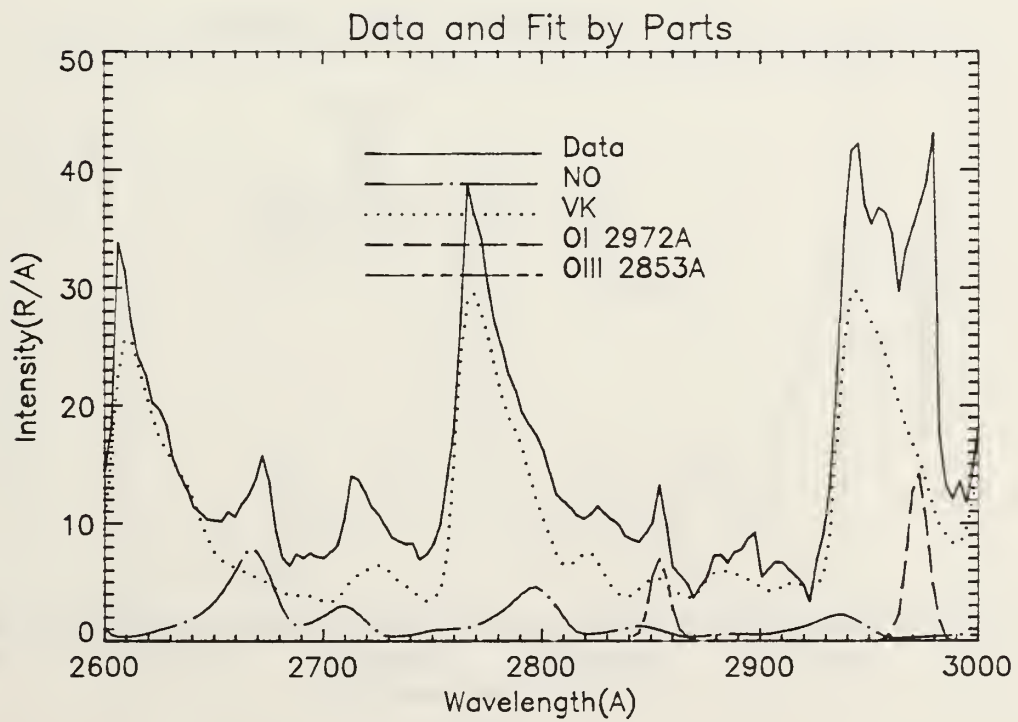
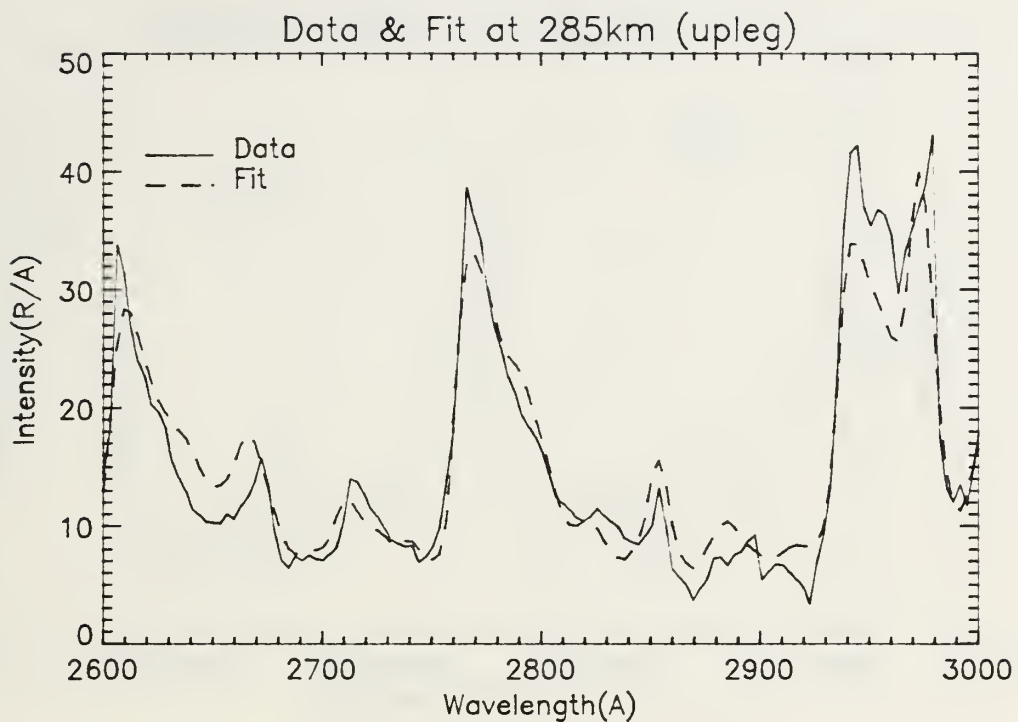


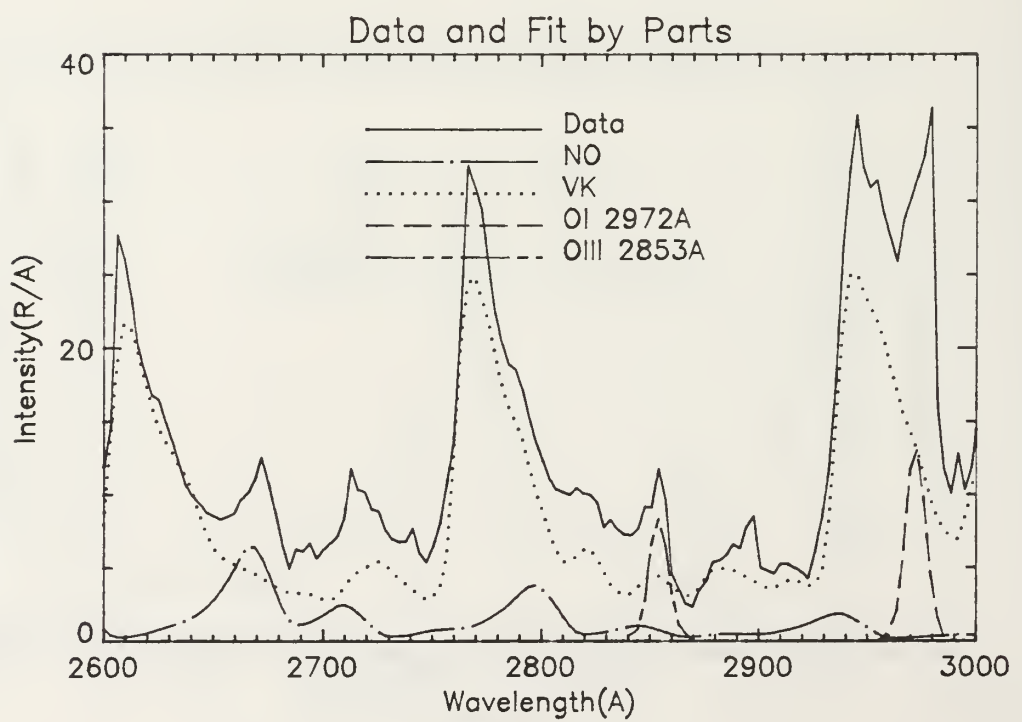
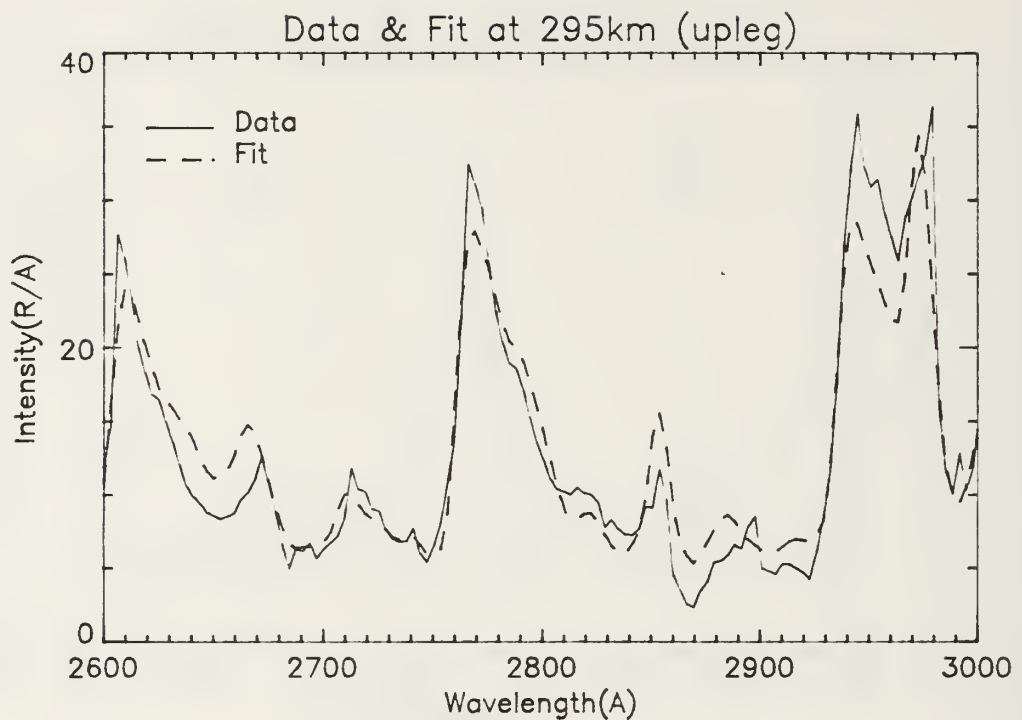


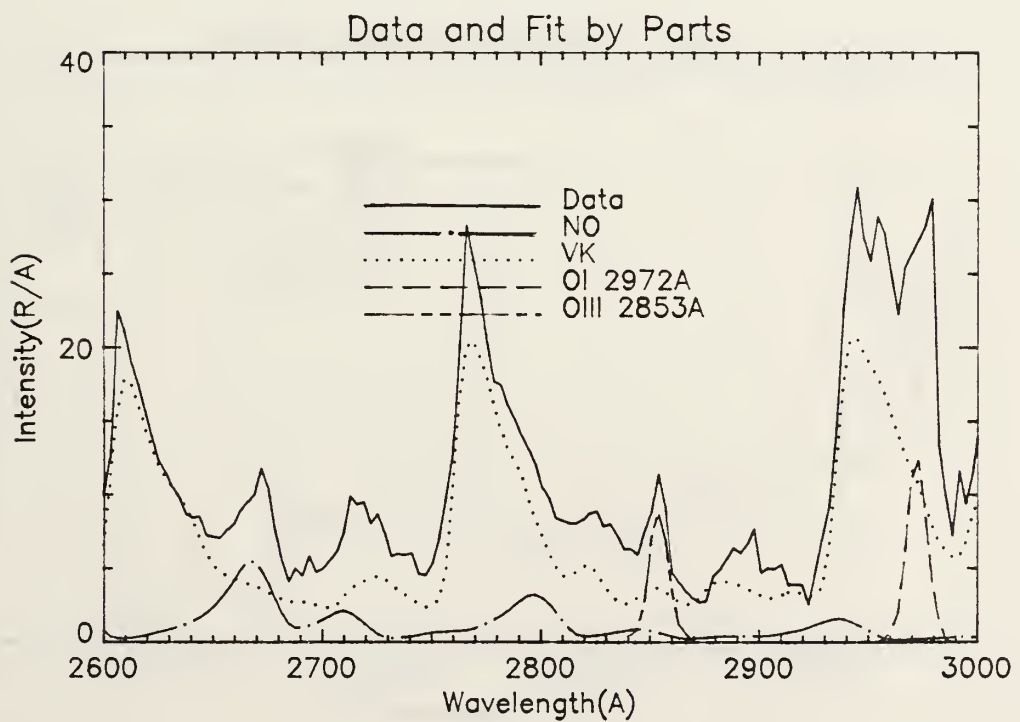
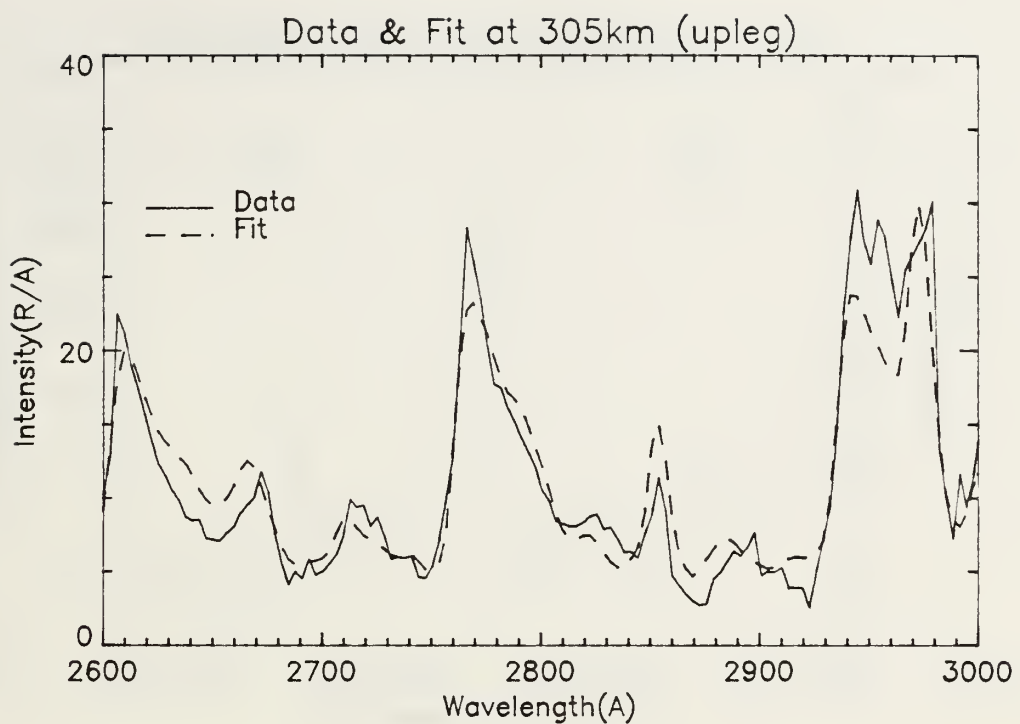




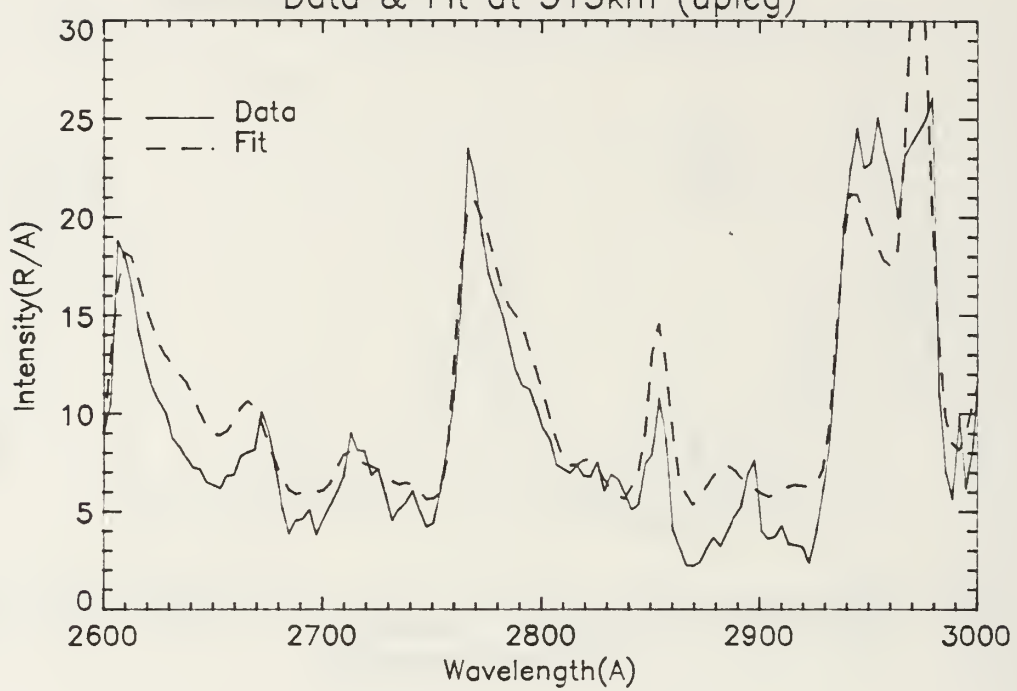




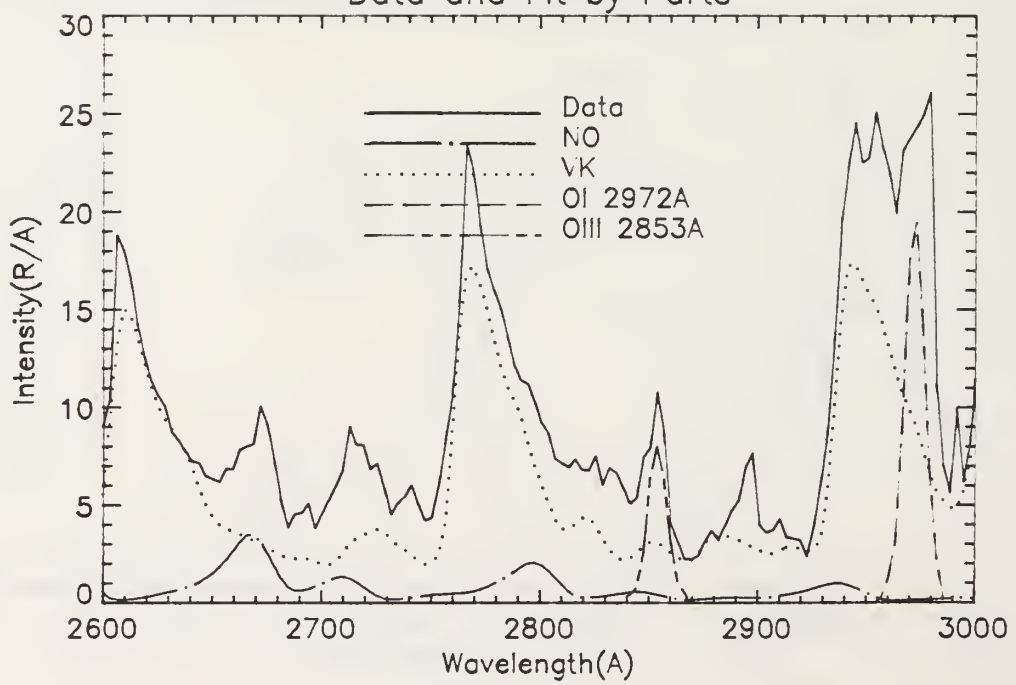


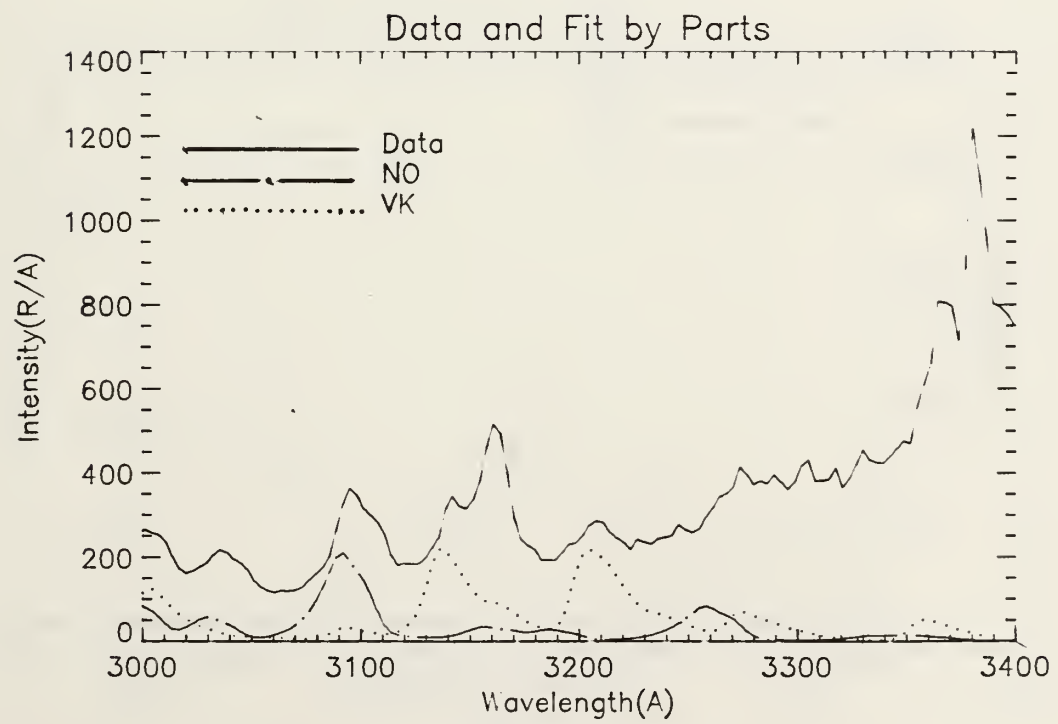
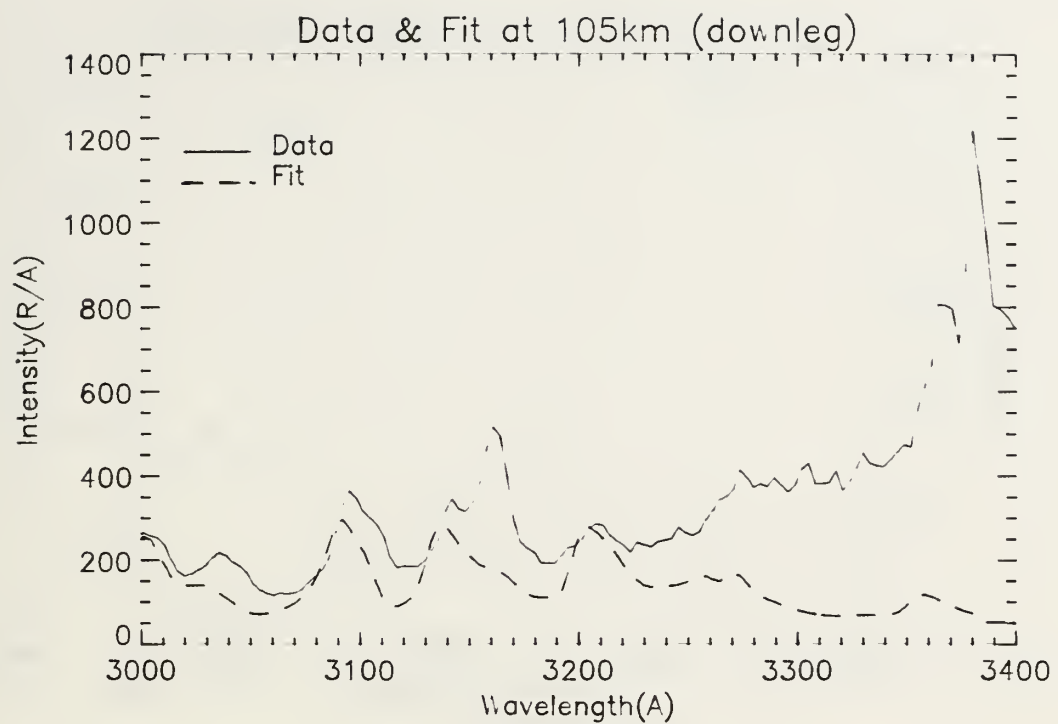


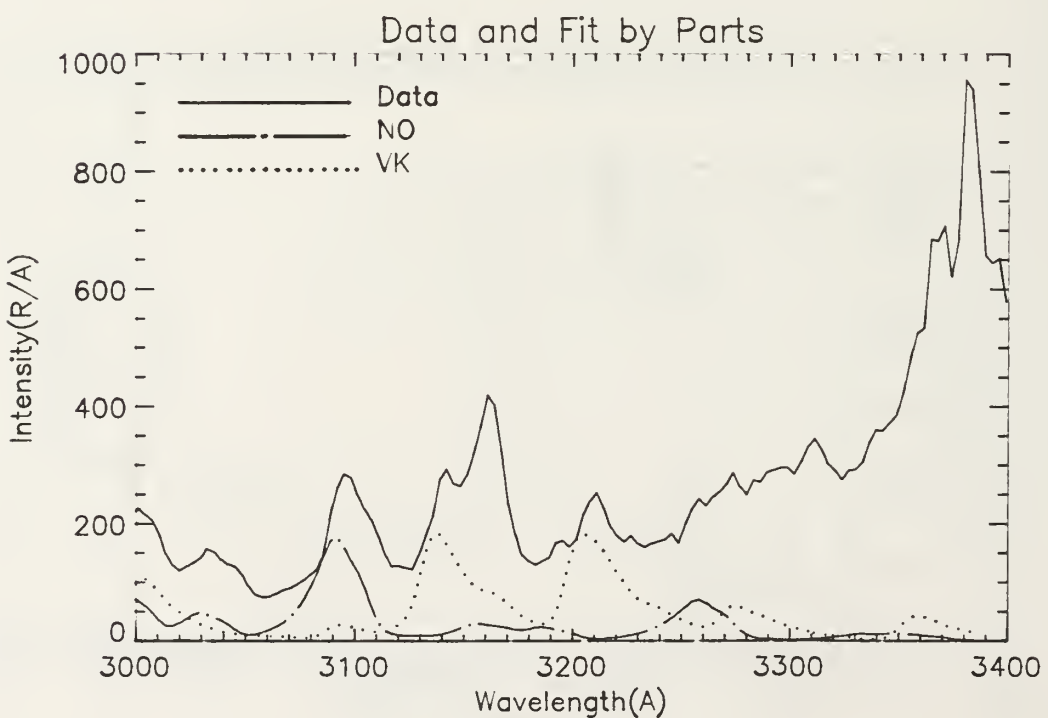
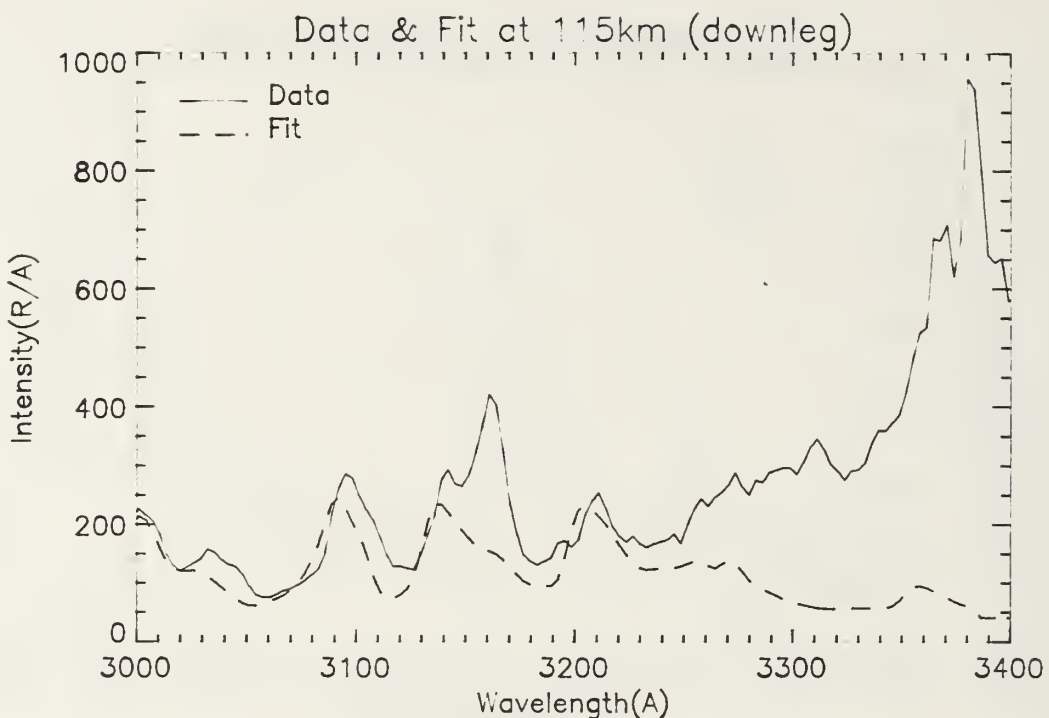
Data & Fit at 315km (upleg)

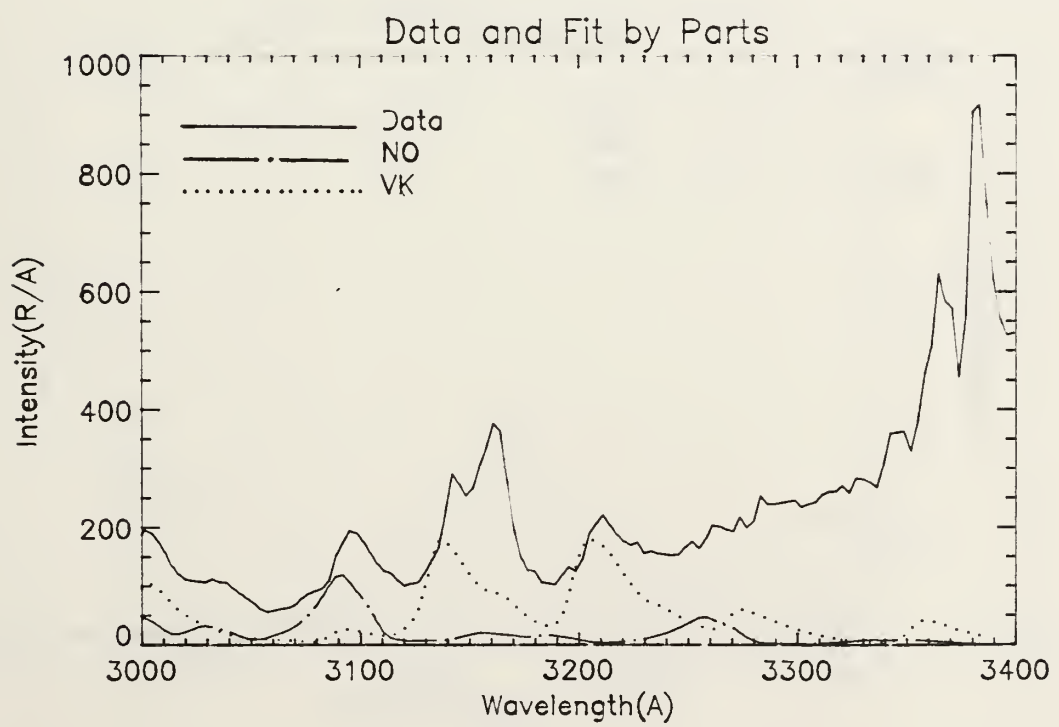
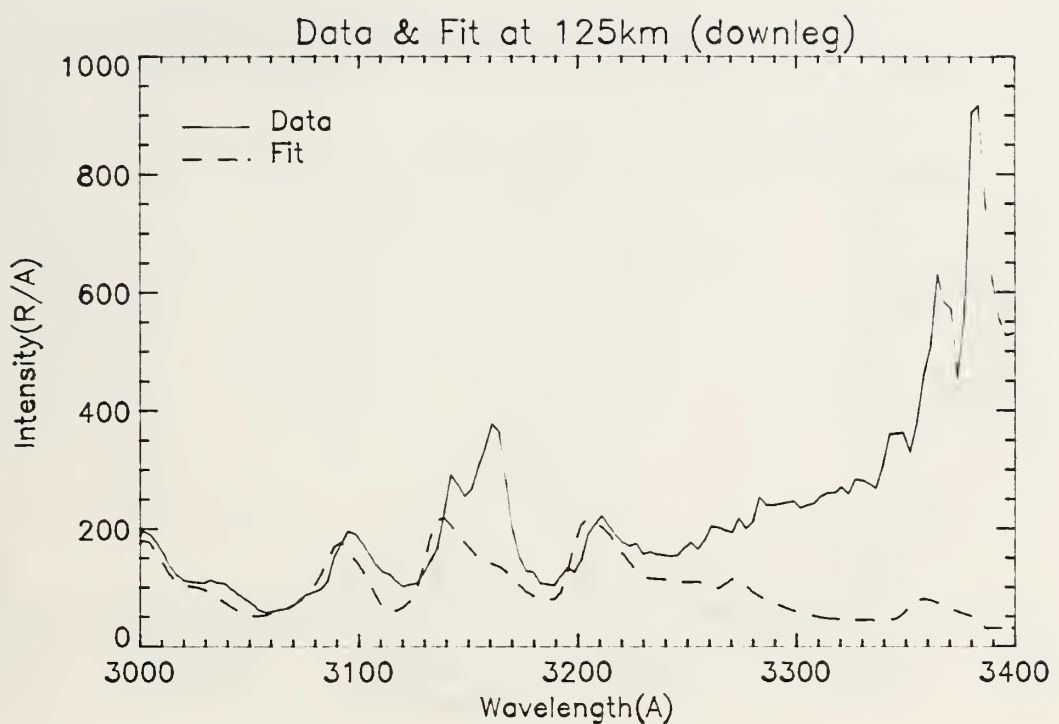


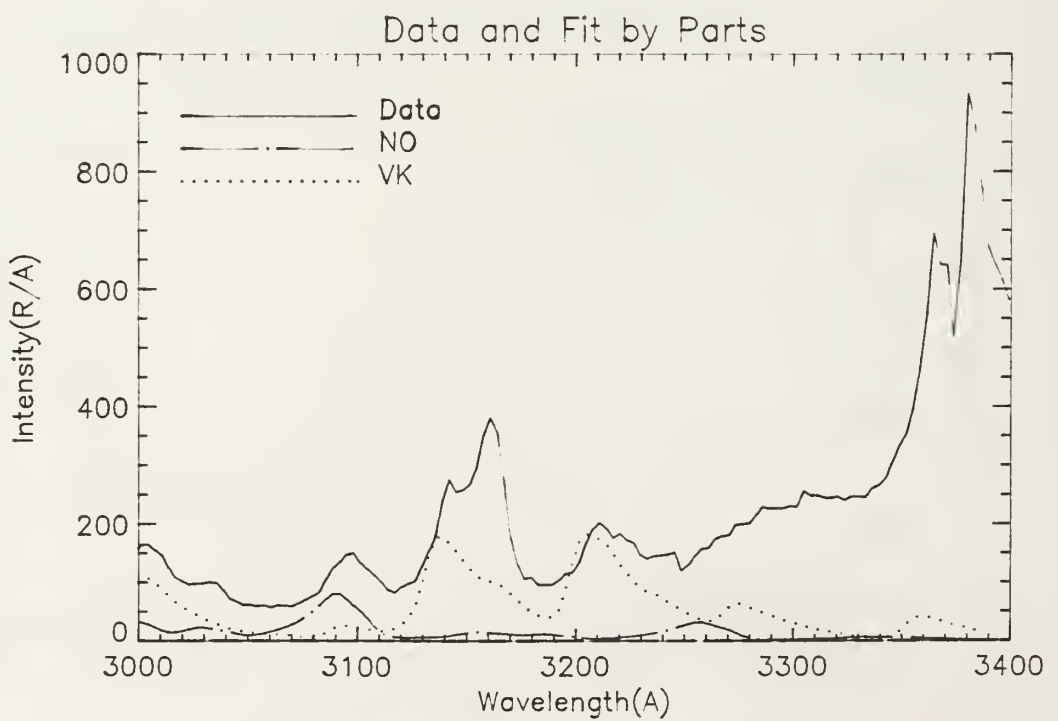
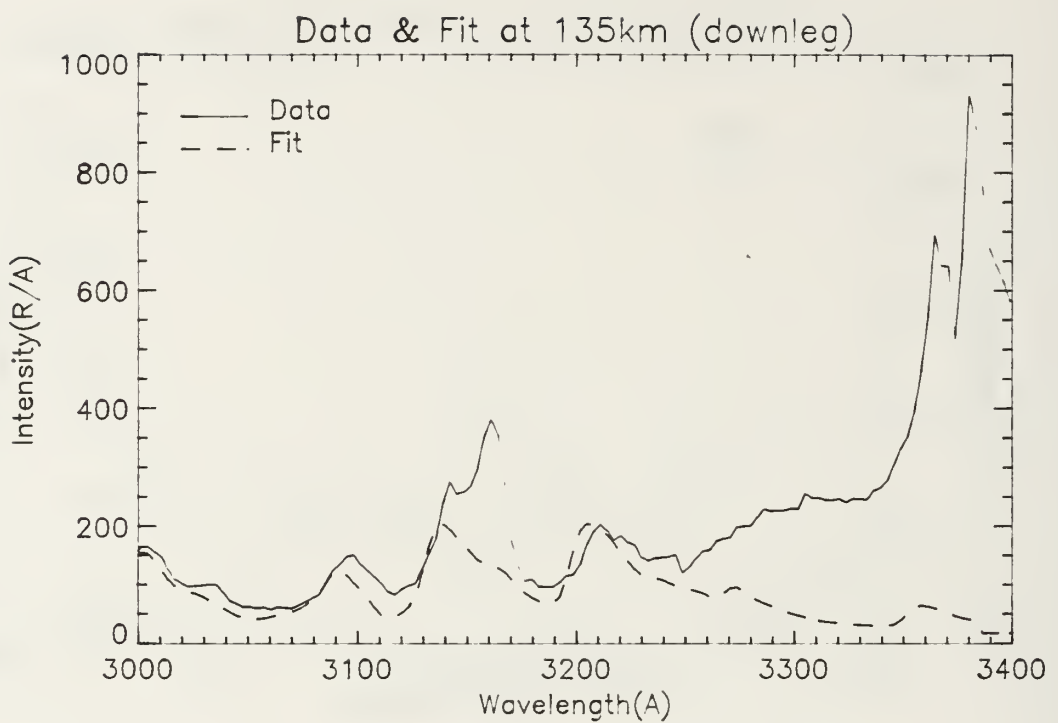
Data and Fit by Parts

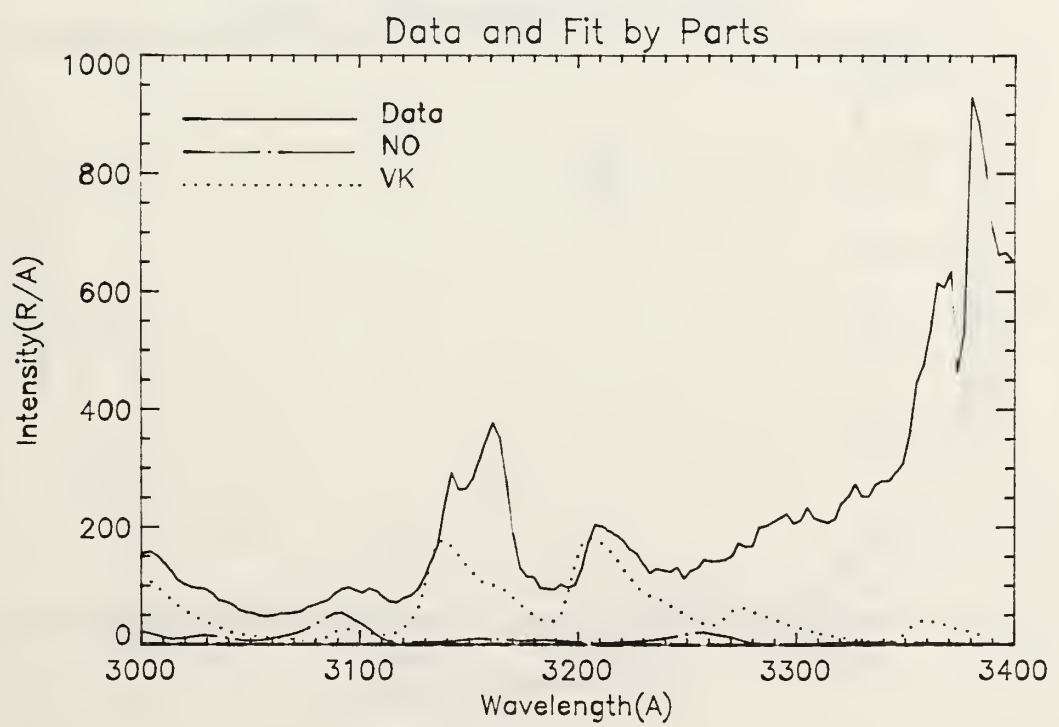
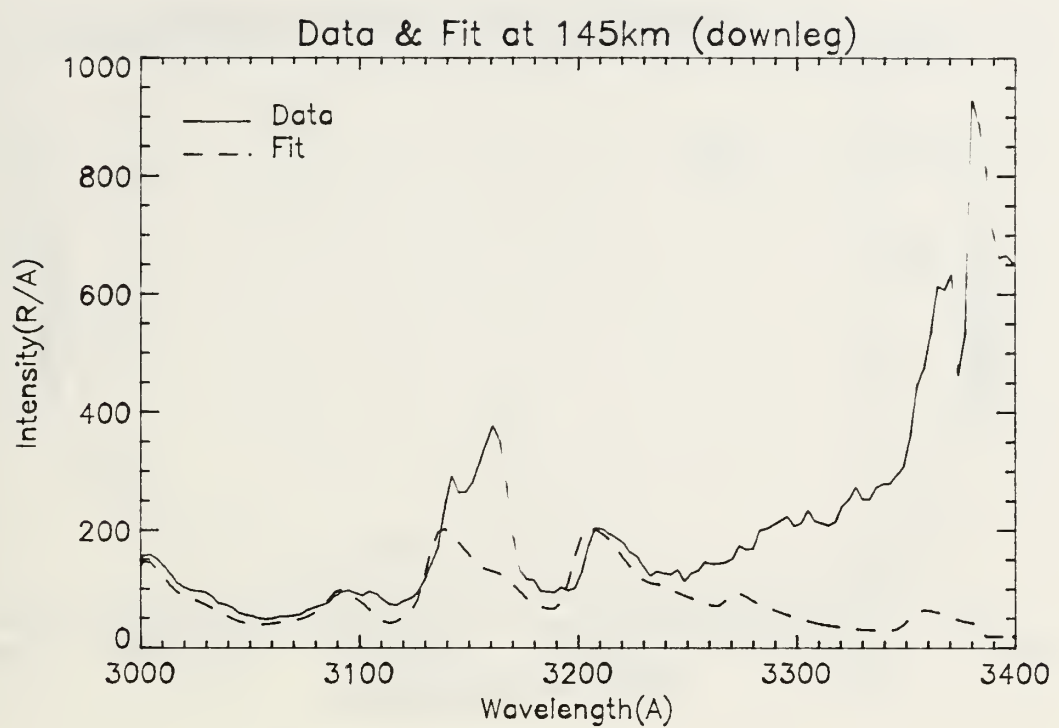


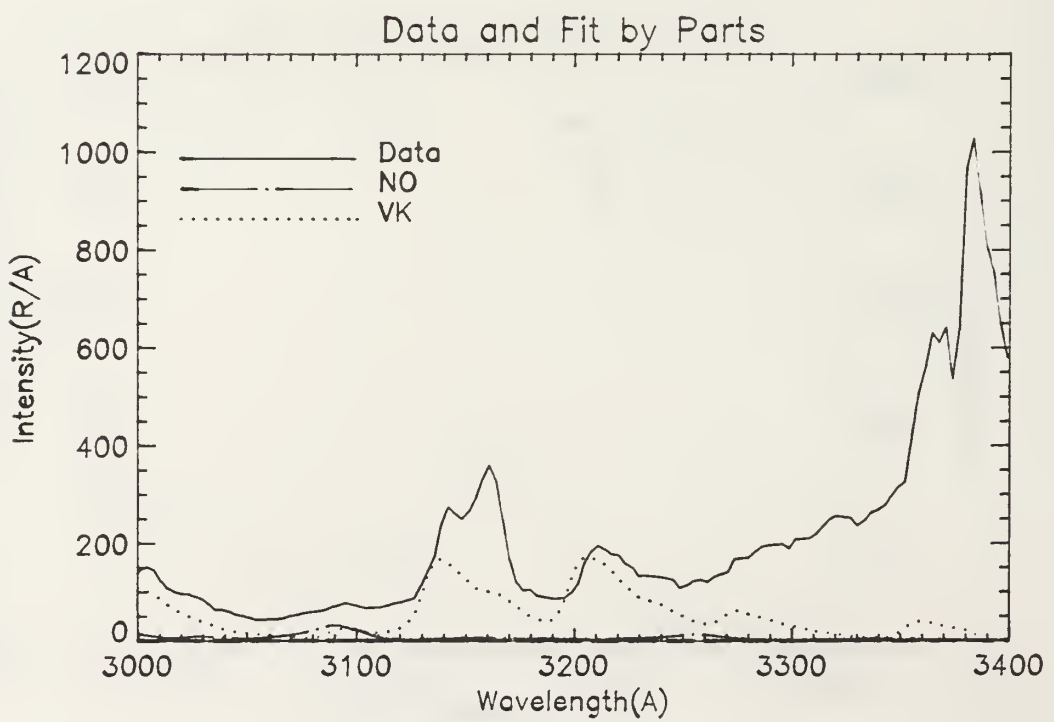
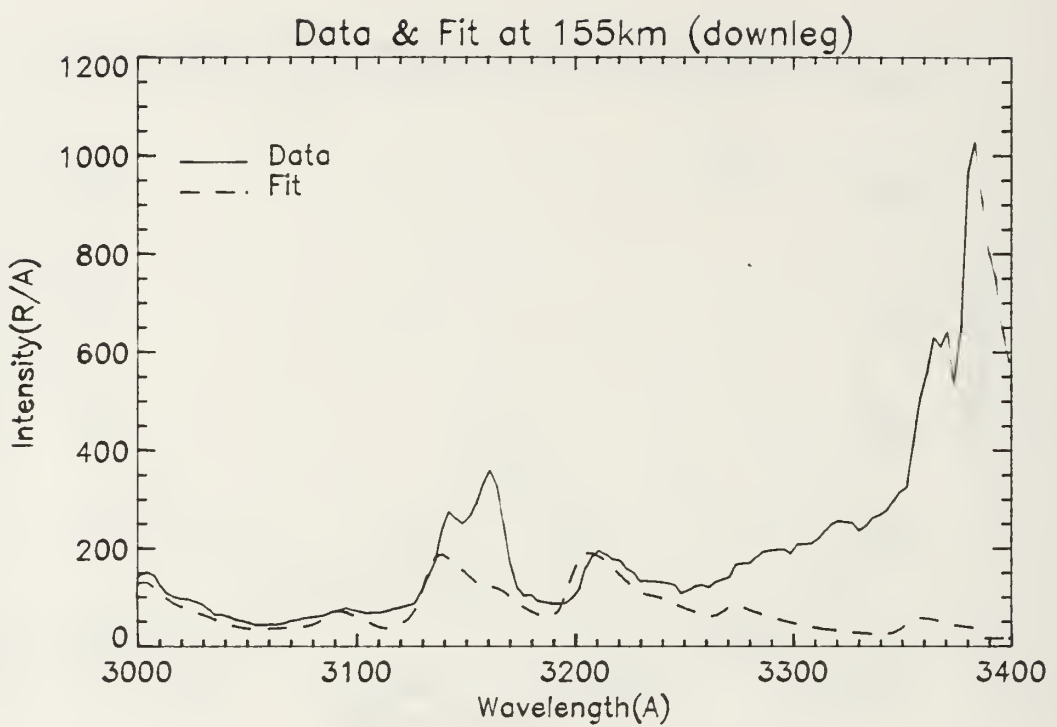


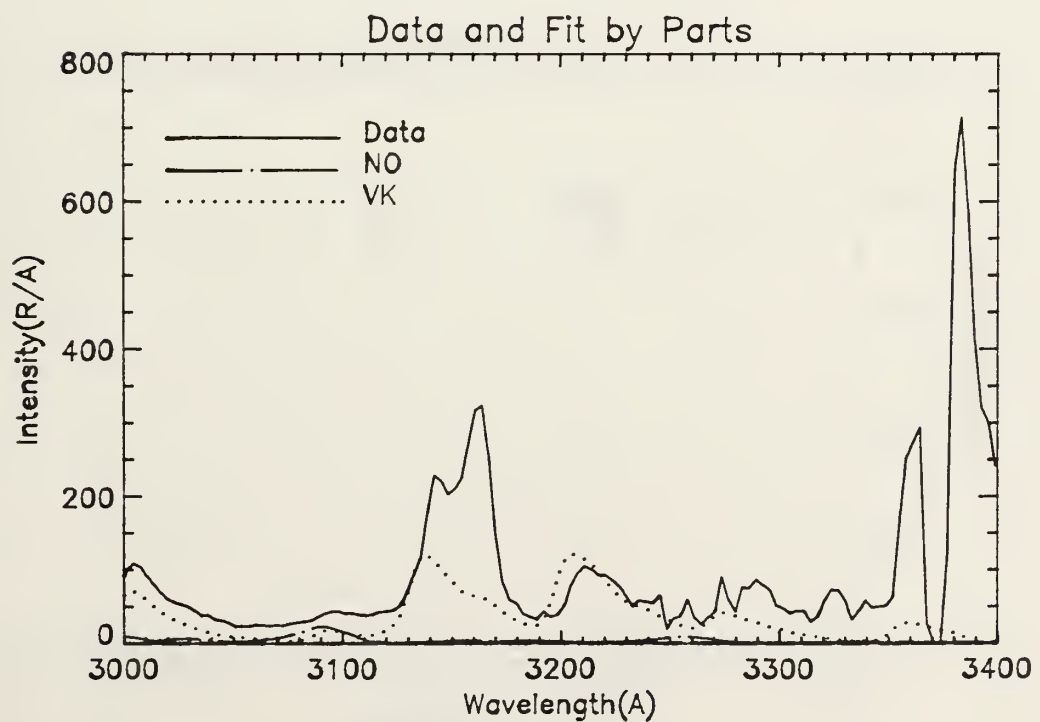
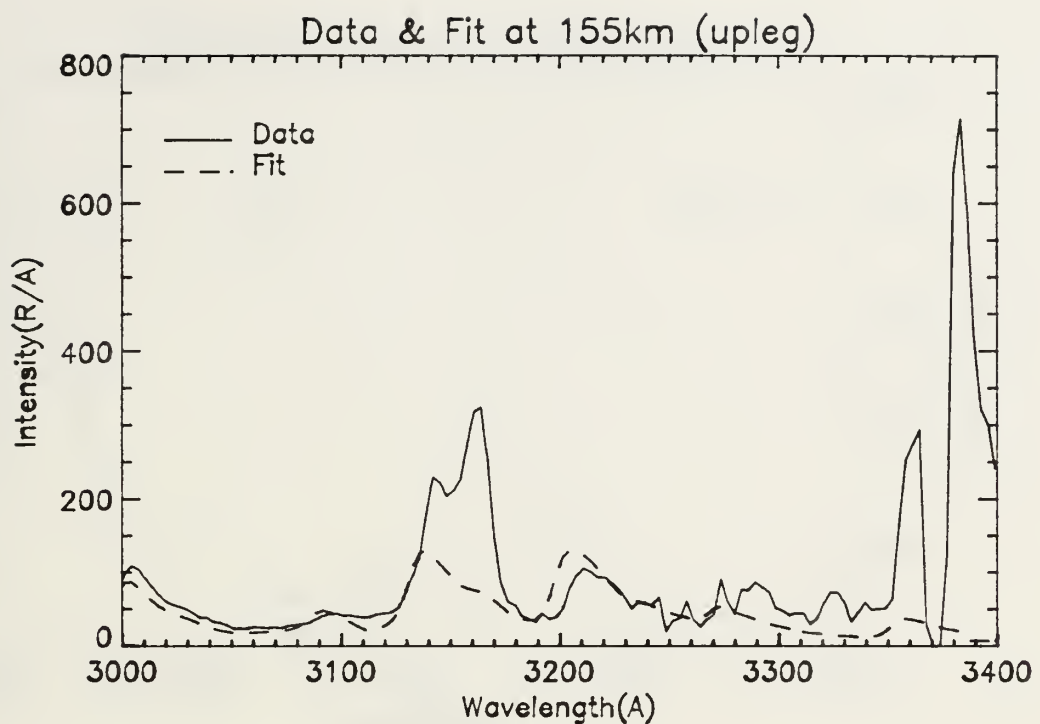


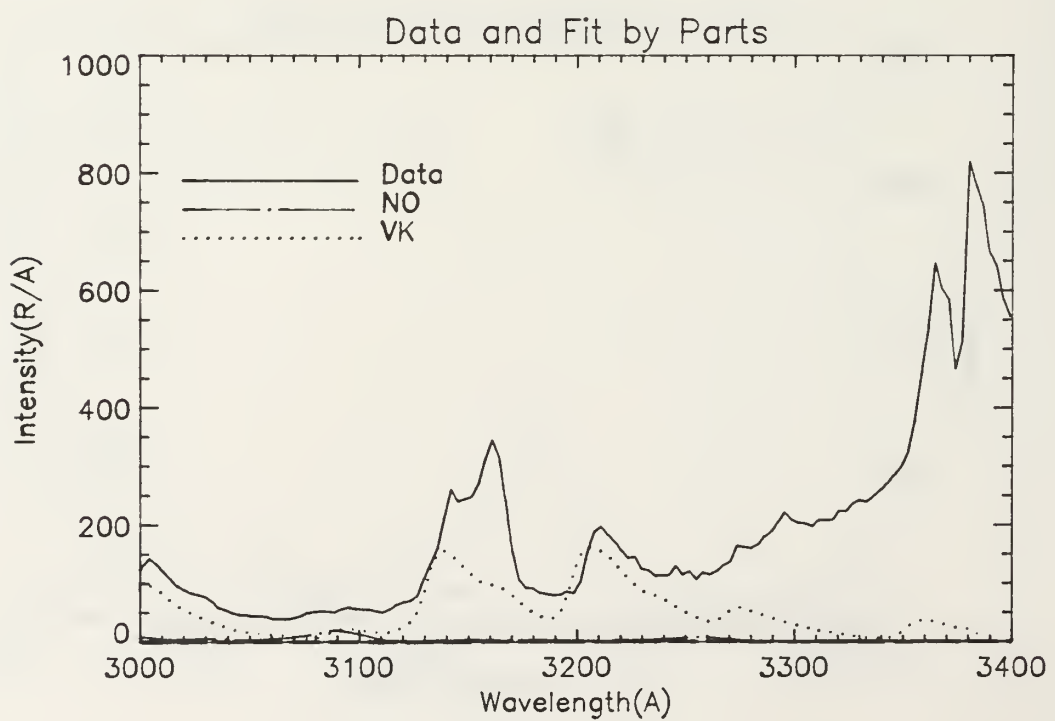
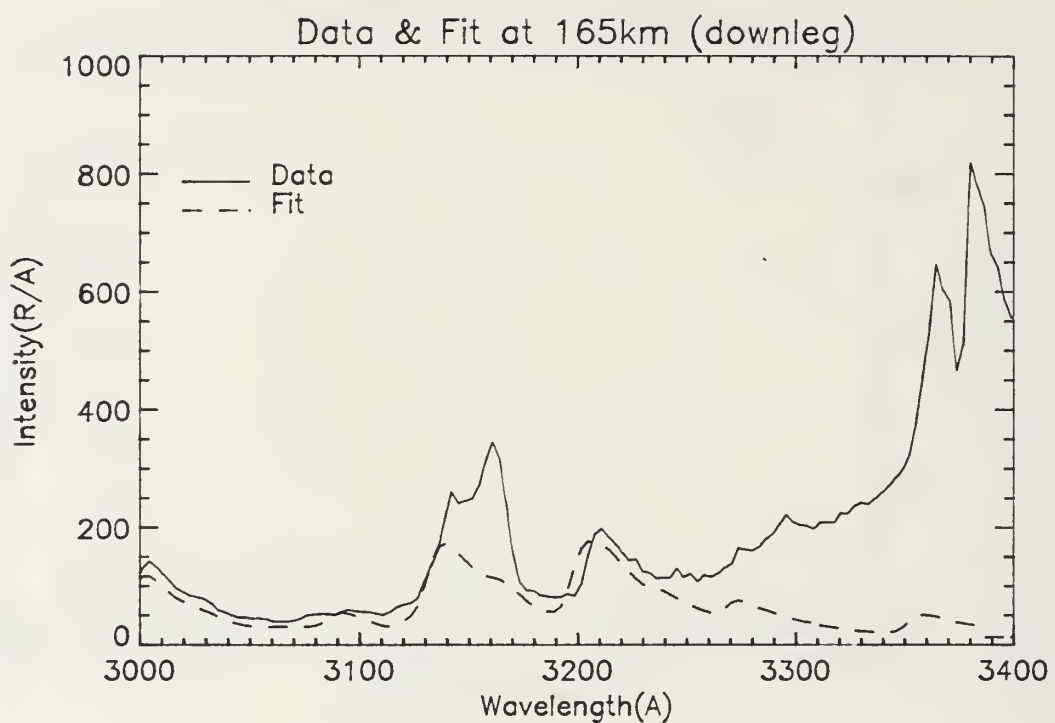


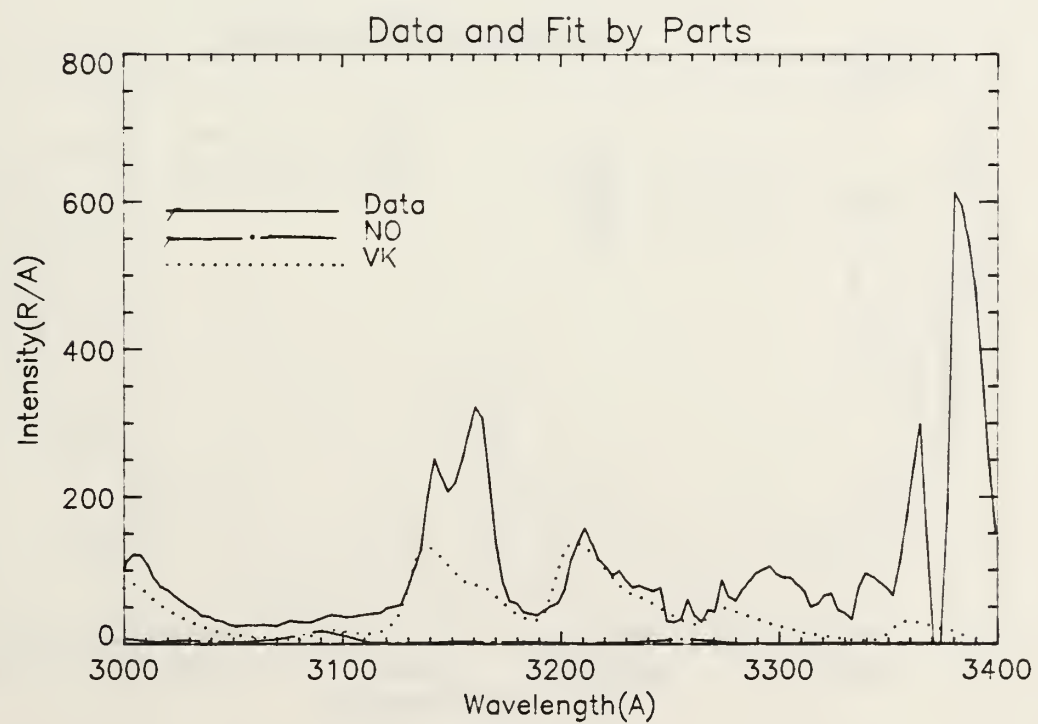
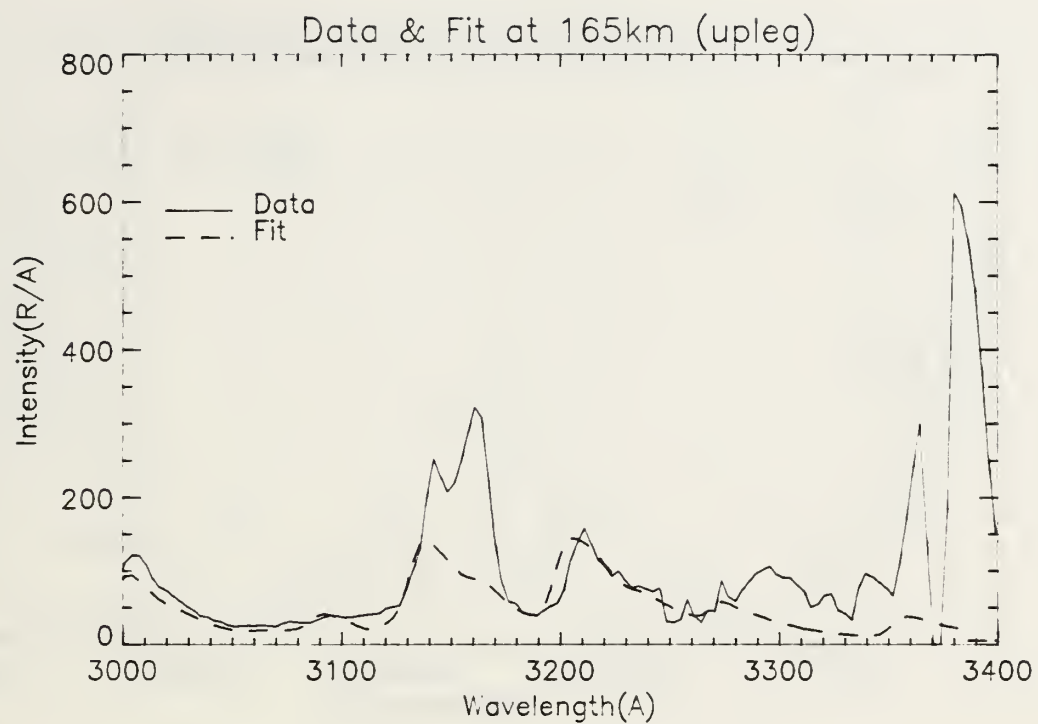


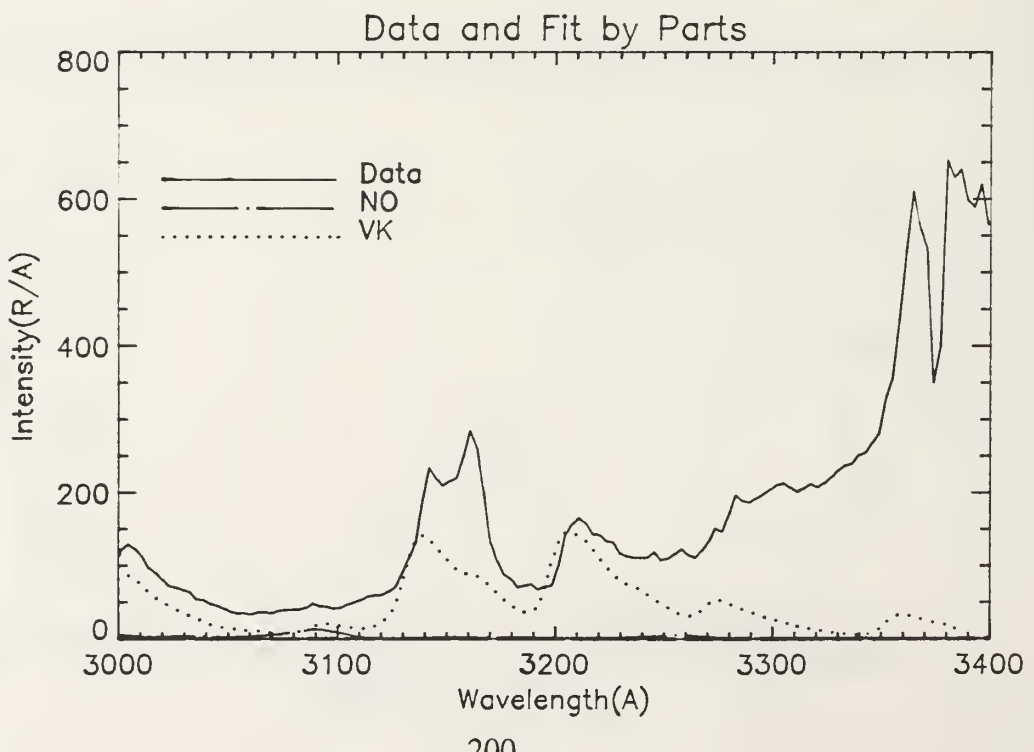
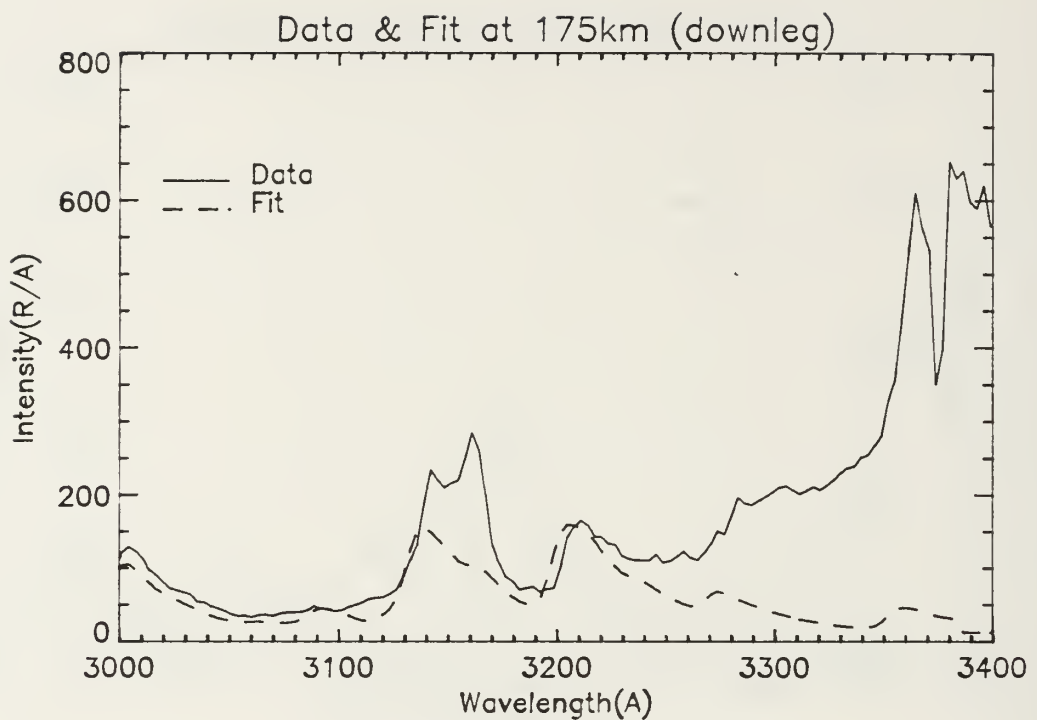


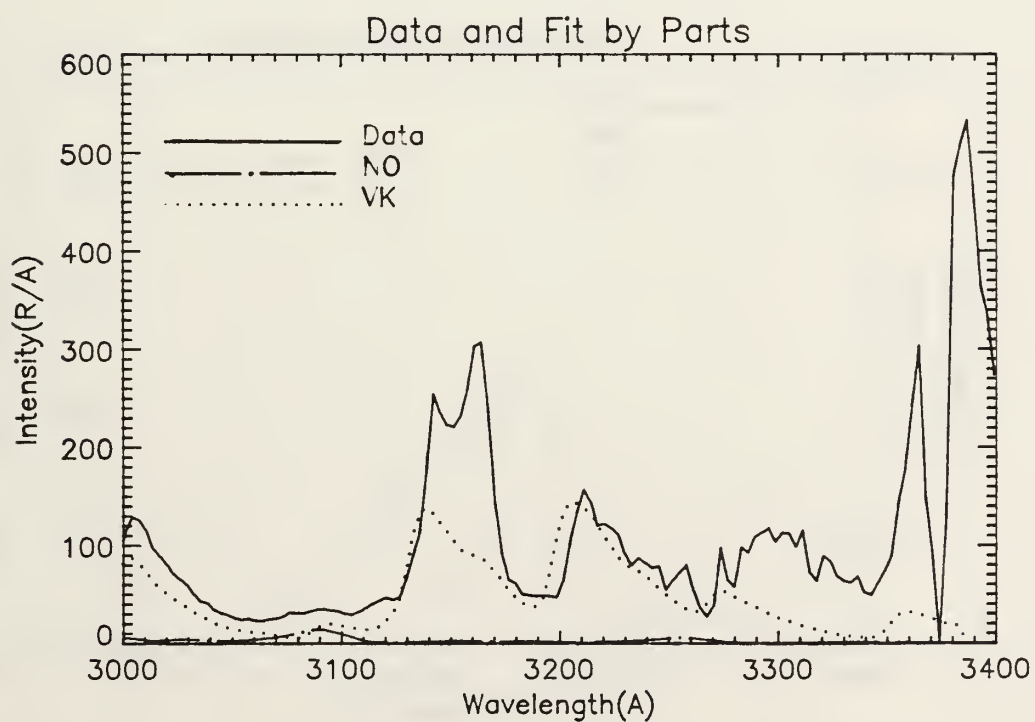
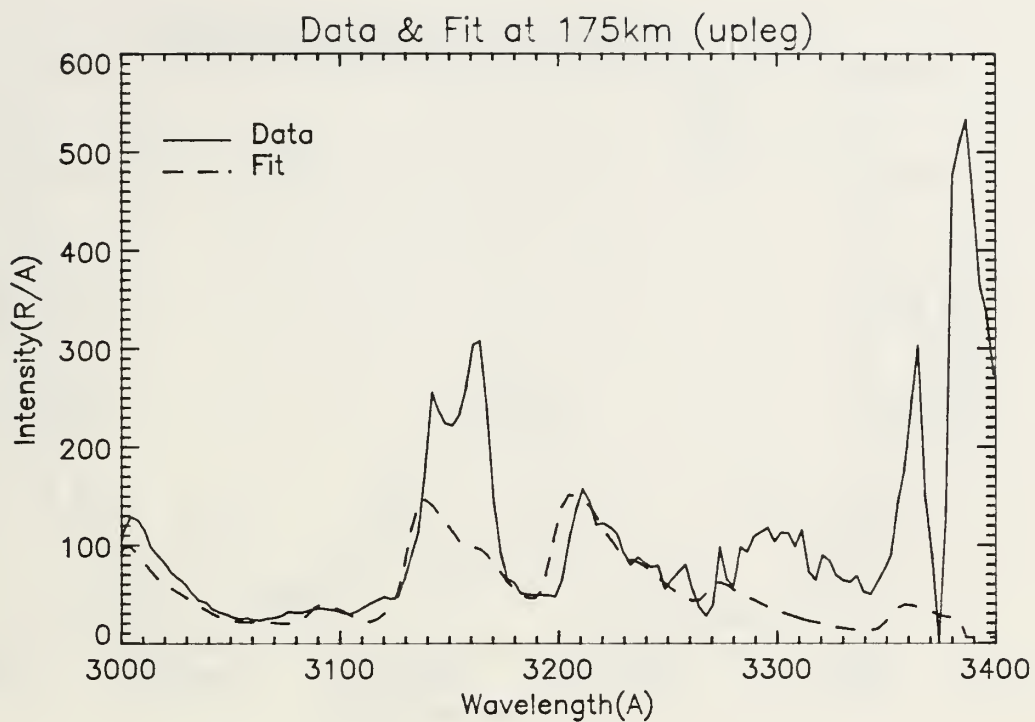


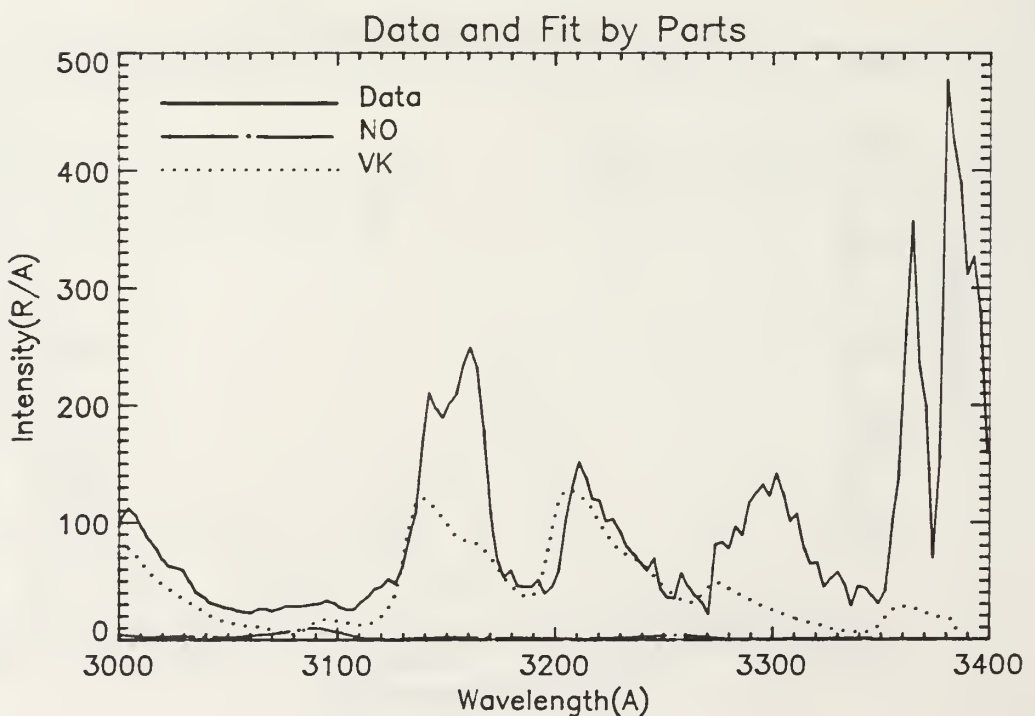
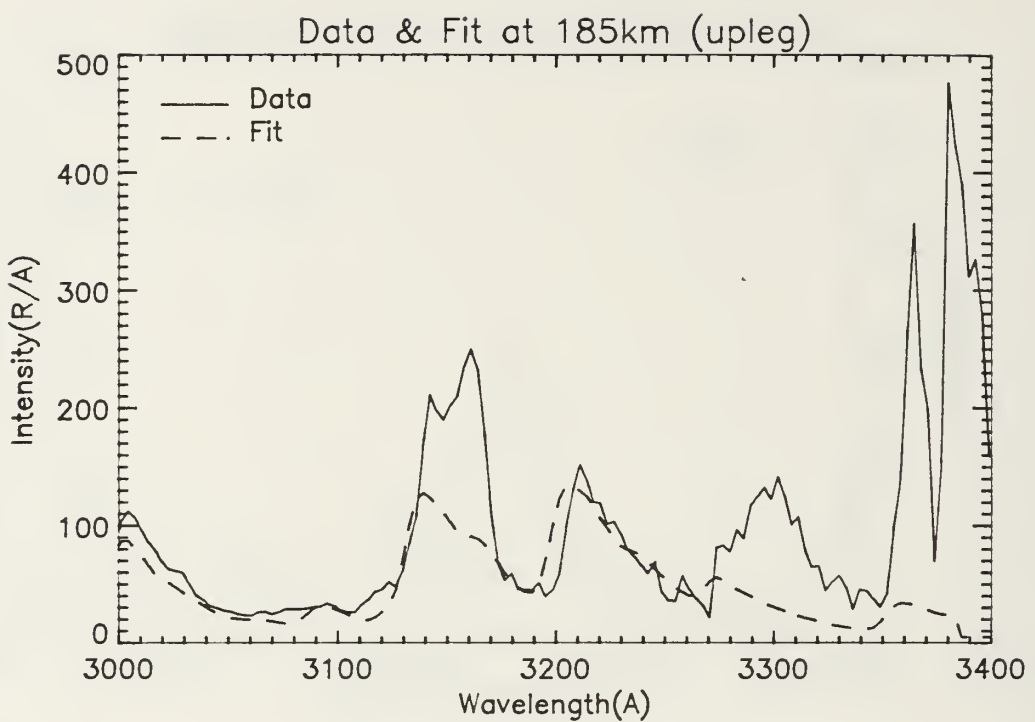


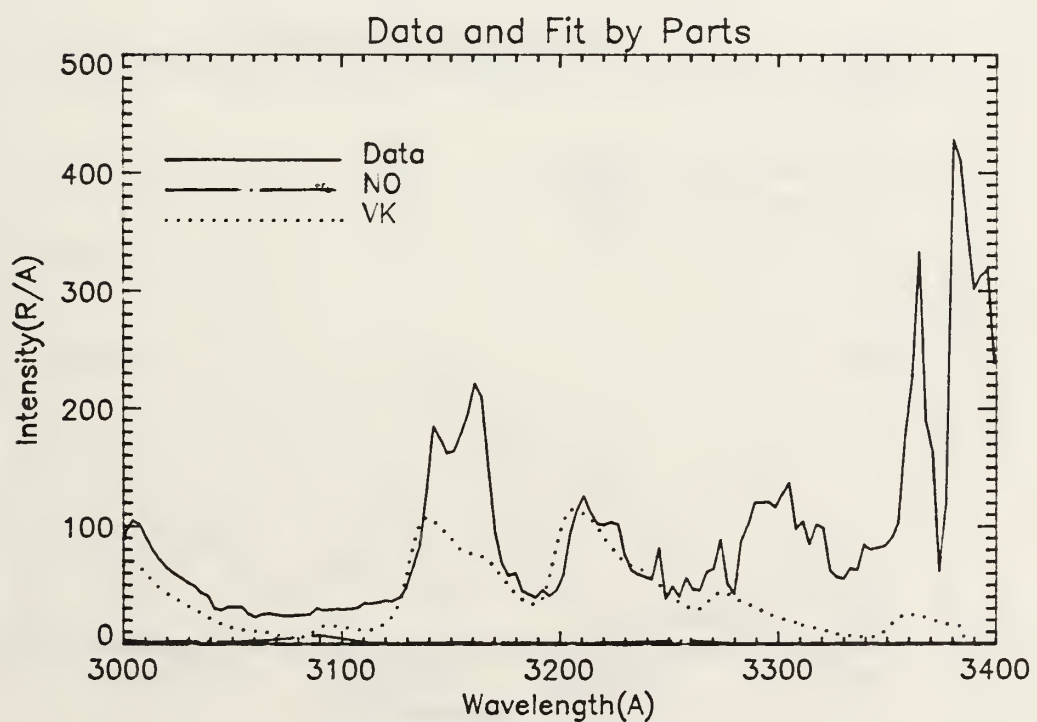
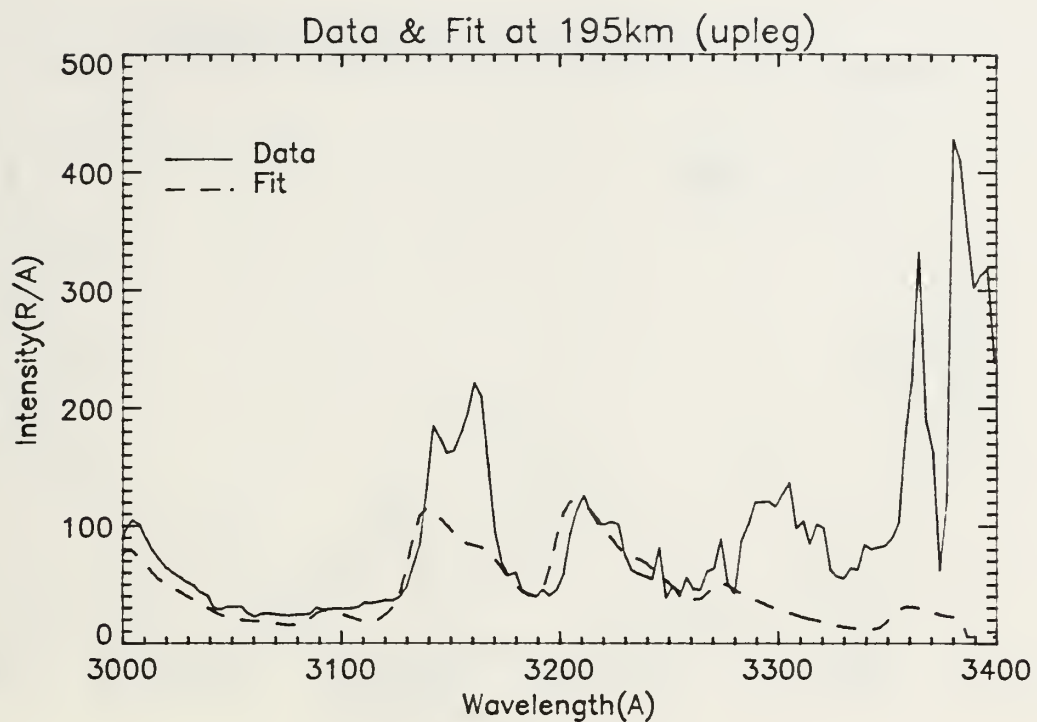


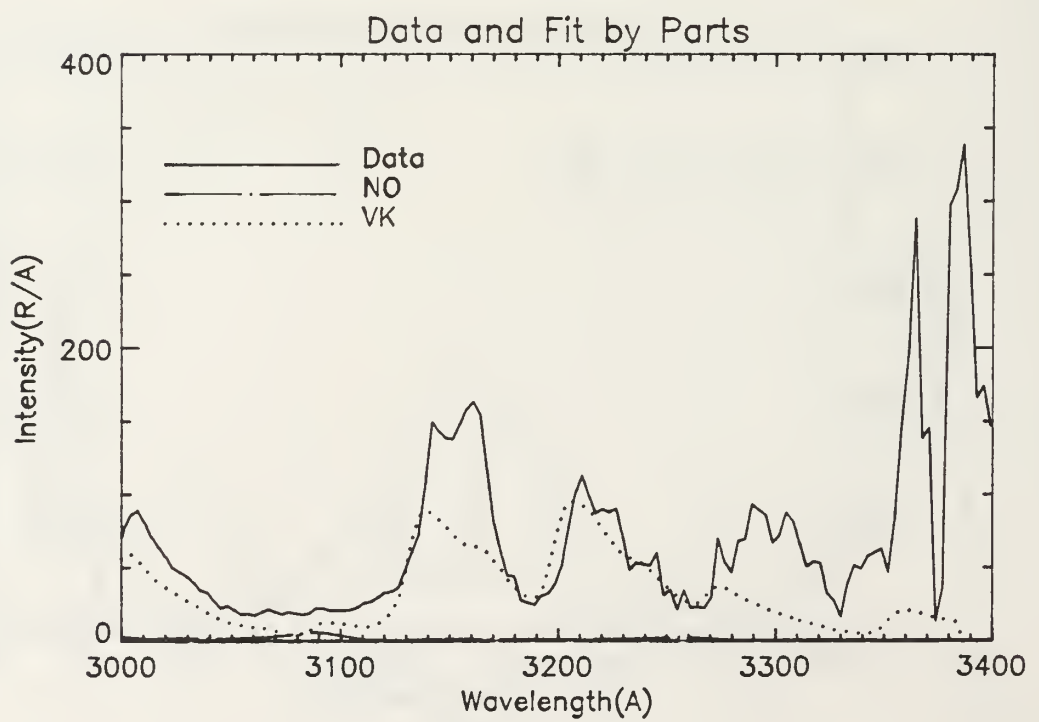
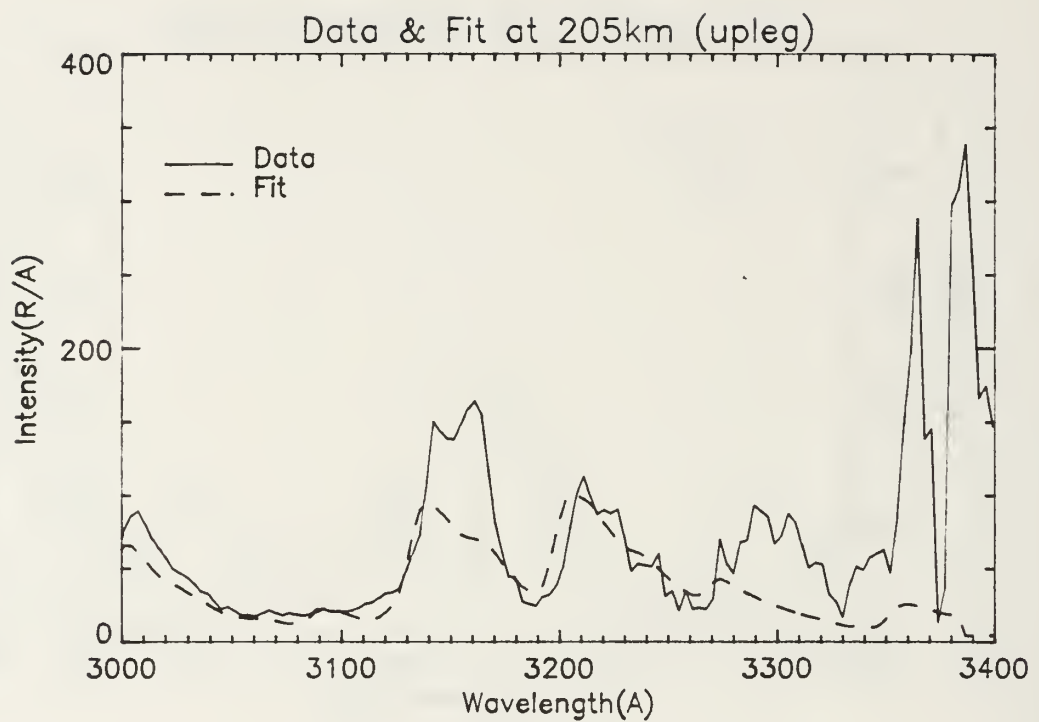


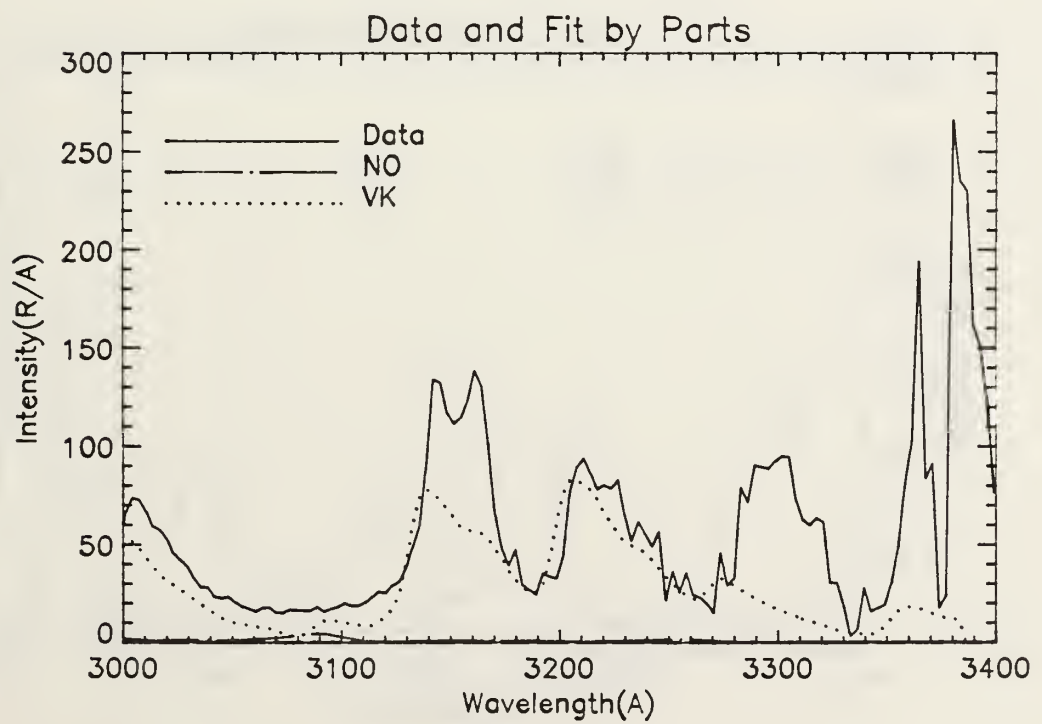
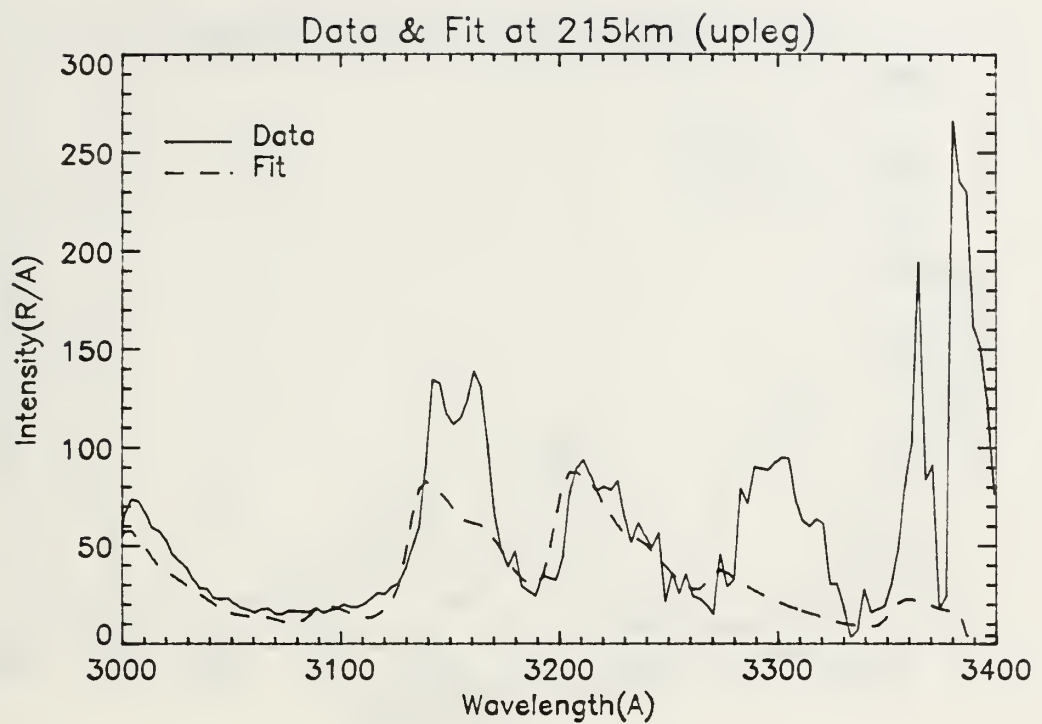


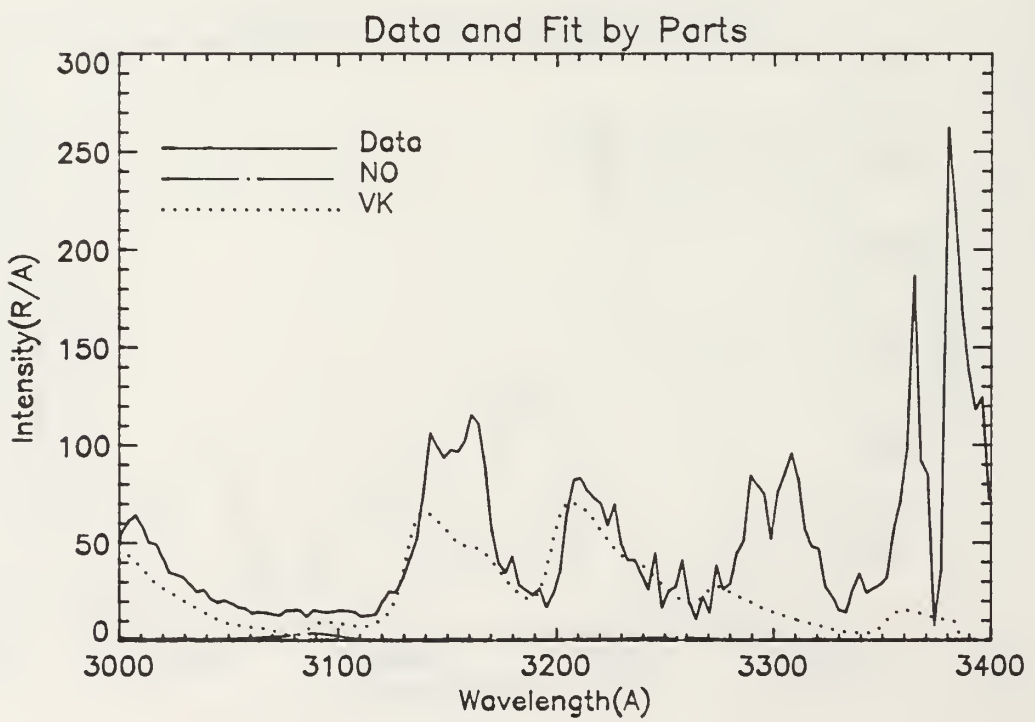
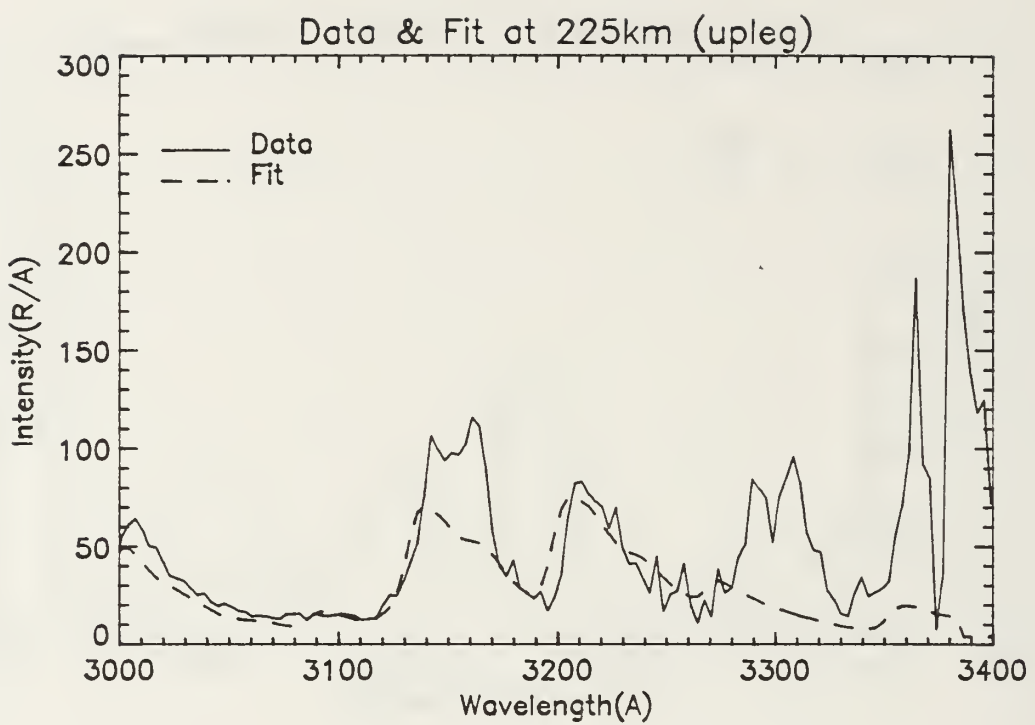


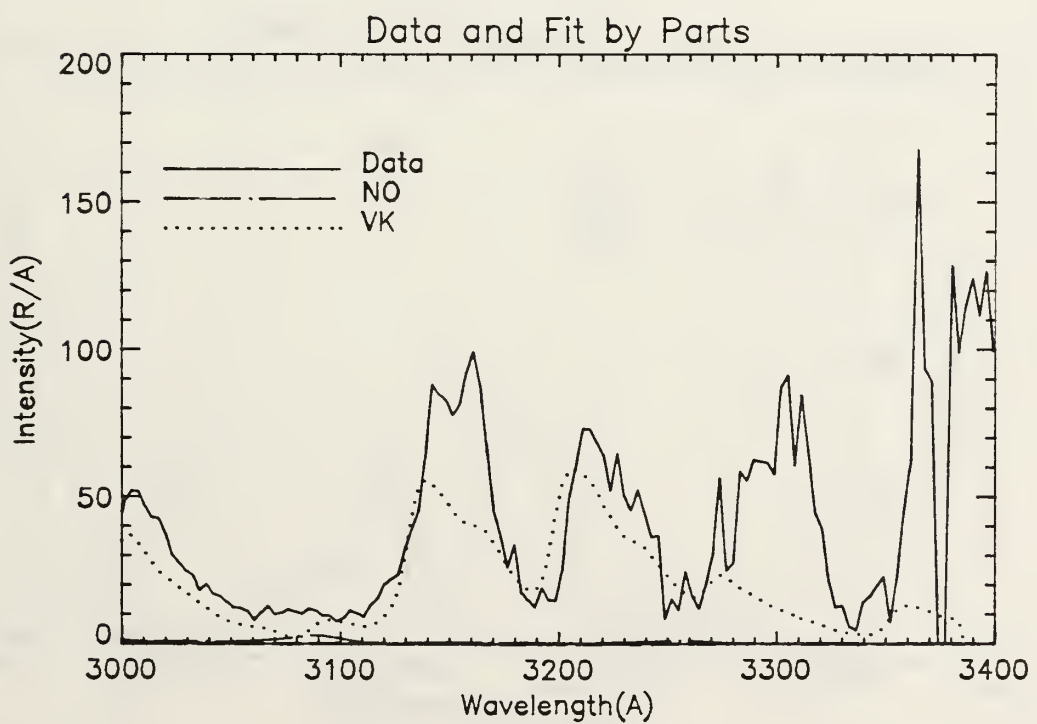
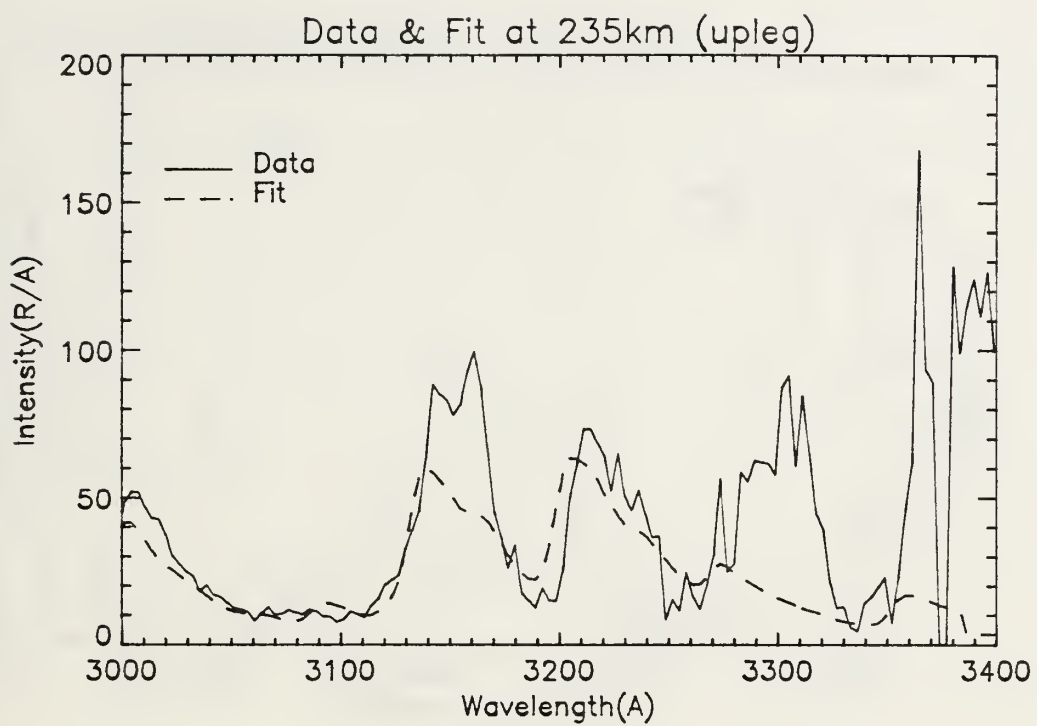


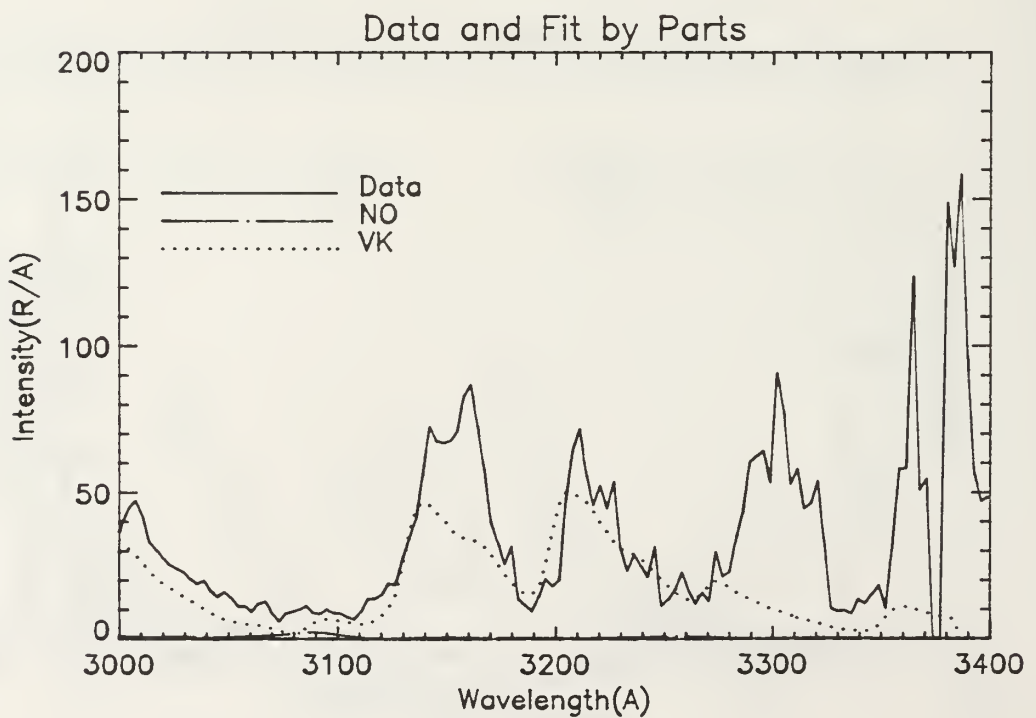
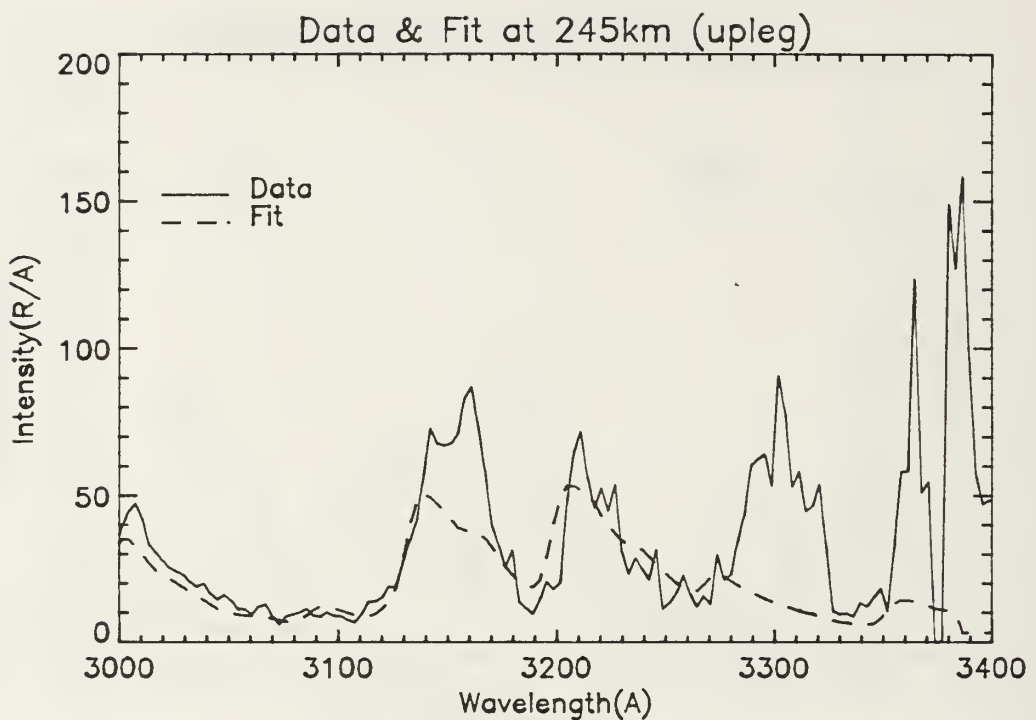


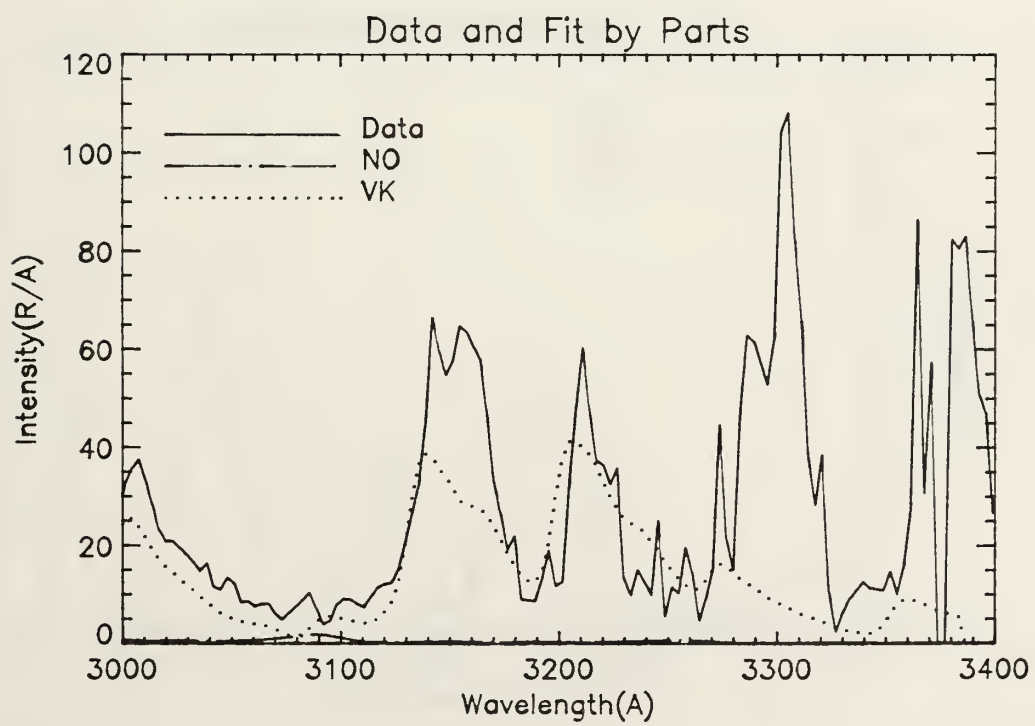
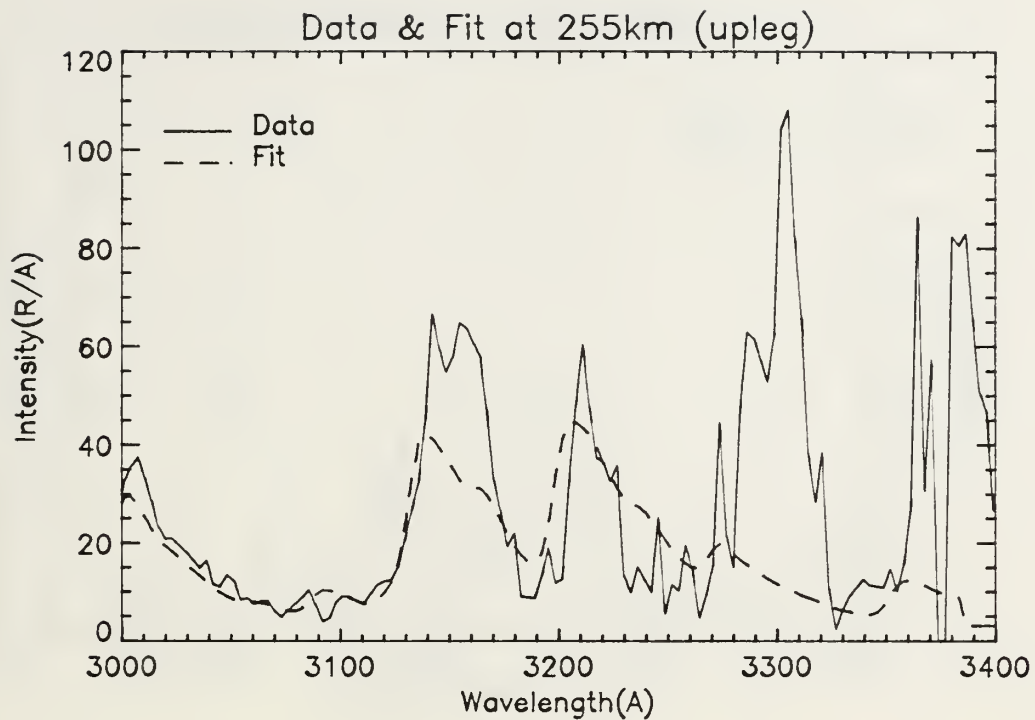


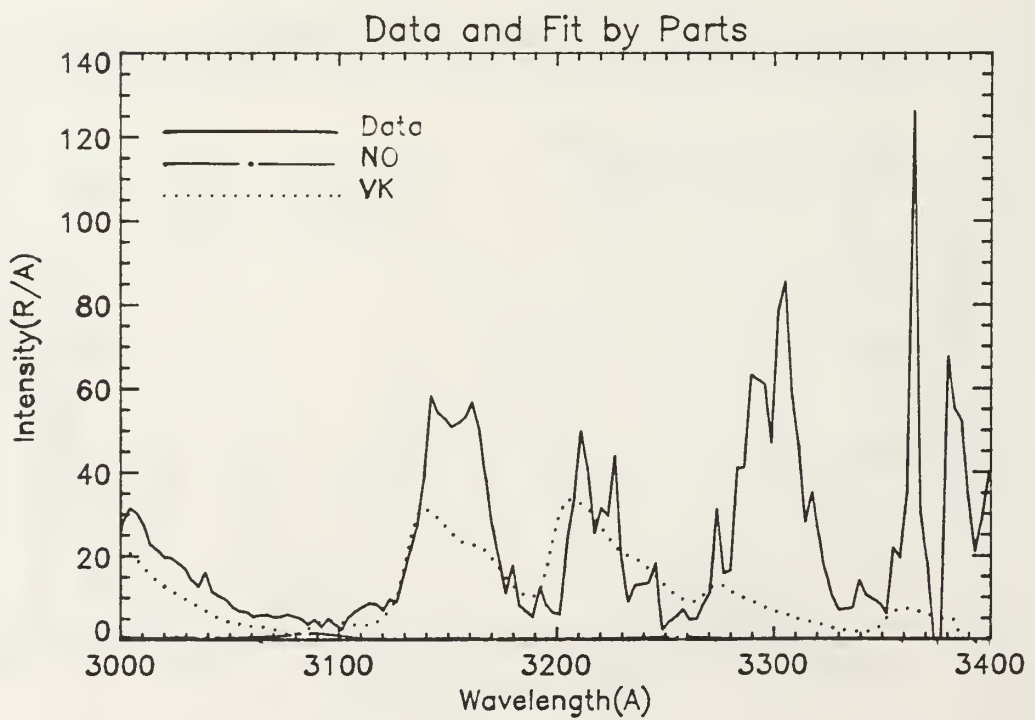
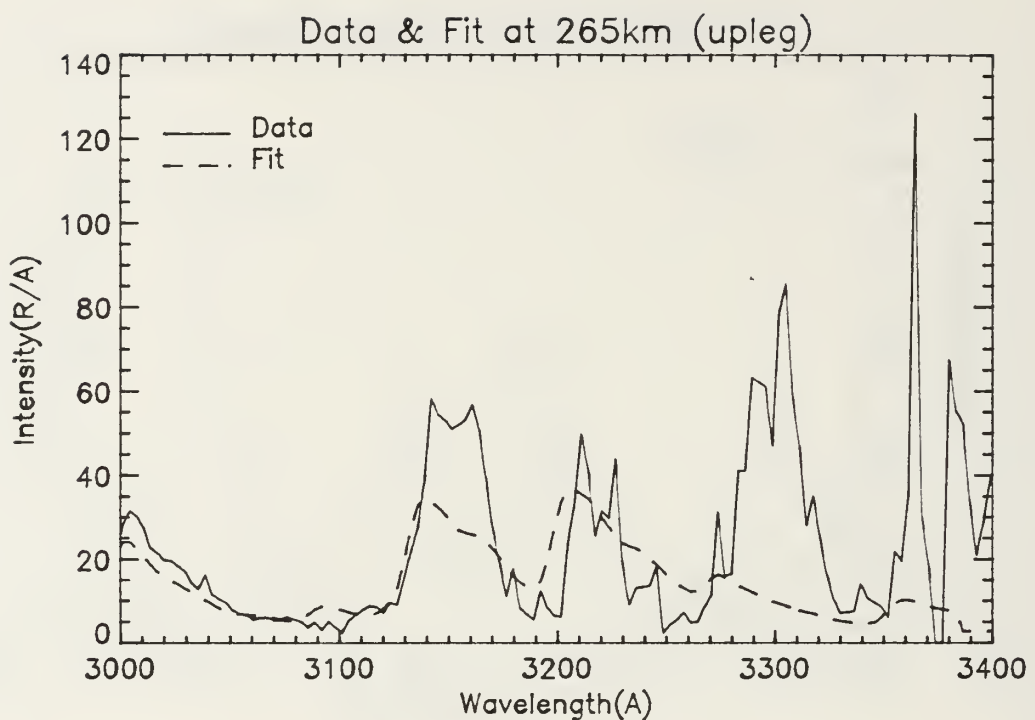


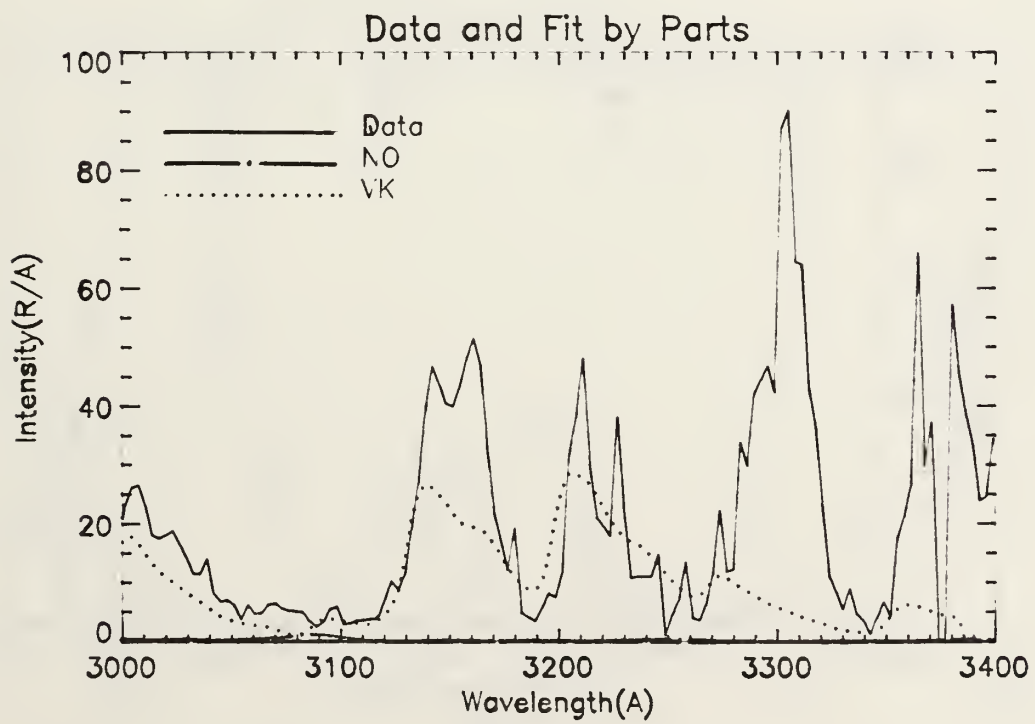
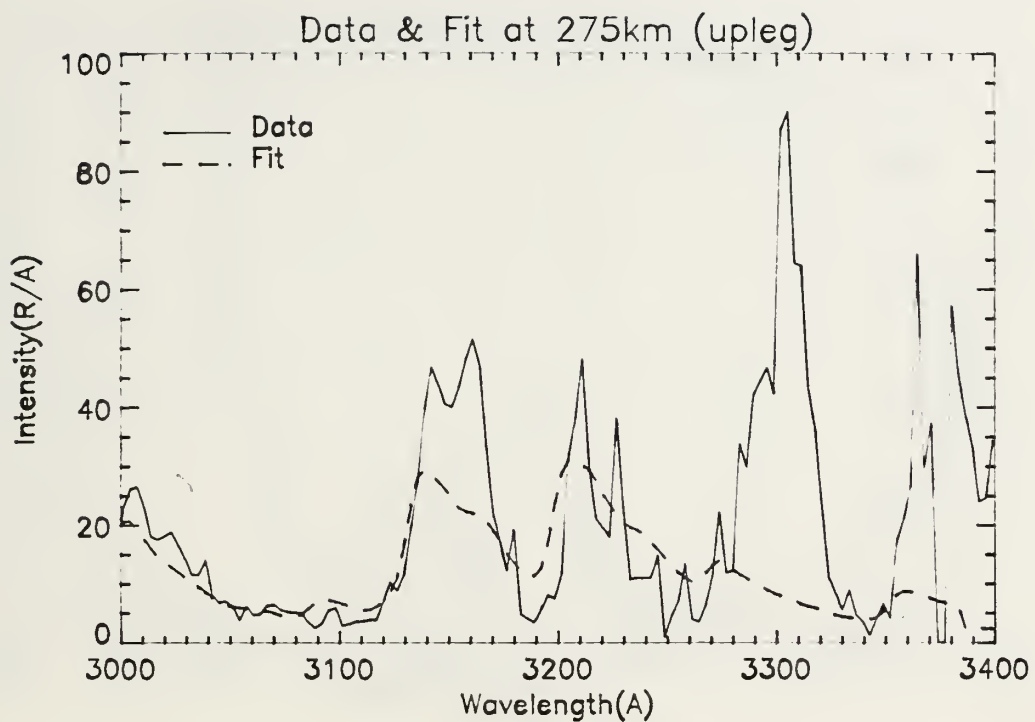


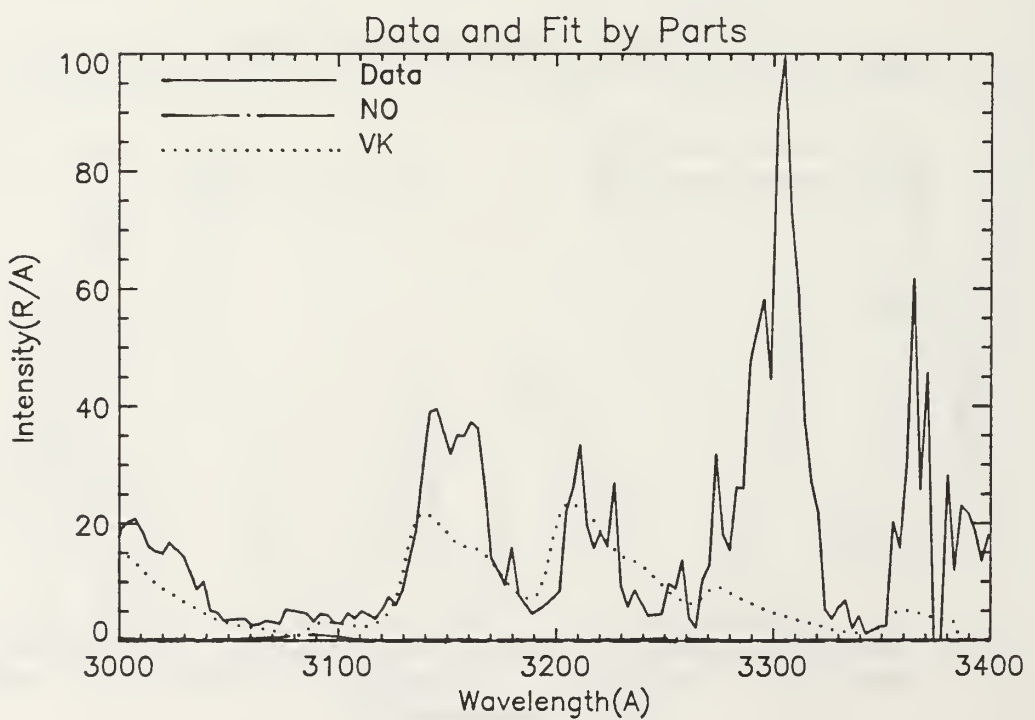
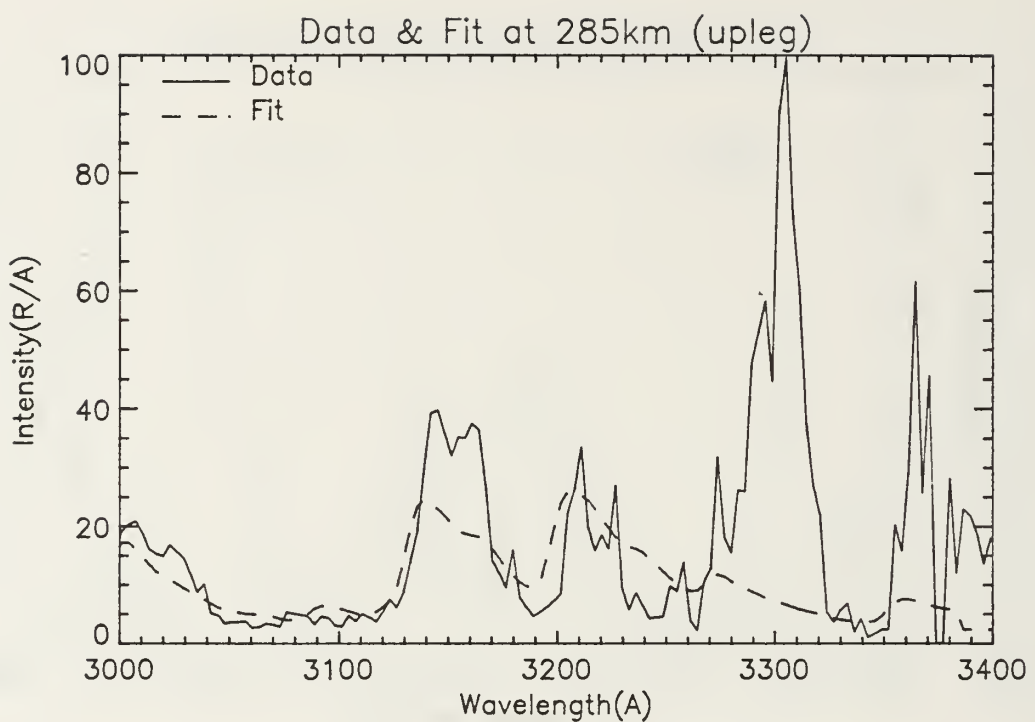


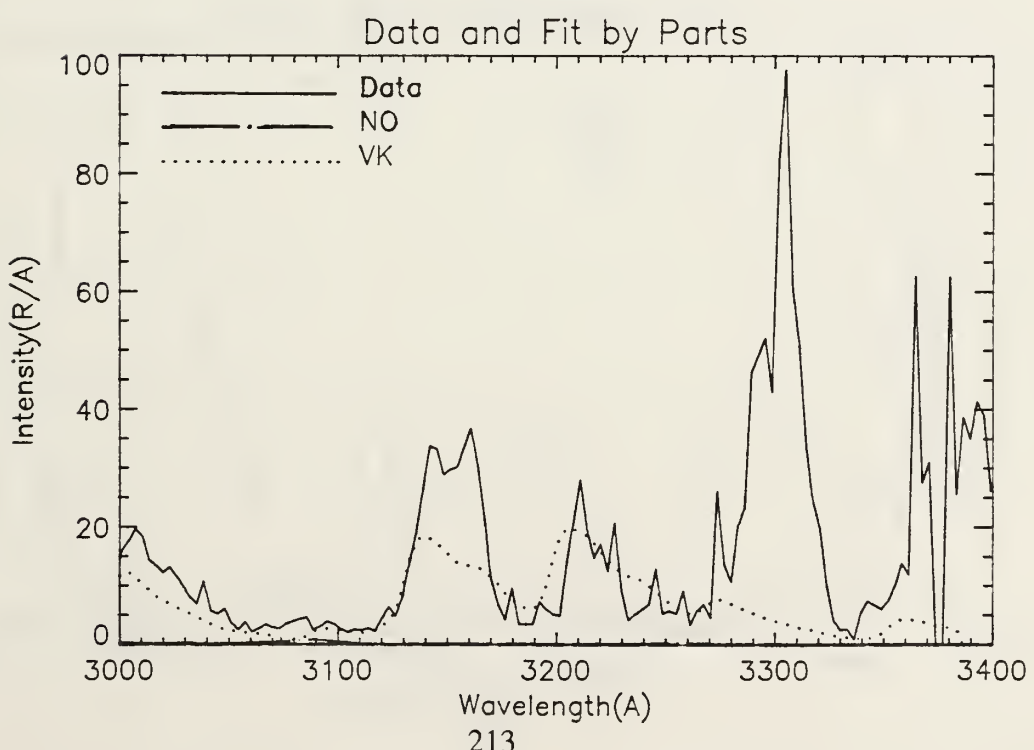
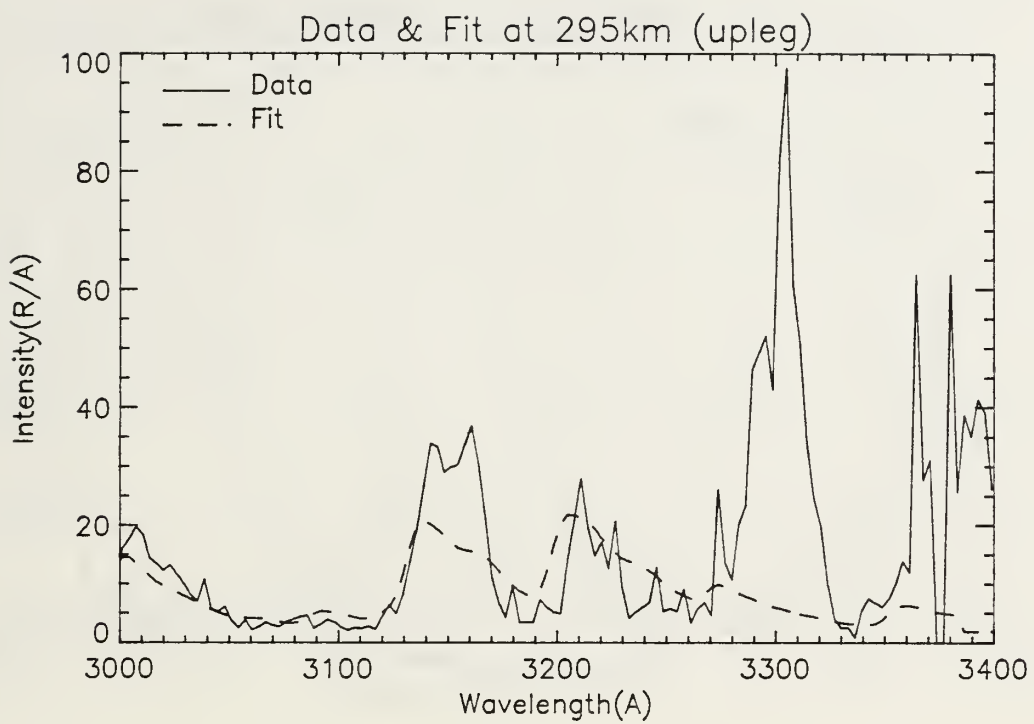


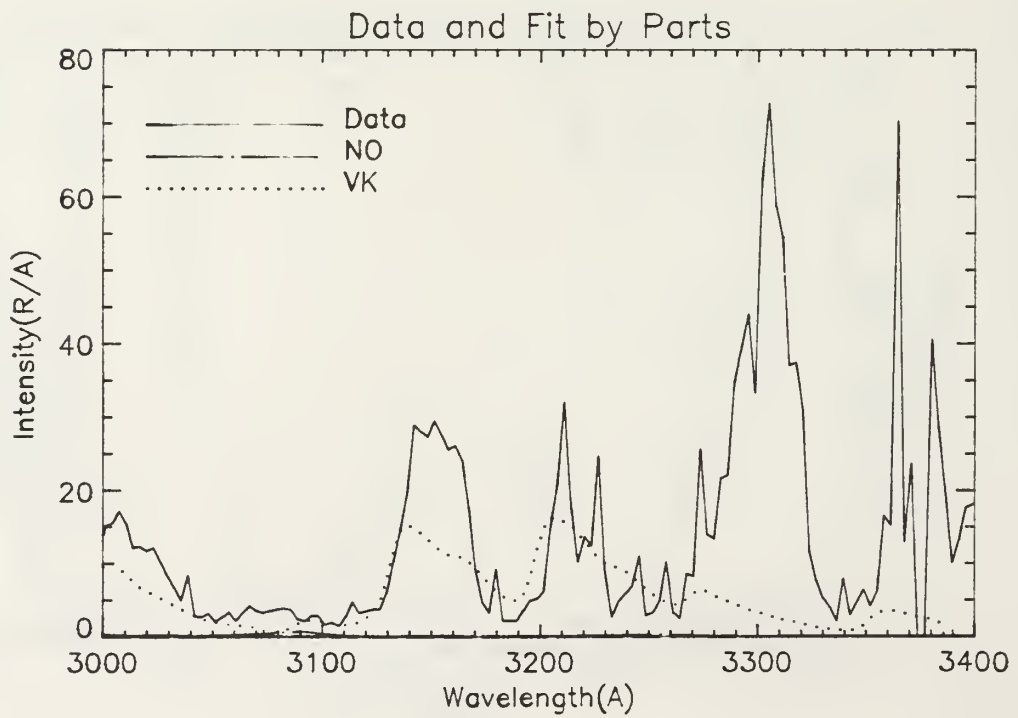
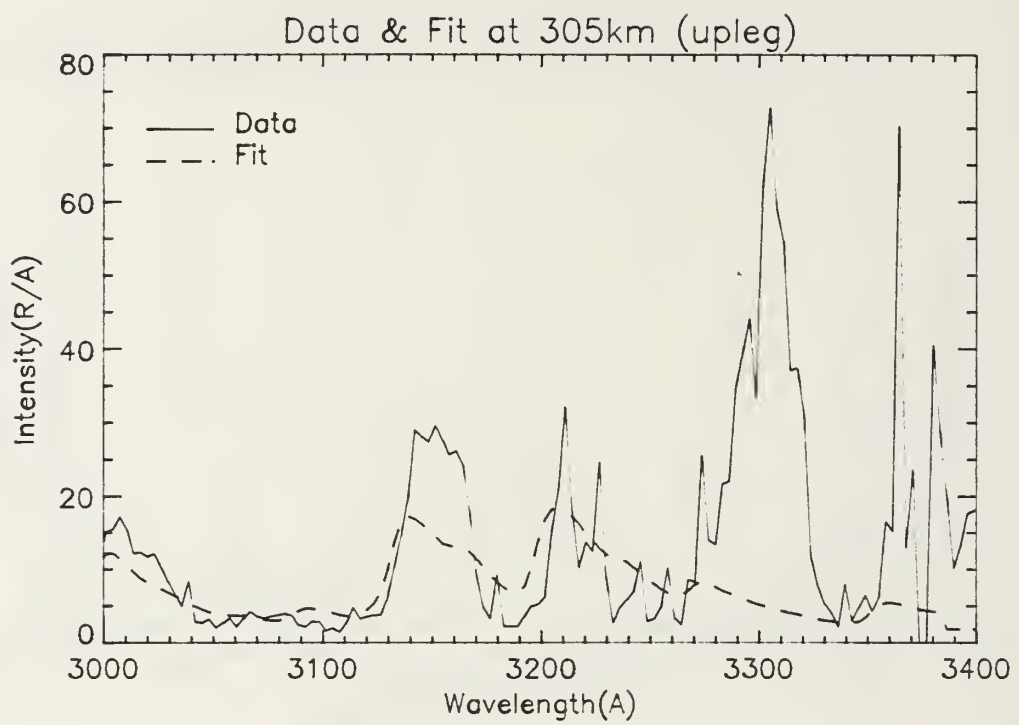


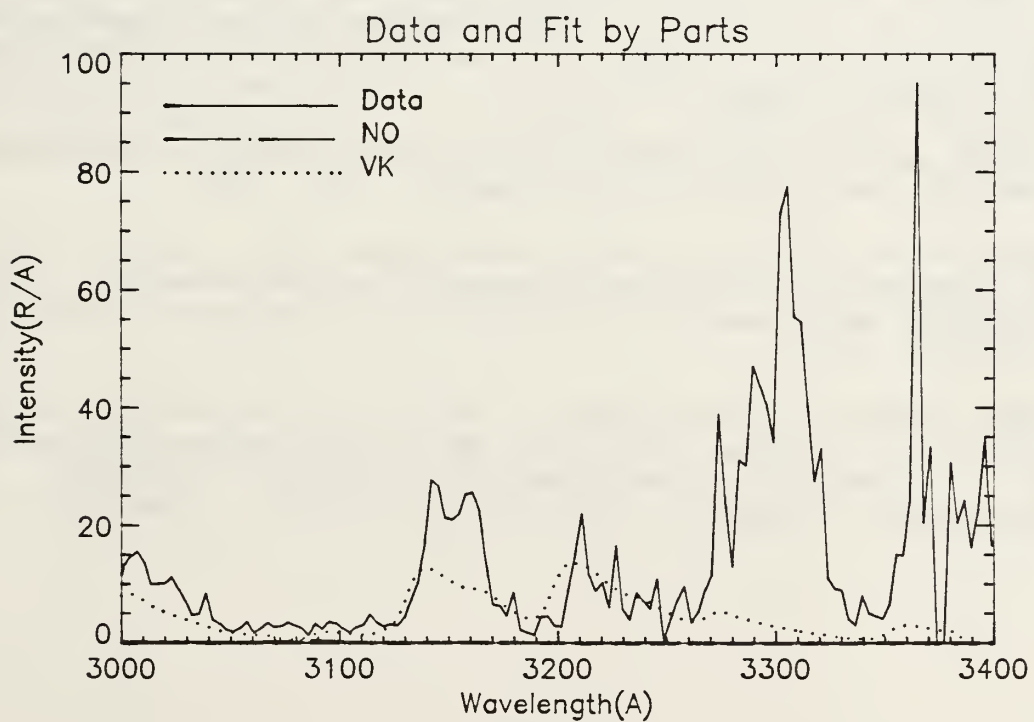
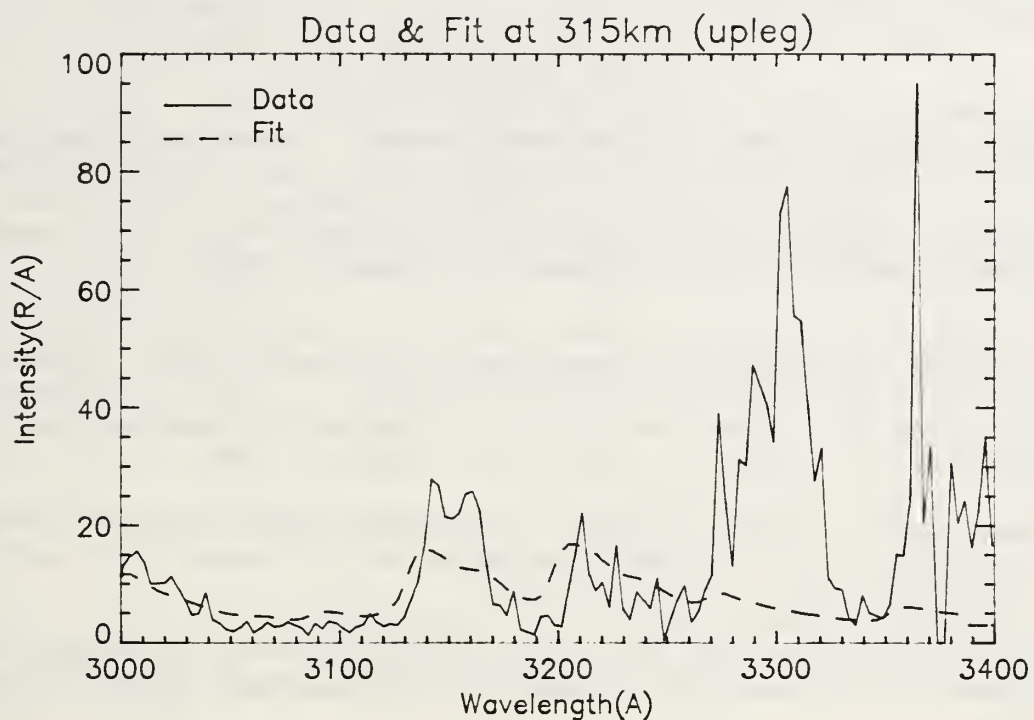












#### LIST OF REFERENCES

Andersen, Carl K., *A Calibration of the Naval Postgraduate School Middle Ultraviolet Spectrograph and an Analysis of the OII 2470 Å and OI 2972 Å Emissions Obtained from Mid-Latitude Rocket Observations*, Master's Thesis, Naval Postgraduate School, Monterey, California, September 1990.

Bevington, Philip R., *Data Reduction and Error Analysis for the Physical Sciences*, McGraw-Hill Book Company, 1969.

Brehm, John J., and Mullin, William J., *Introduction to the Structure of Matter*, John Wiley & Sons, 1989.

Bucsela, E.J., and Sharp, W.E., "The Relative Line Strength and Intensity of the NII 2143 Doublet," *Journal of Geophysical Research*, v.94, p.12069, 1989.

Chamberlain, Joseph P., *Theory of Planetary Atmospheres: An Introduction to Their Physics and Chemistry*, Academic Press, 1978.

Clayton, Michael J., *Analysis of the Ultraviolet Emissions of Nitric Oxide from Mid-Latitude Rocket Observations*, Master's Thesis, Naval Postgraduate School, Monterey, California, June 1990.

Cleary, D. D., "Daytime High-Latitude Rocket Observations of the NO  $\gamma$ ,  $\delta$ , and  $\epsilon$  Bands," *Journal of Geophysical Research*, v. 91, p.11337, 1986.

Green, A.E.S., and Wyatt, Philip J., *Atomic and Space Physics*, Addison-Wesley Publishing Company, Inc., 1965.

The Joint Chiefs of Staff Memorandum MJCS Serial 154-86 to Undersecretary of Defense (Research and Engineering), Subject: Military Requirements for Defense Environmental Satellites, 1 August 1986.

Mack, Bryan D., *An Analysis of Middle Ultraviolet Emissions of Molecular Nitrogen and Nitric Oxide and Vacuum Calibration of an Ultraviolet Spectrograph*, Master's Thesis, Naval Postgraduate School, Monterey, California, June 1991.

McCoy, R.P., Anderson, D.E., Jr., and Chakrabarti, S., "F2 Region Ion Densities from Analysis of O<sup>+</sup> 834Å Airglow," *Journal of Geophysical Research*, v. 90, p.12257, 1985.

Meier, R.R., "Ultraviolet Spectroscopy and Remote Sensing of the Upper Atmosphere," *Space Science Reviews*, v. 58, nos. 1 & 2, October 1991.

National Aeronautics and Space Administration Technical Report 32-822, *Ultraviolet Spectroscopy of Planets*, Charles A. Barth, 15 December 1965.

National Aeronautics and Space Administration Technical Memorandum 80268, *Atomic Emission Lines in the near Ultraviolet; Hydrogen Through Krypton Section II*, Raymond L. Kelly, April 1979.

Private conversation between D. Cleary, Naval Postgraduate School, and the author, 17 August 1990.

Quint, John H., *Development of an NPS Middle Ultraviolet Spectrograph (MUSTANG) Electronic Interface Package*, Master's Thesis, Naval Postgraduate School, Monterey, California, December 1991.

Rees, M.H., *Physics and Chemistry of the Upper Atmosphere*, Cambridge University Press, 1989.

Sharp, William E., "Sources of the Emissions Features Between 2000 and 8000 Å in the Thermosphere," *Canadian Journal of Physics*, v.64, p.1594, 1986.

Siskind, D. E., and Barth, C. A., "Rocket Observations of the NII 2143Å Emission in an Aurora," *Geophysical Research Letters*, v.14, p.479, 1987.

#### BIBLIOGRAPHY

Beiting, Edward J., and Feldman, Paul D., "Ultraviolet Spectrum of the Aurora (2000-2800Å)," *Journal of Geophysical Research*, v. 84, no. A4, 1 April 1979.

Bosserman, James L., *Analysis of Thermospheric Dayglow Spectra from the Spacelab 1 Shuttle Mission*, Master's Thesis, Naval Postgraduate School, Monterey, California, December 1989.

Cleary, David D., *Analysis of Nitric Oxide Fluorescence Bands from High Latitude Rocket Observations of the Thermospheric Dayglow*, Ph.D. Dissertation, University of Colorado, 1985.

Cleary, D. D., and Barth, C. A., "The NII 2143 Å Emission in the Dayglow," *Journal of Geophysical Research*, v. 92, no. A12, 1 December 1987.

Danczyk, Gary Michael, *Identification of Thermospheric Dayglow Emissions for the MUSTANG Experiment*, Master's Thesis, Naval Postgraduate School, Monterey, California, December 1989.

Harrison, George R., and others, *Massachusetts Institute of Technology Wavelength Tables*, John Wiley & Sons, 1960 ed., 1939.

Heicklen, Julian, *Atmospheric Chemistry*, Academic Press, 1976.

Herzberg, Gerhard, *Atomic Spectra and Atomic Structure*, 2nd ed., Dover Publications, 1944.

Herzberg, Gerhard, *Molecular Spectra and Molecular Structure*, 2nd ed., D. Van Nostrand Company, Inc., 1950.

McEwan, Murray J., and Phillips, Leon F., *Chemistry of the Atmosphere*, John Wiley & Sons, 1975.

Nichols, James W., *The Design of a New Far Ultraviolet Interferometer for Ionospheric Spectroscopy*, Master's Thesis, Naval Postgraduate School, Monterey, California, December 1990.

Reader, Joseph, and Corliss, Charles H., *Wavelengths and Transition Probabilities for Atoms and Atomic Ions: Part I. Wavelengths*, National Standards Reference Data System, 1980.

Sharp, William E., "Rocket-Borne Spectroscopic Measurements in the Ultraviolet Aurora: Nitrogen Vegard-Kaplan Bands," *Journal of Geophysical Research*, v. 76, no. 4, 1 February 1971.

Sharp, William E., and Eastes, Richard W., "Rocket-Borne Spectroscopic Measurements in the Ultraviolet Aurora: The Lyman-Birge-Hopfield Bands," *Journal of Geophysical Research*, v. 92, no. A9, 1 September 1987.

Wallace, L., "Band-Head Wavelengths of  $C_2$ , CH, CN, CO, NH, NO,  $O_2$ , OH, and Their Ions," *The Astrophysical Journal Supplement Series*, no. 68, October, 1962.

### INITIAL DISTRIBUTION LIST

1. Defense Technical Information Center Cameron Station Alexandria, Virginia 22304-6145	2
2. Library, Code 052 Naval Postgraduate School Monterey, California 93943-5002	2
3. Dr. K.E. Woehler, Chairman PH Physics Department Naval Postgraduate School Monterey, California 93943-5000	1
4. Dr. D.D. Cleary Physics Department, PH-Cl Naval Postgraduate School Monterey, California 93943-5002	3
5. Dr. S. Gnanalingam Physics Department, PH-Gm Naval Postgraduate School Monterey, California 93943-5002	1
6. LT Billie Sue Walden c/o Mr. J.W. Dickson, Jr. 3060 Shipley Street Kingsport, Tennessee 37664	2
7. Dr. Robert McCoy Code 4140 Naval Research Laboratory Washington, D.C. 20375	1
8. Dr. Larry Paxton Mail Stop 24-E115 Applied Physics Laboratory Johns Hopkins Road Laurel, Maryland 20723	1

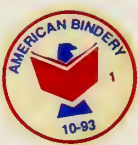
844-215





Thesis  
W22016 Walden  
c.1 An analysis of middle  
ultraviolet dayglow  
spectra.

Thesis  
W22016 Walden  
c.1 An analysis of middle  
ultraviolet dayglow  
spectra.



DUDLEY KNOX LIBRARY



3 2768 00034303 2